34

BINARY-ENCOUNTER AND MONTE-CARLO METHODS

IN

ATOMIC COLLISION THEORY

by

Derek Banks, B.Sc.

Thesis submitted to the University of Stirling

for the degree of Doctor of Philosophy.

Physics Department,

University of Stirling,

STIRLING.

Aug. 1972.

ProQuest LLC.
789 East Eisenhower Parkway
P.O. Box 1346
Ann Arbor, MI 48106 – 1346

ABSTRACT

Collisions between various charged particles and excited hydrogenic atoms and ions are described using the binary-encounter (classical-impulse) approximation and the exact-classical orbit-integration technique. In particular, emphasis is made on strong collisions such as rearrangement and ionization processes, rather than excitations. The classical methods have been justified rigorously by Abrines and Percival (1966b) for the cases in which all the initial and final quantum numbers of the target atom are large and all changes in the initial quantum numbers are also much greater than unity. In these regions quantal methods are particularly complicated and unpractical, whereas the classical approach can often be applied without having to make additional dynamical approximations. This approach is complementary to the standard quantal techniques, which are most useful for low initial and final quantum numbers, and the correspondence-principle methods of Percival and Richards (1970a,b, 1971a,b) which work best when the initial quantum numbers are large and all changes are small.

Because the classical techniques, which have been used to calculate total cross sections, enable simple scaling laws to be applied, these cross sections can also be compared with quantal and experimental values for states with low initial quantum numbers including the ground state. Although there is no solid theoretical justification for applying classical theories in this region, a considerable amount of empirical

evidence is presented, which suggests that accurate classical theories can be superior to quantal approximations for intermediate energies of the incident particle, provided that the changes in quantum number are large. Specific failures at low or high energies must, however, be expected since purely-quantal effects such as barrier penetration and interference are often dominant here.

Many of the cross sections are of importance in the study of astrophysical and laboratory plasmas. The exact-classical results can also be used to test the validity of an existing dynamical approximation, or possibly to suggest a new simple model.

ACKNOWLEDGMENTS

I am grateful to my supervisor, Professor I.C. Percival for suggesting the work investigated in this thesis and for his continual guidance throughout. I should like to thank the Mathematics Department at Queen Mary College, London University and the Physics Department at the University of Stirling for allowing me to carry out this research. My thanks are also due to Dr. N.A. Valentine for his collaboration on the exact-classical work presented in sections (3.3) and (3.4), to T.F.M. Bonsen for his cooperation on the calculations described in section (3.5), to Dr. L. Vriens for helpful discussions on the binary-encounter approximations, and to Mrs N. Littlefair for typing this thesis. I am indebted to the Science Research Council for support.

CONTENTS

CHAPTER I

A GENERAL DISCUSSION OF CLASSICAL METHODS IN ATOMIC COLLISION THEORY

1.1 Introduction

The central theme of this thesis is the description of simple atomic collision phenomena in terms of classical mechanics rather than quantum mechanics. The latter, though superior theoretically, is so complicated to apply exactly in practice that serious dynamical approximations have to be made, whereas in the classical treatment, once the approximation of replacing quantum mechanics by classical mechanics has been made, it is often possible to obtain a solution without the need to invoke further dynamical approximations.

The main arguments in favour of the classical approach are outlined in section (1.2) and a brief survey of the historical development of this approach is presented in section (1.3).

The early sections of chapter 2 contain the basic theory of the classical-impulse or binary-encounter theory. The later sections deal with the results for ionization, electron loss and excitation of hydrogenic atoms and ions by incident charged particles, and the comparison with the exact-classical results for singly-charged particles incident upon neutral hydrogen atoms. Estimates of the electron exchange and interference contributions to ionization of hydrogenic atoms and ions by electron impact are made using the symmetric binary-encounter model based on the Mott scattering formula (see for example Burgess 1963,

1964, Vriens 1966 b).

The first two sections of chapter 3 are devoted to the exact-classical theory necessary to treat collisions involving more than two particles. In the later sections the exact-classical theory of Abrines, Percival and Valentine for three particles is applied to collisions of protons with hydrogen and helium target atoms. The ranges of incident proton velocities selected correspond to regions in which the binary-encounter theory and the classical adiabatic theory of Bates and Reid (1969b) are not necessarily valid. Where relevant these simplified classical theories are compared with the exact-classical results.

Chapter 4 contains miscellaneous points which arise from the theory and results of chapters 2 and 3.

Throughout this work the classical results are contrasted with experimental and quantal results. Semi-classical WKB theories and extensions of the classical approach to include quantal effects using classical path expansions are not reviewed or used in this work. The latter theory has been discussed by Percival (1971), who also displays several of the results obtained in this thesis. Relativistic effects are ignored throughout.

1.2 Justifications for the Classical Approach

As pointed out in section (1.1) the first justification for using the classical approach is a purely-practical reason arising from the present impossibility of solving quantal treatments without making serious dynamical simplifications.

A second justification arises from correspondence principle arguments. Abrines and Percival (1966b) have shown that purely-classical methods are valid when all the quantum numbers associated in the problem are large and when the changes in all quantum numbers resulting from the collision are also large. Percival and Richards (1970a,b) have shown that classical mechanics can also be used when all quantum numbers are large and when the changes in all quantum numbers are small, but in this region Fourier components of the motion must be used rather than dynamical variables themselves. The region, in which all quantum numbers are large, some changes are small and others are large, has not yet been treated consistently. Quantal methods work best when all quantum numbers and all changes in quantum numbers are small. A classical treatment of the region in which all quantum numbers are initially small, but some or al changes are large, cannot be justified, but empirical evidence particularly from the exact-classical results suggests that even here exact-classical results are often surprisingly accurate, especially for intermediate incident energies for which the incident and target velocities are comparable.

One possible reason for the good agreement in the last region of the previous paragraph is that correspondence identities hold for just

two distinguishable charged particles. These and other related identities have been the subject of a thesis by Norcliffe (1970) and a review by Percival (1969). These identities consist of the Rutherford scattering identity which states that the quantal and classical centre-of-mass angular differential cross sections for distinguishable charged particles are identical, the Bohr-Sommerfeld identity, which states that the quantal discrete bound-state energy spectrum of hydrogenic atoms and ions is given exactly by the Bohr-Sommerfeld model, and the Fock identity, which states that quantal momentum distribution for the ground state or any uniformly-populated excited level of a hydrogenic atom or ion is identical to the classical momentum distribution derived from the classical microcanonical statistical distribution of the same binding energy. Thus, although no correspondence identities are known for more than two charged particles, the two-particle identities may be a factor contributing to the good agreement of the exact-classical approach.

A final justification of the exact-classical method adopted here is that powerful scaling laws can be used to obtain classical cross sections corresponding to different uniformly-populated levels of atomic hydrogen from the results at one level, which may be taken conveniently as the ground state. For sufficiently high levels the classical approach is valid.

1.3 Historical Development

The historical development of the classical approach has been

outlined by several authors. Burgess and Percival (1968) and Valentine (1968) give general reviews with greater emphasis on exact-classical methods. Vriens (1969) stresses the connection between binary-encounter and first-Born calculations, particularly for differential cross sections which provide a more stringent test of a theory than the total cross sections alone. Recent advances in heavy particle collisions have been reviewed by Bates and Kingston (1970). Classical, path-integral and correspondence-principle theories have been discussed by Percival (1971). A section on heavy-particle classical scattering has also been included by McDowell and Coleman (1970).

The simplest binary-encounter treatment of excitation and ionization of atoms by fast charged particles was first employed by Thomson (1912). He assumed that the orbital speed of the electron(s) in the target atom could be neglected for collisions with fast charged particles with incident energy E_1 . The Thomson (and all other realistic purely-classical) ionization and excitation cross sections exhibit a E_1^{-1} high energy law, in disagreement with experimental and later quantal values, which generally obey a $E_1^{-1} \log E_1$ high energy law, apart from optically forbidden excitations. This specific failure of the classical approach was one of the main reasons for the decline in its popularity after the introduction of the quantum theory and probably accounted for the fact that improvements over the crude Thomson model made by Williams (1927) and Thomas (1927a, b) were overlooked until very recently. Indeed, their model, in which allowance is made for the motion of the atomic electron, forms a basis for the presently-accepted binary-encounter theory.

After the development of the quantum theory the first important revival of the classical approach was made by Williams (1945). In particular he compared and contrasted the classical and quantal first-Born theories of the scattering by simple central potentials and showed that each approach was valid in separate extremes and hence that the theories were complementary. For the special case of a coulomb potential of the form $z_1 z_2 e^2/r$ he showed that the classical treatment was valid when the dimensionless parameter $S = z_1 z_2 e^2/\hbar v_1$, where v_1 is the incident velocity, $\hbar = 2\pi\hbar$ is Planck's constant and e is the charge on a proton, satisfied $S \gg 1$ and that in contrast the quantal first-Born approximation was valid when $S \ll 1$ (the parameter S occurs explicitly in the exact quantal treatment of the scattering of two identical particles, outlined in chapter 2 of this thesis).

The revival of classical methods was greatly stimulated by the work of Gryzinski (1959). However the binary-encounter theory was developed more carefully by Thomas (1927a), Ochkur and Petrunkin (1963), Stabler (1964), Kingston (1966) and McDowell (1966) using the unsymmetric model for incident electrons, by Thomas (1927a), McDowell (1966) and Vriens (1967) for incident protons, by Gerjuoy (1966) for arbitrary masses, and by Burgess (1963, 1964) and Vriens (1966a, b) for the symmetric treatment of incident electrons.

In a parallel development Abrines and Percival (1966 b), Abrines, Percival and Valentine (1966) and Percival and Valentine (1967) obtained exact-classical results for ionization and charge-changing collisions in which singly-charged incident particles were in collision with neutral

target hydrogen atoms. The theory described in Abrines and Percival (1966a) is similar to related classical work in the field of chemical kinetics (see Burgess and Percival (1968) and the references therein). The exact-classical results for ionization demonstrated that the agreement with experiment was improved even for ground-state targets when the binary-encounter approximation was relaxed. For incident protons the results for charge transfer were also in remarkably good agreement with available experimental data over the energy ranges considered. The scaling laws and generalised correspondence principle derived in Abrines and Percival (1966b) implied that the related exact-classical results for ionization and charge-changing collisions obtained by scaling the results for the ground state would be accurate for target atoms in sufficiently highly-excited initial levels.

In another approach Percival and Richards (1970a,b, 1971a,b) have developed correspondence principles which resolve the failure of purely-classical methods at high energies, in the case of weak excitations of highly-excited hydrogenic atoms and ions by fast charged particles. By using Fourier components of classical variables, rather than the values of the variables directly, they (1970a) obtain excitation cross sections which exhibit the correct high energy behaviour, which agree here to within a few per cent with the more complicated calculations of the first-Born theory.

CHAPTER 2

THE BINARY-ENCOUNTER APPROXIMATION

2.1 General Remarks on the Geometry of an Individual Classical Binary Encounter.

(a) A Standard Derivation Given the Initial Velocities of the Particles.

Consider a system of two mutually-interacting particles in the absence of any external force field. Suppose that the motion of the particles can be adequately described by classical mechanics. Then the interaction experienced by one particle is equal and opposite to that experienced by the second particle, but is not necessarily directed along the line joining them. Suppose that one particle is called the incident particle and is labelled by 1 and that the other particle is termed the target particle and is labelled by 2. Let particle 1 of mass m_1 have an initial velocity $\underline{V}_{L1}$ and particle 2 of mass m_2 have an initial velocity $\underline{V}_{L2}$ in some Galilean frame of reference L, termed the laboratory or observation frame, and suppose that the particles are sufficiently far apart initially for their mutual interactions to be negligible (the frame dependence of any dynamical variable is stressed here by the use of a subscripted Roman capital letter to denote the particular Galilean frame of reference in which the variable is measured). Now let the particles approach one another,

collide and then separate so that their interactions can again be neglected. Let the final velocities in the frame L be $\underline{v}_{L1}'$ and $\underline{v}_{L2}'$ respectively.

Such a collision or scattering event is here termed an individual classical binary encounter. Many of the properties of such a collision can be determined for general forms of particle-particle interaction. These properties arise from basic conservation laws.

Firstly, the law of conservation of total linear momentum holds throughout the encounter and so, as a special case,

$$m_1\underline{v}_{L1} + m_2\underline{v}_{L2} = m_1\underline{v}_{L1}' + m_2\underline{v}_{L2}' \quad . \tag{2.1.1}$$

In velocity space the encounter is therefore completely described by the momentum-transfer vector $\underline{q}$ which may be defined as

$$\underline{q} = m_2\underline{v}_{L2}' - m_2\underline{v}_{L2} = m_1\underline{v}_{L1} - m_1\underline{v}_{L1}' \quad . \tag{2.1.2}$$

The vector $\underline{q}$ is particularly suitable because it is a Galilean frame invariant. Further, $\underline{q}$ remains well-defined and finite in the important limiting cases in which either m_1 , or m_2 , but not both, tend to infinity. However, the collision may often be described in terms of other dynamical variables which may be frame dependent. The most important alternatives are various scattering angles and energy transfers. These variables are particularly suitable for measurement in an experiment.

Scattering angles can be defined by any distinct pair of the

velocity directions $\hat{\underline{v}}_{L1}$, $\hat{\underline{v}}_{L2}$, $\hat{\underline{v}}'_{L1}$ and $\hat{\underline{v}}'_{L2}$. The polar scattering angles may be written θ_{LIJ} , θ'_{LIJ} and θ''_{LIJ} where

$$\theta_{LIJ} = \cos^{-1}(\hat{\underline{v}}_{LJ} \cdot \hat{\underline{v}}_{LI}) \quad \text{for } J = 3-I \text{ and } I = 1,2 \ ,$$

$$\theta'_{LIJ} = \cos^{-1}(\hat{\underline{v}}'_{LJ} \cdot \hat{\underline{v}}_{LI}) \quad \text{for } I \text{ and } J = 1,2 \ ,$$

and

$$\theta''_{LIJ} = \cos^{-1}(\hat{\underline{v}}'_{LJ} \cdot \hat{\underline{v}}'_{LI}) \quad \text{for } J = 3-I \text{ and } I = 1,2 \ .$$

Obviously these polar angles do not depend upon the order of the subscripts I and J . However, for each polar scattering angle there is an associated azimuthal angle, which will depend upon which of the two unit vectors, used to define the polar angle, is selected as the reference $\hat{\underline{z}}$ axis. The azimuthal scattering angles corresponding to θ_{LIJ} , θ'_{LIJ} and θ''_{LIJ} may be written ϕ_{LIJ} , ϕ'_{LIJ} and ϕ''_{LIJ} respectively. The polar angles are always defined in the range $(0, \pi)$ and so are uniquely determined by the corresponding velocity directions. The azimuthal angles must be defined over a complete period 2π, so the corresponding range may be $(-\pi, \pi)$ or $(0, 2\pi)$, say. Further, the azimuthal angles can only be defined with respect to additional arbitrary axes.

The appropriate polar scattering angles become indeterminate if one or more of the initial or final velocities is zero. An azimuthal scattering angle is indeterminate when its corresponding polar angle is 0 or π ; that is, when the appropriate velocity directions are parallel or anti-parallel.

The energy transfers ΔE_{L1} and ΔE_{L2} are here defined by

$$\Delta E_{L2} = \tfrac{1}{2} m_2 v'^2_{L2} - \tfrac{1}{2} m_2 v^2_{L2} = \underline{v}_{L2} \cdot \underline{q} + \frac{1}{2m_2} q^2 , \qquad (2.1.3)$$

and

$$\Delta E_{L1} = \tfrac{1}{2} m_1 v^2_{L1} - \tfrac{1}{2} m_1 v'^2_{L1} = \underline{v}_{L1} \cdot \underline{q} - \frac{1}{2m_1} q^2 . \qquad (2.1.4)$$

In many applications of the binary-encounter theory the particle-particle interactions are conservative. This implies that the law of conservation of energy holds throughout the collision. In particular, if this law is applied initially and finally, the potential energy terms may be neglected and so

$$\tfrac{1}{2} m_1 v^2_{L1} + \tfrac{1}{2} m_2 v^2_{L2} = \tfrac{1}{2} m_1 v'^2_{L1} + \tfrac{1}{2} m_2 v'^2_{L2} . \qquad (2.1.5)$$

From this it follows that

$$\Delta E_{L1} = \Delta E_{L2} = \Delta E_L , \qquad (2.1.6)$$

say. So, if energy is conserved in the collision, the kinetic energy gained by the target particle is equal to the kinetic energy lost by the incident particle.

The law of conservation of energy places a heavy restriction upon the permitted values of the momentum transfer vector $\underline{q}$, namely

$$(\underline{v}_{L1} - \underline{v}_{L2}) \cdot \underline{q} = \frac{1}{2} \frac{(m_1 + m_2)}{m_1 m_2} q^2 , \qquad (2.1.7)$$

which follows from equations (2.1.3), (2.1.4) and (2.1.6). This

restriction can be explained simply, if the laboratory velocities $\underline{v}_{L1}$ and $\underline{v}_{L2}$ are combined to form the centre-of-mass velocity $\underline{v}_{LG}$ and a relative velocity $\underline{v}_R$, where

$$(m_1+m_2)\underline{v}_{LG} = m_1\underline{v}_{L1} + m_2\underline{v}_{L2} , \tag{2.1.8}$$

and it is convenient to choose

$$\underline{v}_R = \underline{v}_{L1} - \underline{v}_{L2} . \tag{2.1.9}$$

By equation (2.1.1) with the usual notation for corresponding final velocities

$$\underline{v}_{LG} = \underline{v}_{LG}' , \tag{2.1.10}$$

and, by the law of conservation of linear momentum, the velocity of the centre of mass is conserved throughout the collision. The relative velocity $\underline{v}_R$ is a frame invariant. Henceforth the subscript R will be used to denote a quantity defined in a frame moving with a particle even though the variable may be a Galilean frame invariant.

Equations (2.1.8) and (2.1.9) can be solved directly for $\underline{v}_{L1}$ and $\underline{v}_{L2}$ in terms of $\underline{v}_{LG}$ and $\underline{v}_R$. The resulting expressions are

$$\underline{v}_{L1} = \underline{v}_{LG} + \frac{m_2}{(m_1+m_2)}\underline{v}_R = \underline{v}_{LG} + \underline{v}_{G1} , \tag{2.1.11}$$

and

$$\underline{v}_{L2} = \underline{v}_{LG} - \frac{m_1}{(m_1+m_2)}\underline{v}_R = \underline{v}_{LG} + \underline{v}_{G2} , \tag{2.1.12}$$

where the velocities $\underline{v}_{G1}$ and $\underline{v}_{G2}$ are proportional to $\underline{v}_R$ and are the initial velocities of the colliding particles as measured in the centre-of-mass frame G. Let the respective final velocities be $\underline{v}_R'$, $\underline{v}_{G1}'$ and $\underline{v}_{G2}'$. Then

$$\underline{v}_{L1}' = \underline{v}_{LG}' + \frac{m_2}{(m_1+m_2)}\underline{v}_R' = \underline{v}_{LG} + \underline{v}_{G1}' , \qquad (2.1.13)$$

and

$$\underline{v}_{L2}' = \underline{v}_{LG}' - \frac{m_1}{(m_1+m_2)}\underline{v}_R' = \underline{v}_{LG} + \underline{v}_{G2}' . \qquad (2.1.14)$$

If these expressions for $\underline{v}_{L1}$, $\underline{v}_{L2}$, $\underline{v}_{L1}'$ and $\underline{v}_{L2}'$ are substituted into equation (2.1.5) and the result (2.1.10) is used, the following equality is obtained:

$$v_R^2 = v_R'^2 . \qquad (2.1.15)$$

Hence the law of conservation of energy implies that the relative speed is unaltered by the collision. Further,

$$v_{G1}^2 = v_{G1}'^2 , \qquad (2.1.16)$$

and

$$v_{G2}^2 = v_{G2}'^2 . \qquad (2.1.17)$$

Thus the speed of each particle in the centre-of-mass frame is unaltered by the encounter.

The restriction upon $\underline{q}$ arising from equation (2.1.7) can be

written

$$\underline{q} \cdot (2 m_R \underline{v}_R - \underline{q}) = 0 \,, \tag{2.1.18}$$

where

$$m_R = m_1 m_2 / (m_1 + m_2) \,, \tag{2.1.19}$$

is the reduced mass of particles 1 and 2 .

Equation (2.1.18) is the equation of the surface of a sphere in momentum-transfer space. The sphere passes through the origin $\underline{q} = \underline{0}$ and through the diametrically opposite point $\underline{q} = 2 m_R \underline{v}_R$.

The momentum transfer $\underline{q}$ may also be expressed in terms of the velocity transfers $\underline{w}_1$ and $\underline{w}_2$ where

$$m_1 \underline{w}_1 = -\underline{q} \,, \tag{2.1.20}$$

and

$$m_2 \underline{w}_2 = \underline{q} \,, \tag{2.1.21}$$

so that

$$\underline{v}_{L1}' = \underline{v}_{L1} + \underline{w}_1 \,, \tag{2.1.22}$$

and

$$\underline{v}_{L2}' = \underline{v}_{L2} + \underline{w}_2 \,. \tag{2.1.23}$$

In figure (2.1.1) the velocity vectors $\underline{v}_{L1}$, $\underline{v}_{L2}$, $\underline{v}_{Lq}$,

Figure 2.1.1 Velocity-space diagram for an individual binary encounter. The final velocity of the incident particle $\vec{OP_1'}$ must lie on the sphere Σ_1 centred at G and passing through P_1. The final velocity of the target particle $\vec{OP_2'}$ lies diametrically opposite P_1' on the concentric sphere Σ_2 passing through P_2.

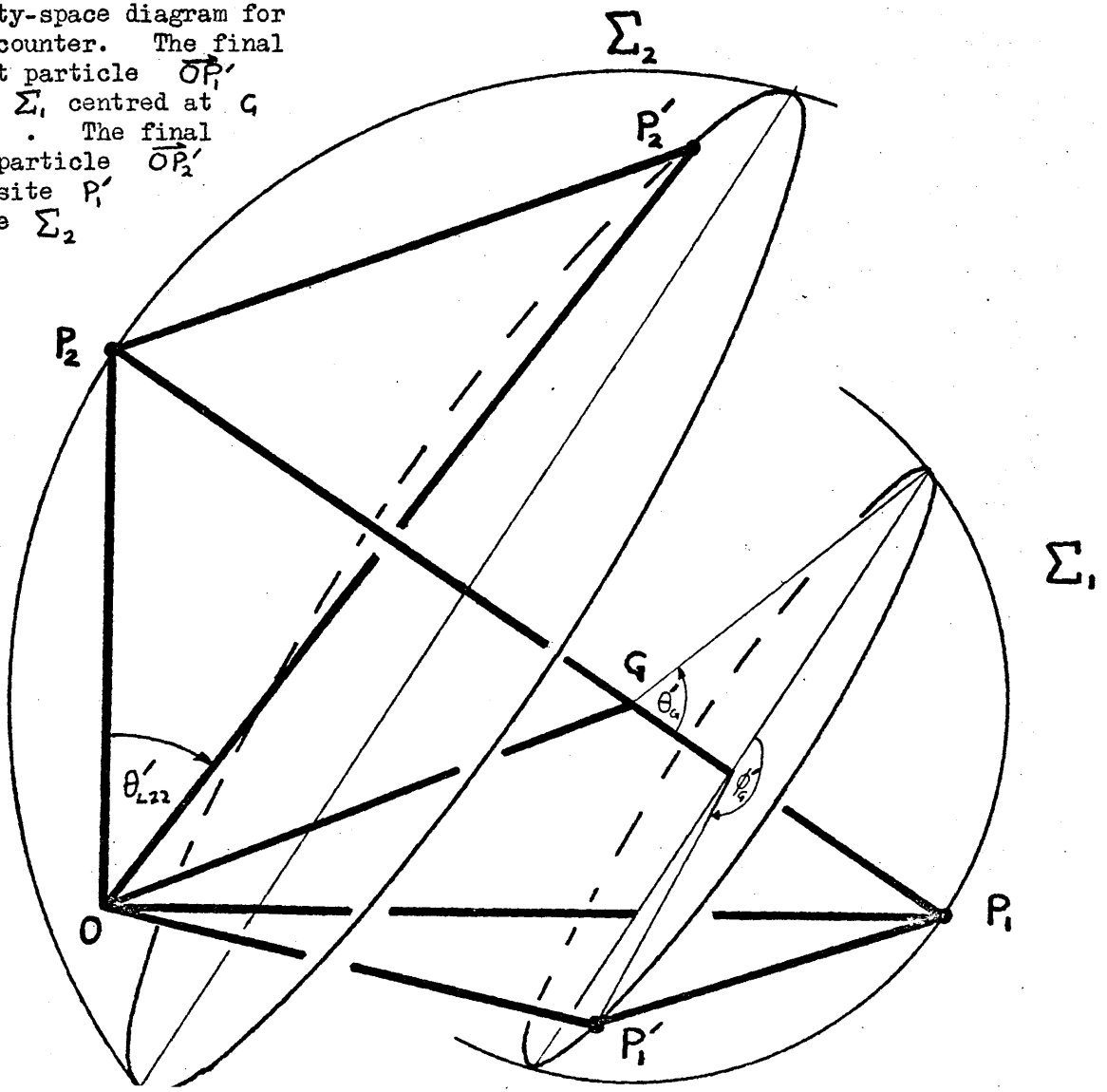

$\underline{v}_R$, $\underline{v}_{G1}$, $\underline{v}_{G2}$, $\underline{w}_1$ and $\underline{w}_2$ are represented by $\overrightarrow{OP_1}$, $\overrightarrow{OP_2}$, $\overrightarrow{OG}$, $\overrightarrow{P_2P_1}$, $\overrightarrow{GP_1}$, $\overrightarrow{GP_2}$, $\overrightarrow{P_1P_1'}$ and $\overrightarrow{P_2P_2'}$ respectively, where O is the origin (that is, the rest point of the velocity space). The final velocities $\underline{v}'_{G1}$, $\underline{v}'_{G2}$, $\underline{v}'_{L1}$ and $\underline{v}'_{L2}$ are represented by $\overrightarrow{GP_1'}$, $\overrightarrow{GP_2'}$, $\overrightarrow{OP_1'}$ and $\overrightarrow{OP_2'}$.

The laboratory angle θ'_{L22} is also displayed. By equations (2.1.10) and (2.1.16) P_1' must lie on a unique sphere $\sum_1$ centred at G and passing through P_1 . Equations (2.1.11), (2.1.12), (2.1.13) and (2.1.14) imply that P_2' must lie diametrically opposite P_1' on the concentric sphere $\sum_2$ passing through P_2 . As a consequence it is impossible for the velocities $\underline{v}_{L1}$ and $\underline{v}_{L2}$ to be exactly exchanged by the collision unless $m_1 = m_2$.

The collision is commonly parametrized by the standard spherical-polar angles $\theta'_{G11} = \theta'_{G22} = \theta'_G$, say, and $\phi'_{G11} = 2\pi - \phi'_{G22} = \phi'_G$, say, with respect to $\overrightarrow{GP_1} = \underline{v}_{G1}$ as $\hat{\underline{z}}$ axis, when the collision is viewed in the centre-of-mass frame. These angles may be used to determine $\underline{q}$ or any other scattering variable in any other frame of reference L . Thus, given θ'_G , ϕ'_G it is easy to show that

$$q = 2 m_R v_R \sin \tfrac{1}{2}\theta'_G \quad , \qquad (2.1.24)$$

and

$$\Delta E_L = v_{L2} q \left(\cos \tfrac{1}{2}\theta'_G \cos \phi'_G \sin \chi_{L2} - \sin \tfrac{1}{2}\theta'_G \cos \chi_{L2} \right) + \frac{1}{2m_2} q^2 \quad , \qquad (2.1.25)$$

by equation (2.1.3), or equivalently,

$$\Delta E_L = v_{L1} q \left(\cos \tfrac{1}{2}\theta'_q \cos \phi'_q \sin \chi_{L1} + \sin \tfrac{1}{2}\theta'_q \cos \chi_{L1} \right) - \frac{1}{2m_1} q^2 , \tag{2.1.26}$$

by equation (2.1.4), where the angles χ_{L1} and χ_{L2} are given by

$$\cos \chi_{L1} = \hat{\underline{v}}_{L1} . \hat{\underline{v}}_R , \tag{2.1.27}$$

and

$$\cos \chi_{L2} = \hat{\underline{v}}_{L2} . \hat{\underline{v}}_R . \tag{2.1.28}$$

Conversely it is possible to express θ'_q and ϕ'_q in terms of q and ΔE_L. In fact

$$\theta'_q = 2 \sin^{-1} \{ q / (2 m_R v_R) \} , \tag{2.1.29}$$

and

$$\phi'_q = \cos^{-1} \{ (\Delta E_L - \tfrac{1}{2m_2} q^2 + v_{L2} q \sin \tfrac{1}{2}\theta'_q \cos \chi_{L2}) / (v_{L2} q \cos \tfrac{1}{2}\theta'_q \sin \chi_{L2}) \} , \tag{2.1.30}$$

or, equivalently,

$$\phi'_q = \cos^{-1} \{ (\Delta E_L + \tfrac{1}{2m_1} q^2 - v_{L1} q \sin \tfrac{1}{2}\theta'_q \cos \chi_{L1}) / (v_{L1} q \cos \tfrac{1}{2}\theta'_q \sin \chi_{L1}) \} . \tag{2.1.31}$$

Because the range of θ'_q is only $(0, \pi)$, θ'_q is uniquely prescribed by equation (2.1.29). However, since the range of ϕ'_q is $(0, 2\pi)$, say, there are two possible values of ϕ'_q for each value of q and ΔE_L. Exceptional cases occur when ΔE_L is independent of the azimuthal angle ϕ'_q. This is only true if $\underline{v}_{L1}$ and $\underline{v}_{L2}$ are parallel or anti-parallel, but it does include all collisions both in the centre-of-mass frame C (since ΔE_C is always zero) and in the simplest laboratory frame S defined by $\underline{v}_{S2} = \underline{0}$, for by equation (2.1.3) $\Delta E_S - \frac{1}{2m_2} q^2$ is always zero.

It should be noted that these inverse transformations are not defined for arbitrary values of the momentum-transfer magnitude q and the energy transfer ΔE_L, but only for

$$0 \leq q \leq 2 m_R v_R \ ,$$

and

$$-v_{L2} q \cos \tfrac{1}{2}\theta'_q \sin \chi_{L2} \leq \Delta E_L - \frac{1}{2m_2} q^2 + v_{L2} q \sin \tfrac{1}{2}\theta'_q \cos \chi_{L2} \leq v_{L2} q \cos \tfrac{1}{2}\theta'_q \sin \chi_{L2} \ ,$$

or, equivalently,

$$-v_{L1} q \cos \tfrac{1}{2}\theta'_q \sin \chi_{L1} \leq \Delta E_L + \frac{1}{2m_1} q^2 - v_{L1} q \sin \tfrac{1}{2}\theta'_q \cos \chi_{L1} \leq v_{L1} q \cos \tfrac{1}{2}\theta'_q \sin \chi_{L1} \ .$$

Equations (2.1.1) to (2.1.31) have been derived using classical mechanics alone. However, since only relations between velocities, momenta and kinetic energies, before and after the collision, have been employed, the uncertainty principle has not been violated, and so these formulae remain valid in a quantal treatment of an individual collision of two distinguishable particles. In particular, the variables q and ΔE_L are subject to the same restrictions as in the classical theory treated here. If the particles are identical, then they may be treated firstly as if they were distinguishable and then all variables can be symmetrised by interchanging the velocities $\underline{v}'_{L1}$ and $\underline{v}'_{L2}$.

(b) An Alternative Approach Given the Initial and Final Velocities of the Incident Particle.

In the preceding section the range of allowed values of the momentum-transfer vector was determined for elastic collisions from prescribed values of m_1 , m_2 , $\underline{v}_{L1}$ and $\underline{v}_{L2}$. It is also possible to find the restriction on the values of the initial velocity $\underline{v}_{L2}$ of the target particle, given the values of m_1 , m_2 , $\underline{v}_{L1}$ and $\underline{v}'_{L1}$ (and hence $\underline{q}$). This resriction can be used to infer properties of an unknown initial velocity distribution of a thin gas of target particles. Alternatively, if the initial velocity distribution of the target particle(s) is known then any function f of $\underline{v}_{L1}$ and $\underline{v}'_{L1}$ can be averaged over all values of $\underline{v}_{L2}$ consistent with $\underline{v}_{L1}$ and $\underline{v}'_{L1}$. This is especially important if f is a quantum-mechanical scattering amplitude when the average will include interference effects.

The restriction upon $\underline{v}_{L2}$ can be obtained immediately, once the equations (2.1.1) to (2.1.31) have been presented. Since $\underline{v}_{L1}$ and $\underline{q}$ are known, then by equation (2.1.4) the energy transfer ΔE_{L1} is also prescribed. However, for elastic collisions $\Delta E_{L1} = \Delta E_{L2} = \Delta E_L$. Hence by equation (2.1.3)

$$\underline{v}_{L2} \cdot \underline{q} = \Delta E_L - \tfrac{1}{2} m_2 q^2 = \text{constant}. \quad (2.1.32)$$

This equation is the required restriction on $\underline{v}_{L2}$, and is just

the equation in velocity space of a plane $\Pi_{\underline{q}\,\underline{v}_{L1}}$, perpendicular to the direction $\hat{\underline{q}}$ and with its shortest distance (that is, speed) from the origin given by

$$v_{L2\,min} = |(\Delta E_L - \tfrac{1}{2}m_2 q^2)/q| \,. \qquad (2.1.33)$$

These relations have been used by Vriens and Bonsen (1968) and by Banks, Vriens and Bonsen (1969) in their comparisons between binary-encounter and first-Born double-differential cross sections for the ejection of electrons from various levels of atomic hydrogen by fast charged particles.

2.2 The Dynamics of Two Particles in a General Observation Frame L.

In this section the classical and quantum-mechanical methods of solution of the two-particle problem are outlined. In both theories it is convenient to change the representation so that, instead of solving for the motion of the individual particles in frame L, the free motion of the centre of mass and the relative motion can be solved independently.

(a) Classical Dynamics.

In section (2.1a) the conservation laws were used to determine the domain of the scattering variables of interest, for example $\underline{q}$. However it was not possible to say which value of $\underline{q}$ was obtained in a given collision, since in a classical treatment more information is required. If the initial positions $\underline{r}_{L1}$ and $\underline{r}_{L2}$ of the two particles at the initial time t are also known, then Newton's equations of motion:

$$\left.\begin{aligned} \frac{d\underline{r}''_{LI}}{dt''} &= \underline{v}''_{LI} \\ m_I \frac{d\underline{v}''_{LI}}{dt''} &= \underline{F}''_{IJ} \end{aligned}\right\} \quad \text{for } J = 3-I \text{ and } I = 1,2 \quad , \qquad (2.2.1)$$

where $\underline{r}''_{LI}$ and $\underline{v}''_{LI}$ are the position and velocity of particle I at a general time t'' and $\underline{F}''_{IJ}$ is the force on particle I exerted by particle J, together with the boundary conditions:

$$\left.\begin{aligned} \underline{r}''_{LI} &= \underline{r}_{LI} \\ \underline{v}''_{LI} &= \underline{v}_{LI} \end{aligned}\right\} \quad \text{for } I = 1,2 \text{ at } t'' = t \quad , \qquad (2.2.2)$$

have a unique solution, which may be determined (possibly numerically) at any time t'' . The scattering parameters of the encounter may be obtained from the given initial positions and velocities $\underline{r}_{L1}$, $\underline{r}_{L2}$, $\underline{v}_{L1}$, $\underline{v}_{L2}$ and from the final coordinates $\underline{r}'_{L1}$, $\underline{r}'_{L2}$, $\underline{v}'_{L1}$, $\underline{v}'_{L2}$ which are the solutions of equations (2.2.1) for sufficiently large t'' . Equations (2.2.1) constitute twelve coupled ordinary first-order differential equations with t'' as the independent variable. These twelve equations can be transformed into the equations of motion of the centre of mass G and the independent equations of motion of the frame-invariant relative position and velocity vectors $\underline{r}''_R = \underline{r}''_{L1} - \underline{r}''_{L2}$ and $\underline{v}''_R = \underline{v}''_{L1} - \underline{v}''_{L2}$. The separation can be achieved because the force $\underline{F}''_{IJ} = -\underline{F}''_{JI}$ only depends upon the relative position and velocity and not upon the position and velocity of the centre of mass, since there are no external forces present.

The transformed equations for the motion of the centre of mass are:

$$\left.\begin{aligned} \frac{d\underline{r}''_{LG}}{dt''} &= \underline{v}''_{LG} \\ \frac{d\underline{v}''_{LG}}{dt''} &= \underline{0} \end{aligned}\right\} , \qquad (2.2.3)$$

where the position $\underline{r}''_{LG}$ of the centre of mass satisfies

$$(m_1 + m_2)\,\underline{r}''_{LG} = m_1\underline{r}''_{L1} + m_2\underline{r}''_{L2} , \qquad (2.2.4)$$

with the boundary conditions

$$\left.\begin{aligned} \underline{r}''_{LG} &= \underline{r}_{LG} \\ \underline{v}''_{LG} &= \underline{v}_{LG} \end{aligned}\right\} \text{ at } t'' = t . \qquad (2.2.5)$$

These equations have the solutions

$$\left.\begin{aligned} \underline{r}''_{LG} &= \underline{r}_{LG} + (t''-t)\,\underline{v}_{LG} \\ \underline{v}''_{LG} &= \underline{v}_{LG} \end{aligned}\right\} \text{ for all } t''. \qquad (2.2.6)$$

The equations of relative motion are:

$$\left.\begin{aligned} \frac{d\underline{r}''_R}{dt''} &= \underline{v}''_R \\ m_R \frac{d\underline{v}''_R}{dt''} &= \underline{F}''_R \end{aligned}\right\}, \qquad (2.2.7)$$

where

$$\underline{F}''_R = \underline{F}''_{12}(\underline{r}''_R, \underline{v}''_R), \qquad (2.2.8)$$

together with the boundary conditions

$$\left.\begin{aligned} \underline{r}''_R &= \underline{r}_R \\ \underline{v}''_R &= \underline{v}_R \end{aligned}\right\} \text{ at } t''=t. \qquad (2.2.9)$$

These last three equations are equivalent to the equations of motion of a fictitious particle of mass $m = m_R$ at the position $\underline{r}'' = \underline{r}''_R$ and moving with velocity $\underline{v}'' = \underline{v}''_R$ in a fixed force field $\underline{F}''(\underline{r}'', \underline{v}'') = \underline{F}''_R(\underline{r}''_R, \underline{v}''_R)$ centred at the origin. Further the relative momentum transfer $\underline{q}_R = m_R \underline{v}_R - m_R \underline{v}'_R$ is the same as the original momentum transfer $\underline{q}$.

2.2(b) The Quantal Solution of Two Particles Moving in a General Observation Frame L.

In a quantal treatment it is not possible to know simultaneously the exact positions and velocities of the particles at any time t'' because of the uncertainty principle. However, the Schrödinger equation may also be transformed so that the centre-of-mass motion and the relative

motion may be solved independently. The solution of the centre-of-mass motion is trivial and the solution of the relative motion again leads naturally to the reduced-mass problem. A more complete discussion is given in Mott and Massey (1965, pp. 286 - 9).

2.3 Scattering of a Particle by a Fixed Centre of Force.

(a) Classical Theory

Suppose that the force field is central; that is, $\underline{F}''(\underline{r}'',\underline{v}'') = \underline{F}''(r'')$. Then it is easy to show that the angular momentum $\underline{l}'' = m\underline{r}''\times\underline{v}''$ of the particle about the centre of force is constant for any orbit. It is convenient to choose a cartesian coordinate system located with origin at the centre of force and oriented so that $\underline{l}'' = \underline{l} = |\underline{l}|\,\hat{\underline{z}}$ and the initial velocity $\underline{v} = |\underline{v}|\,\hat{\underline{y}}$. The orbit then lies wholly in the $(\hat{\underline{x}},\hat{\underline{y}})$ plane and, if the interaction were negligible, the trajectory of the particle would be a straight line parallel to the $\hat{\underline{y}}$ axis and cutting the $\hat{\underline{x}}$ axis in the point $\underline{b} = (b,0,0)$, where

$$mbv = l \quad , \tag{2.3.1}$$

with $v = |\underline{v}|$ and $l = |\underline{l}|$. The vector $\underline{b}$ is called the impact-parameter vector and would be the shortest position vector of the particle from the centre of force if the force could be neglected. Obviously

$$\underline{v}.\underline{b} = 0 \, . \tag{2.3.2}$$

If the interaction is fully included each orbit is still completely characterised by $\underline{b}$ and $\underline{v}$. Hence, any scattering parameter, for example $\underline{q}$, may be determined uniquely from $\underline{b}$ and $\underline{v}$. Because the orbit is planar, $\underline{q}$ lies in the plane defined by $\underline{b}$ and $\underline{v}$. In an alternative approach $\underline{v}$ and $\underline{v}'$ and hence $\underline{q}$ may be prescribed instead of $\underline{b}$ and $\underline{v}$. In such cases the orbit is uniquely determined

only if there is a unique $\underline{b}$ for each value of $\underline{q}$. For many forms of central force, different values of $\underline{b}$ can lead to the same value of $\underline{q}$ and so there may be more than one orbit leading from the given initial velocity $\underline{v}$ to the given final velocity $\underline{v}'$. This alternative approach is used in semi-classical path-integral theories and can lead to simple interference phenomena (see for example Percival 1971).

(b) Quantal Theory

The solution of this problem is standard and may be found in many general works on atomic scattering theory (see for example Mott and Massey 1965, chapters II-VII). The most important points for contrast are that the outcome of an individual collision cannot be predicted and that the impact parameter can no longer be accurately defined.

(c) The Classical Angular Differential Cross Section $\frac{d\sigma^c}{d\Omega}$

Consider a uniform beam of incident particles all of which are scattered independently by the centre of force. The angular differential cross section $\frac{d\sigma^c}{d\Omega}.d\Omega$ may be defined as the flux of particles scattered into an element of solid angle $d\Omega$ divided by the flux of particles per unit area in the incident beam. The cartesian frame of reference defined in section (2.3a) is no longer suitable because different particles in the incident beam will have different impact-parameter vectors $\underline{b}$. Choose a new frame $O(\hat{\underline{x}}',\hat{\underline{y}}',\hat{\underline{z}}')$ so that $\hat{\underline{y}}' = \hat{\underline{y}}$ and with origin at the centre of force. Let the $\hat{\underline{x}}'$ and $\hat{\underline{z}}'$ axes be fixed in space. In this frame the incident velocity has coordinates $\underline{v} = (0, v, 0)$ as before, but the coordinates of the impact-parameter vector are $\underline{b} = (b\sin\phi_b, 0, b\cos\phi_b)$ where ϕ_b is the angle between $\underline{b}$ and

the $\hat{z}'$ axis. Classically, all particles in the element of area $b\,db\,d\phi_b$ in the incident beam are scattered into the solid-angle element $d\Omega = d(\cos\theta')d\phi'$ where θ' and ϕ' are the polar and azimuthal scattering angles. Hence,

$$\frac{d\sigma^c}{d\Omega} = \left|\frac{b\,db\,d\phi_b}{d(\cos\theta')\,d\phi'}\right| . \qquad (2.3.3)$$

For central forces $\frac{d\sigma^c}{d\Omega}$ is independent of ϕ' and $d\phi_b = d\phi'$ so that

$$\frac{d\sigma^c}{d(\cos\theta')} = 2\pi \frac{d\sigma^c}{d\Omega} = 2\pi b \left|\frac{db}{d(\cos\theta')}\right| . \qquad (2.3.4)$$

Now, θ' is uniquely determined by b, but there may be more than one value of b which leads to the same value of θ'. In this case

$$\frac{d\sigma^c}{d(\cos\theta')} = \sum_{\substack{\text{all branches} \\ \text{of } \theta'(b)}} 2\pi b \left|\frac{db}{d(\cos\theta')}\right| . \qquad (2.3.5)$$

For Rutherford scattering $\underline{F}''(r'') = \frac{\alpha}{r''^3}\underline{r}''$.

It is easy to prove that

$$b^2 = \frac{\alpha^2}{m^2 v^4}\cot^2\tfrac{1}{2}\theta' , \qquad (2.3.6)$$

(see, for example, Corben and Stehle 1966, p.102). Since $0 \leq \theta' \leq \pi$, b is uniquely determined by θ'. Hence

$$\frac{d\sigma^c}{d\Omega} = \frac{\alpha^2}{4m^2v^4}\frac{1}{\sin^4\frac{1}{2}\theta'} . \qquad (2.3.7)$$

This result is known as the Rutherford scattering law and is identical for both attractive and repulsive fields.

(d). The Quantal Angular Differential Cross Section $\frac{d\sigma^Q}{d\Omega}$

The quantal angular-differential cross section $\frac{d\sigma^Q}{d\Omega}$ is defined in exactly the same way as $\frac{d\sigma^C}{d\Omega}$. However it is not possible to equate the number of particles in the element of area $b\,db\,d\phi_b$ of the incident beam with the number of particles scattered into an element of solid angle $d\Omega$. Nevertheless it is possible to obtain an angular differential cross section which in general will be different to the corresponding classical result. One of the strange properties of the Coulomb potential is that the quantum-mechanical angular-differential cross section is identical to the classical Rutherford formula.

2.4 Angular-Differential Cross Sections in the Centre-of-Mass Frame C_I

(a) Classical Scattering

The scattering in the centre-of-mass frame may be directly related to the scattering in the reduced-mass system since the polar scattering angles are the same in both problems. Hence, for distinguishable particles the centre-of-mass angular-differential cross section $\frac{\partial \sigma_{C_I}^{c}}{\partial \Omega_{C_I}}$ is given by

$$\frac{\partial \sigma_{C_I}^{c}}{\partial \Omega_{C_I}} = \frac{\partial \sigma^{c}}{\partial \Omega} , \qquad (2.4.1)$$

where $d\Omega_{C_I} = d(\cos\theta_{C_I}') \, d\phi_{C_I}'$ and $\frac{\partial \sigma^{c}}{\partial \Omega}$ is the corresponding classical angular-differential cross section for the reduced-mass system. If, however, the particles are identical, the classical angular-differential cross section $\frac{\partial \sigma_{C_I}^{cs}}{\partial \Omega_{C_I}}$ must be symmetrised to allow for contributions from both the particles. The correction is trivial because the centre-of-mass polar scattering angles $\theta_{C_I 1}' = \theta_{C_I}'$ and $\theta_{C_I 2}'$ of the two particles are supplementary. So,

$$\frac{\partial \sigma_{C_I}^{cs}}{\partial \Omega_{C_I}}(\theta_{C_I}') = \frac{\partial \sigma^{c}}{\partial \Omega}(\theta') + \frac{\partial \sigma^{c}}{\partial \Omega}(\pi - \theta') , \qquad (2.4.2)$$

if the interaction is central. The first term on the right-hand side of equation (2.4.2) is known as the direct scattering term and may be written $\frac{\partial \sigma_{C_I}^{cD}}{\partial \Omega_{C_I}}$. The latter is known as the exchange scattering term and may be written $\frac{\partial \sigma_{C_I}^{cE}}{\partial \Omega_{C_I}}$. If in an individual encounter the orbits are specified by the positions and velocities of both particles then there is no uncertainty over which particle is scattered into a

solid angle $d\Omega_c$. However, the uncertainty cannot be avoided if the orbits are prescribed by the initial and final velocities.

(b) Quantal Scattering

Analogously, for distinguishable particles the quantal centre-of-mass angular-differential cross section $\frac{\partial\sigma_c^Q}{\partial\Omega_c}$ is given by

$$\frac{\partial\sigma_c^Q}{\partial\Omega_c} = \frac{\partial\sigma^Q}{\partial\Omega} \quad , \tag{2.4.3}$$

where $\frac{\partial\sigma^Q}{\partial\Omega}$ is the corresponding quantal angular-differential cross section for the reduced-mass problem. Again, equation (2.4.3) must be modified if the particles are identical and the symmetrised quantal angular-differential cross section $\frac{\partial\sigma_c^{QS}}{\partial\Omega_c}$ may be defined by

$$\frac{\partial\sigma_c^{QS}}{\partial\Omega_c} = \frac{\partial\sigma^Q}{\partial\Omega}(\theta') + \frac{\partial\sigma^Q}{\partial\Omega}(\pi-\theta') + 2\cos\{F(\theta')\}\left[\frac{\partial\sigma^Q}{\partial\Omega}(\theta')\frac{\partial\sigma^Q}{\partial\Omega}(\pi-\theta')\right]^{1/2}, \tag{2.4.4}$$

where, as in the classical case, the direct scattering term $\frac{\partial\sigma_c^{QD}}{\partial\Omega_c} = \frac{\partial\sigma^Q}{\partial\Omega}(\theta')$ and the exchange scattering term $\frac{\partial\sigma_c^{QE}}{\partial\Omega_c} = \frac{\partial\sigma^Q}{\partial\Omega}(\pi-\theta')$. The third term is called the interference term and is written $\frac{\partial\sigma_c^{QIF}}{\partial\Omega_c}$. It is present because it is not possible to say which particle is scattered into the solid angle $d\Omega_c$ and has no analogue in a purely-classical approach. The interference term contains a factor $2\left[\frac{\partial\sigma_c^{QD}}{\partial\Omega_c}\cdot\frac{\partial\sigma_c^{QE}}{\partial\Omega_c}\right]^{1/2}$ which may be written $\frac{\partial\sigma_c^{QIB}}{\partial\Omega_c}$ and which is often useful as a bound on the magnitude of the interference term. The function $F(\theta')$ is a phase factor which depends not only upon the relative phase of the direct and exchange scattering amplitudes but also upon the type

of particle involved. The interference term may be positive or negative but the inequality

$$\left[\left\{\frac{\partial\sigma^{Q}}{\partial\Omega}(\theta')\right\}^{1/2}-\left\{\frac{\partial\sigma^{Q}}{\partial\Omega}(\pi-\theta')\right\}^{1/2}\right]^{2}\leq\frac{\partial\sigma_{q}^{QS}}{\partial\Omega_{q}}\leq\left[\left\{\frac{\partial\sigma^{Q}}{\partial\Omega}(\theta')\right\}^{1/2}+\left\{\frac{\partial\sigma^{Q}}{\partial\Omega}(\pi-\theta')\right\}^{1/2}\right]^{2},$$

is always satisfied, so that $\frac{\partial\sigma_{q}^{QS}}{\partial\Omega_{q}}$ is never negative. In the classical limit $|F(\theta')|$ becomes very large. The interference term then oscillates very rapidly, so it can be approximated by its zero mean value.

(c) Rutherford Scattering

Suppose particle 1 has charge Z_1 and particle 2 has charge Z_2. Then for distinguishable particles

$$\frac{\partial\sigma_{q}^{C}}{\partial\Omega_{q}}=\frac{\partial\sigma_{q}^{Q}}{\partial\Omega_{q}}=\frac{Z_1^2Z_2^2}{4m_R^2v_R^4}\cdot\frac{1}{\sin^4\frac{1}{2}\theta_q'}\,. \qquad (2.4.5)$$

For identical particles,

$$\frac{\partial\sigma_{q}^{CS}}{\partial\Omega_{q}}=\frac{Z_1^4}{4m_R^2v_R^4}\cdot\left(\frac{1}{\sin^4\frac{1}{2}\theta_q'}+\frac{1}{\cos^4\frac{1}{2}\theta_q'}\right). \qquad (2.4.6)$$

For unpolarised beams of electrons or positrons ($m_1=m_2=m_e$ and $Z_1^2=e^2$) the symmetrised quantal angular-differential cross section is

$$\frac{\partial\sigma_{q}^{QS}}{\partial\Omega_{q}}=\frac{\partial\sigma_{q}^{CS}}{\partial\Omega_{q}}-\frac{\partial\sigma_{q}^{QIF}}{\partial\Omega_{q}}\,, \qquad (2.4.7)$$

where

$$\frac{\partial\sigma_{q}^{QIF}}{\partial\Omega_{q}}=\frac{\partial\sigma_{q}^{QIB}}{\partial\Omega_{q}}\cos\left\{\frac{v_0}{v_R}\log\left(\tan^2\tfrac{1}{2}\theta_q'\right)\right\}\,, \qquad (2.4.8)$$

and

$$\frac{\partial \sigma_q^{QIB}}{\partial \Omega_q} = \frac{4e^4}{m_e^2 v_R^4} \cdot \frac{1}{\sin^2 \frac{1}{2}\theta_q' \cos^2 \frac{1}{2}\theta_q'} \quad . \quad (2.4.9)$$

In equation (2.4.8) $v_o = e^2/\hbar$ is the atomic unit of velocity. Equation (2.4.7) has a different interference term to that in equation (2.4.4). The interference term in equation (2.4.7) and the bound in equation (2.4.9) are obtained by averaging over singlet and triplet orientations of the resultant spin of the two particles in the collision (see for example Vriens 1969).

There is an important difference between the interference term in equation (2.4.6) and the remaining terms, since the phase factor contains a unit of velocity. Hence, unlike the remaining terms, the interference term does not scale classically. However, in the limit $v_R \gg v_o$, which may be termed the extreme quantal limit, the interference term tends to the bound, which scales classically, even though it is not a classical term. The classical limit is obtained if $v_R \ll v_o$.

2.5 The Effective Differential Cross Section $\frac{\partial^2\sigma_L(\underline{v}_{L1},\underline{v}_{L2})}{\partial q\,\partial\Delta E_L}$ in the Frame L

The classical or quantal effective differential cross section $\frac{\partial^2\sigma_L(\underline{v}_{L1},\underline{v}_{L2})}{\partial q\,\partial\Delta E_L}$ per unit momentum transfer magnitude q and per unit energy transfer ΔE_L may be defined as the differential cross section for the scattering of the incident particle 1 by a fictitious stationary target which yields identical scattering results to that of the original moving target beam. Now the differential rate $\frac{\partial^2\alpha}{\partial q\,\partial\Delta E_L}$ of a reaction is a Galilean frame invariant so that the effective differential cross section $\frac{\partial^2\sigma_L}{\partial q\,\partial\Delta E_L}$ may be related to the centre-of-mass differential cross section $\frac{\partial^2\sigma_q}{\partial q\,\partial\Delta E_L}$ by

$$v_{L1}\,\frac{\partial^2\sigma_L(\underline{v}_{L1},\underline{v}_{L2})}{\partial q\,\partial\Delta E_L} = \frac{\partial^2\alpha}{\partial q\,\partial\Delta E_L} = v_R\,\frac{\partial^2\sigma_q}{\partial q\,\partial\Delta E_L}\,. \qquad (2.5.1)$$

This relation has been used by Ochkur and Petrunkin (1963), Stabler (1964), Gryzinski (1965a), Gerjuoy (1966), Vriens (1966b), Burgess and Percival (1968), Vriens (1969) and McDowell and Coleman (1970). An alternative formula, given by equation (2.5.1) without the velocity factors v_{L1} and v_R and without using the rate as an intermediate step, was used by Burgess (1963) and by Percival and Valentine (1966). It was pointed out by Vriens (1967) after discussion with Percival that, when the differential cross sections in the latter approach were averaged over random orientations of $\hat{\underline{v}}_{L2}$, the resulting expressions did not correspond to the scattering of a beam of incident particles by a thin monoenergetic target gas, as it should. Now if $v_{L1} \gg v_{L2}$, the

two methods converge. For $v_{L1} \sim v_{L2}$ Valentine (1968) compared the two binary-encounter approaches with exact-classical three-body calculations for ionization of atomic hydrogen by electron impact. He concluded that the "invariant rate" approach yielded simpler and more accurate results. This approach is adopted here.

The classical centre-of-mass differential cross section $\frac{\partial^2\sigma_q^c}{\partial q\,\partial\Delta E_L}$ is defined by

$$\frac{\partial^2\sigma_q^c}{\partial q\,\partial\Delta E_L} = \sum_{\text{all branches}} \frac{\partial^2\sigma_q^c}{\partial(\cos\theta_q')\,\partial\phi_q'} \cdot \left| \frac{\partial(\cos\theta_q')\,\partial\phi_q'}{\partial q\;\partial\Delta E_L} \right| . \qquad (2.5.2)$$

In section (2.1a) it was shown that θ_q' and hence $\cos\theta_q'$ was uniquely determined in the range $(0, \pi)$ by q but that there were two values of ϕ_q' (ϕ_{qA}' and $\phi_{qB}' = 2\pi - \phi_{qA}'$, say) in the range $(0, 2\pi)$ for each value of ΔE_L. Thus there are two branches of the transformation from $(q, \Delta E_L)$ to $(\cos\theta_q', \phi_q')$ and so

$$\frac{\partial^2\sigma_q^c}{\partial q\,\partial\Delta E_L} = \frac{\partial^2\sigma_q^c(\phi_{qA}')}{\partial(\cos\theta_q')\,\partial\phi_q'} \cdot \frac{1}{J(\phi_{qA}')} + \frac{\partial^2\sigma_q^c(\phi_{qB}')}{\partial(\cos\theta_q')\,\partial\phi_q'} \cdot \frac{1}{J(\phi_{qB}')} , \qquad (2.5.3)$$

where

$$J(\phi_q') = \left| \frac{\partial q\;\partial\Delta E_L(\phi_q')}{\partial(\cos\theta_q')\,\partial\phi_q'} \right| . \qquad (2.5.4)$$

Now ΔE_L is given by equation (2.1.26) and q is given by equation (2.1.24) and it is easy to show that

$$J(\phi_q') = \tfrac{1}{2} m_R v_R v_{L1} q \left| \frac{\cos\tfrac{1}{2}\theta_q' \sin\chi_{L1} \sin\phi_q'}{\sin\tfrac{1}{2}\theta_q'} \right| . \qquad (2.5.5)$$

Hence $J(\phi_{qA}') = J(\phi_{qB}')$ and thus for central interactions

$$\frac{\partial^2\sigma_q^c}{\partial q\,\partial\Delta E_L} = \frac{2}{J} \frac{\partial^2\sigma_q^c}{\partial(\cos\theta_q')\,\partial\phi_q'} . \qquad (2.5.6)$$

It follows immediately that for central interactions

$$\frac{\partial^2 \sigma_q^Q}{\partial q \, \partial \Delta E_L} = \frac{2}{J} \frac{\partial^2 \sigma_q^Q}{\partial(\cos\theta_q') \, \partial \phi_q'} \quad . \qquad (2.5.7)$$

However, if $\frac{\partial^2 \sigma_q^Q}{\partial(\cos\theta_q') \partial\phi_q'}$ depends upon ϕ_q', there will be additional interference contributions to $\frac{\partial^2 \sigma_q^Q}{\partial q \, \partial \Delta E_L}$. The Jacobian J can be expressed in a simpler form, if certain geometrical relations of the triangle OP_1P_2 defined by the initial velocities $\underline{v}_{L1}$, $\underline{v}_{L2}$ and $\underline{v}_R$ are used. Now $\cos\chi_{L1} = \hat{\underline{v}}_{L1} \cdot \hat{\underline{v}}_R$, $\cos\chi_{L2} = \hat{\underline{v}}_{L2} \cdot \hat{\underline{v}}_R$ and $\cos\theta_{L12} = \hat{\underline{v}}_{L1} \cdot \hat{\underline{v}}_{L2}$ and so

$$v_{L2} \sin\theta_{L12} = v_R \sin\chi_{L1} \quad , \qquad (2.5.8)$$

and hence

$$J = m_R^2 v_{L1} v_{L2} v_R \left| \cos\tfrac{1}{2}\theta_q' \sin\theta_{L12} \sin\phi_q' \right| .$$

But, it is easy to show that

$$\hat{\underline{v}}_{L1} \times \hat{\underline{v}}_{L2} \cdot \hat{\underline{q}} = \cos\tfrac{1}{2}\theta_q' \sin\theta_{L12} \sin\phi_q' \, ,$$

and so

$$J = m_R^2 v_{L1} v_{L2} v_R \left| \hat{\underline{v}}_{L1} \times \hat{\underline{v}}_{L2} \cdot \hat{\underline{q}} \right| . \qquad (2.5.9)$$

Hence

$$\frac{\partial^2 \sigma_L(v_{L1}, v_{L2})}{\partial q \, \partial \Delta E_L} = \frac{2}{m_R^2 v_{L1}^2 v_{L2}} \cdot \frac{\partial^2 \sigma_q}{\partial(\cos\theta_q') \partial\phi_q'} \cdot \frac{1}{\left| \hat{\underline{v}}_{L1} \times \hat{\underline{v}}_{L2} \cdot \hat{\underline{q}} \right|} \, , \qquad (2.5.10)$$

which is valid both classically and quantally for central interactions. In the special case of charged-particle collisions

$$\frac{\partial^2 \sigma_q}{\partial(\cos\theta_q') \partial\phi_q'} = \frac{Z_1^2 Z_2^2}{4 m_R^2 v_R^4 \sin^4\frac{1}{2}\theta_q'} = \frac{4 m_R^2 Z_1^2 Z_2^2}{q^4} \, , \qquad (2.5.11)$$

for distinguishable particles and so

$$\frac{\partial^2\underline{\sigma}_L(\underline{v}_{L1},\underline{v}_{L2})}{\partial q\,\partial\Delta E_L} = \frac{8Z_1^2Z_2^2}{v_{L1}^2 v_{L2} q^4 |\hat{\underline{v}}_{L1}\times\hat{\underline{v}}_{L2}\cdot\hat{\underline{q}}|} \quad . \qquad (2.5.12)$$

This result has not been given previously and shows that the effective differential cross section is inversely proportional to the volume of the parallelepiped bounded by the unit vectors $\hat{\underline{v}}_{L1}$, $\hat{\underline{v}}_{L2}$ and $\hat{\underline{q}}$. For electrons or positrons,

$$\frac{\partial^2\underline{\sigma}_L^{CD}(\underline{v}_{L1},\underline{v}_{L2})}{\partial q\,\partial\Delta E_L} = \frac{\partial^2\underline{\sigma}_L^{QD}(\underline{v}_{L1},\underline{v}_{L2})}{\partial q\,\partial\Delta E_L} = \frac{8e^4}{v_{L1}^2 v_{L2} q^4 |\hat{\underline{v}}_{L1}\times\hat{\underline{v}}_{L2}\cdot\hat{\underline{q}}|} \quad , \qquad (2.5.13)$$

$$\frac{\partial^2\underline{\sigma}_L^{CE}(\underline{v}_{L1},\underline{v}_{L2})}{\partial q\,\partial\Delta E_L} = \frac{\partial^2\underline{\sigma}_L^{QE}(\underline{v}_{L1},\underline{v}_{L2})}{\partial q\,\partial\Delta E_L} = \frac{8e^4}{v_{L1}^2 v_{L2}(m_e^2v_R^2-q^2)^2}\cdot\frac{1}{|\hat{\underline{v}}_{L1}\times\hat{\underline{v}}_{L2}\cdot\hat{\underline{q}}|} \quad , \qquad (2.5.14)$$

$$\frac{\partial^2\underline{\sigma}_L^{QIF}(\underline{v}_{L1},\underline{v}_{L2})}{\partial q\,\partial\Delta E_L} = \frac{\partial^2\underline{\sigma}_L^{QIB}(\underline{v}_{L1},\underline{v}_{L2})}{\partial q\,\partial\Delta E_L}\cdot\cos\left[\frac{v_0}{v_R}\log\{q^2/(m_e^2v_R^2-q^2)\}\right] \quad , \qquad (2.5.15)$$

and

$$\frac{\partial^2\underline{\sigma}_L^{QIB}(\underline{v}_{L1},\underline{v}_{L2})}{\partial q\,\partial\Delta E_L} = \frac{8e^4}{v_{L1}^2 v_{L2} q^2(m_e^2v_R^2-q^2)}\cdot\frac{1}{|\hat{\underline{v}}_{L1}\times\hat{\underline{v}}_{L2}\cdot\hat{\underline{q}}|} \quad . \qquad (2.5.16)$$

In equations (2.5.10) and (2.5.12) to (2.5.16) not all values of q and ΔE_L are simultaneously physical. The allowed ranges of q and ΔE_L are given by the inverse transformations defined in equations (2.1.29) and (2.1.31). Thus

$$0 \leq q \leq 2m_R v_R \quad ,$$

and $$\left|\Delta E_L + \frac{1}{2m_1}q^2 - v_{L1}q\sin\tfrac{1}{2}\theta_q'\cos\chi_{L1}\right| \leq v_{L1}q\cos\tfrac{1}{2}\theta_q'\sin\chi_{L1} \quad ,$$

are the required restrictions on q and ΔE_L .

2.6 The Effective Double-Differential Cross Section $\frac{\partial^2\sigma}{\partial q\,\partial\Delta E_L}(v_{L1}, v_{L2})$ averaged over different orientations of the target velocity

(a) Geometrical Restrictions on the Momentum-Transfer Vector $\underline{q}$

For fixed initial velocities $\underline{v}_{L1}$ and $\underline{v}_{L2}$ and for any conservative interaction it was shown in section (2.1a) that the physically-allowed values of $\underline{q}$ lie on the sphere

$$\underline{q}\cdot(2m_R\underline{v}_R - \underline{q}) = 0 \quad . \tag{2.6.1}$$

Since $\underline{v}_R = \underline{v}_{L1} - \underline{v}_{L2}$, this result may be written in the form

$$\hat{\underline{q}}\cdot\hat{\underline{v}}_{L2} = \frac{2m_R v_{L1}\,\hat{\underline{q}}\cdot\hat{\underline{v}}_{L1} - q}{2m_R v_{L2}} \quad , \tag{2.6.2}$$

provided $v_{L2}q \neq 0$. If all orientations of $\underline{v}_{L2}$ are allowed then $\underline{q}$ must lie inside the region bounded between the surfaces $\sum_{min}$ and $\sum_{max}$ whose equations are

$$\sum_{min} \equiv \left\{ \hat{\underline{q}}\cdot\hat{\underline{v}}_{L2} + 1 = 0 \right\} \equiv \left\{ q = 2m_R v_{L1}(\hat{\underline{q}}\cdot\hat{\underline{v}}_{L1}) - 2m_R v_{L2} \right\}, \tag{2.6.3}$$

and

$$\sum_{max} \equiv \left\{ \hat{\underline{q}}\cdot\hat{\underline{v}}_{L2} - 1 = 0 \right\} \equiv \left\{ q = 2m_R v_{L1}(\hat{\underline{q}}\cdot\hat{\underline{v}}_{L1}) + 2m_R v_{L2} \right\} \quad . \tag{2.6.4}$$

Let a rectangular cartesian coordinate system with origin $\underline{q} = \underline{0}$ have $\hat{\underline{z}}$ axis along $\underline{v}_{L1}$ and suppose $\underline{q}$ has spherical-polar coordinates $(q, \theta_{Lq1}, \phi_{Lq1})$ so that $\cos\theta_{Lq1} = \hat{\underline{q}}\cdot\hat{\underline{v}}_{L1}$. In this frame the surfaces $\sum_{min}$ and $\sum_{max}$ are independent of the azimuthal angle ϕ_{Lq1} and hence are symmetric about $\hat{\underline{v}}_{L1}$. Let Γ_{min} and Γ_{max} be plane curves from which the surfaces $\sum_{min}$ and $\sum_{max}$ are obtained by revolution about $\hat{\underline{v}}_{L1}$. The equations of Γ_{min} and Γ_{max} in plane-polar coordinates (q, θ_{Lq1}) are

$$\Gamma_{min} \equiv \left\{ q = a\cos\theta_{Lq1} - b \right\} \quad , \tag{2.6.5}$$

and

$$\Gamma_{max} \equiv \{ q = a \cos\theta_{Lq1} + b \} \quad , \tag{2.6.6}$$

where

$$a = 2 m_R v_{L1} \quad , \tag{2.6.7}$$

and

$$b = 2 m_R v_{L2} \quad . \tag{2.6.8}$$

Equations (2.6.5) and (2.6.6) are of limacon form, the properties of which depend upon the relative magnitudes of a and b. If $a<b$ (that is, if $v_{L1}<v_{L2}$) Γ_{min} has no real points and Γ_{max} is an oval curve enclosing the origin. Thus if $v_{L1}<v_{L2}$, $\underline{q}$ may take any value within the surface of revolution Σ_{max} which encloses the origin.

In the case $a=b$ (that is, $v_{L1}=v_{L2}$) Σ_{min} has $\underline{q}=\underline{0}$ as its only real point and Γ_{max} simplifies to a cardioid. The allowed region for $\underline{q}$ is a cardioid of revolution with cusp at the origin.

If $a>b$ (that is, $v_{L1}>v_{L2}$) Γ_{min} has real points for $\cos\theta_{Lq1} \geq b/a$ and Γ_{max} has real points for $\cos\theta_{Lq1} \geq -b/a$. The branches Γ_{min} and Γ_{max} are complementary in that the slopes of the tangents at the origin are equal in magnitude and opposite in sign. Thus, for $v_{L1}>v_{L2}$, $\underline{q}$ must lie inside the surface of revolution Σ_{max} but outside the interior surface of revolution Σ_{min}. This case is illustrated in figure (2.6.1), where the velocity transfer $\underline{w}_1 = -\underline{q}/m_1$ has been used instead of the momentum

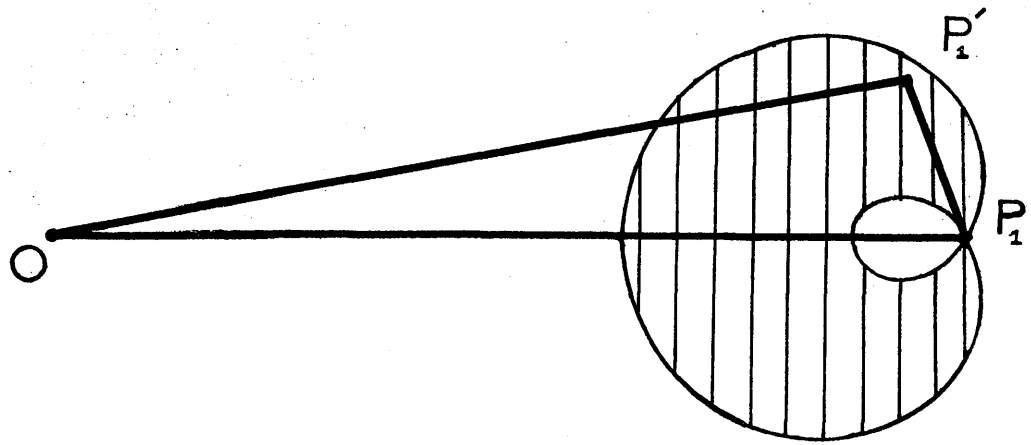

Figure 2.6.1 Velocity-space diagram for the final velocity $\underline{v}_{L1}' = \overrightarrow{OP_1'}$ of a particle of initial velocity $\underline{v}_{L1} = \overrightarrow{OP_1}$ incident upon a thin distribution of monoenergetic target particles moving initially with speed v_{L2}, all orientations of $\underline{v}_{L2}$ being allowed. The final incident velocity $\underline{v}_{L1}'$ must lie inside the volume obtained by rotating the shaded area around the $\overrightarrow{OP_1}$ axis. The plane boundary is a Limacon, whose coefficients depend upon m_1, m_2, v_{L1} and v_{L2} only. The case illustrated corresponds to $m_1 > m_2$, $v_{L1} > v_{L2}$ and $2m_1m_2(v_{L1} + v_{L2}) < m_1(m_1+m_2)v_{L1}$.

transfer itself. In the extreme limit $v_{L1} \gg v_{L2}$, small values of $\underline{q}$ are directed almost perpendicular to the incident velocity direction.

(b) The Geometrical Restrictions in $(q, \Delta E_L)$ Space.

Since $q = 2m_R v_R \sin\frac{1}{2}\theta'_q$, the accessible values of q satisfy

$$0 \leq q \leq 2m_R (v_{L1} + v_{L2}) .$$

Further, $\Delta E_L = \underline{v}_{L1} \cdot \underline{q} - q^2/2m_1 = \underline{v}_{L2} \cdot \underline{q} + q^2/2m_2$, so that it is obvious that

$$-v_{L1} q - \frac{1}{2m_1} q^2 \leq \Delta E_L \leq v_{L1} q - \frac{1}{2m_1} q^2 ,$$

and that

$$-v_{L2} q + \frac{1}{2m_2} q^2 \leq \Delta E_L \leq v_{L2} q + \frac{1}{2m_2} q^2 .$$

Let the parabolae Γ_{11}, Γ_{12}, Γ_{21} and Γ_{22} be defined by

$$\Gamma_{11} \equiv \left\{ \frac{1}{2m_1} q^2 + q v_{L1} + \Delta E_L = 0 \right\} , \qquad (2.6.9)$$

$$\Gamma_{12} \equiv \left\{ \frac{1}{2m_2} q^2 - q v_{L2} - \Delta E_L = 0 \right\} , \qquad (2.6.10)$$

$$\Gamma_{21} \equiv \left\{ \frac{1}{2m_1} q^2 - q v_{L1} + \Delta E_L = 0 \right\} , \qquad (2.6.11)$$

and

$$\Gamma_{22} \equiv \left\{ \frac{1}{2m_2} q^2 + q v_{L2} - \Delta E_L = 0 \right\} . \qquad (2.6.12)$$

Let A_{IJ} be the point of intersection $\Gamma_{I1} \cap \Gamma_{J2}$ with $q \neq 0$. Each of the four points A_{IJ} is uniquely determined for all positive values of m_1, m_2, v_{L1} and v_{L2}. It is easy to show that the coordinates $(q_{IJ}, \Delta E_{LIJ})$ of A_{IJ} are

$$-q_{11} = q_{22} = 2m_R (v_{L1} - v_{L2}) , \qquad (2.6.13)$$

$$-q_{12} = q_{21} = 2m_R (v_{L1} + v_{L2}) , \qquad (2.6.14)$$

$$\Delta E_{L11} = \Delta E_{L22} = \frac{2m_R}{(m_1 + m_2)} (v_{L1} - v_{L2})(m_1 v_{L1} + m_2 v_{L2}) , \qquad (2.6.15)$$

and

$$\Delta E_{L12} = \Delta E_{L21} = \frac{2m_R}{(m_1+m_2)}(v_{L1}+v_{L2})(m_1v_{L1}-m_2v_{L2}) \quad (2.6.16)$$

The physically-allowed region $(q, \Delta E_L)$ space is bounded by a "polygon" whose sides consist of segments of parabolae and whose vertices are the origin (which corresponds to a collision with negligible interaction) together with those points A_{IJ} for which q_{IJ} satisfies $0 \leq q_{IJ} \leq 2m_R(v_{LI}+v_{LJ})$. Since none of the q_{IJ} is larger than $2m_R(v_{L1}+v_{L2})$ only those A_{IJ} for which q_{IJ} is negative need be rejected. Now q_{12} is always negative and q_{11} or q_{22} is negative according as v_{L1} is less than or greater than v_{L2}. Let A_+ be the point $(|q_{22}|, \Delta E_{L22})$. The accessible region in $(q, \Delta E_L)$ space is therefore a "triangle" with vertices $(0,0)$, A_+ and A_{21}. The case in which $m_1 > m_2$ and $v_{L1} > v_{L2}$ is shown in figure (2.6.2) and corresponds to that in figure (2.6.1), approximately.

The following additional remarks on the relative positions of the three vertices are useful. Firstly, since $|q_{22}| \leq q_{21}$, the point A_{21} always has the largest value of q. Further, the ordinate ΔE_{L21} is positive, zero or negative according as v_{L1} is greater than, equal to or less than v_{L2}, and similarly the ordinate ΔE_{L22} is positive, zero or negative according as m_1v_{L1} is greater than, equal to or less than m_2v_{L2}. Finally, the energy-transfer difference

$$\Delta E_{L21} - \Delta E_{L22} = \frac{4m_R(m_1-m_2)v_{L1}v_{L2}}{(m_1+m_2)}, \quad (2.6.17)$$

is positive, zero or negative according as m_1 is greater than, equal

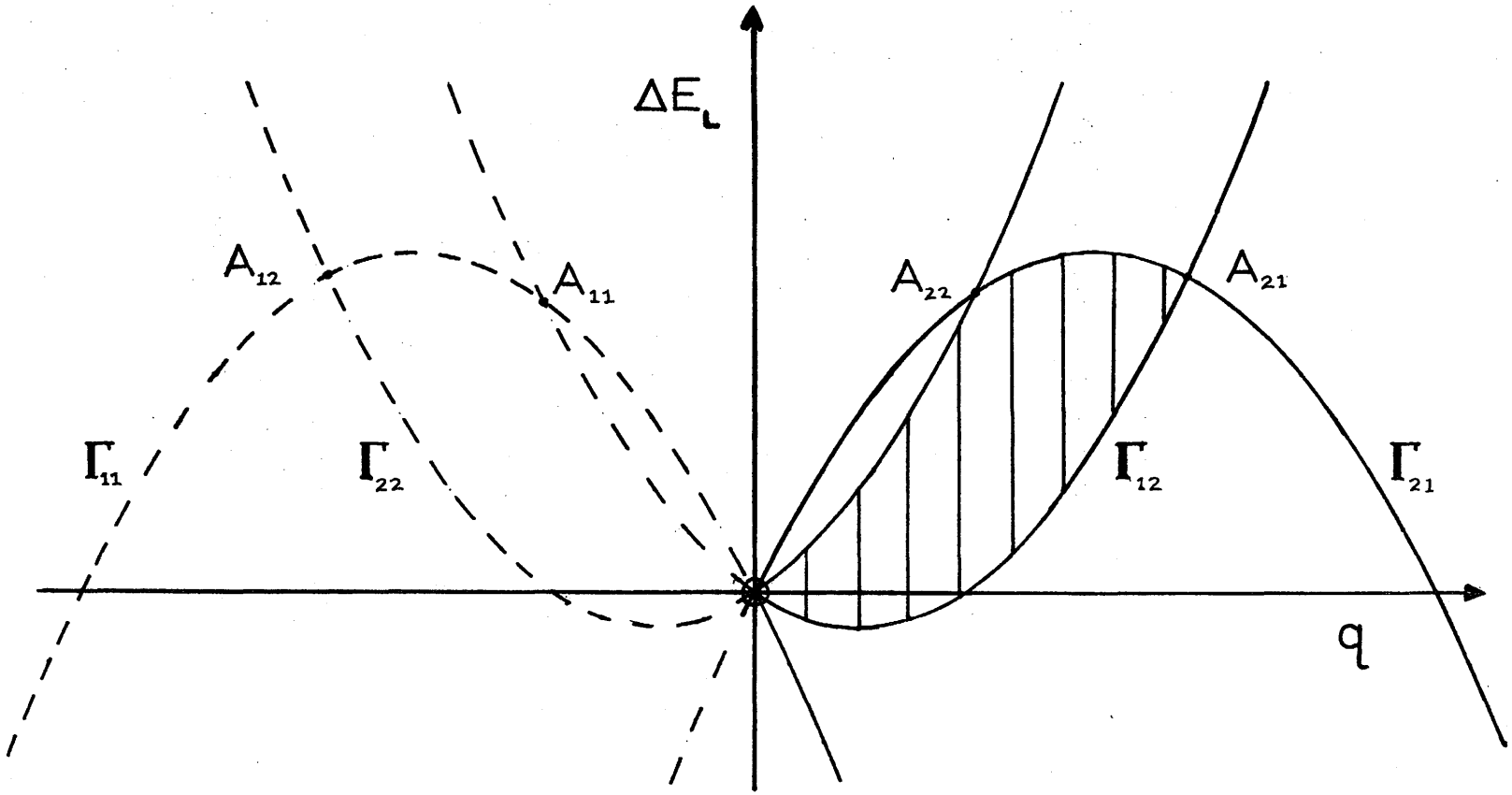

Figure 2.6.2 The allowed region in $(q\ ,\ \Delta E_L)$ space for a particle with initial velocity $\underline{v}_1$ incident upon a thin distribution of monoenergetic target particles moving initially with speed v_{L2}; all orientations of $\underline{v}_{L2}$ being possible. Values of $(q\ ,\ \Delta E_L)$ are restricted to the shaded region, bounded by the parabolae Γ_{11}, Γ_{12}, Γ_{21} and Γ_{22}. The case illustrated corresponds to $m_1 > m_2$, $v_{L1} > v_{L2}$ and

$$2 m_1 m_2 (v_{L1} - v_{L2}) < m_1 (m_1 + m_2) v_{L1} < 2 m_1 m_2 (v_{L1} + v_{L2}).$$

to or less than m_2 .

The condition that the incident particle may transfer all its initial kinetic energy to the target is that the point $(m_1 v_{L1}, \frac{1}{2} m_1 v_{L1}^2)$ on Γ_{21} is accessible, which is true only if

$$2 m_R (v_{L1} - v_{L2}) \leq m_1 v_{L1} \leq 2 m_R (v_{L1} + v_{L2}) .$$

Similarly, the condition that the target may transfer all its initial kinetic energy to the incident particle is that the point $(m_2 v_{L2}, -\frac{1}{2} m_2 v_{L2}^2)$ on Γ_{12} is accessible, which is true only if

$$2 m_R (v_{L2} - v_{L1}) \leq m_2 v_{L2} \leq 2 m_R (v_{L1} + v_{L2}) .$$

(c) $\frac{\partial^2 \sigma_L (v_{L1}, v_{L2})}{\partial q \, \partial \Delta E_L}$ With $\hat{z}$ Axis along the Incident-Velocity Direction

Let $\hat{v}_{L2}$ be described by the spherical-polar angles θ_{L21} and ϕ_{L21} in a rectangular cartesian coordinate system with $\hat{z}$ axis along $\hat{v}_{L1}$, and suppose that $f(\theta_{L21}, \phi_{L21})$ is the distribution function describing the orientations of $\hat{v}_{L2}$ with respect to $\hat{v}_{L1}$. The classical orientation-averaged effective double-differential cross section $\frac{\partial^2 \sigma_L^c (v_{L1}, v_{L2})}{\partial q \, \partial \Delta E_L}$ is given by

$$\frac{\partial^2 \sigma_L^c (v_{L1}, v_{L2})}{\partial q \, \partial \Delta E_L} = \int_0^{2\pi} d\phi_{L21} \int_{-1}^{1} d(\cos \theta_{L21}) \, f(\theta_{L21}, \phi_{L21}) \frac{\partial^2 \sigma_L^c (v_{L1}, v_{L2})}{\partial q \, \partial \Delta E_L} \quad (2.6.18)$$

In the quantal approach the orientation average should be performed on the scattering amplitude so that interference effects, arising from the uncertainty over which $\hat{v}_{L2}$ is involved in a particular collision, can be incorporated. The interference effect which arises here must be distinguished from the special interference properties arising from the scattering of identical particles, but is similar to that mentioned in

section (2.1b) and occurs for all particles and all conservative interactions.

If this interference is included, the integrals involved cannot usually be treated analytically. However, with the approximation that cross sections - not amplitudes - can be averaged over different initial conditions, an equation identical to (2.6.18) is obtained for $\frac{\partial^2 \sigma_L^Q}{\partial q \, \partial \Delta E_L}(v_{L1}, v_{L2})$. Henceforth it must be remembered that the results for quantal scattering by this method are only approximate whereas the results for classical scattering remain exact.

Let $\frac{\partial^2 \tilde{\sigma}_L^Q}{\partial q \, \partial \Delta E_L}(v_{L1}, v_{L2})$ be the approximate quantal result obtained using the approximation of averaging over cross sections. Equation (2.6.18) can be simplified since

$$|\hat{v}_{L1} \times \hat{v}_{L2} \cdot \hat{q}|^2 = X^2 \quad , \text{ say}$$
$$= 1 - \{ (\hat{v}_{L1} \times \hat{v}_{L2}) \times \hat{q} \}^2 \quad ,$$

$$= 1 + 2(\hat{v}_{L1} \cdot \hat{v}_{L2})(\hat{v}_{L1} \cdot \hat{q})(\hat{v}_{L2} \cdot \hat{q}) - (\hat{v}_{L1} \cdot \hat{v}_{L2})^2 - (\hat{v}_{L1} \cdot \hat{q})^2 - (\hat{v}_{L2} \cdot \hat{q})^2 . \quad (2.6.19)$$

However, from equations (2.1.3) and (2.1.4)

$$\hat{q} \cdot \hat{v}_{L1} = \cos \theta_{Lq1} \quad , \text{ say}$$
$$= (\Delta E_L + \frac{1}{2m_1} q^2) / q v_{L1} = \text{constant} , \quad (2.6.20)$$

and

$$\hat{q} \cdot \hat{v}_{L2} = \cos \theta_{Lq2} \quad , \text{ say}$$
$$= (\Delta E_L - \frac{1}{2m_2} q^2) / q v_{L2} = \text{constant} . \quad (2.6.21)$$

Thus the function X^2 may be written

$$X^2 = (\mu_{max} - \cos \theta_{L21})(\cos \theta_{L21} - \mu_{min}) , \quad (2.6.22)$$

where

$$\mu_{max} = \cos\left(\theta_{Lq1} - \theta_{Lq2}\right), \tag{2.6.23}$$

and

$$\mu_{min} = \cos\left(\theta_{Lq1} + \theta_{Lq2}\right). \tag{2.6.24}$$

Further, since $X^2 \geq 0$ then

$$-1 \leq \mu_{min} \leq \cos\theta_{L21} \leq \mu_{max} \leq 1,$$

otherwise q and ΔE_L are not physically accessible.

Let

$$\cos\theta_{L21} = \mu_{min}\cos^2\eta + \mu_{max}\sin^2\eta, \tag{2.6.25}$$

where

$$0 \leq \eta \leq \frac{\pi}{2}.$$

Thus

$$\frac{d(\cos\theta_{L21})}{X} = 2\,d\eta. \tag{2.6.26}$$

Hence, for distinguishable particles

$$\frac{\partial^2\sigma_L^C(v_{L1},v_{L2})}{\partial q\,\partial\Delta E_L} = \frac{\partial^2\tilde{\sigma}_L^Q(v_{L1},v_{L2})}{\partial q\,\partial\Delta E_L} = \frac{16Z_1^2Z_2^2}{v_{L1}^2v_{L2}q^4}\int_0^{2\pi}d\phi_{L21}\int_0^{\pi/2}d\eta\; f(\eta(\theta_{L21}),\phi_{L21}). \tag{2.6.27}$$

For an isotropic distribution of $\hat{v}_{L2}$, $f(\eta,\phi_{L21}) = 1/4\pi$,

and so

$$\frac{\partial^2\sigma_L^C(v_{L1},v_{L2})}{\partial q\,\partial\Delta E_L} = \frac{\partial^2\tilde{\sigma}_L^Q(v_{L1},v_{L2})}{\partial q\,\partial\Delta E_L} = \frac{4\pi Z_1^2Z_2^2}{v_{L1}^2v_{L2}q^4}. \tag{2.6.28}$$

This equation is an important intermediate result and was first obtained by Thomas (1927a), though his method was not explained in detail.

For unpolarised electrons or positrons

$$\frac{\partial^2\sigma_L^{CD}(v_{L1},v_{L2})}{\partial q\,\partial\Delta E_L} = \frac{\partial^2\tilde{\sigma}_L^{QD}}{\partial q\,\partial\Delta E_L} = \frac{4\pi e^4}{v_{L1}^2v_{L2}q^4}, \tag{2.6.29}$$

as before. Further,

$$\frac{\partial^2 \sigma_L^{CE}}{\partial q\, \partial \Delta E_L}(v_{L1}, v_{L2}) = \frac{\partial^2 \tilde{\sigma}_L^{QE}}{\partial q\, \partial \Delta E_L}(v_{L1}, v_{L2}) = \frac{4\pi e^4}{v_{L1}^2 v_{L2}} \left\{ \frac{m_e^2 (v_{L1}^2 + v_{L2}^2)}{q^6} - \frac{1}{2q^4} - 2m_e \Delta E_L / q^6 \right\}, \quad (2.6.30)$$

$$\frac{\partial^2 \tilde{\sigma}_L^{QIF}}{\partial q\, \partial \Delta E_L}(v_{L1}, v_{L2}) = \frac{2\pi e^4}{v_{L1}^2 v_{L2} q^2} \int_{-1}^{1} d\gamma\, g(v_{L1}, v_{L2}, v_0, q, \Delta E_L, \gamma), \quad (2.6.31)$$

where

$$g(v_{L1}, v_{L2}, v_0, q, \Delta E_L, \gamma) = \frac{1}{(m_e^2 v_R^2(\gamma) - q^2)} \cos\left\{ \frac{v_0}{v_R(\gamma)} \log \frac{q^2}{m_e^2 v_R^2(\gamma) - q^2} \right\}, \quad (2.6.32)$$

with

$$(\gamma + 1)\pi = 4\eta \quad , \quad (2.6.33)$$

and

$$v_R^2(\gamma) = v_{L1}^2 + v_{L2}^2 - 2v_{L1} v_{L2} (\mu_{min} \cos^2\eta + \mu_{max} \sin^2\eta) . \quad (2.6.34)$$

Let

$$\tilde{g} = \frac{1}{m_e^2 v_R^2 - q^2} \quad , \quad (2.6.35)$$

so that $\tilde{g} = g$ if the phase factor

$$\Psi = \frac{v_0}{v_R} \log \frac{q^2}{(m_e^2 v_R^2 - q^2)} \quad , \quad (2.6.36)$$

is zero. Then it can be shown that

$$\int_{-1}^{1} d\gamma\, \tilde{g} = \frac{2}{(m_e^2 v_{L1}^2 - m_e^2 v_{L2}^2 - 2m_e \Delta E_L)} \quad , \quad (2.6.37)$$

and so

$$\frac{\partial^2 \tilde{\sigma}_L^{QIB}}{\partial q\, \partial \Delta E_L}(v_{L1}, v_{L2}) = \frac{4\pi e^4}{v_{L1}^2 v_{L2} q^2} \cdot \frac{1}{(m_e^2 v_{L1}^2 - m_e^2 v_{L2}^2 - 2m_e \Delta E_L)} . \quad (2.6.38)$$

Equations (2.6.30) and (2.6.37) can be derived from the expressions

$(\mu_{max} + \mu_{min})$ and $(\mu_{max}\,\mu_{min})$ without having to solve equation (2.6.22) for $\chi^2 = 0$ to obtain both μ_{min} and μ_{max}. However, in equation (2.6.31) the integral cannot be handled analytically and so it is necessary to solve for μ_{min} and μ_{max} separately. Equations (2.6.30) and (2.6.38) agree with those of Vriens (1966b).

(d) $\dfrac{\partial^2\sigma_L}{\partial q\,\partial\Delta E_L}(v_{L1}, v_{L2})$ with $\hat{z}$ Axis along the Momentum-Transfer Direction $\hat{q}$

An alternative derivation is convenient for this case.

Let the centre-of-mass angular-differential cross section $\dfrac{\partial^2\sigma_q}{\partial(\cos\theta_q')\,\partial\phi_q'}$ for an arbitrary conservative particle - particle interaction be denoted $\sigma_q(\cos\theta_q', \phi_q')$. The magnitude of the momentum-transfer vector $|\underline{q}|$ is related to the polar scattering angle θ_q' by equation (2.1.29). Hence

$$\frac{\partial^2\sigma_q}{\partial q\,\partial\phi_q'} = \frac{q}{m_R^2 v_R^2}\,\sigma_q(\cos\theta_q', \phi_q')\,H\left(1 - \frac{q^2}{4m_R^2 v_R^2}\right), \qquad (2.6.39)$$

where $H(x) = 0$ for $x < 0$ and $H(x) = 1$ for $x \geq 0$. Suppose $\underline{q}$ has spherical-polar coordinates $(q, \theta_{Rq}, \phi_{Rq})$ in a rectangular cartesian frame of reference with $\hat{z}$ axis along $\underline{v}_R$. Then, without loss of generality, ϕ_{Rq} may be taken equal to ϕ_q' and so

$$\frac{\partial^2\sigma_q}{\partial q\,\partial\phi_{Rq}} = \frac{q}{m_R^2 v_R^2}\,\sigma_q(\cos\theta_q', \phi_q')\,H\left(1 - \frac{q^2}{4m_R^2 v_R^2}\right). \qquad (2.6.40)$$

Since, for a conservative interaction

$$q = 2m_R v_R \cos\theta_{Rq}\,, \qquad (2.6.41)$$

which follows from equation (2.1.18)

$$\frac{\partial^2\sigma_q}{\partial(\cos\theta_{Rq})\,\partial\phi_{Rq}} = 4\cos\theta_{Rq}\,.\,\sigma_q(\cos\theta_q', \phi_q')\,H(\cos\theta_{Rq}). \qquad (2.6.42)$$

Equations (2.6.40) and (2.6.42) can be conveniently combined by defining a generalised triple-differential cross section $\frac{d\sigma_q}{d\tau_q}$ per unit volume of momentum-transfer space by

$$\frac{d\sigma_q}{d\tau_q} = \frac{\partial^3\sigma_q}{q^2\partial q\,\partial(\cos\theta_{Rq})\,\partial\phi_{Rq}} = \frac{2}{m_R v_R}\,\sigma_q(\cos\theta_q', \phi_q').\,\delta(2m_R\underline{v}_R\cdot\underline{q} - q^2), \tag{2.6.43}$$

which reduces to equations (2.6.40) and (2.6.42) on integrating over the relevant variables. The generalised triple-differential cross section $\frac{d\sigma_q}{d\tau_q}$ is not defined uniquely off the conservation-of-energy shell $\delta(2m_R\underline{v}_R\cdot\underline{q} - q^2)$ but off-shell values will not be required in subsequent averaging and integrating operations. The differential cross section $\sigma_q(\cos\theta_q', \phi_q')$ may be written $\sigma_q(\underline{v}_R, \underline{q})$. Then

$$\frac{d\sigma_q}{d\tau_q} = \frac{2}{m_R v_R}\,\sigma_q(\underline{v}_R, \underline{q}).\,\delta(2m_R\underline{v}_R\cdot\underline{q} - q^2)\,. \tag{2.6.44}$$

As in the previous section the centre-of-mass differential cross section $\frac{d\sigma_q}{d\tau_q}$ may be related to the effective differential cross section $\frac{d\sigma_L(\underline{v}_{L1}, \underline{v}_{L2})}{d\tau_q}$ in a general laboratory frame of reference L by

$$\frac{d\sigma_L(\underline{v}_{L1}, \underline{v}_{L2})}{d\tau_q} = \frac{v_R}{v_{L1}}\frac{d\sigma_q}{d\tau_q} = \frac{2}{m_R v_{L1}}\,\sigma_q(\underline{v}_R, \underline{q}).\,\delta(2m_R\underline{v}_R\cdot\underline{q} - q^2), \tag{2.6.45}$$

since $d\tau_q$ is frame invariant.

In the case of charged-particle collisions

$$\sigma_q(\underline{v}_R, \underline{q}) = \frac{4z_1^2 z_2^2 m_R^2}{q^4}, \tag{2.6.46}$$

and so

$$\frac{d\sigma_L(\underline{v}_{L1}, \underline{v}_{L2})}{d\tau_q} = \frac{8 m_R z_1^2 z_2^2}{v_{L1}\,q^4}\,\delta(2m_R\underline{v}_R\cdot\underline{q} - q^2)\,. \tag{2.6.47}$$

By choosing a rectangular cartesian frame of reference with $\hat{\underline{z}}$ axis along $\underline{v}_{L1}$ it is possible to rederive equation (2.5.10) since in this case

$$d\tau_q = q^2 dq\, d(\hat{\underline{v}}_{L1}\cdot\hat{\underline{q}})\, d\phi_{Lq1} = \frac{q}{v_{L1}}\, dq\, d\Delta E_L\, d\phi_{Lq1}, \quad (2.6.48)$$

by equation (2.1.4), and

$$\frac{\partial^2\sigma_L}{\partial q\,\partial\Delta E_L} = \int_0^{2\pi} d\phi_{Lq1}\, \frac{\partial^3\sigma_L}{\partial q\,\partial\Delta E_L\,\partial\phi_{Lq1}} . \quad (2.6.49)$$

However, if the $\hat{\underline{z}}$ axis is chosen along $\underline{q}$, the differential cross section $\frac{d\sigma_L}{d\tau_q}(v_{L1}, v_{L2})$ averaged over all possible orientations of $\hat{\underline{v}}_{L2}$ with $\underline{v}_{L1}$ fixed is given by

$$\frac{d\sigma_L}{d\tau_q}(v_{L1}, v_{L2}) = \frac{8 m_R z_1^2 z_2^2}{v_{L1} q^4} \int_0^{2\pi} d\phi_{qL2} \int_{-1}^{1} d(\cos\theta_{qL2})\, f(\cos\theta_{qL2}, \phi_{qL2}) \times \delta(2m_R \underline{v}_R\cdot\underline{q} - q^2), \quad (2.6.50)$$

where $\cos\theta_{qL2} = \hat{\underline{v}}_{L2}\cdot\hat{\underline{q}}$, ϕ_{qL2} is the corresponding azimuthal angle, and $f(\cos\theta_{qL2}, \phi_{qL2})$ is the required distribution function of orientations of $\hat{\underline{v}}_{L2}$ with respect to $\hat{\underline{q}}$.

It was shown in section (2.1b) that for fixed values of $\underline{v}_{L1}$ and $\underline{q}$, $\underline{v}_{L2}$ was restricted to the plane $\Pi_{\underline{q}\,\underline{v}_{L1}}$ with equation

$$\underline{v}_{L2}\cdot\underline{q} = \Delta E_L - \frac{1}{2m_2} q^2 = \text{constant}. \quad (2.6.51)$$

The argument of the delta function in equation (2.6.50) may be written in the form

$$2m_R \underline{v}_{L1}\cdot\underline{q} - 2m_R \underline{v}_{L2}\cdot\underline{q} - q^2 = 2m_R\left(\Delta E_L - \frac{1}{2m_2} q^2\right) - v_{L2} q \cos\theta_{qL2}. \quad (2.6.52)$$

Hence

$$\frac{d\sigma_L}{d\tau_q}(v_{L1}, v_{L2}) = \frac{8 m_R z_1^2 z_2^2}{v_{L1} q^4} \int_0^{2\pi} d\phi_{qL2} \int_{-1}^{1} d(\cos\theta_{qL2})\; f(\cos\theta_{qL2}, \phi_{qL2}) \times \delta\left\{2m_R v_{L2} q\left(\mu_{q2} - \cos\theta_{qL2}\right)\right\}, \quad (2.6.53)$$

where

$$\mu_{q2} = \frac{\Delta E_L - \frac{1}{2m_2} q^2}{v_{L2}\, q} . \qquad (2.6.54)$$

Now $\delta(ax) = \delta(x)/|a|$ and so

$$\frac{d\sigma_L}{d\tau_q}(v_{L1}, v_{L2}) = \frac{4 z_1^2 z_2^2}{v_{L1} v_{L2} q^5} \int_0^{2\pi} d\phi_{qL2}\, f(\mu_{q2}, \phi_{qL2})\, H(1-\mu_{q2}^2) . \qquad (2.6.55)$$

For isotropic orientations of v_{L2}, $f(\mu_{q2}, \phi_{qL2}) = \frac{1}{4\pi}$ and so

$$\frac{d\sigma_L}{d\tau_q}(v_{L1}, v_{L2}) = \frac{2 z_1^2 z_2^2}{v_{L1} v_{L2} q^5} H(1-\mu_{q2}^2) . \qquad (2.6.56)$$

Now $d\tau_q = \frac{q}{v_{L1}} dq\, d\Delta E_L\, d\phi_{qL1}$ and thus

$$\frac{\partial^2 \sigma_L}{\partial q\, \partial \Delta E_L}(v_{L1}, v_{L2}) = \frac{4\pi z_1^2 z_2^2}{v_{L1}^2 v_{L2} q^4} H(1-\mu_{q1}^2)\, H(1-\mu_{q2}^2) , \qquad (2.6.57)$$

as before, where

$$\mu_{q1} = \frac{\Delta E_L + \frac{1}{2m_1} q^2}{v_{L1}\, q} . \qquad (2.6.58)$$

Now suppose that $f(\cos\theta_{qL2}, \phi_{qL2}) = \frac{3}{4\pi} \cos^2\theta_{qL2}$, which is the case for any $(2p, 0)$ angular state of an atom.

Then it is easy to show that

$$\frac{\partial^2 \sigma_L}{\partial q\, \partial \Delta E_L} = \frac{12\pi z_1^2 z_2^2}{v_{L1}^2 v_{L2} q^4} \left\{ \frac{\Delta E_L - \frac{1}{2m_2} q^2}{v_{L2}\, q} \right\}^2 H(1-\mu_{q1}^2)\, H(1-\mu_{q2}^2) , \qquad (2.6.59)$$

which is zero at $\Delta E_L = \frac{1}{2m_2} q^2$ and non-zero around this region.

This result has been used by Banks, Vriens and Bonsen (1969) for the special case of hydrogenic target atoms.

2.7 The Effective Differential Cross Section $\frac{d\sigma}{d\Delta E}(v_1, v_2)$ Averaged over Uniformly-Distributed Orientations of the Target Velocity for Charged-Particle Collisions.

(a) Distinguishable Particles

Henceforth, unless otherwise stated, the arbitrary frame of reference L will be chosen to be that for which the target velocity distribution is spherically distributed, corresponding in the case of charged-particle atom collisions to the frame in which the target nucleus (assumed to be of infinite mass) is at rest. The subscript L may therefore be omitted. It is also convenient to define $\frac{d\sigma}{d\Delta E} = \frac{d\sigma^c}{d\Delta E} = \frac{d\tilde{\sigma}^Q}{d\Delta E}$ for distinguishable charged particles.

The effective differential cross section $\frac{d\sigma}{d\Delta E}$ is obtained by integrating the Thomas formula (see equation (2.6.28) over the momentum-transfer magnitude q in the range $0 \leq q_{min} \leq q \leq q_{max}$ for a given value of ΔE in the range $-E_2 \leq \Delta E \leq E_1$ where $E_1 = \frac{1}{2} m_1 v_1^2$ and $E_2 = \frac{1}{2} m_2 v_2^2$ are the respective initial kinetic energies. Hence

$$\frac{d\sigma}{d\Delta E}(v_1, v_2) = \frac{4\pi z_1^2 z_2^2}{3 v_1^2 v_2} \left\{ \frac{1}{q_{min}^3} - \frac{1}{q_{max}^3} \right\} , \qquad (2.7.1)$$

where the integration limits lie on the boundary of the accessible region in $(q, \Delta E)$ space for fixed ΔE. In general $\frac{d\sigma}{d\Delta E}$ is a function of m_1, m_2, v_1, v_2 and ΔE.

For positive ΔE the relevant boundaries are

$$\Delta E = v_1 q - \frac{1}{2m_1} q^2 , \qquad (2.7.2)$$

$$\Delta E = v_2 q + \frac{1}{2m_2} q^2 , \qquad (2.7.3)$$

and

$$\Delta E = -v_2 q + \frac{1}{2m_2} q^2 . \qquad (2.7.4)$$

Since $q \geq 0$ the possible values of q_{min} and q_{max} are

$$q^{+}_{min\,1} = (2m_1E_1)^{1/2} - \{2m_1(E_1-\Delta E)\}^{1/2}, \tag{2.7.5}$$

$$q^{+}_{max\,1} = (2m_1E_1)^{1/2} + \{2m_1(E_1-\Delta E)\}^{1/2}, \tag{2.7.6}$$

$$q^{+}_{min\,2} = \{2m_2(E_2+\Delta E)\}^{1/2} - (2m_2E_2)^{1/2}, \tag{2.7.7}$$

and

$$q^{+}_{max\,2} = \{2m_2(E_2+\Delta E)\}^{1/2} + (2m_2E_2)^{1/2}. \tag{2.7.8}$$

Then

$$q_{min} = \max\,(q^{+}_{min\,1},\ q^{+}_{min\,2}), \tag{2.7.9}$$

and

$$q_{max} = \min\,(q^{+}_{max\,1},\ q^{+}_{max\,2}). \tag{2.7.10}$$

The appropriate values in any particular case are determined by the relative values of ΔE, ΔE_{21} and ΔE_{22}, the last two of which are defined by equations (2.6.15) and (2.6.16). Let

$$\frac{d\sigma_{IJ}}{d\Delta E} = \frac{4\pi z_1^2 z_2^2}{3v_1^2 v_2}\left\{\frac{1}{q^{+3}_{min\,I}} - \frac{1}{q^{+3}_{max\,J}}\right\}, \text{ for } I, J = 1, 2. \tag{2.7.11}$$

Then

$$\frac{d\sigma_{IJ}}{d\Delta E} = \pi\left(\frac{m_1}{m_2}\right)\frac{z_1^2 z_2^2}{E_1\,\Delta E^2}(F_{I1} + F_{J2}), \tag{2.7.12}$$

where

$$F_{11} = \left(\frac{m_2}{m_1}\right)^{3/2}\left(\frac{2}{3}\frac{E_1}{\Delta E} - \frac{1}{6}\right)\left\{\frac{E_1-\Delta E}{E_2}\right\}^{1/2} + \left(\frac{m_2}{m_1}\right)^{3/2}\left(\frac{2}{3}\frac{E_1}{\Delta E} - \frac{1}{2}\right)\left(\frac{E_1}{E_2}\right)^{1/2}, \tag{2.7.13}$$

$$F_{12} = \left(\frac{m_2}{m_1}\right)^{3/2}\left(\frac{2}{3}\frac{E_1}{\Delta E} - \frac{1}{6}\right)\left\{\frac{E_1-\Delta E}{E_2}\right\}^{1/2} - \left(\frac{m_2}{m_1}\right)^{3/2}\left(\frac{2}{3}\frac{E_1}{\Delta E} - \frac{1}{2}\right)\left(\frac{E_1}{E_2}\right)^{1/2}, \tag{2.7.14}$$

$$F_{21} = \left(\frac{2}{3}\frac{E_2}{\Delta E} + \frac{1}{2}\right) + \left(\frac{2}{3}\frac{E_2}{\Delta E} + \frac{1}{6}\right)\left(\frac{E_2+\Delta E}{E_2}\right)^{1/2}, \tag{2.7.15}$$

and

$$F_{22} = \left(\frac{2}{3}\frac{E_2}{\Delta E} + \frac{1}{2}\right) - \left(\frac{2}{3}\frac{E_2}{\Delta E} + \frac{1}{6}\right)\left(\frac{E_2+\Delta E}{E_2}\right)^{1/2}. \tag{2.7.16}$$

The regions of validity of the different formulae are shown shaded in figure (2.7.1a) for $m_1 > m_2$ and in figure (2.7.1b) for $m_1 < m_2$. In both diagrams the dimensionless variable $\Delta E/E_1$, which is the fraction of the initial incident kinetic energy transferred to the target, is plotted against the dimensionless ratio v_2/v_1. Since ΔE is assumed positive and is always less than or equal to E_1 the permitted values of $\Delta E/E_1$ lie only in the range $[0,1]$. In contrast there is no upper bound on the ratio v_2/v_1. The region of validity of $\frac{d\sigma_{IJ}}{d\Delta E}$ is denoted by the symbol " IJ ". The boundary separating the regions of validity of $\frac{d\sigma_{22}}{d\Delta E}$ and $\frac{d\sigma_{12}}{d\Delta E}$ in case (a) and that separating $\frac{d\sigma_{11}}{d\Delta E}$ and $\frac{d\sigma_{21}}{d\Delta E}$ in case (b) is that segment of the parabola $\Delta E = \Delta E_{11}$ (see equation (2.6.15)) lying in the positive quadrant in $\left(\frac{v_2}{v_1}, \frac{\Delta E}{E_1}\right)$ space and passing through the points $\{0, 4m_1m_2/(m_1+m_2)^2\}$ and $(1,0)$. Similarly the boundary separating the regions of validity of $\frac{d\sigma_{12}}{d\Delta E}$ and $\frac{d\sigma_{11}}{d\Delta E}$ in case (a) and that separating $\frac{d\sigma_{21}}{d\Delta E}$ and $\frac{d\sigma_{22}}{d\Delta E}$ in case (b) is that segment of the parabola $\Delta E = \Delta E_{21}$ (see equation (2.6.16)) which lies in the positive quadrant and passes through the points $\{0, 4m_1m_2/(m_1+m)^2\}$ and $(m_1/m_2, 0)$. The two parabolae are complementary in the sense that each is the reflection of the other in the $\Delta E/E_1$ axis. The greater of the two parabolae has its maximum at the point $(|m_1-m_2|/2m_2, 1)$ and the region between this point and the $\Delta E/E_1$ axis lying above the larger of the two parabolae and below the line $\Delta E = E_1$ is excluded by the conditions

$$2m_R(v_1-v_2) \leq m_1v_1 \leq 2m_R(v_1+v_2)$$

which were derived in section (2.6b) after equation (2.6.17).

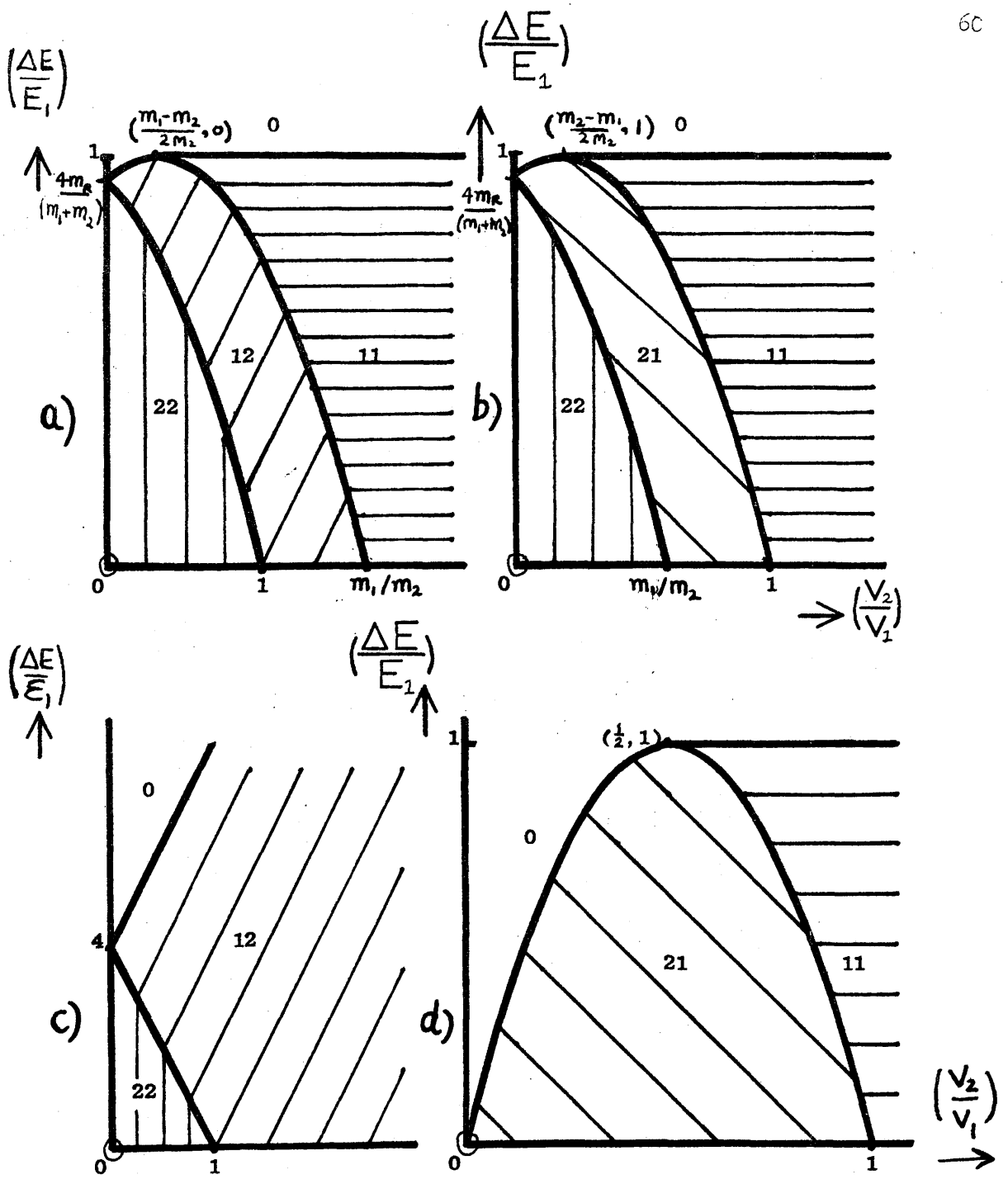

Figure 2.7.1 Regions of validity of $\frac{d\sigma}{d\Delta\varepsilon}^{IJ}$ for I,J=1,2 in the space defined by the dimensionless parameters $\Delta E/E_1$ and v_2/v_1 for positive ΔE. The regions for each value of I and J are shaded differently and are denoted by 11, 12, 21 and 22 respectively. Case a) $m_1 > m_2$; b) $m_1 < m_2$; c) m_1 infinite (E_1 has been replaced by $\varepsilon_1 = \frac{1}{2} m_2 v_1^2$); d) m_2 infinite.

In the limit as v_2/v_1 tends to zero $\frac{d\sigma_{22}}{d\Delta E}$ tends to the expression

$$\frac{d\sigma_{22}}{d\Delta E}(v_1, v_2=0) = \pi\left(\frac{m_1}{m_2}\right)\frac{z_1^2 z_2^2}{E_1 \Delta E^2}, \quad \text{for } 0 \leq \Delta E \leq 4m_1 m_2 E_1/(m_1+m_2)$$
$$= 0, \quad \text{otherwise}, \tag{2.7.17}$$

which is the result first obtained by Thomson (1912) for a target particle initially at rest.

The differential cross sections and regions of validity for $\Delta E < 0$ may be obtained from the stated results for $\Delta E > 0$ using the detailed-balance relation

$$v_1 \frac{d\sigma_{IJ}}{d|\Delta E|}(m_1, m_2, v_1, v_2, -|\Delta E|) = v_2 \frac{d\sigma_{3-I,3-J}}{d|\Delta E|}(m_2, m_1, v_2, v_1, |\Delta E|), \quad \text{for } I, J = 1, 2, \tag{2.7.18}$$

since, for $\Delta E < 0$ the relevant boundaries in $(q, \Delta E)$ space are

$$\Delta E = v_1 q - \frac{1}{2m_1} q^2, \tag{2.7.19}$$

$$\Delta E = -v_1 q - \frac{1}{2m_1} q^2, \tag{2.7.20}$$

and

$$\Delta E = -v_2 q + \frac{1}{2m_2} q^2, \tag{2.7.21}$$

and so the possible limits of integration over q are

$$q^-_{min\,1} = \{2m_1(E_1 + |\Delta E|)\}^{1/2} - (2m_1 E_1)^{1/2} = q^+_{min\,2}(m_1, v_1, |\Delta E|), \tag{2.7.22}$$

$$q^-_{max\,1} = \{2m_1(E_1 + |\Delta E|)\}^{1/2} + (2m_1 E_1)^{1/2} = q^+_{max\,2}(m_1, v_1, |\Delta E|), \tag{2.7.23}$$

$$q^-_{min\,2} = (2m_2 E_2)^{1/2} - \{2m_2(E_2 - |\Delta E|)\}^{1/2} = q^+_{min\,1}(m_2, v_2, |\Delta E|), \tag{2.7.24}$$

and

$$q^-_{max\,2} = (2m_2 E_2)^{1/2} + \{2m_2(E_2 - |\Delta E|)\}^{1/2} = q^+_{max\,1}(m_2, v_2, |\Delta E|). \tag{2.7.25}$$

Note that on the right-hand side of equation (2.7.18) the particles have been interchanged.

The general formulae for $\frac{d\sigma}{d\Delta E}$ and their regions of validity presented in this section are more explicit versions of the results obtained by Gerjuoy (1966) using a different method. In some special cases the results have been used to obtain simple approximate analytical formulae for the excitation and ionization of atoms and ions by incident electrons, positrons and ions. These results are presented below for completeness and convenience.

(i) Distinguishable Particles of Equal Mass

For equal masses the two parabolae separating the different regions of validity of $\frac{d\sigma}{d\Delta E}$ coincide and so the expressions $\frac{d\sigma_{21}}{d\Delta E}$ and $\frac{d\sigma_{12}}{d\Delta E}$ defined between them are irrelevant. The results for $\Delta E > 0$ are

$$\frac{d\sigma_{22}}{d\Delta E} = \frac{\pi z_1^2 z_2^2}{E_1 \Delta E^2}\left(1 + \frac{4E_2}{3\Delta E}\right), \quad \text{for} \quad 0 \le \Delta E \le \max\{(E_1 - E_2), 0\}, \tag{2.7.26}$$

which was first given by Thomas (1927a) and

$$\frac{d\sigma_{11}}{d\Delta E} = \frac{\pi z_1^2 z_2^2}{E_1 \Delta E^2}\left(\frac{4E_1}{3\Delta E} - \frac{1}{3}\right)\left(\frac{E_1 - \Delta E}{E_2}\right)^{1/2}, \quad \text{for} \quad \max\{(E_1 - E_2), 0\} \le \Delta E \le E_1, \tag{2.7.27}$$

which was first given by Stabler (1964) (it should be emphasised that many authors including Stabler label the target particle by 1 and the incident particle by 2).

Equation (2.7.27) has no analogue for a stationary target. Equation (2.7.26) reduces to equation (2.7.17) when $E_2 = 0$.

(ii) Infinite-Mass Projectile

Since the initial incident kinetic energy E_1 is infinite it is convenient to define the equivalent incident energy by $\mathcal{E}_1 = \frac{1}{2} m_2 v_1^2$.

In $(q, \Delta E)$ space the boundaries derived from the mass and velocity of the incident particle become

$$\Delta E = v_1 q \ , \tag{2.7.28}$$

and

$$\Delta E = -v_1 q \ . \tag{2.7.29}$$

The physically-accessible region in $(v_2/v_1, \Delta E/\mathcal{E}_1)$ space for $\Delta E > 0$ is shown in figure (2.7.1c). The differential cross sections are

$$\frac{d\sigma_{22}}{d\Delta E} = \frac{\pi z_1^2 z_2^2}{\mathcal{E}_1 \Delta E^2}\left(1 + \frac{4E_2}{3\Delta E}\right) , \quad \text{for} \quad 0 \le \Delta E \le \max\{0, 2m_2 v_1(v_1 - v_2)\} , \tag{2.7.30}$$

which was also first derived by Thomas (1927a) and

$$\frac{d\sigma_{12}}{d\Delta E} = \frac{\pi z_1^2 z_2^2}{2\mathcal{E}_1 \Delta E^2}\left[1 + \frac{8}{3}\left(\frac{v_1}{v_2}\right)\left(\frac{\mathcal{E}_1}{\Delta E}\right) + \frac{4}{3}\left(\frac{E_2}{\Delta E}\right) - \frac{4}{3}\left(\frac{E_2}{\Delta E} + \frac{1}{4}\right)\left(1 + \frac{\Delta E}{E_2}\right)^{1/2}\right] , \tag{2.7.31}$$

$$\text{for} \quad \max\{0, 2m_2 v_1(v_1 - v_2)\} \le \Delta E \le 2m_2 v_1 (v_1 + v_2) ,$$

which was first given by Vriens (1967).

Note that equation (2.7.30) is identical to equation (2.7.26) if $\mathcal{E}_1$ is replaced by E_1 , though the regions of validity are different. Equation (2.7.31) demonstrates that the general results for $\frac{d\sigma}{d\Delta E}$ can become extremely tedious and illustrates the danger that direct evaluation can lead to large numerical errors for $\Delta E \ll E_2$.

(iii) Infinite-Mass Target

As in case (ii) it is convenient to introduce the equivalent initial kinetic energy $\mathcal{E}_2 = \frac{1}{2} m_1 v_2^2$. The boundaries derived from the target particle become

$$\Delta E = v_2 q \ , \tag{2.7.32}$$

and

$$\Delta E = -v_2 q \ . \tag{2.7.33}$$

The physically-allowed region in $\left(\frac{v_2}{v_1}, \frac{\Delta E}{E_1}\right)$ space is shown in figure (2.7.1d). The relevant differential cross sections are

$$\frac{d\sigma_{11}}{d\Delta E} = \frac{\pi z_1^2 z_2^2}{E_1 \Delta E^2}\left(\frac{4E_1}{3\Delta E} - \frac{1}{3}\right)\left(\frac{E_1-\Delta E}{E_2}\right)^{1/2},$$

$$\text{for} \quad 0 \leq \Delta E \leq \max\{0, 2m_1 v_2 (v_1 - v_2)\}, \tag{2.7.34}$$

and

$$\frac{d\sigma_{21}}{d\Delta E} = \frac{\pi z_1^2 z_2^2}{E_1 \Delta E^2}\left[\frac{4\mathcal{E}_2}{3\Delta E} + \left(\frac{2E_1}{3\Delta E} - \frac{1}{6}\right)\left\{\left(\frac{E_1-\Delta E}{\mathcal{E}_2}\right)^{1/2} - \left(\frac{E_1}{\mathcal{E}_2}\right)^{1/2}\right\}\right],$$

$$\text{for} \quad \max\{0, 2m_1 v_2 (v_1 - v_2)\} \leq \Delta E \leq E_1 . \tag{2.7.35}$$

Equations (2.7.34) and (2.7.35) have not been given previously.

(b) Identical Electrons or Positrons

It was shown in sections (2.7 a(i)) that for equal masses $\Delta E_{11} = \Delta E_{21} = E_1 - E_2$. For later applications it is necessary to choose $E_1 > E_2$ so that the relative velocity is never zero. The full range of ΔE can be divided into four intervals, only two of which are physically distinct because the energy transfers $\Delta E = E_2' - E_2$ say, and $\Delta E = E_1' - E_2$ cannot be distinguished. Since $E_1' = E_1 - \Delta E$ the energy transfers ΔE and $E_1 - E_2 - \Delta E$ lead to identical final conditions. The two distinct energy-transfer ranges may be chosen to be

$$0 \leq \Delta E \leq \Delta E_0 = \tfrac{1}{2}(E_1 - E_2),$$

which is equivalent to

$$\Delta E_0 \leq \Delta E \leq 2\Delta E_0 = E_1 - E_2,$$

and secondly

$$2\Delta E_0 \leq \Delta E \leq E_1,$$

which is equivalent to

$$-E_2 \leq \Delta E \leq 0 .$$

A collision in which $0 \leq \Delta E \leq \Delta E_0$ may be described as an "excitation" because the final kinetic energies of both particles are greater than the initial kinetic energy of the target particle. A collision for which $\Delta E = \Delta E_0$ is such that the final kinetic energies are equal. A collision in which $-E_2 \leq \Delta E \leq 0$ may be termed a "de-excitation" since the final kinetic energy of one particle is greater than the initial incident energy E_1. The excitation region will now be considered in detail.

Let $$\frac{d\sigma_L^{CD}}{d\Delta E_L} = \frac{d\tilde{\sigma}_L^{QD}}{d\Delta E_L} = \frac{d\sigma^D}{d\Delta E}, \quad \frac{d\sigma_L^{CE}}{d\Delta E_L} = \frac{d\tilde{\sigma}_L^{QE}}{d\Delta E_L} = \frac{d\sigma^E}{d\Delta E},$$

$$\frac{d\sigma_L^{CS}}{d\Delta E_L} = \frac{d\sigma^{CS}}{d\Delta E}, \quad \frac{d\tilde{\sigma}_L^{QIB}}{d\Delta E_L} = \frac{d\sigma^{QIB}}{d\Delta E}, \quad \frac{d\tilde{\sigma}_L^{QIF}}{d\Delta E_L} = \frac{d\sigma^{QIF}}{d\Delta E},$$

and $$\frac{d\tilde{\sigma}_L^{QS}}{d\Delta E_L} = \frac{d\sigma^{QS}}{d\Delta E} = \frac{d\sigma^{CS}}{d\Delta E} - \frac{\partial\sigma^{QIF}}{\partial\Delta E}.$$ Then it is easy to show that for $0 \leq \Delta E \leq \Delta E_0$

$$\frac{d\sigma^D}{d\Delta E} = \frac{\pi e^4}{E_1 \Delta E^2}\left(1 + \frac{4E_2}{3\Delta E}\right), \tag{2.7.36}$$

$$\frac{d\sigma^E}{d\Delta E} = \frac{\pi e^4}{E_1 (E_1 - E_2 - \Delta E)^2}\left\{1 + \frac{4E_2}{3(E_1 - E_2 - \Delta E)}\right\}, \tag{2.7.37}$$

and

$$\frac{d\sigma^{QIF}}{d\Delta E} = \frac{\pi e^4}{E_1 v_2}\int_{q^+_{min\,2}}^{q^+_{max\,2}} \frac{dq}{q^2}\int_{-1}^{1} d\gamma\, g(v_1, v_2, v_0, q, \Delta E, \gamma), \tag{2.7.38}$$

where $g(v_1, v_2, v_0, q, \Delta E, \gamma)$ is defined by equation (2.6.32). The expression for $\frac{d\sigma^{QIF}}{d\Delta E}$ can only be evaluated numerically, however,

it can be transformed so that its convergence properties are improved, by replacing the variable q by the dimensionless parameter x where

$$\frac{1}{q} = \frac{1}{q^+_{min\,2}} - \frac{(1+x)v_2}{2\Delta E} \quad . \tag{2.7.39}$$

Then

$$\frac{dq}{q^2} = \frac{v_2}{2\Delta E}\,dx \quad , \tag{2.7.40}$$

and the range $q^+_{min2} \leq q \leq q^+_{max\,2}$ is transformed into the range $-1 \leq x \leq 1$. Hence for $0 \leq \Delta E \leq \Delta E_0$

$$\frac{d\sigma^{QIF}}{d\Delta E} = \frac{\pi e^4}{2E_1\Delta E}\int_{-1}^{1}dx\int_{-1}^{1}d\gamma\, g(v_1,v_2,v_0,x,\Delta E,\gamma) \quad . \tag{2.7.41}$$

The bound $\frac{d\sigma^{QIB}}{d\Delta E}$ is obtained by replacing $g(v_1,v_2,v_0,x,\Delta E,\gamma)$ by its approximate value $\tilde{g} = 1/\{m_e^2 v_R^2(\gamma) - q^2(x)\}$ in equation (2.7.41). The integrals can now be evaluated analytically giving, for $0 \leq \Delta E \leq \Delta E_0$

$$\frac{d\sigma^{QIB}}{d\Delta E} = \frac{\pi e^4}{E_1\Delta E\,(E_1 - E_2 - \Delta E)} \quad . \tag{2.7.42}$$

Equations (2.7.37) and (2.7.42) were first obtained by Vriens (1966b) after pioneering work by Burgess (1963). If, in equations (2.7.36), (2.7.37) and (2.7.42) E_2 is replaced by zero the corresponding "Thomson" symmetrised formulae are obtained, namely

$$\frac{d\sigma^{D}}{d\Delta E} = \frac{\pi e^4}{E_1\,\Delta E^2} \quad , \tag{2.7.43}$$

$$\frac{d\sigma^{E}}{d\Delta E} = \frac{\pi e^4}{E_1\,(E_1-\Delta E)^2} \quad , \tag{2.7.44}$$

and

$$\frac{d\sigma^{QIB}}{d\Delta E} = \frac{\pi e^4}{E_1\,\Delta E\,(E_1-\Delta E)} \quad . \tag{2.7.45}$$

These results are valid for $0 \leq \Delta E \leq \frac{1}{2}E_1$ and can be obtained directly from the centre-of-mass angular-differential cross sections (see equations (2.4.6) to (2.4.9)). Further, in this case the result for the interference term can also be obtained, for

$$\frac{d\sigma^{QIF}}{d\Delta E} = \frac{\pi e^4}{E_1 \Delta E (E_1 - \Delta E)} \cos\left\{\frac{v_0}{v_1} \log\left(\frac{\Delta E}{E_1 - \Delta E}\right)\right\}, \qquad (2.7.46)$$

provided $0 \leq \Delta E \leq \frac{1}{2}E_1$. It is interesting to note that equation (2.7.46) simplifies to equation (2.7.45) when $\Delta E = \Delta E_0 = \frac{1}{2}E_1$.

In the case in which E_2 is not zero Vriens (1966b) approximated $\frac{d\sigma^{QIF}}{d\Delta E}$ by

$$\frac{d\sigma_A^{QIF}}{d\Delta E} = \frac{d\sigma^{QIB}}{d\Delta E} \cos\left[\left(\frac{U_0}{E_1 - E_2}\right)^{1/2} \log\left(\frac{\Delta E}{E_1 - E_2 - \Delta E}\right)\right], \qquad (2.7.47)$$

where $U_0 = \frac{1}{2}m_e v_0^2$. Equation (2.7.47) reduces to equation (2.7.42) for $\Delta E = \Delta E_0$. An alternative approximation for ΔE close to ΔE_0 is

$$\frac{d\sigma_B^{QIF}}{d\Delta E} = \frac{d\sigma^{QIB}}{d\Delta E}\left\{A_0 + B_0\left(\frac{E_1 - E_2 - 2\Delta E}{E_1 - E_2}\right)^2\right\}, \qquad (2.7.48)$$

where A_0 and B_0 are dimensionless parameters which can be determined only by fitting to the numerical values. In particular A_0 is determined by $\frac{d\sigma^{QIF}}{d\Delta E}$ at $\Delta E = \Delta E_0$. If A_0 is not close to unity then the approximation $\frac{d\sigma_A^{QIF}}{d\Delta E}$ has little value. The parameter A_0 measures the extent to which the interference is coherent.

In the accelerated symmetric model (see Thomas 1927a, Vriens 1966b) the incident electron is assumed to gain energy before it collides with a target electron in an atom or ion. In the case of a hydrogenic target, E_1 is set equal to $E_{1\infty} + U + E_2$, where $E_{1\infty}$ is the true incident energy

and U is the ionization potential of the target atom. However no correction is included for the kinetic energy of the target electron and focus-ing effects are ignored. Nevertheless, the improvement in the agreement with more accurate results is significant. The relevant differential cross sections are

$$\frac{d\sigma^{D}}{d\Delta E} = \frac{\pi e^4}{(E_{1\infty}+U+E_2)\Delta E^2}\left(1+\frac{4E_2}{3\Delta E}\right), \qquad (2.7.49)$$

$$\frac{d\sigma^{E}}{d\Delta E} = \frac{\pi e^4}{(E_{1\infty}+U+E_2)(E_{1\infty}+U-\Delta E)^2}\left\{1+\frac{4E_2}{3(E_{1\infty}+U-\Delta E)}\right\}, \qquad (2.7.50)$$

$$\frac{d\sigma^{QIF}}{d\Delta E} = \frac{\pi e^4}{(E_{1\infty}+U+E_2)\Delta E}\int_{-1}^{1}dx\int_{-1}^{1}d\gamma\, g(v_{1\infty},v_2,v_0,x,\Delta E,\gamma), \qquad (2.7.51)$$

and

$$\frac{d\sigma^{QIB}}{d\Delta E} = \frac{\pi e^4}{(E_{1\infty}+U+E_2)\Delta E\,(E_{1\infty}+U-\Delta E)}, \qquad (2.7.52)$$

all of which are valid for $0\le\Delta E\le\frac{1}{2}(E_{1\infty}+U)$, provided $E_{1\infty}$ is greater than U, the ionization potential. A complication arises if $E_{1\infty}$ is less than U. In this case those energy transfers in the range $\{E_{1\infty},\frac{1}{2}(E_{1\infty}+U)\}$ result in both incident and target electrons being temporarily trapped by the target nucleus to form a classical H^- atom. In such collisions the two electrons repeatedly collide until one of them is free to escape. This means that the contributions to the differential cross section $\frac{d\sigma}{d\Delta E}$ in the closed-channel range $\{E_{1\infty},\frac{1}{2}(E_{1\infty}+U)\}$ should be redistributed over the two open-channel ranges $\{0,E_{1\infty}\}$ and

$-E_2 \leq \Delta E \leq 0$. The possibility of such collisions was not discussed by Vriens (1966b). In the unsymmetric model of Stabler (1964) these complicated collisions are ignored because the incident electron is regarded as free from the influence of the target nucleus.

2.8 The Effective Differential Cross Section $\frac{d\sigma}{d\Delta E}(v_1)$ Averaged over a Spherical Distribution of Target Velocities for Charged-Particle Collisions.

The velocity-averaged effective differential cross section $\frac{d\sigma}{d\Delta E}(v_1)$ may be obtained by averaging $\frac{d\sigma_{IJ}}{d\Delta E}$ over a given spherical velocity distribution $\rho(v_2)$ using the relevant regions as indicated in figures (2.7.1a) to (2.7.1d). The resulting formulae are extremely complicated for all but the simplest of expressions for $\rho(v_2)$.

In many applications the target particle is an atomic electron whose velocity distribution is usually spherically distributed in the frame of reference in which the atomic nucleus is at rest. In all but the simplest cases the exact expression for $\rho(v_2)$ is not known. Commonly used approximations are the stationary target model $\rho(v_2) = \delta(v_2)$ where $\delta(x)$ is the well-known Dirac delta function and the circular-orbit model $\rho(v_2) = \delta(v_2 - v)$ where v is some velocity characteristic of the particular target electron. In the exceptional case in which the target atom is hydrogenic the exact target electron velocity distribution, termed the Fock distribution, is given by

$$\rho(v_2) = \frac{32}{\pi} \cdot \frac{v^5 v_2^2}{(v_2^2 + v^2)^4} \quad , \qquad (2.8.1)$$

for both the ground state and all uniformly-populated excited levels (see Fock 1935), where $\frac{1}{2} m_e v^2 = U$.

Vriens (1966b) proposed an approximate formula for $\frac{d\sigma}{d\Delta E}(v_1)$ averaged over the Fock distribution in the case of the accelerated model for identical electrons. However, he also incorporated some additional

approximations in order to eliminate less important collisions and obtained (see equation (28) of Vriens 1966b)

$$\frac{d\sigma_D^D(v_{1\infty})}{d\Delta E} = \frac{\pi e^4}{(E_{1\infty}+2U)}\left\{\frac{0.924}{\Delta E^2} + \frac{2U}{3\Delta E^3}\right\} , \qquad (2.8.2)$$

$$\frac{d\sigma_D^E(v_{1\infty})}{d\Delta E} = \frac{\pi e^4}{(E_{1\infty}+2U)(E_{1\infty}+U-\Delta E)^2}\left\{0.924 + \frac{2U}{3(E_{1\infty}+U-\Delta E)}\right\} , \qquad (2.8.3)$$

and

$$\frac{d\sigma_D^{QIB}(v_{1\infty})}{d\Delta E} = \frac{0.924\ \pi e^4}{(E_{1\infty}+2U)(E_{1\infty}+U-\Delta E)\,\Delta E} , \qquad (2.8.4)$$

all being valid for $0 \leqslant \Delta E \leqslant \frac{1}{2}(E_{1\infty}+U)$. The interference term quoted in equation (28) is incorrect since it contains E_2 . An expression of the same type is

$$\frac{d\sigma_D^{QIF}(v_{1\infty})}{d\Delta E} = \frac{d\sigma_D^{QIB}}{d\Delta E}\cos\left\{\left(\frac{U_o}{E_{1\infty}+U}\right)^{\frac{1}{2}}\log\left(\frac{\Delta E}{E_{1\infty}+U-\Delta E}\right)\right\} . \qquad (2.8.5)$$

In the same case, but without excluding particular collisions , Valentine (1968) computed $\frac{d\sigma^D}{d\Delta E}$ and $\frac{d\sigma^E}{d\Delta E}$ numerically for comparisons with more accurate classical calculations.

The analytical results in this case are for $E_{1\infty} \geqslant U$

$$\frac{d\sigma^D(v_{1\infty})}{d\Delta E} = \frac{\pi e^4}{E_{1\infty}\Delta E^2}\left\{(1-T) + \frac{4U}{3\Delta E}(1+T-2X)\right\} , \qquad (2.8.6)$$

$$\frac{d\sigma^E(v_{1\infty})}{d\Delta E} = \frac{\pi e^4}{E_{1\infty}(E_{1\infty}+U-\Delta E)^2}\left\{(1-T) + \frac{4U(1+T-2X)}{3(E_{1\infty}+U-\Delta E)}\right\} , \qquad (2.8.7)$$

and

$$\frac{d\sigma}{d\Delta E}^{QIB}(v_{1\infty}) = \frac{\pi e^4 (1-T)}{E_{1\infty}\,\Delta E\,(E_{1\infty}+U-\Delta E)} \quad , \qquad (2.8.8)$$

all being valid for $0 \leq \Delta E \leq \frac{1}{2}(E_{1\infty}+U)$ where $E_{1\infty} = \frac{1}{2} m_e v_{1\infty}^2$ and the dimensionless quantities $X(E_{1\infty}/U)$ and $T(E_{1\infty}/U)$ are given by

$$X(E_{1\infty}/U) = 4\left(\frac{U}{E_{1\infty}}\right)\left[1 - 2\left(\frac{U}{E_{1\infty}}\right)\left\{\left(1+\frac{E_{1\infty}}{U}\right)^{1/2} - 1\right\}\right] \quad , \qquad (2.8.9)$$

and

$$T(E_{1\infty}/U) = 2\left(\frac{U}{E_{1\infty}}\right)\left\{1 - X(E_{1\infty}/U)\right\} \quad . \qquad (2.8.10)$$

As in previous cases, the interference term can only be integrated numerically. It can be seen that the exact integrations differ from the approximations of Vriens, especially in the second term of $\frac{d\sigma_D}{d\Delta E}^{D}$ and $\frac{d\sigma_D}{d\Delta E}^{E}$. However, no analytic results can be obtained for the interference term.

These differential cross sections should be modified for $E_{1\infty} < U$, because of the complications caused by temporary trapping of both electrons as discussed at the end of section (2.7).

In the general-mass case and even in the special limiting cases of interest no other explicit results are available for $\frac{d\sigma}{d\Delta E}$ averaged over the Fock distribution or over any comparable velocity distribution for non-hydrogenic targets.

2.9 Total Effective Cross Sections for Charged-Particle Collisions

It is convenient to classify the total cross sections into four types. Firstly, ionization cross sections may be defined as cross sections which include all collisions with energy transfers in excess of a fixed positive amount U . In contrast excitation cross sections may be defined as cross sections which include all collisions with energy transfers lying between two positive values $U_1 < U_2$, even if part of this energy-transfer range may be inaccessible. By a suitable choice of U_2 ionization cross sections can be included in excitation cross sections, but to avoid possible confusion they will be treated separately. De-excitations (collisions for which ΔE is negative) will not be considered here but can be handled in a similar way.

Both excitation and ionization cross sections may be further classified according to whether they have been averaged over the magnitudes of the target velocities. The unaveraged total cross section $\sigma(v_1, v_2)$ may be obtained by integrating $\frac{d\sigma(v_1,v_2)}{d\Delta E}$ over the relevant range of ΔE . The averaged total cross section $\sigma(v_1)$ may be obtained either by averaging $\sigma(v_1, v_2)$ over $\rho(v_2)$ or by integrating $\frac{d\sigma(v_1)}{d\Delta E}$ over the relevant range of ΔE .

(a) Unaveraged Total Cross Sections.

The most important cases of physical interest are listed below.

(i) Infinite-Mass Projectile.

The ionization cross section $\sigma(v_1, v_2, U)$ is

$$\sigma(v_1, v_2, U) = \frac{\pi z_1^2 z_2^2}{\mathcal{E}_1 U}\left\{1 - \frac{U}{4(\mathcal{E}_1 - E_2)} + \frac{2E_2}{3U}\right\} ; \qquad (2.9.1)$$

$$\text{for} \quad 0 \leq U \leq 2m_2 v_1 (v_1 - v_2) , \quad \mathcal{E}_1 = \tfrac{1}{2} m_2 v_1^2 ,$$

$$\sigma(v_1,v_2,U) = \frac{\pi z_1^2 z_2^2}{2\mathcal{E}_1 U}\left[1 + \frac{U}{2m_2 v_1(v_1+v_2)} + \frac{m_2}{3v_2 U}\left\{2v_1^3 + v_2^3 - \left(v_2^2 + \frac{2U}{m_2}\right)^{\frac{3}{2}}\right\}\right],$$

$$\text{for} \quad 2m_2 v_1(v_1-v_2) \leq U \leq 2m_2 v_1(v_1+v_2), \qquad (2.9.2)$$

and

$$\sigma(v_1,v_2,U) = 0, \quad \text{for} \quad U \geq 2m_2 v_1(v_1+v_2). \qquad (2.9.3)$$

These results were first given by Vriens (1967) though the invariant cross sections of Percival and Valentine (1966) had the same regions of validity and the same high incident energy form in the important region given by equation (2.9.1).

The excitation cross section $\sigma(v_1,v_2,U_1,U_2)$ is more complicated. The simplest and most important result is

$$\sigma(v_1,v_2,U_1,U_2) = \frac{\pi z_1^2 z_2^2}{\mathcal{E}_1 U_1 U_2}(U_2-U_1)\left\{1 + \frac{2(U_1+U_2)E_2}{3U_1U_2}\right\},$$

$$\text{for} \quad 0 \leq U_1 \leq U_2 \leq 2m_2 v_1(v_1-v_2). \qquad (2.9.4)$$

The other cases are considerably more complicated but may be obtained directly by integrating equation (2.7.31) over ΔE and by investigating the respective magnitudes of U_1, U_2, $2m_2 v_1(v_1-v_2)$ and $2m_2 v_1(v_1+v_2)$.

(ii) Equal-Mass Distinguishable Particles

The ionization cross section is

$$\sigma(v_1,v_2,U) = \frac{\pi z_1^2 z_2^2}{E_1 U}\left\{1 - \frac{U}{(E_1-E_2)} + \frac{2E_2}{3U}\right\},$$

$$\text{for} \quad E_1 - E_2 \geq U, \qquad (2.9.5)$$

$$\sigma(v_1,v_2,U) = \frac{2\pi z_1^2 z_2^2}{3E_1 U}\cdot\frac{(E_1-U)^{\frac{3}{2}}}{U E_2^{\frac{1}{2}}},$$

$$\text{for} \quad E_1 - E_2 \leq U \leq E_1, \qquad (2.9.6)$$

and

$$\sigma(v_1, v_2, U) = 0 \quad , \text{for} \quad U > E_1 \, . \tag{2.9.7}$$

Equations (2.9.5), (2.9.6) and (2.9.7) were first given by Stabler (1964), though Thomas (1927a) had derived expression (2.9.5) and Ochkur and Petrunkin (1963) had obtained equivalent numerical results.

The excitation cross section $\sigma(v_1, v_2, U_1, U_2)$ has also been given by Stabler. He considered four separate cases together with another added in the footnotes. The simplest and most important result is

$$\sigma(v_1, v_2, U_1, U_2) = \frac{\pi z_1^2 z_2^2 (U_2 - U_1)}{E_1 U_1 U_2} \left\{ 1 + 2 \frac{E_2 (U_1 + U_2)}{3 U_1 U_2} \right\}, \tag{2.9.8}$$

$$\text{for} \quad 0 \leq U_1 \leq U_2 \leq E_1 - E_2 \, .$$

(iii) Identical Electrons

The ionization cross sections can be obtained from equations (2.7.36), (2.7.37), (2.7.41) and (2.7.42) and may be written

$$\sigma^D(v_1, v_2, U) = \frac{\pi e^4}{E_1 U} \left\{ 1 - \frac{2U}{(E_1 - E_2)} \right\} \cdot \left[1 + \frac{2E_2}{3U} \left\{ 1 + \frac{2U}{(E_1 - E_2)} \right\} \right], \tag{2.9.9}$$

$$\sigma^E(v_1, v_2, U) = \frac{\pi e^4}{E_1 U} \left\{ \frac{2U}{(E_1 - E_2)} - \frac{U}{(E_1 - E_2 - U)} \right\} \cdot \left[1 + \frac{2E_2}{3U} \left\{ \frac{2U}{(E_1 - E_2)} + \frac{U}{(E_1 - E_2 - U)} \right\} \right], \tag{2.9.10}$$

$$\sigma^{CS}(v_1, v_2, U) = \sigma^D + \sigma^E = \frac{\pi e^4}{E_1 U} \left\{ 1 - \frac{U}{(E_1 - E_2 - U)} \right\} \left[1 + \frac{2E_2}{3U} \left\{ 1 + \frac{U}{(E_1 - E_2 - U)} \right\} \right], \tag{2.9.11}$$

$$\sigma^{QIF}(v_1, v_2, U) = \frac{\pi e^4}{2E_1} \int_U^{\frac{1}{2}(E_1-E_2)} \frac{d\Delta E}{\Delta E} \int_{-1}^{1} dx \int_{-1}^{1} d\gamma \, . \, g \quad , \qquad (2.9.12)$$

and

$$\sigma^{QIB}(v_1, v_2, U) = \frac{\pi e^4}{E_1(E_1-E_2)} \log \frac{(E_1-E_2-U)}{U} \quad , \qquad (2.9.13)$$

all being valid for $0 \leq U \leq \frac{1}{2}(E_1-E_2)$.

Equations (2.9.9), (2.9.10) and (2.9.13) were obtained by Vriens (1966b), though the last equation was given incorrectly in Vriens (1966a). The interference term has not been given previously, but cannot be evaluated analytically. Vriens (1966b) proposed an approximation

$$\sigma_c^{QIF}(v_1, v_2, U) = \sigma^{QIB} \cos\left\{\left(\frac{U_o}{E_1-E_2}\right)^{\frac{1}{2}} \log \frac{(E_1-E_2-U)}{U}\right\} . \qquad (2.9.14)$$

Two other approximations can be obtained by integrating the approximate expressions in equations (2.7.47) and (2.7.48) for $\frac{d\sigma^{QIF}}{d\Delta E}$. The former cannot be integrated analytically. The latter is easily integrated, but it is more convenient to use the value obtained from equation (2.9.12) to fix the value of the parameter B_o in equation (2.7.48).

In the accelerated treatment for ionization E_1 is replaced by $E_{1\infty}+U+E_2$ so that the modified cross sections are valid for $E_{1\infty} \geq U$. For convenience these cross sections are also listed below.

$$\sigma^{D}(v_{1\infty}, v_2, U) = \frac{\pi e^4}{(E_{1\infty}+U+E_2)U} \left\{1-\frac{2U}{(E_{1\infty}+U)}\right\}\left[1+\frac{2E_2}{3U}\left\{1+\frac{2U}{(E_{1\infty}+U)}\right\}\right], \qquad (2.9.15)$$

$$\sigma^{E}(v_{1\infty}, v_2, U) = \frac{\pi e^4}{(E_{1\infty}+U+E_2)U}\left\{\frac{2U}{(E_{1\infty}+U)} - \frac{U}{E_{1\infty}}\right\}\left[1 + \frac{2E_2}{3U}\left\{\frac{2U}{(E_{1\infty}+U)} + \frac{U}{E_{1\infty}}\right\}\right], \tag{2.9.16}$$

$$\sigma^{CS}(v_{1\infty}, v_2, U) = \frac{\pi e^4}{(E_{1\infty}+U+E_2)U}\left(1 - \frac{U}{E_{1\infty}}\right)\left\{1 + \frac{2E_2}{3U}\left(1 + \frac{U}{E_{1\infty}}\right)\right\}, \tag{2.9.17}$$

$$\sigma^{QIB}(v_{1\infty}, v_2, U) = \frac{\pi e^4}{(E_{1\infty}+U+E_2)(E_{1\infty}+U)} \log \frac{E_{1\infty}}{U}, \tag{2.9.18}$$

$$\sigma^{QIF}(v_{1\infty}, v_2, U) = \frac{\pi e^4}{2(E_{1\infty}+U+E_2)} \int_{U}^{\frac{1}{2}(E_{1\infty}+U)} \frac{d\Delta E}{\Delta E} \int_{-1}^{1} dx \int_{-1}^{1} d\gamma\, g(v_{1\infty}), \tag{2.9.19}$$

and

$$\sigma^{QS}(v_{1\infty}, v_2, U) = \sigma^{CS} - \sigma^{QIF}. \tag{2.9.20}$$

The excitation cross sections in the symmetric unaccelerated model can be treated in a similar way and if required they can be derived from the expressions for the accelerated model treated below.

Firstly, suppose that $E_{1\infty}$ is greater than U. Then the excitation cross sections for ΔE lying between U_1 and U_2 are given by

$$\sigma^{D}(v_{1\infty}, v_2, U_1, U_2) = \frac{\pi e^4 (U_2 - U_1)}{(E_{1\infty}+U+E_2)U_1 U_2}\left\{1 + \frac{2E_2(U_1+U_2)}{3U_1U_2}\right\}, \tag{2.9.21}$$

$$\sigma^{E} = \frac{\pi e^4 (U_2 - U_1)}{(E_{1\infty}+U+E_2)(E_{1\infty}+U-U_1)(E_{1\infty}+U-U_2)}\left\{1 + \frac{2E_2(2E_{1\infty}+2U-U_1-U_2)}{3(E_{1\infty}+U-U_1)(E_{1\infty}+U-U_2)}\right\}, \tag{2.9.22}$$

$$\sigma^{CS}(v_{1\infty}, v_2, U_1, U_2) = \sigma^D + \sigma^E \quad , \tag{2.9.23}$$

$$\sigma^{QIB}(v_{1\infty}, v_2, U_1, U_2) = \frac{\pi e^4}{(E_{1\infty}+U+E_2)(E_{1\infty}+U)} \cdot \log\left\{\frac{U_2(E_{1\infty}+U-U_1)}{U_1(E_{1\infty}+U-U_2)}\right\}, \tag{2.9.24}$$

$$\sigma^{QIF}(v_{1\infty}, v_2, U_1, U_2) = \frac{\pi e^4}{2(E_{1\infty}+U+E_2)} \int_{U_1}^{U_2} \frac{d\Delta E}{\Delta E} \int_{-1}^{1} dx \int_{-1}^{1} d\gamma\, g \quad , \tag{2.9.25}$$

and

$$\sigma^{QS}(v_{1\infty}, v_2, U_1, U_2) = \sigma^{CS} - \sigma^{QIF} \quad , \tag{2.9.26}$$

all being valid for $0 \leq U_1 \leq U_2 \leq \left(\frac{E_{1\infty}+U}{2}\right) \leq E_{1\infty}$.

If $U_2 > \left(\frac{E_{1\infty}+U}{2}\right)$ and $E_{1\infty} > U$ then U_2 should be replaced by $\frac{1}{2}(E_{1\infty}+U)$ in equations (2.9.21) to (2.9.26). Equations (2.9.21) to (2.9.24) were given by Vriens (1966b), but the condition $U_2 > \frac{1}{2}(E_{1\infty}+U)$ was not considered.

Now suppose that $E_{1\infty}$ is less than the ionization threshold U . If $E_{1\infty} > U_2$ equations (2.9.21) to (2.9.26) are unchanged, but if $U_2 < E_{1\infty}$, U_2 should be replaced by $E_{1\infty}$, since the remaining range $\{E_{1\infty}, \frac{1}{2}(E_{1\infty}+U)\}$ leads to temporary capture of both electrons (see section (2.7b)). The contribution to the excitation cross sections from this capture region could be obtained using a random walk procedure (see for example Hammersley and Handscomb 1964) but the additional effort would not be justified because even the symmetrised accelerated binary-encounter model considerably overestimates the exact-

classical excitation cross section for incident energies below the ionization threshold (see for example Valentine 1968). A simple analytic estimate for this correction can be obtained by assuming that a fraction α of the capture collisions is redistributed uniformly in the excitation range $[0, E_{1\infty}]$ and that the remaining fraction $1-\alpha$ leads to de-excitations. Now the total capture cross section can be obtained from equations (2.9.21) to (2.9.26) with U_1 and U_2 replaced by $E_{1\infty}$ and $\frac{1}{2}(E_{1\infty}+U)$ respectively. The contributions to the required excitation cross sections can be determined by multiplying the total capture cross section by the factor $\alpha(U_2-U_1)/E_{1\infty}$ if $E_{1\infty}>U_2$ and by the factor $\alpha(E_{1\infty}-U_1)/E_{1\infty}$ if $U_1<E_{1\infty}<U_2$. For most purposes $\alpha=\frac{1}{2}$ should suffice.

Clearly, all excitation cross sections are zero if $E_{1\infty}<U_1$ and all ionization cross sections are zero if $E_{1\infty}<U$.

(b) Averaged Total Cross Sections

In the general-mass case the results are too tedious to be presented in detail, but the more important special cases are considered below.

(i) Infinite-Mass Projectile

The total ionization cross section averaged over the Fock distribution given in equation (2.8.1) was calculated numerically both by Percival and Valentine (1966), using invariant cross sections, and by McDowell (1966) using invariant rates. Vriens (1967) obtained an analytic formula for the incident velocity region $v_1 > \frac{1}{2}v$, though the expression is so complicated that it is not immediately obvious what high incident velocity form the cross section takes. No formula was given for the low incident

velocity region $v_1 < \frac{1}{2}v$ in which the corresponding Thomson formula is zero. The low-velocity form of the ionization cross section can be obtained by expanding the terms in equation (2.9.2) for small v_1 and simultaneously $v_2 \geq (v^2-4v_1^2)/v_1$ and then averaging over v_2. Direct evaluation of equation (2.9.2) for numerical integration, say, can lead to numerical errors for small v_1, since the expansion of the separate terms contains leading terms of order v_1^{-4}, v_1^{-2} and v_1^{0}, all of which exactly cancel when they are collected together. The low incident velocity form of the ionization cross section averaged over the Fock distribution is

$$\sigma(v_1/v) = k\,(v_1/v)^7 + O\{(v_1/v)^9\}\,. \qquad (2.9.27)$$

Fairly accurate target electron velocity distributions have been used to obtain total ionization cross sections for non-hydrogenic atoms by proton impact (see for example Catlow and McDowell 1967 and Bates and Kingston 1970), but, in contrast, no exact results are available for averaged proton-excitation cross sections for any atomic targets.

(ii) Equal-Mass Distinguishable Particles.

Fock-averaged electron-hydrogen ionization cross sections have been evaluated numerically by Kingston (1966) and analytically by McDowell (1966). In this case the result is simpler than the corresponding expression derived by Vriens (1967) for infinite-mass projectiles. McDowell obtained

$$\sigma(E_1,U) = \frac{8e^4}{3U^2\pi}\,x^{-2}(x^2+1)^{-4}\left\{(5x^4+15x^3-3x^2-7x+6)(x-1)^{1/2}\right.$$
$$+(5x^5+17x^4+15x^3-25x^2+20x)\tan^{-1}(x-1)^{1/2}$$
$$\left.-24\,x^{3/2}\log\left|\frac{x^{1/2}+(x-1)^{1/2}}{x^{1/2}-(x-1)^{1/2}}\right|\right\}, \text{ with } x=\frac{E_1}{U}\,. \qquad (2.9.28)$$

Kingston (1968) has also obtained numerical values for electron-hydrogen ionization cross sections in which the atom is initially in different excited levels (n,l) which are obtained by averaging uniformly over all orientations m_l. The first non-hydrogenic targets were considered by Catlow and McDowell (1967) for ionization only. Flannery (1970a) has presented some numerical values for Fock-averaged electron-hydrogen excitation cross sections in the special case of $n \to n+1$ transitions with $n = 20$ and $n = 100$.

(iii) Identical Electrons

The total ionization cross section averaged over the Fock distribution for the symmetric accelerated model was evaluated numerically by Valentine (1968). The analytic results can be obtained very simply from the averaged differential cross sections $\frac{d\sigma}{d\Delta E}(v_\infty)$ in equations (2.8.6) to (2.8.8). The results may be written

$$\sigma^D(E_\infty,U) = \frac{\pi e^4}{U^2}\left(\frac{U}{E_\infty}\right)\left[\left\{1-\frac{2U}{(E_\infty+U)}\right\}(1-T)+\frac{2}{3}\left\{1-\frac{4U^2}{(E_\infty+U)^2}\right\}(1+T-2X)\right], \tag{2.9.29}$$

$$\sigma^E(E_\infty,U) = \frac{\pi e^4}{U^2}\left(\frac{U}{E_\infty}\right)\left[\left\{\frac{2U}{(E_\infty+U)}-\frac{U}{E_\infty}\right\}(1-T)+\frac{2}{3}\left\{\frac{4U^2}{(E_\infty+U)^2}-\frac{U^2}{E_\infty^2}\right\}(1+T-2X)\right], \tag{2.9.30}$$

$$\sigma^{CS}(E_\infty,U) = \frac{\pi e^4}{U^2}\left(\frac{U}{E_\infty}\right)\left[\left(1-\frac{U}{E_\infty}\right)(1-T)+\frac{2}{3}\left(1-\frac{U^2}{E_\infty^2}\right)(1+T-2X)\right], \tag{2.9.31}$$

$$\sigma^{QIB}(E_\infty,U) = \frac{\pi e^4}{U^2}\left(\frac{U}{E_\infty+U}\right)\cdot\frac{U}{E_\infty}\cdot(1-T)\log\frac{E_\infty}{U}, \tag{2.9.32}$$

and

$$\sigma^{QIF}(E_\infty,U) = \frac{\pi e^4}{2}\int_0^\infty \frac{dv_2\,\rho(v_2)}{(E_\infty+U+E_2)}\int_U^{\frac{(E_\infty+U)}{2}}\frac{d\Delta E}{\Delta E}\int_{-1}^{1}dx\int_{-1}^{1}d\gamma\, g, \tag{2.9.33}$$

where $X(E_{\infty}/U)$ and $T(E_{\infty}/U)$ are defined in equations (2.8.9) and (2.8.10) respectively. Vriens (1966b) obtained the approximate formulae

$$\sigma_E^{CS}(E_{\infty},U) = \frac{\pi e^4}{U^2}\left(\frac{U}{E_{\infty}+2U}\right)\left[0.924\left(1-\frac{U}{E_{\infty}}\right)+\frac{1}{3}\left(1-\frac{U^2}{E_{\infty}^2}\right)\right], \quad (2.9.34)$$

$$\sigma_E^{QIB}(E_{\infty},U) = 0.924\,\frac{\pi e^4}{U^2}\left(\frac{U}{E_{\infty}+2U}\right)\left(\frac{U}{E_{\infty}+U}\right)\log\frac{E_{\infty}}{U}, \quad (2.9.35)$$

and

$$\sigma_E^{QIF}(E_{\infty},U) = \sigma_E^{QIB}\cos\left\{\left(\frac{U_o}{E_{\infty}+U}\right)^{1/2}\log\frac{E_{\infty}}{U}\right\}, \quad (2.9.36)$$

where U_o is the ionization potential of the ground state of atomic hydrogen (that is, U_o is equal to the Rydberg unit of energy).

The total excitation cross sections can also be obtained from equations (2.8.6) to (2.8.8) and may be written

$$\sigma^{D}(E_{\infty},U_1,U_2) = \frac{\pi e^4}{U^2}\left(\frac{U}{E_{\infty}}\right)\left\{\frac{U(U_2-U_1)}{U_1U_2}\right\}\left\{(1-T)+\frac{2U(U_1+U_2)}{3U_1U_2}(1+T-2X)\right\}, \quad (2.9.37)$$

$$\sigma^{E}(E_{\infty},U_1,U_2) = \frac{\pi e^4}{U^2}\left(\frac{U}{E_{\infty}}\right)\left\{\frac{U(U_2-U_1)}{(E_{\infty}+U-U_1)(E_{\infty}+U-U_2)}\right\}\times\left\{(1-T)+\frac{2U(2E_{\infty}+2U-U_1-U_2)}{3(E_{\infty}+U-U_1)(E_{\infty}+U-U_2)}\times(1+T-2X)\right\}, \quad (2.9.38)$$

$$\sigma^{QIB}(E_{\infty},U_1,U_2) = \frac{\pi e^4}{U^2}\left(\frac{U}{E_{\infty}}\right)\left(\frac{U}{E_{\infty}+U}\right)(1-T)\log\left\{\frac{U_2(E_{\infty}+U-U_1)}{U_1(E_{\infty}+U-U_2)}\right\}, \quad (2.9.39)$$

and

$$\sigma^{QIF}(E_{\infty},U_1,U_2) = \frac{\pi e^4}{2}\int_0^{\infty}\frac{dv_2\,\rho(v_2)}{(E_{\infty}+U+E_2)}\int_{U_1}^{U_2}\frac{d\Delta E}{\Delta E}\int_{-1}^{1}dx\int_{-1}^{1}d\gamma\; g, \quad (2.9.40)$$

for $0 \le U_1 \le U_2 \le \frac{1}{2}(E_{\infty}+U) \le E_{\infty}$.

If $U_1 \le \frac{1}{2}(E_{\infty}+U) \le U_2 \le E_{\infty}$ then U_2 should be replaced by $\frac{1}{2}(E_{\infty}+U)$ in

equations (2.9.37) to (2.9.40). This region was not considered correctly by Vriens (1966b). The results for $E_{1\infty}<U$ are less reliable because of the difficulty in treating the capture region $E_{1\infty} \leq \Delta E \leq \frac{1}{2}(E_{1\infty}+U)$. Nevertheless, if this region is neglected then the results are unchanged if $E_{1\infty} \geq U_2$ and can be obtained from equations (2.9.37) to (2.9.40) by replacing U_2 by $E_{1\infty}$. An approximate formula for the correction arising from the redistribution of capture orbits can be derived in a similar way to that described in section (2.9a(iii)) except that in the present case the total capture cross section can be derived from equations (2.9.37) to (2.9.40) by replacing U_1 and U_2 by $E_{1\infty}$ and $\frac{1}{2}(E_{1\infty}+U)$ respectively.

The symmetric accelerated model has been applied to ionization and excitation of non-hydrogenic atoms by Tripathi et al. (1969).

(iv) A Semi-Empirical Decelerated Model for Total Ionization of Hydrogen Atoms by Incident Positrons

The accelerated symmetric model for identical electrons is obtained from the unsymmetric case by substituting $E_{1\infty}+U+E_2$ for E_1. In this way, the region $E_1-E_2 \leq U \leq E_1$, which is important for low incident energies in the unsymmetric treatment, is automatically excluded in the symmetric model. Suppose that for incident positrons a decelerated model is defined by replacing E_1 by $E_{1\infty}-\alpha U-\beta E_2$ in the unsymmetric case, where α and β are positive constants. Now, the region $E_1-E_2 \leq U \leq E_1$ is enhanced rather than excluded and the threshold energy for ionization is given by $(1+\alpha)U+\beta E_2$. The natural choice $\alpha=1$ and $\beta=1$ therefore leads to the wrong threshold energy. In fact

$\alpha=0$, but β need not necessarily be zero since E_2 may assume a range of values including zero. By comparison with the symmetric treatment $\beta=1$ is used henceforth. Finally, the modified total ionization cross section obtained from equations (2.9.5) - (2.9.7) with $E_1 = E_{1\infty} - E_2$ may be averaged numerically over the Fock velocity distribution of the atomic electron 2 .

2.10 Comparison of Binary-Encounter Total Ionization Cross Sections with Exact-Classical Results

In the special case of charged particles incident upon hydrogen atoms which are initially in a uniformly-populated level n, the binary-encounter results for ionization can be compared with exact-classical calculations. It is obvious from the explicit formulae for the binary-encounter ionization cross sections $\sigma(E_1, U)$ for incident energy E_1 and target binding energy U, that, with the exception of the interference contribution, $\sigma(E_1, U)$ obeys the classical scaling law

$$\sigma(E_1, U) = \theta^2 \sigma(\theta E_1, \theta U), \text{ for arbitrary } \theta > 0. \quad (2.10.1)$$

Abrines and Percival (1966b) have shown that the same law applies to cross sections derived from the exact-classical approach for three interacting charged particles. Hence all comparisons can be made at a single value of the binding energy U which can be conveniently set equal to the ionization potential of the ground state of atomic hydrogen. Cross sections from any other level n can be obtained from those for the ground state via equation (2.10.1) with $\theta = n^{-2}$.

Various types of incident particle have been employed in exact-classical calculations. Abrines and Percival (1966b) considered the case of incident protons, Abrines, Percival and Valentine (1966) investigated electron collisions and Percival and Valentine (1967) studied incident positrons. In all three cases the mass of the proton was not taken to be infinite. Electron collisions have also been studied by Brattsev and Ochkur (1967) using a very similar technique

but with an infinitely-massive target nucleus. Each of these processes is compared separately below.

(a) Infinite-Mass Projectile

No averaged binary-encounter results for finite-mass incident protons are available. However, at incident proton energies E_1 above 1 Kev., the approximation of replacing the incident proton by an infinite-mass projectile moving with the same speed should have a negligible effect on the binary-encounter ionization cross sections. A very convenient approximate relationship between the incident proton energy E_1 in Kev. and the equivalent incident energy $\mathcal{E}_1 = \frac{1}{2} m_e v_1^2$ for the infinite-mass projectile is given by

$$E_1 = \left(\frac{\mathcal{E}_1}{U}\right) .25 \text{ Kev.} \quad . \tag{2.10.2}$$

The relevant cross sections are displayed in figure (2.10.1) in the form of a Bethe plot (σE_1 versus $\log E_1$) so that the high incident energy form of the ionization cross section

$$\sigma(E_1) \sim \frac{20}{3} \left(\frac{25}{E_1}\right) \pi a_0^2 \; ; \tag{2.10.3}$$

can be demonstrated clearly.

The simplest of the binary-encounter results is the Thomson formula given by equation (2.9.1) with $E_2 = 0$. By comparison with more refined binary-encounter models and with the exact-classical results the Thomson formula is too small by a factor $5/3$ at high incident energies and so the Thomson formula scaled up by the factor $5/3$ has been plotted. The reason for this disagreement at high incident energies is that the neglected term in equation (2.9.1) contains a factor E_2/U whose

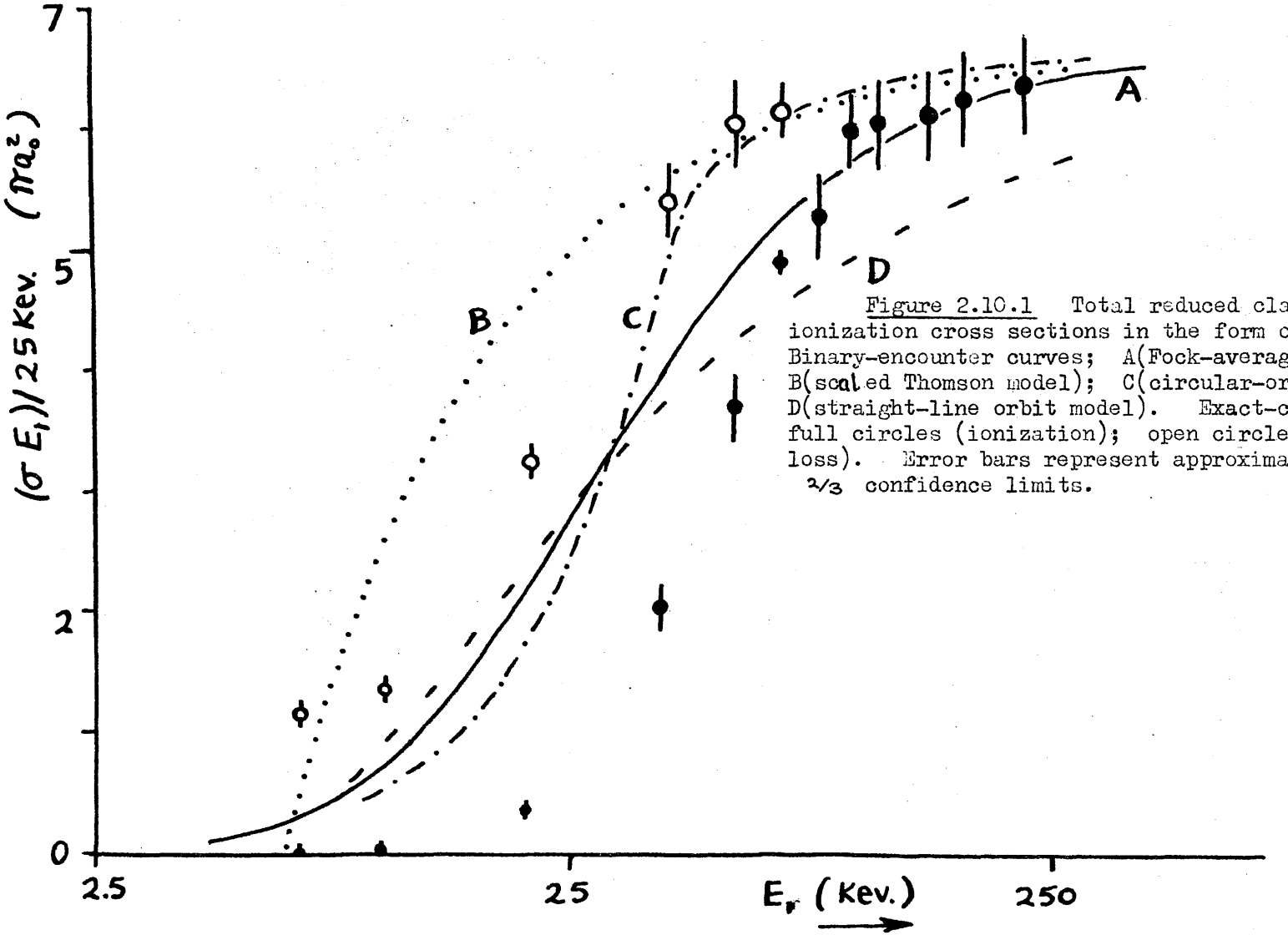

Figure 2.10.1 Total reduced classical p-H ionization cross sections in the form of a Bethe plot Binary-encounter curves; A(Fock-averaged model); B(scaled Thomson model); C(circular-orbit model); D(straight-line orbit model). Exact-classical values: full circles (ionization); open circles (electron-loss). Error bars represent approximate statistical 2/3 confidence limits.

average over the initial target velocity distribution is equal to unity by the Virial Theorem for charged particles. The neglected term is therefore of the same order of magnitude as the first term in equation (2.9.1) even for high incident energies. It is clear from equation (2.7.30) that the Thomson model is only accurate if $\Delta E \gg E_2 \sim U$.

The circular-orbit model given by equations (2.9.1), (2.9.2) and (2.9.3) with $E_2 = U$ and the Fock-averaged model of McDowell (1966) and Vriens (1967) are also displayed. The incident energy range below about 6.25 Kev. was not covered by Vriens and McDowell but was determined numerically and was found to agree at low energies with the threshold law given by equation (2.9.27).

The exact-classical results of Abrines and Percival (1966b) have been supplemented at lower incident energies (see section (3.3)). It was pointed out by Percival and Valentine (1966) that the binary-encounter results should be interpreted as electron-loss cross sections rather than purely ionization values. For this reason both ionization and electron-loss results are displayed in figure (2.10.1). It is worth noting that the 7 points with highest incident energy were obtained from the same pseudo-random numbers so that the shape of the curve in this region is more reliable than the absolute values.

(b) Incident Electrons

In this case there are more possible binary-encounter ionization models. The cross sections in units of πa_0^2 are listed in table (2.10.2) as functions of the incident energy $E_{1\infty}$ in units of the ionization potential of the ground state of atomic hydrogen and are

$E_{1\infty}/U$	σ_1 (πa_0^2)	σ_2 (πa_0^2)	σ_3 (πa_0^2)	σ_4 (πa_0^2)	σ_5 (πa_0^2)	σ_6 (πa_0^2)	σ_7 (πa_0^2)	σ_8 (πa_0^2)
1.05	0.181	0.028	0.144	0.047	0.098	0.155	0.132	-
1.10	0.331	0.077	0.267	0.122	0.183	0.289	0.245	0.19∓04
1.15	0.454	0.135	0.372	0.208	0.256	0.404	0.342	-
1.20	0.556	0.199	0.463	0.296	0.319	0.505	0.426	-
1.25	0.640	0.267	0.542	0.384	0.375	0.593	0.499	0.34∓04
1.30	0.710	0.337	0.610	0.469	0.423	0.669	0.562	-
1.40	0.816	0.482	0.720	0.627	0.502	0.794	0.665	-
1.50	0.889	0.629	0.804	0.763	0.563	0.889	0.743	-
1.60	0.937	0.775	0.868	0.879	0.610	0.962	0.803	0.61∓06
1.80	0.988	1.060	0.953	1.055	0.675	1.058	0.883	-
2.00	1.000	1.333	1.000	1.170	0.712	1.111	0.928	0.81∓06
2.50	0.960	1.600	1.031	1.292	0.741	1.143	0.960	0.83∓02
3.20	0.859	1.515	0.992	1.275	0.720	1.091	0.926	0.79∓04
4.00	0.750	1.333	0.917	1.175	0.670	1.000	0.859	0.76∓04
6.40	0.527	0.926	0.711	0.873	0.526	0.760	0.672	0.67∓04
8.00	0.437	0.762	0.613	0.732	0.455	0.648	0.581	-
10.00	0.360	0.622	0.520	0.605	0.387	0.545	0.496	0.51∓02
12.00	0.306	0.525	0.451	0.515	0.336	0.470	0.432	-
16.00	0.234	0.400	0.356	0.395	0.266	0.368	0.343	0.35∓02
20.00	0.190	0.323	0.294	0.320	0.220	0.302	0.284	-
25.21	0.152	0.258	0.239	0.256	0.179	0.244	0.232	0.25∓02
40.00	0.097	0.164	0.156	0.164	0.117	0.159	0.153	0.16∓01
60.00	0.066	0.110	0.106	0.110	0.080	0.107	0.105	-
100.00	0.040	0.066	0.065	0.066	0.049	0.065	0.064	-

Table 2.10.2 Total reduced classical $\bar{e}$–H ionization cross sections as a function of the incident energy $E_{1\infty}$ in units of the target ionization potential U. Binary-encounter values; σ_1 to σ_7 (see text). Exact-classical values σ_8. Errors in σ_8 represent approximate statistical 2/3 confidence limits.

defined below.

σ_1 is the unsymmetric Thomson formula given by equation (2.9.5) with $E_1 = E_{1\infty}$ and $E_2 = 0$.

σ_2 is the unsymmetric circular-orbit model of Stabler given by equations (2.9.5) and (2.9.6) with $E_1 = E_{1\infty}$ and $E_2 = U$.

σ_3 is the accelerated symmetric circular-orbit model of Vriens given by equation (2.9.17) with $E_2 = U$.

σ_4 is the Fock-averaged unsymmetric model given by equation (2.9.28).

σ_5 is the approximate Fock-averaged accelerated symmetric model given by equation (2.9.34).

σ_6 is the scaled accelerated symmetric Thomson model given by equation (2.9.17) with $E_2 = 0$ and then multiplied by $5/3$.

σ_7 is the exact Fock-averaged accelerated symmetric model given by equation (2.9.31).

σ_8 is the exact-classical ionization cross section with its associated statistical error taken from Valentine (1968).

One should expect the binary-encounter results for incident electrons or positrons to be no better than the proton results at the same velocity since in the proton case the motion of the incident particle is not affected by the collision. At high incident energies the electron binary-encounter cross sections should approach the exact-classical values. In order to emphasise the high energy form, the binary-encounter cross sections may be expanded in inverse powers of the incident energy as follows:

$$\sigma_1 = 4\left(\frac{U}{E_{1\infty}}\right)\left\{1 - \left(\frac{U}{E_{1\infty}}\right)\right\}\pi a_0^2 \text{, exactly,} \qquad (2.10.4)$$

$$\sigma_2 = \frac{20}{3}\left(\frac{U}{E_\infty}\right)\left\{1 - \frac{3}{5}\left(\frac{U}{E_\infty}\right)\right\} + O\left\{\left(\frac{U}{E_\infty}\right)^3\right\} \pi a_0^2, \quad (2.10.5)$$

$$\sigma_3 = \frac{20}{3}\left(\frac{U}{E_\infty}\right)\left\{1 - \frac{13}{5}\left(\frac{U}{E_\infty}\right)\right\} + O\left\{\left(\frac{U}{E_\infty}\right)^3\right\} \pi a_0^2, \quad (2.10.6)$$

$$\sigma_4 = \frac{20}{3}\left(\frac{U}{E_\infty}\right)\left\{1 - \frac{3}{5}\left(\frac{U}{E_\infty}\right)\right\} + O\left\{\left(\frac{U}{E_\infty}\right)^{5/2}\right\} \pi a_0^2, \quad (2.10.7)$$

$$\sigma_5 = \frac{15.1}{3}\left(\frac{U}{E_\infty}\right)\left\{1 - 3\left(\frac{U}{E_\infty}\right)\right\} + O\left\{\left(\frac{U}{E_\infty}\right)^3\right\} \pi a_0^2, \quad (2.10.8)$$

$$\sigma_6 = \frac{20}{3}\left(\frac{U}{E_\infty}\right)\left\{1 - 2\left(\frac{U}{E_\infty}\right)\right\} + O\left\{\left(\frac{U}{E_\infty}\right)^3\right\} \pi a_0^2, \quad (2.10.9)$$

$$\sigma_7 = \frac{20}{3}\left(\frac{U}{E_\infty}\right)\left\{1 - \frac{13}{5}\left(\frac{U}{E_\infty}\right)\right\} + O\left\{\left(\frac{U}{E_\infty}\right)^{5/2}\right\} \pi a_0^2, \quad (2.10.10)$$

and

$$\sigma_8 = \frac{20}{3}\left(\frac{U}{E_\infty}\right) + ? \quad . \quad (2.10.11)$$

As expected the Thomson result σ_1 is too small by a factor $5/3$ at high energies. All other approximations apart from the Vriens result σ_5 agree with the leading term in the high-energy expansion of the exact-classical values. Vriens obtains σ_5 by omitting certain regions of integration for which this approximation is poor. However, either this operation has not been carried out correctly, or else his assumptions are wrong, since such modifications should not affect the leading term in the expansion if the unmodified term agrees with the exact-classical value. For this reason σ_5 may be regarded as empirical and may be eliminated from the rest of this discussion. It is interesting to note that the first two leading terms of the velocity-averaged cross

sections σ_4 and σ_7 agree with those of the corresponding unaveraged formulae σ_2 and σ_3, showing that the velocity-averaging procedure gives different results only for intermediate or low incident energies. It is not difficult to show that this result is also true for incident protons. The statistical errors in the exact-classical results are too large to accurately specify the second term in the expansion, but, by comparison in table (2.10.2) σ_6 appears to agree best, yet σ_7 is also within the statistical errors.

Although none of the binary-encounter models should be accurate just above the ionization threshold, it is interesting to compare the behaviour of the various models here. The unsymmetric models σ_2 and σ_4 have a $3/2$ power law at threshold, as also does the quantal first-Born calculation (see for example Rudge and Seaton 1965), whereas the Thomson model σ_1, the symmetric models σ_3, σ_6 and σ_7 have a linear threshold law, favoured by Rudge and Seaton in the quantal case. It is now known that the exact-classical threshold law is neither a linear nor a $3/2$ power law (see Banks, Percival and Valentine 1969, Peterkop and Tsukerman 1969), but is close to the unusual power $\frac{1}{4}\left\{\left(\frac{91}{3}\right)^{1/2}-1\right\}\simeq 1.127$ derived by Wannier (1953) for the classical case. This law has also been derived in the semi-classical WKB approximation (Peterkop and Liepinsh 1969, Peterkop 1971).

The unsymmetric models σ_2 and σ_4 are worse than the symmetric models at low and intermediate incident energies for two reasons. Firstly, in the unsymmetric treatment the effect of the nucleus on the incident electron, after the collision with the target electron, is ignored. Thus, at low and intermediate energies, if the incident electron loses all its

initial energy to the target electron, the incident electron should be captured by the nucleus, whereas in the unsymmetric treatment the collision is counted as an ionization. A second reason is that the unsymmetric treatment does not distinguish between incident electrons or incident positrons, whereas, for low and intermediate energies the two cross sections (see, for example, Valentine 1968 and figure (2.10.3)) are quite different. The empirical symmetric model σ_6, based on the symmetrised Thomson model is extremely simple yet is superior to both unsymmetric treatments for $E_{1\infty} \geq 2U$. The symmetric models σ_3 and σ_7 are surprisingly close to exact-classical values for all incident energies above $E_{1\infty} \sim 1.5\,U$. The better model is the velocity-averaged cross section σ_7, but both models must be regarded as semi-empirical since, in the symmetrisation the incident energy E_1 is replaced by $E_{1\infty}+U+E_2$ whereas the initial kinetic energy of the target electron is unchanged. Nevertheless, if a binary-encounter model is to be used at all, then it should be the symmetrised velocity-averaged model, rather than an unsymmetric treatment, as is used by Catlow and McDowell (1967) for non-hydrogenic target atoms and by Flannery (1970α) for excitation of atomic hydrogen.

(c) Incident Positrons

The cross sections σ_1, σ_2 and σ_4 defined in the previous section are equally valid for incident positrons. The exact-classical ionization cross section is tabulated in Percival and Valentine (1967). As in the case of incident protons the binary-encounter results for positrons can be interpreted as electron-loss values rather than purely

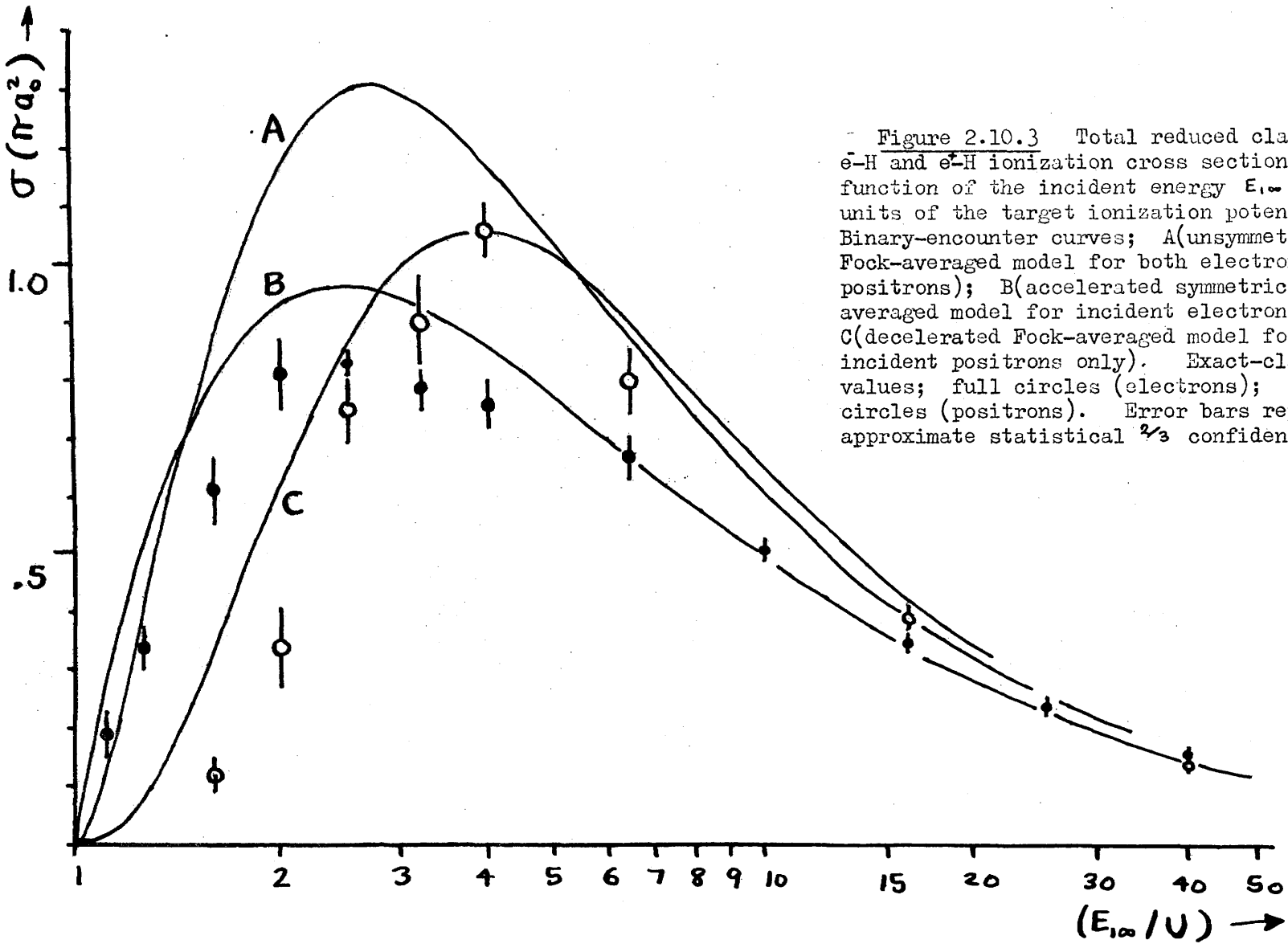

Figure 2.10.3 Total reduced classical e^--H and e^+-H ionization cross sections as a function of the incident energy $E_{1\infty}$ in units of the target ionization potential U. Binary-encounter curves; A(unsymmetric Fock-averaged model for both electrons and positrons); B(accelerated symmetric Fock-averaged model for incident electrons only); C(decelerated Fock-averaged model for incident positrons only). Exact-classical values; full circles (electrons); open circles (positrons). Error bars represent approximate statistical $^2/_3$ confidence limits

as ionization. The exact-classical electron and positron results are compared in figure (2.10.3) with the Fock-averaged unsymmetric model σ_4 of McDowell, with the Fock-averaged symmetric model σ_7 for incident electrons alone and with the semi-empirical decelerated model for incident positrons (see section (2.9(b)iv)). The improvement over the unsymmetric model σ_4 is remarkable.

2.11 Binary-Encounter Estimates of the Interference Contribution to Total Ionization Cross Sections for Electrons Incident upon Hydrogenic Ions.

In quantal calculations exchange and interference effects are particularly difficult to treat exactly and are therefore often neglected. At intermediate incident energies the inclusion of exchange in the binary-encounter model reduces the total ionization cross sections by as much as 30% for target classical hydrogen atoms (see for example figure (2.10.3)). This suggests that exchange and interference contributions to the quantal ionization cross sections are not negligible here, but are sufficiently small to be estimated using a binary-encounter model.

The ionization potential U of a target hydrogenic ion with general nuclear charge Z in an arbitrary uniformly-populated initial level n may be written

$$U = \left(\frac{Z}{n}\right)^2 U_0 \quad , \qquad (2.11.1)$$

where U_0 is the binding energy of the ground state of atomic hydrogen. The direct, exchange and interference-bound contributions to the total symmetrised binary-encounter ionization cross sections of the target hydrogenic ions may be calculated from the reduced cross sections for ionization of the ground-state neutral hydrogen atom using the scaling law given by equation (2.10.1), apart from a focusing factor F which partially allows for the effect of the net charge of the target system on the incident electron. A simple expression for F has been given by Percival (1966), who took

$$F = 1 + \frac{2.3}{(1-Z^{-1})^{-2} + 2(\varepsilon-1)^2} \quad , \qquad (2.11.2)$$

for $Z>1$ and $F=1$ for $Z=1$. This factor is identical for all initial levels n. In equation (2.11.2) ε is the ratio of incident energy $E_{1\infty}$ to the binding energy U.

The binary-encounter interference contributions do not satisfy this classical scaling law. The corresponding reduced contributions are therefore functions, not of ε alone, but of ε and of (Z/n) or some equivalent parameter, say $t=n/(n+Z)$, but not of n and Z separately. For t close to zero Z is much larger than n, the interference is maximal and the extreme quantal limit is approached. For t close to unity n is much larger than Z, the interference is destructive and the classical limit is approached.

In order to avoid additional averages over the magnitude of the velocity of the target electron the accelerated symmetric unaveraged circular orbit binary-encounter model was selected firstly to study the effects of including interference exactly using numerical integration. In this comparison E_1 is replaced by $E_{1\infty}+2U$ and E_2 by U. Then ε is defined as $E_{1\infty}/U$.

The differential contribution $\frac{d\sigma^{QIF}}{d\Delta E}$, given by equations (2.7.41) and (2.6.32), was evaluated using Gaussian numerical integration for different values of ε, t and ΔE. The approximations $\frac{d\sigma_A^{QIF}}{d\Delta E}$, given by equation (2.7.47), and $\frac{d\sigma_B^{QIF}}{d\Delta E}$, given by equation (2.7.48), can be gauged from the symmetric case $\Delta E=\frac{1}{2}(E_{1\infty}+U)$ for which both electrons have the same kinetic energy finally. By construction the approximation $\frac{d\sigma_B^{QIF}}{d\Delta E}$ is exact here, whereas $\frac{d\sigma_A^{QIF}}{d\Delta E}$ reduces to the bound $\frac{d\sigma^{QIB}}{d\Delta E}$, given by equation (2.7.42). The coefficient A_0 is the ratio $\left\{\frac{d\sigma^{QIF}}{d\Delta E}/\frac{d\sigma^{QIB}}{d\Delta E}\right\}$ evaluated at $\Delta E=\frac{1}{2}(E_{1\infty}+U)$. The approximation $\frac{d\sigma_A^{QIF}}{d\Delta E}$ of Vriens

is therefore accurate only if A_o is close to unity. The function $\cos^{-1}(A_o)$ is plotted against the variable t for various values of ε in the range $1<\varepsilon\leq 7$ in figure (2.11.1). It is apparent that A_o is only close to unity for small t . For $0\leq t\leq \frac{1}{2}$ the function $\cos^{-1}(A_o)$ is not particularly complicated and could possibly be approximated sufficiently simply to allow further analytic integration over ΔE . However the region $\frac{1}{2}\leq t\leq 1$ contains rapid oscillations close to $t=1$, which suggests that analytic approximations may not be easily obtained. For other values of ΔE the coefficient B_o in equation (2.7.48) is also required. A comparison with the Vriens approximation $\frac{d\sigma_A^{QIF}}{d\Delta E}$ is not made here since it was found that $\frac{d\sigma_A^{QIF}}{d\Delta E}$ was poor except where A_o was close to unity. The value of B_o was chosen so that exact integration over ΔE of equation (2.7.48) lead to the correct value of the total interference contribution σ^{QIF} obtained by an equally-spaced numerical integration of $\frac{d\sigma^{QIF}}{d\Delta E}$ over ΔE . The approximation $\frac{d\sigma_B^{QIF}}{d\Delta E}$ is therefore only accurate when B_o is small and when $\frac{d\sigma^{QIF}}{d\Delta E}$ varies smoothly with ΔE . Values of A_o and B_o for the particular case $\varepsilon=2$ are listed in table (2.11.2) as functions of t . The approximation $\frac{d\sigma_B^{QIF}}{d\Delta E}$ is poor for $t\geq 1/2$ over the complete ionization range $U\leq \Delta E\leq \frac{1}{2}(E_\infty+U)$ but is always accurate close to $\Delta E=\frac{1}{2}(E_\infty+U)$ since $\frac{d\sigma^{QIF}}{d\Delta E}$ has a stationary value here, as $\frac{d\sigma^{QIF}}{d\Delta E}\left\{\frac{1}{2}(E_\infty+U)-\Delta E\right\}=\frac{d\sigma^{QIF}}{d\Delta E}\left\{\Delta E-\frac{1}{2}(E_\infty+U)\right\}$ by symmetry arguments. Table (2.11.2) also contains the ratio R of the total interference contribution σ^{QIF} to its bound σ^{QIB} , the total ionization cross section σ^{QS} given by equation (2.9.20), and the ratios R_A and R_c of two approximations $\sigma_A^{QIF}, \sigma_B^{QIF}$

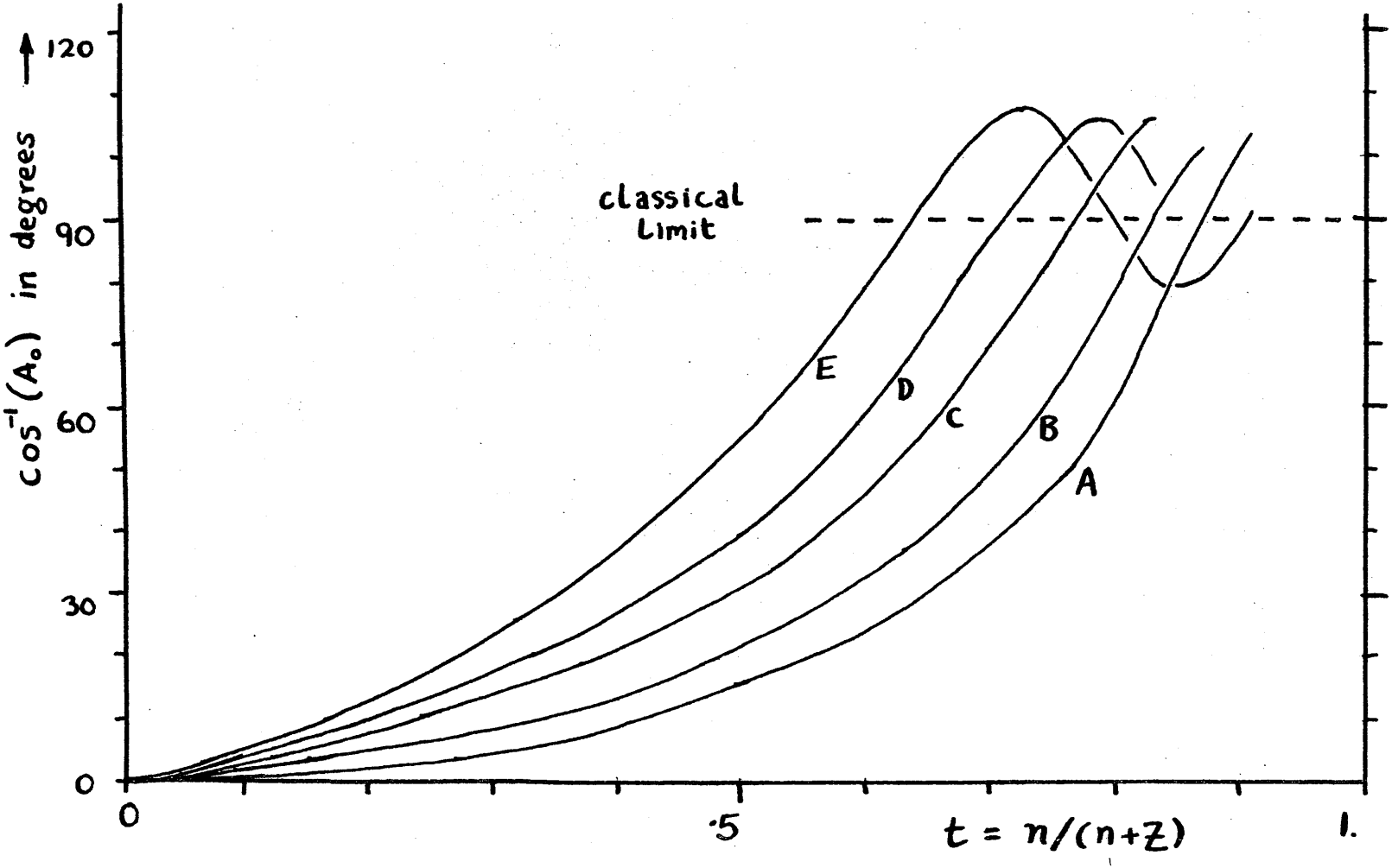

Figure 2.11.1 The dependence of $\cos^{-1} A_0$ as a function of $t = n/(n+Z)$ for different values of $\varepsilon = E_{1,\infty}/u$. Curves; A($\varepsilon$ = 1.08); B(ε = 2); C(ε = 3); D(ε = 5); E(ε = 7). See text.

$t = n/(n+Z)$	σ^{QS} in πa_o^2	R	R_A	R_C	A_o	B_o
0/1	0.769	1.000	1.000	1.000	1.000	0.000
1/11	0.770	0.997	1.000	0.999	0.998	-0.017
1/6	0.772	0.988	0.999	0.997	0.990	-0.067
3/13	0.775	0.973	0.998	0.993	0.978	-0.148
1/4	0.777	0.966	0.997	0.991	0.973	-0.183
2/7	0.780	0.952	0.996	0.987	0.961	-0.259
1/3	0.786	0.925	0.993	0.980	0.940	-0.397
3/8	0.794	0.893	0.990	0.971	0.914	-0.558
2/5	0.799	0.869	0.988	0.965	0.895	-0.677
1/2	0.833	0.721	0.974	0.921	0.772	-1.345
3/5	0.897	0.445	0.941	0.825	0.530	*
5/8	0.919	0.349	0.927	0.786	0.441	*
2/3	0.961	0.168	0.897	0.696	0.261	*
5/7	1.011	-0.048	0.841	0.540	0.014	*
3/4	1.039	-0.167	0.777	0.362	-0.170	*
10/13	1.044	-0.193	0.729	0.235	-0.245	*
5/6	1.003	-0.013	0.454	-0.417	-0.092	*
1/1	1.000	-	-	-	-	*

Table 2.11.2 The accelerated circular-orbit binary-encounter reduced ionization cross section σ^{QIF} for $\bar{e}$-H and $\bar{e}$-(H-like ion) collisions together with several interference parameters versus $t=n/(n+Z)$ for the case $\mathcal{E}=2$. See text.

of Vriens to the interference bound. R_A is the ratio of the interference term σ_A^{QIF} to the bound σ^{QIB}, where σ_A^{QIF} is obtained by integrating $\frac{d\sigma_A^{QIF}}{d\Delta E}$ numerically over ΔE, using an equally-spaced formula. R_C is the ratio of the expression $\sigma_C^{QIF}/\sigma^{QIB}$ proposed by Vriens and given by equation (2.9.14). It should be noted that the ratio R_B given by $\sigma_B^{QIF}/\sigma^{QIB}$ is just R by construction.

Again, the ratios R_A and R_C are accurate only over a limited range of small t where the bound itself is probably sufficiently close. For values of t close to unity R_C oscillates rapidly between -1 and 1 whereas the exact values of R oscillate with a damped amplitude. The behaviour of R is similar to that of A_o. Hence for $t \gtrsim \frac{1}{2}$ no simple analytic approximations may be expected to be found.

The Fock-averaged symmetrised accelerated total interference contribution for $t = \frac{1}{2}$ is given by equation (2.9.33). This term has an analytic bound given by equation (2.9.32). Numerical values of this interference term have been calculated using the crude and control Monte-Carlo estimates of the four-dimensional integrals required. These estimates are given by equations (3.1.51) and (3.1.74) respectively, where the bound obtained by replacing the function g, given by equation (2.6.32), by the simpler expression $\tilde{g}$, given by equation (2.6.35), has been used as the control. At each incident energy five hundred function values corresponding to less than five in each dimension were selected. The statistical errors from the control method were found to be smaller

than those of the crude estimate by approximately a factor of three, yielding a reduction by a factor of nine in computing time over the crude method of comparable accuracy. The results are shown in figure (2.11.3). Also displayed are the velocity-averaged bound, the unaveraged interference estimate and the empirical bound obtained by symmetrising the Thomson formula, given by equation (2.9.18) with $E_2 = 0$.

It is worth noting that for large $\mathcal{E}$ the high-energy limit of the direct, interference and exchange contributions given by equations (2.9.29), (2.9.32) and (2.9.30) are $\frac{20}{3}\mathcal{E}^{-1}$, $4\mathcal{E}^{-2}\log\mathcal{E}$ and $4\mathcal{E}^{-2}$ respectively, in units of πa_0^2, so that the interference contribution is larger here than the exchange term. This is expected since the interference bound in the basic Mott formula given by equations (2.4.6), (2.4.7) and (2.4.9), is the geometric mean of the direct and exchange contributions.

The equations of the unaveraged symmetric accelerated model of Vriens (1966b) have been applied by Tripathi, Mathur and Joshi (1969) to ionization and excitation of several non-hydrogenic atoms. However, since the interference term σ_C^{QIF} , which they use, is not reliable, and since they did not compare either with the unsymmetric model of Stabler (1964) or the direct, exchange and interference contributions separately, it is difficult to assess the significance of including the exchange and interference contributions.

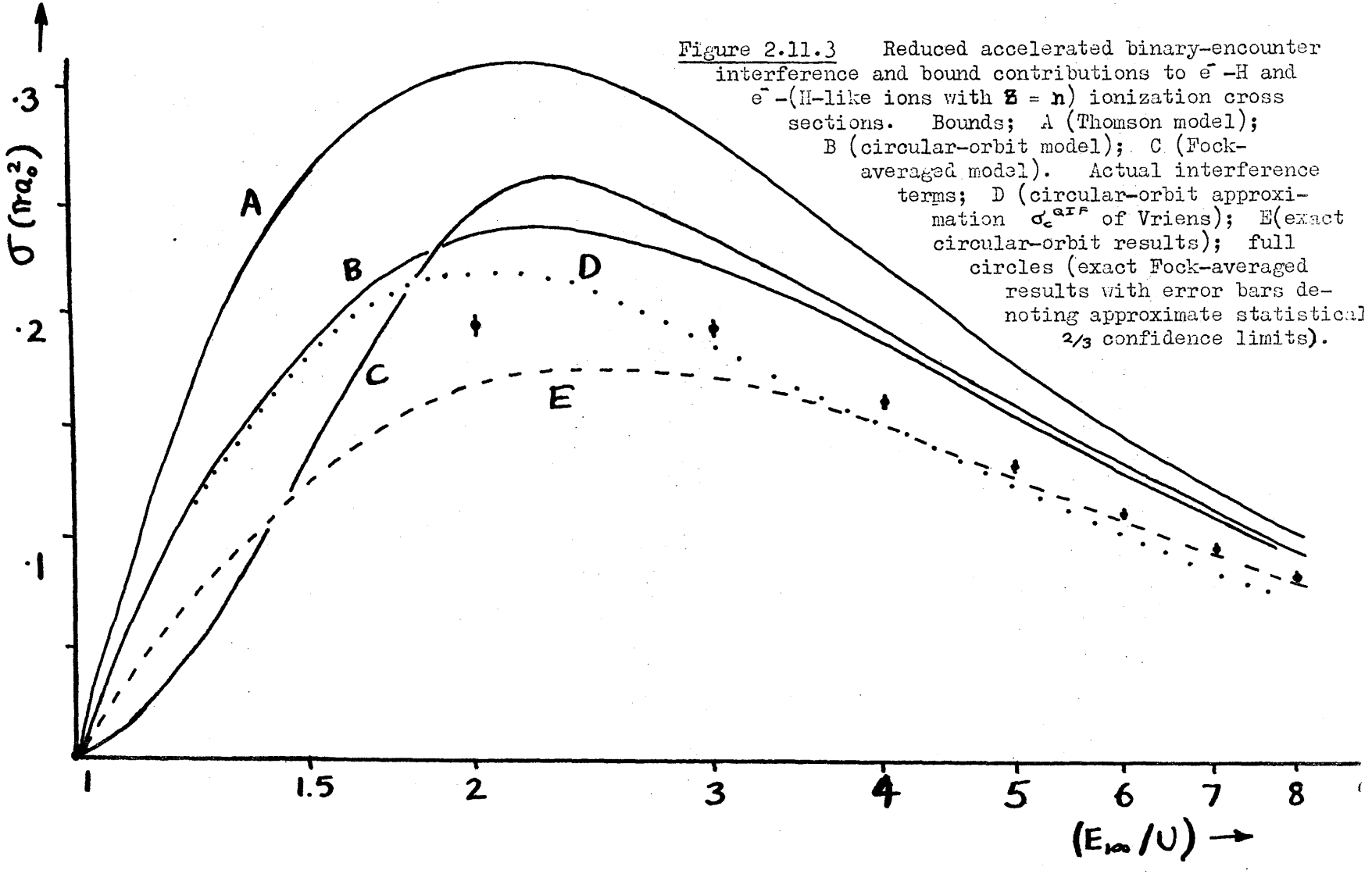

Figure 2.11.3 Reduced accelerated binary-encounter interference and bound contributions to e^--H and e^--(H-like ions with $Z = n$) ionization cross sections. Bounds; A (Thomson model); B (circular-orbit model); C (Fock-averaged model). Actual interference terms; D (circular-orbit approximation σ_c^{AIF} of Vriens); E(exact circular-orbit results); full circles (exact Fock-averaged results with error bars denoting approximate statistical 2/3 confidence limits).

CHAPTER 3

MONTE-CARLO ORBIT-INTEGRATION THEORY

3.1 A Review of the Theory

In the important special case of three charged particles the theory is described fully by Abrines and Percival (1966a,b) and by Valentine (1968). This theory has also been outlined by McDowell and Coleman (1970). The more general theory for arbitrary particle-particle interactions is reviewed by Burgess and Percival (1968). In order to avoid excessive cross-referencing the relevant parts of the theory are discussed below, using a terminology developed by Banks, Percival and Wilson (1971, 1972b,c).

(a) The Geometry of an N – Particle System.

In this theory a particle is supposed to have no shape or internal structure which affects its interaction and all N particles are assumed to be distinguishable. In order to describe the positions and velocities of all the particles at any time it is convenient to define a body as a non-empty set of particles. In particular a simple body is a particle, a composite body consists of two or more particles and a K- particle body has exactly K particles. Two bodies are distinct if there is a particle in one body which does not belong to the other. Two bodies are disjoint if there are no particles belonging to both. Since the empty set of particles is not a body and since each particle may or may not belong to a body there are $NB = 2^N - 1$ distinct bodies in an N – particle system and there are $\binom{N}{K}$ distinct K– particle bodies

where $\binom{N}{K}$ is the well-known binomial coefficient.

Each body may be labelled by a positive integer I where $1 \leq I \leq NB$. In particular the labels may be ordered so that the label of a K_1 – particle body is smaller than the label of a K_2 – particle body if $K_1 < K_2$. If $K_1 = K_2$ there is no natural order but, once the particles have been arbitrarily ordered with labels $I = 1, N$, a particular order within the K_1 – particle bodies may be suggested by symmetry arguments. Thus, in the 3 – particle system the seven bodies can be labelled so that 1, 2 and 3 are the particles, 4, 5 and 6 are the 2 – particle bodies $(2,3)$, $(3,1)$ and $(1,2)$, and 7 is the 3 – particle body $(1,2,3)$.

In the N – particle system each body I has a mass m_I which is defined as the sum of the masses of its constituent particles. At a given time t each body I also has a position $\underline{r}_{LI}$ and a velocity $\underline{v}_{LI}$ in an arbitrary Galilean rectangular cartesian frame of reference L. The position and velocity of a composite body are defined as the position and velocity of the centre of mass of its constituent particles.

In addition to the laboratory coordinates $\underline{r}_{LI}$, $\underline{v}_{LI}$ of each body I, it is also convenient to introduce relative coordinates between disjoint bodies. The relative coordinates between bodies which are not disjoint are not usually required since these bodies overlap. The number NR of sets of relative coordinates of position and velocity is not trivial to obtain, but can be determined by considering the square array of distinct-body labels against distinct-body labels. The value of NR is obviously less than the number of array elements lying above the diagonal

of this square array. Since the body (2^N-1) contains all the particles, it is not disjoint with any other body and hence the final row and column of the array can also be deleted. Then

$$NR \leq (2^{N-1}-1)(2^N-3) .$$

The precise value of NR can be found by considering the possible number of relative coordinates between K_1 – particle bodies and disjoint K_2 – particle bodies. Then

$$NR = \sum_{K_1=1}^{N-1} \left[\left\{ \sum_{K_2=1}^{K_1-1} \binom{N-K_1}{K_2} \right\} + \frac{1}{2} \binom{N-K_1}{K_1} \right], \tag{3.1.1}$$

where the binomial factor $\binom{I}{J}$ is zero for $I<J$ and $\sum_{K=I}^{J} a_K$ is to be interpreted as zero if $J<I$. The factor $\frac{1}{2}$ multiplying the term $\binom{N-K_1}{K_1}$ is necessary to avoid counting cases in which $K_1 = K_2$ twice. For $N = 1, 2, 3, 4$ and 5 the values of NR are $0, 1, 6, 25$ and 90 .

As in the case of the laboratory coordinates, the relative coordinates may be labelled by RI , $I = 1, NR$. The labelling may be arranged so that the label for a relative coordinate between a K_1– particle body and a disjoint (K_1+K_2)-particle body is less than the label for a relative coordinate between a K_3– particle body and a disjoint (K_3+K_4)-particle body if $K_3>K_1$. If $K_3=K_1$ then $K_4>K_2$. If $K_1=K_3$ and $K_2=K_4$ there is no natural order, but as in the laboratory-coordinate case, a particular ordering may be suggested by symmetry arguments. In the 3– particle system the six relative-coordinate labels are defined by the pairs of disjoint bodies $(2,3), (3,1), (1,2), \{1,(2,3)\}$, $\{2,(3,1)\}$ and $\{3,(1,2)\}$. Hence

$$\left.\begin{aligned} \underline{r}_{R1} &= \underline{r}_{L2} - \underline{r}_{L3} \\ \underline{v}_{R1} &= \underline{v}_{L2} - \underline{v}_{L3} \end{aligned}\right\} , \tag{2.1.2}$$

etc. The convention governing the signs in equation (3.1.2) is arbitrary, but must be used consistently.

Each set of relative coordinates RI has an associated relative body I whose mass m_{RI} is equal to the reduced mass of the two disjoint bodies from which the relative body is formed.

It can be seen that the list of useful bodies and relative bodies and their positions and velocities at any instant may be formidable. However, not all these vectors are required to determine the motion of the $N-$ particle system at all times. The motion of the system can be obtained if a time t and the positions and velocities of all the particles at that time are prescribed, for then, Newton's equations of motion can be solved, provided all the particle-particle interactions are known. The set of $(6N+1)$ real numbers defines the classical state of the $N-$ particle system in the laboratory representation. This state may be regarded as a point in a $(6N+1)$ dimensional space. The motion of this point is determined by Newton's equations of motion. Any equivalent set of $(6N+1)$ or more real numbers which also defines this point defines the state. Useful alternative sets of numbers may be termed representations. In particular the standard representation may be defined as the set consisting of the time t , the laboratory position and velocity of body (2^N-1) together with all the relative positions and velocities of the particles. The equations of motion are simpler in this representation, since the motion of the centre of mass (2^N-1) may be solved independently of the relative motion and since the particle-particle interactions depend on the relative

positions and velocities only. The laboratory and standard representations are extreme cases of the useful representations. The laboratory representation is most useful when the particles are all sufficiently far apart from one another for the interactions to be negligible. Intermediate cases are also possible. To describe the intermediate cases it is convenient to define an arrangement of the $N-$ particle system as an exhaustive set of mutually disjoint bodies. Thus, no particle is common to any two bodies, yet every particle is included in some body. For each distinct arrangement a representation can be defined by the set of real numbers consisting of the time t and standard representations of each of the disjoint bodies at that time where, for this purpose, each body may be regarded as an independent $K-$ particle system, where K is equal to the number of particles in the relevant body. In the special case in which $N=1$ the standard representation is identical to the laboratory representation. The total number of such representations can be determined as the number of ways N distinguishable particles can be placed independently into N boxes without regard to the order of the boxes or the order of the particles within each box. The total number of representations N_{REP} of the $N-$ particle system under this scheme is therefore given by

$$N_{REP} = \sum_{\substack{\text{all cases } a_i \\ \text{such } \sum a_i = N,\ a_i \geq 0}} (N; a_1, a_2, \dots, a_N) , \qquad (3.1.3)$$

where $(N; a_1, a_2, \dots, a_N)$ is the multinomial coefficient defined and tabulated by Abramowitz and Stegun (1965 pp. 823 and 831). N_{REP} is also given by

$$N_{REP} = \sum_{m=1}^{N} \mathcal{S}_N^{(m)} , \qquad (3.1.4)$$

where $\mathcal{S}_N^{(m)}$ is a Stirling number of the second kind and defined and tabulated by Abramowitz and Stegun (1965, pp. 824 and 835).

Alternative representation schemes are possible but may not generalise easily and efficiently for systems of more particles. The present scheme is identical to that used by Abrines and Percival (1966a) for $N=3$, in the case of the standard and laboratory representations, but is different for the intermediate $(2+1)$ – particle representations, though the arrangements are identical. They chose the $(2+1)$- particle representation I to consist of the laboratory position and velocity of the centre of mass 7 at time t, together with the relative positions and velocities $\underline{r}_{RI}$ and $\underline{v}_{RI}$ between particles J and K, and $\underline{r}_{R(I+3)}$ and $\underline{v}_{R(I+3)}$ between particle I and body $(I+3)$, where I, J and K are cyclic permutations of $(1,2,3)$, which will be written henceforth in the form $[(I,J,K)]$. In the natural extension of their scheme to the N – particle system the representation of a general arrangement of disjoint bodies consists of the relative positions and velocities between all particles in each disjoint composite body, as in the present scheme, together with the relative positions and velocities between all disjoint bodies at some time t, and, finally, the laboratory position and velocity of the centre of mass (2^N-1) of the N – particle system at that time. This scheme has the advantage that all important relative positions and velocities are immediately available for computational purposes, but suffers from the disadvantage that the intermediate representations do not factorise into a sum of independent standard representations for each disjoint body.

The case $N=2$ is also identical in both schemes and

has been treated in Chapter 2 where the symbol C has been used in place of 3 for the centre of mass of the two particles.

Neither of these schemes is exhaustive in the sense that certain laboratory or relative vectors are excluded from all representations for all $N \geqslant 3$. However, given a representation in either scheme, all other representations and all laboratory and relative vectors of significance can be determined from linear geometrical relations.

(b) The Equations of Motion

Given the forces between the particles and given prescribed initial conditions, the equations of motion of the $N-$ particle system can be solved exactly (usually numerically) in any representation, though, in practice, the equations are simpler in certain representations.

Thus, in the case of an isolated system of three particles with charges z_1, z_2 and z_3 the equations of motion in the laboratory representation are

$$\left.\begin{aligned} \dot{\underline{r}}_{LI} &= \underline{v}_{LI} \\ \dot{\underline{v}}_{LI} &= f_{LII}\,\underline{r}_{LI} + f_{LIJ}\,\underline{r}_{LJ} + f_{LIK}\,\underline{r}_{LK} \end{aligned}\right\}, \qquad (3.1.5)$$

where

$$f_{LII}(\underline{r}_{L1}, \underline{r}_{L2}, \underline{r}_{L3}) = N_I\left(\frac{z_I z_J}{r_{RK}^3} - \frac{z_K z_I}{r_{RJ}^3}\right), \qquad (3.1.6)$$

$$f_{LIJ}(\underline{r}_{L1}, \underline{r}_{L2}, \underline{r}_{L3}) = -N_I \cdot \frac{z_I z_J}{r_{RK}^3}, \qquad (3.1.7)$$

$$f_{LIK}(\underline{r}_{L1}, \underline{r}_{L2}, \underline{r}_{L3}) = N_I \cdot \frac{z_K z_I}{r_{RJ}^3}, \qquad (3.1.8)$$

$$\underline{r}_{RI} = \underline{r}_{LJ} - \underline{r}_{LK} \quad , \tag{3.1.9}$$

and

$$N_I = 1/m_I \quad , \tag{3.1.10}$$

for $I = 1, 2$ and 3 and all $[\{I,J,K\}]$. Equations (3.1.5) constitute eighteen coupled first-order non-linear differential equations, which partition into three independent sets of six coupled equations of motion for each particle separately, if the nine functions $f_{LMM'}$ satisfy the conditions

$$f_{LMM'}(\underline{r}_{L1}, \underline{r}_{L2}, \underline{r}_{L3}) = \delta_{MM'} f_{LM}(\underline{r}_{LM}) \quad , \tag{3.1.11}$$

for all M and $M' = 1,2,3$, where $\delta_{MM'}$ is the well-known Kronecker delta symbol. These conditions are equivalent to the condition that the nine coupling terms $g_{LMM'}(\underline{r}_{L1}, \underline{r}_{L2}, \underline{r}_{L3})$ where

$$g_{LMM'} = f_{LMM'} - \delta_{MM'} f_{LM}(\underline{r}_{LM}) \quad , \tag{3.1.12}$$

for all $M, M' = 1,2,3$ are all identically zero, which is only true either if the charges are all zero or else the masses are all infinite. In either case the particles move uniformly since then $f_{LM}(\underline{r}_{LM})$ is also zero for $M = 1,2,3$. Even if the coupling terms are not all zero the equations of motion (3.1.5) partition approximately if the $g_{MM'}$ are all sufficiently small, which is true when the distances between all three particles are sufficiently large.

In the standard representation the equations of motion are

$$\left.\begin{aligned} \dot{\underline{r}}_{L7} &= \underline{v}_{L7} \\ \dot{\underline{v}}_{L7} &= \underline{0} \end{aligned}\right\} \quad , \tag{3.1.13}$$

for the uniform motion of the centre of mass 7 together with the

independent equations of motion of particle J **relative to** K, and K **relative to** I, say,

$$\left.\begin{aligned} \dot{\underline{r}}_{RI} &= \underline{v}_{RI} \\ \dot{\underline{v}}_{RI} &= f_{RII}\,\underline{r}_{RI} + f_{RIJ}\,\underline{r}_{RJ} \end{aligned}\right\}, \tag{3.1.14}$$

and

$$\left.\begin{aligned} \dot{\underline{r}}_{RJ} &= \underline{v}_{RJ} \\ \dot{\underline{v}}_{RJ} &= f_{RJI}\,\underline{r}_{RI} + f_{RJJ}\,\underline{r}_{RJ} \end{aligned}\right\}, \tag{3.1.15}$$

where

$$\underline{r}_{RI} + \underline{r}_{RJ} + \underline{r}_{RK} = \underline{v}_{RI} + \underline{v}_{RJ} + \underline{v}_{RK} = \underline{0}\ , \tag{3.1.16}$$

$$f_{RII}(\underline{r}_{RI}, \underline{r}_{RJ}) = N_{RI}\,\frac{z_J z_K}{r_{RI}^3} + N_J\,\frac{z_I z_J}{r_{RK}^3}\ , \tag{3.1.17}$$

$$f_{RIJ}(\underline{r}_{RI}, \underline{r}_{RJ}) = N_J\,\frac{z_I z_J}{r_{RK}^3} - N_K\,\frac{z_K z_I}{r_{RJ}^3}\ , \tag{3.1.18}$$

$$f_{RJI}(\underline{r}_{RI}, \underline{r}_{RJ}) = N_I\,\frac{z_I z_J}{r_{RK}^3} - N_K\,\frac{z_J z_K}{r_{RI}^3}\ , \tag{3.1.19}$$

$$f_{RJJ}(\underline{r}_{RI}, \underline{r}_{RJ}) = N_{RJ}\,\frac{z_K z_I}{r_{RJ}^3} + N_I\,\frac{z_I z_J}{r_{RK}^3}\ , \tag{3.1.20}$$

and

$$N_{RI} = 1/m_{RI}\ , \tag{3.1.21}$$

for $[\{I, J, K\}]$. The twelve coupled equations of relative motion (3.1.14) and (3.1.15) are simpler to solve than the laboratory form (3.1.5). They partition into two independent sets of six coupled equations for the motion of particles J and K separately relative to particles K and I, if the coupling terms

$$g_{RMM'}(\underline{r}_{RI}, \underline{r}_{RJ}) = f_{RMM'}(\underline{r}_{RI}, \underline{r}_{RJ}) - \delta_{MM'} f_{RM}(\underline{r}_{RM}), \tag{3.1.22}$$

for $M, M' = I, J$.

all are zero, which is true as in the laboratory cases, and in the two additional cases $Z_I = N_K = 0$ with $N_J \neq 0$, and $N_K = Z_J = 0$ with $N_I \neq 0$, which correspond respectively to uniform motion of particle I or J relative to particle K, of infinite mass, together with non-uniform motion of particle J or I relative to K. The solution of the latter two-particle problem is discussed in chapter 2. Even if the coupling terms are not all zero, the equations of relative motion partition approximately, if all the coupling terms are sufficiently small. These conditions are satisfied by a classical model of a highly-charged helium-like ion when $r_{R1} \sim r_{R2} \sim r_{R3}$.

The equations of motion in the $(2+1)$ - particle representation I of Abrines and Percival may be written

$$\left.\begin{aligned} \dot{\underline{r}}_{L7} &= \underline{v}_{L7} \\ \dot{\underline{v}}_{L7} &= \underline{0} \end{aligned}\right\} ,$$

as above, together with the equations of motion of particle J relative to particle K, and of particle I relative to body $(I+3)$, the centre of mass of J and K,

$$\left.\begin{aligned} \dot{\underline{r}}_{RI} &= \underline{v}_{RI} \\ \dot{\underline{v}}_{RI} &= f_{RII}\,\underline{r}_{RI} + f_{RI(I+3)}\,\underline{r}_{R(I+3)} \end{aligned}\right\} , \qquad (3.1.23)$$

and

$$\left.\begin{aligned} \dot{\underline{r}}_{R(I+3)} &= \underline{v}_{R(I+3)} \\ \dot{\underline{v}}_{R(I+3)} &= f_{R(I+3)I}\,\underline{r}_{RI} + f_{R(I+3)(I+3)}\,\underline{r}_{R(I+3)} \end{aligned}\right\} , \qquad (3.1.24)$$

where

$$N_J \underline{r}_{RJ} = -N_J \underline{r}_{R(I+3)} - N_{(I+3)}\,\underline{r}_{RI} , \qquad (3.1.25)$$

$$\underline{r}_{RK} = -\underline{r}_{RI} - \underline{r}_{RJ} , \qquad (3.1.26)$$

$$f_{RII}\{\underline{r}_{RI}, \underline{r}_{R(I+3)}\} = N_{RI}\frac{Z_J Z_K}{r_{RI}^3} + m_J N_K N_{(I+3)}\frac{Z_K Z_I}{r_{RJ}^3} + m_K N_J N_{(I+3)}\cdot\frac{Z_I Z_J}{r_{RK}^3}, \quad (3.1.27)$$

$$f_{RI(I+3)}\{\underline{r}_{RI}, \underline{r}_{R(I+3)}\} = N_K\frac{Z_K Z_I}{r_{RJ}^3} - N_J\frac{Z_I Z_J}{r_{RK}^3}, \quad (3.1.28)$$

$$f_{R(I+3)I}\{\underline{r}_{RI}, \underline{r}_{R(I+3)}\} = N_{R(I+3)}\, m_{RI}\, f_{RI(I+3)}, \quad (3.1.29)$$

and

$$f_{R(I+3)(I+3)}\{\underline{r}_{RI}, \underline{r}_{R(I+3)}\} = N_{R(I+3)}\frac{Z_K Z_I}{r_{RJ}^3} + N_{R(I+3)}\frac{Z_I Z_J}{r_{RK}^3}, \quad (3.1.30)$$

for all $[\{I, J, K\}]$.

The twelve equations of relative motion (3.1.23) and (3.1.24) partition into two independent sets of six coupled equations for the motion of particle J relative to particle K and, separately, of particle I relative to body $(I+3)$ if the four coupling terms

$$g_{RMM'}\{\underline{r}_{RI}, \underline{r}_{R(I+3)}\} = f_{RMM'} - \delta_{MM'} f_{RM}(\underline{r}_{RM}), \quad (3.1.31)$$

for $M, M' = I, (I+3)$, are all zero, which is true, as in the laboratory and standard representation cases, and in the additional case $Z_I = 0$ (without the restriction $N_K = 0$) which corresponds to uniform motion of particle I relative to body $(I+3)$. Even if the coupling terms are not all zero, these equations of relative motion partition approximately when the $g_{RMM'}$ are all sufficiently small, as is the case for a classical hydrogenic atom or ion weakly perturbed by a distant charged particle.

The system of twelve coupled equations of relative motion (3.1.14) and (3.1.15) in the standard representation was selected by Abrines and

Percival for direct numerical computation. Although these equations can be reduced to a system of only six coupled first-order non-linear differential equations by elimination of the constants of the motion and the time (Whittaker 1965, chapter 13), the resulting differential equations are considerably more complicated and so may not be more efficient for numerical work.

In the general case of an N - particle system the coupling terms of the equations of motion in any representation may be defined similarly. If the coupling terms are sufficiently small the solution of the equations of motion may be determined to any degree of accuracy by direct numerical methods or by perturbation expansions (see, for example, Born 1960) of which the zeroth-order expansion is the exact solution when the coupling terms are all zero. In general the exact numerical solution and the perturbation expansion of any finite order will differ, even if only insignificantly, and so it is convenient to distinguish them by introducing the concept of a classical channel of an N - particle system as an arrangement of the system together with prescribed coupling terms, possibly approximate. In particular, for each arrangement there are two important channels, the full-interaction channel, in which all the coupling terms are calculated exactly from the prescribed particle-particle interactions, and, in the other extreme, the non-coupling channel, in which the coupling terms are neglected. Intermediate channels, in which some coupling terms may be included exactly, but others only included approximately or even neglected, may also be useful. Thus given the state of an N -particle system at some time t , each distinct channel may lead to a different state at any time t' . A selection of channels, including a full-interaction

channel, is particularly useful for numerical work, since it is possible, in principle, to choose an optimum channel at any time t, so that the error in the solution satisfies prescribed error bounds, and so that the evolution of the state is most easily achieved. After a finite time interval the error in the solution in the optimum channel may exceed the error conditions, since the coupling terms will generally vary with time. However, a different optimum channel can now be chosen and the solution can be extended in this way to any time t' .

In the case of a collision between two disjoint bodies A and B the error in the corresponding non-coupling channel tends to zero as the time t' tends to minus infinity. In this initial scattering channel the bodies A and B form two separate isolated particle systems, each of which may have well-defined constants of the separated motion. The initial scattering state can then be subdivided according to the values of such constants of the motion. After the collision between bodies A and B, the system will usually partition into a disjoint set of bodies C , D ,..... each of which will form an isolated particle system as the time t' tends to infinity. The corresponding non-coupling channel is termed the final scattering channel, which can also be subdivided according to the values of the constants of the separated motion.

In the case of a collision between a charged particle 1 and a bound pair of charged particles $(2,3)$, in which particle 2 has a charge of opposite sign to that of particle 1 , say, the possible final scattering channels are the <u>direct</u> channel denoted by

$$1 + (2,3) \longrightarrow 1 + (2,3) \quad , \qquad (3.1.32)$$

the ionization channel

$$1 + (2,3) \longrightarrow 1 + 2 + 3 \quad , \tag{3.1.33}$$

and the exchange channel

$$1 + (2,3) \longrightarrow (1,2) + 3 \quad . \tag{3.1.34}$$

It is useful to distinguish the direct-ionization channel, in which particle 2 remains closer to particle 3, and the exchange-ionization channel, in which particle 2 is finally closer to particle 1. Each of the final channels can be subdivided according to the relative velocities of the disjoint bodies and the binding energy and angular momentum of the closest pair of particles.

(c) Formal Classical Scattering Theory

The formal classical scattering theory described by Burgess and Percival (1968) is useful for numerical work. Let the classical state at time t be $X(t)$. Let $U(t,t')$ be the classical evolution operator, that is, the operator which relates the exact solution $X(t)$ at time t to the exact solution $X(t')$ by

$$U(t,t')\,X(t') = X(t) \quad . \tag{3.1.35}$$

Let the evolution operator in the non-coupling channel I be $U_I(t,t')$. Then the classical scattering operator S_{FI}, which relates the initial scattering channel I to the final scattering channel F, may be defined by

$$S_{FI} = \lim_{\substack{t_+ \to \infty \\ t_- \to -\infty}} U_F(t_0,t_+)\,U(t_+,t_-)\,U_I(t_-,t_0) \quad . \tag{3.1.36}$$

Apart from border-line cases the final channel F can be determined uniquely. The classical scattering operator S_{FI} is well-behaved in the limits $t_- \to -\infty$ and $t_+ \to \infty$, provided the long-range forces between the disjoint bodies in the initial and final channels fall off faster than the inverse-square law. If this is the case, S_{FI} relates two artificial states $X_I(t_o)$ and $X_F(t_o)$, the initial and final reference states, say, at the same arbitrary time t_o by

$$X_F(t_o) = S_{FI}\, X_I(t_o) . \qquad (3.1.37)$$

If the long-range forces do not fall to zero faster than the inverse-square law, the difference between the coordinates in the states $X_I(t_o)$ and $X_F(t_o)$ will usually be infinite, corresponding to an infinite time delay in the collision. For such forces it may be possible to construct modified evolution operators $U_I'(t_-,t_o)$ and $U_F'(t_o,t_+)$ to incorporate the long-range behaviour exactly. Thus, for example, in the case of charged particles incident upon target classical hydrogenic ions, $U_I'(t_-,t_o)$ may be chosen to treat the separate motions of the bound ion system and of the incident particle in the overall charge of the target ion. This motion does not correspond to an exact non-coupling channel, but rather to an approximate non-coupling channel for large separations of the disjoint bodies. In terms of these modified evolution operators the classical scattering operator S_{FI} may be constructed similarly and is well-defined.

If the coupling terms in the initial channel I are negligible throughout the collision then $U(t_+,t_-)$ may be replaced by $U_I(t_+,t_-)$ in equation (3.1.36) and hence

$$S_{FI} = \delta_{FI} , \qquad (3.1.38)$$

and the system passes through the artificial reference state $X_I(t_o)$ at time t_o .

It should be noted that the limits in equation (3.1.36) are only taken after all three successive evolutions have been achieved. Hence only approximate initial and final scattering states $X_I(t_-)$ and $X_F(t_+)$ are needed to obtain $X_F(t_o)$ from $X_I(t_o)$, where

$$X_I(t_-) = X(t_-) = U_I(t_-,t_o)\,X_I(t_o) \,, \qquad (3.1.39)$$

and

$$X_F(t_+) = X(t_+) = U(t_+,t_-)\,X(t_-) \,. \qquad (3.1.40)$$

Indeed, if $X_I(t_-)$ or $X_F(t_+)$ includes any internal coordinates which are not conserved in the respective non-coupling channel, it is meaningless to consider exact initial or final scattering states, since the limits of such internal coordinates do not exist. The initial conditions for an individual orbit are therefore prescribed in the initial reference state $X_I(t_o)$, which may be used to generate sequences of initial and final scattering states which lead to a convergent sequence of final reference states. In spite of the fact that the limit of the sequence of final reference states cannot be evaluated in numerical work, the formal theory affords a practical method of determining numerical solutions for individual orbits.

The time t_o in equation (3.1.36) is arbitrary, but, in practice, the initial conditions in the initial reference state may be used to predict approximate properties of the collision, if t_o is chosen to be the time of closest approach of the colliding disjoint bodies A and B in the non-coupling initial channel I .

(d) Classical Models and Cross Sections.

In applications of classical orbit-integration techniques to atomic and molecular collision processes the uncertainty principle prevents an accurate knowledge of any classical state. In the quantum theory this uncertainty leads naturally to a statistical interpretation of atomic and molecular phenomena. Since the classical theory leads to definite results, once the initial conditions have been specified, the desired statistical properties must be introduced into the initial conditions. This is achieved by treating the classical collision model as an ensemble of similar collisions in which the initial conditions are selected from suitable distributions.

In the important case of collisions of a uniform monoenergetic beam of disjoint bodies A with a stationary target body B, a general expression for the distribution $\rho(X_I)$ of initial conditions has been given by Burgess and Percival (1968). They obtained

$$\rho(X_I) = \rho_A(X_A)\,\rho_B(X_B)\,\delta(\underline{r}_B)\,\delta(\underline{v}_B)\,\frac{1}{v_A}\,\delta(\underline{v}_A - v_A\hat{\underline{z}}), \quad (3.1.41)$$

where the position of the centre of mass $\underline{r}_B$ of the target system is chosen at the origin of a fixed laboratory cartesian frame of reference whose $\hat{\underline{z}}$ axis is oriented along the direction of the incident velocity $\underline{v}_A$. The distributions $\rho_A(X_A)$ and $\rho_B(X_B)$ are the distributions of initial conditions specifying the internal motion of the respective isolated systems. These distributions are chosen to represent the physical systems as reasonably as possible. In most cases $\rho_A(X_A)$ and $\rho_B(X_B)$ are stationary and isotropic. In the case of a hydrogenic atom or ion the

distribution is taken to be the classical microcanonical model

$$\rho_H(X_H) = K\,\delta\left(\frac{1}{2}m v^2 - \frac{Ze^2}{r} - E\right), \qquad (3.1.42)$$

where m, r and v are respectively the reduced mass, the relative distance and relative speed of the electron and nucleus of the hydrogenic atom or ion, Ze is the charge on the nucleus, E is the total energy and K is a normalisation constant. Other models are possible. In particular, the Bohr-Sommerfeld model has also been widely used. The contrasting merits of such models are discussed in section (4.1).

The distribution $\rho(X_I)$ is defined at the approximate initial scattering state $X_I(t_-)$. The corresponding distribution at the initial reference state is simple to determine if the force between bodies A and B falls off faster than the inverse-square law. In this case for stationary $\rho_A(X_A)$ and $\rho_B(X_B)$,

$$\rho\{X_I(t_o)\} = \rho\{X_I(t_-)\}. \qquad (3.1.43)$$

Otherwise,

$$\rho\{X_I(t_o)\} = \rho_A(X_A)\rho_B(X_B) f(\underline{r}_A, \underline{r}_B, \underline{v}_A, \underline{v}_B), \qquad (3.1.44)$$

where the distribution $f(\underline{r}_A, \underline{r}_B, \underline{v}_A, \underline{v}_B)$ defined at time t_o may be derived from the standard distribution $\delta(\underline{r}_B)\,\delta(\underline{v}_B)\,\frac{1}{v_A}\,\delta(\underline{v}_A - v_A\hat{\underline{z}})$ defined in the limit as t_- tends to minus infinity, using the classical theory of scattering of two bodies A and B whose motion is governed by the evolution operator $U_I'(t_o, t_-)$.

In the absence of any interaction body A will cross the $(\hat{\underline{x}}, \hat{\underline{y}})$ plane at the impact-parameter vector $\underline{b} = (b\cos\phi_b, b\sin\phi_b, 0)$. Let $\tilde{X}_I(t_o)$ be the set of initial conditions, which, together with the

time t_o , the variables b and ϕ_b and any constants of the distributions $\rho_A(X_A)$ and $\rho_B(X_B)$ (such as the binding energies), make up the initial reference state $X_I(t_o)$. Let $P_{b\phi_b I}(F)$ be the mean probability that the prescribed initial channel I leads to a final channel F for fixed b and ϕ_b . Then

$$P_{b\phi_b I}(F) = \int d\tilde{X}\, \rho(\tilde{X})\, H(F;I) \quad , \qquad (3.1.45)$$

where $H(F;I)$ is unity if $X_I(t_o)$ leads to channel F , and is zero otherwise. The total cross section for the production of channel F from initial channel I is given by

$$\sigma_I(F) = \int_o^\infty db\, b \int_0^{2\pi} d\phi_b\, P_{b\phi_b I}(F) \, . \qquad (3.1.46)$$

Let C be any function of the initial and final reference states. Then the differential cross section for the variable C is given by

$$\frac{d\sigma_I(F)}{dC} = \sigma_I(F;C) = \int_o^\infty db\, b \int_0^{2\pi} d\phi_b\, P_{b\phi_b I}(F;C) \, , \qquad (3.1.47)$$

where

$$P_{b\phi_b I}(F;C_o) = \int d\tilde{X}\, \rho(\tilde{X})\, H(F;I)\, \delta\{C_o - C(X_I, X_F)\} \, . \qquad (3.1.48)$$

Equations (3.1.47) and (3.1.48) may be generalised to include multiple-differential cross sections $\sigma_I(F;C_1,C_2,\ldots)$ for prescribed values of $C_1, C_2, \ldots\ldots$.

If either A or B is composite then, in general, $H(F;I)$ is an unknown function of $X_I(t_o)$, since it is necessary to determine the solution of a three-or-more particle problem in order to evaluate

$H(F;I)$. Thus the cross sections $\sigma_I(F)$, $\sigma_I(F;C)$ and $\sigma_I(F;C_1,C_2,\ldots)$ must be determined numerically. Numerical methods based upon Simpson, Gauss-Laguerre and related techniques (see for example, Buckingham 1962) are unsuitable for two important reasons. Firstly, if the number of dimensions of integration D in equation (3.1.46) is large, then the rate of convergence for such methods is of order $N^{\alpha/D}$ where N is the number of function evaluations and α is a fixed parameter, close to unity and dependent upon the numerical formula used (see, for example, Schreider 1964, chapter II). Secondly, in order to determine the differential cross sections, an elaborate and time-consuming search procedure may be required to find orbits with prescribed values of $C_1,C_2,\ldots$. In contrast, the Monte-Carlo method of numerical integration (see, for example, Hammersley and Handscomb 1964 and Schreider 1964) has a rate of convergence of order $N^{-1/2}$ for large N and all values of D . Furthermore, the function values used to determine the total cross section $\sigma_I(F)$ may also be utilised to determine all differential cross sections in the form of approximate unbiased differential distributions, whose characteristic parameters are accurate to order $N_F^{-1/2}$, where N_F is the total number of orbits which result in final channel F . Thus, in the Monte-Carlo method, the delta-function restrictions for the differential cross sections may be relaxed with the result that the time-consuming search procedures are not required.

(e) The Monte-Carlo Method of Numerical Integration

The method is fully described by Schreider (1964) and by Hammersley and Handscomb (1964). Various refinements have been applied by Abrines,

Percival and Valentine in order to reduce the statistical errors. In order to discuss the relative merits of such refinements the theory is outlined below.

Suppose that

$$\theta_1 = \int_0^1 dx\, f(x) \quad , \tag{3.1.49}$$

and

$$\omega_1 = \int_0^1 dx \left\{ f(x) - \theta_1 \right\}^2 = \int_0^1 dx \left\{ f(x) \right\}^2 - \theta_1^2 \quad , \tag{3.1.50}$$

both exist. Let ξ be a random variable which is uniformly (rectangularly) distributed in the interval $[0,1]$. Then the unbiased crude Monte-Carlo estimate t_1 of θ_1 is given by

$$t_1 = \frac{1}{N} \sum_{i=1}^{N} f(\xi_i) \quad . \tag{3.1.51}$$

The corresponding unbiased estimate w_1 of the variance ω_1 is given by

$$w_1 = \frac{1}{(N-1)} \left[\sum_{i=1}^{N} \left\{ f(\xi_i) \right\}^2 - N t_1^2 \right] \quad . \tag{3.1.52}$$

The standard error δt_1 of the estimate t_1 is given by

$$\delta t_1 = \left(\frac{\omega_1}{N} \right)^{1/2} \simeq \left(\frac{w_1}{N} \right)^{1/2} \quad . \tag{3.1.53}$$

For large N the values of t_1 are distributed normally about θ_1 with standard deviation δt_1 . The standard error δt_1 in t_1 therefore represents approximate $2/3$ confidence limits on t_1 .

The integral θ_1 may be regarded as the area between the curve $y = f(x)$ and the x axis. This area is a special case of an area θ_2 bounded by an arbitrary rectifiable curve Γ with equation $f(x,y) = 0$.

The hit-or-miss Monte-Carlo estimate t_2 is particularly useful for determining the area θ_2 when the boundary Γ is of complicated

form. Suppose that Γ is enclosed in the unit square and that

$$\theta_2 = \int_0^1 dy \int_0^1 dx \; H\{f(x,y)\} \;, \tag{3.1.54}$$

exists, where $H\{f(x,y)\}=1$ if (x,y) lies inside Γ and is zero otherwise. Then

$$\omega_2 = \int_0^1 dy \int_0^1 dx \left[H\{f(x,y)\} - \theta_2 \right]^2 = \theta_2 (1-\theta_2) \;, \tag{3.1.55}$$

also exists. The unbiased hit-or-miss estimate t_2 of θ_2 is given by

$$t_2 = \frac{1}{N} \sum_{i=1}^{N} H\{f(\xi_{2i-1}, \xi_{2i})\} = \frac{M}{N} \;, \tag{3.1.56}$$

where M is the number of points (ξ_{2i-1}, ξ_{2i}) which lie inside Γ. The true distribution of t_2 is binomial. The standard error δt_2 in t_2 is given by

$$\delta t_2 = \left\{ \frac{\theta_2 (1-\theta_2)}{N} \right\}^{1/2} \;, \tag{3.1.57}$$

where θ_2 is, of course, unknown, in general. When N is large and θ_2 is not too extreme, the binomial distribution of t_2 may be approximated by the normal distribution about θ_2 with standard deviation

$$\delta t_2 \simeq \left\{ \frac{t_2 (1-t_2)}{N-1} \right\}^{1/2} . \tag{3.1.58}$$

However, even when N is large, if t_2 is sufficiently close to zero or unity, the normal distribution does not approximate the binomial distribution. The error estimates are then no longer symmetric about t_2 because of the boundary conditions $0 \leq t_2 \leq 1$. If it were true that M tended to a finite value as N tended to infinity, then the distribution of M would be of Poisson form. Although this is not the case, for large N and $M \sim 1$, the Poisson law suggests an error

estimate of the form

$$\delta t_2 \simeq \frac{1}{N} \quad . \tag{3.1.59}$$

In the region between the normal and Poisson limiting forms of the binomial distribution, approximate error estimates are given by Hays (1963, p. 291) and may be written, for small t_2 and large N, in the form

$$t_2^{\pm} \simeq \frac{N}{(N+Z^2)} \left[t_2 + \frac{Z^2}{2N} \pm Z \left\{ \frac{t_2(1-t_2)}{N} + \frac{Z^2}{4N^2} \right\}^{1/2} \right], \tag{3.1.60}$$

where Z is the number of standard deviations required to yield prescribed confidence limits for the normal distribution. Hence, the case $Z=1$ corresponds to approximate $2/3$ confidence limits. It is easy to see that equation (3.1.60) has the correct form in the three limiting cases t_2 tends to zero, Z tends to infinity and $N \gg M \gg 1$. If t_2 is close to unity, then equation (3.1.60) should be applied to $(1-t_2)$.

The arcsine transformation (see for example, Zubin 1935) has also been applied to the case of extreme probabilities in order to obtain error estimates which are approximately independent of θ_2. However, the transformation introduces a small bias of order $1/N$ into the estimate t_2'.

Any integral of the form θ_1 defined in equation (3.1.49) may be expressed in the form θ_2, given by equation (3.1.54) by choosing $H\{f(x,y)\} = H\{f(x)-y\}$ where $H(x)=1$ for $x \geq 0$ and $H(x)=0$, otherwise. However, Hammersley and Handscomb (1964) show, in this case, that the hit-or-miss estimate t_2 has a larger standard error than the crude estimate t_1. Thus, the hit-or-miss techinque should only be applied in preference to the crude method either when the boundary $f(x,y)=0$ cannot be handled easily,

or when several additional integrals of the type

$$\theta_2(c_1, c_2, \cdots, c_K) = \int_0^1 dy \int_0^1 dx\, H\{f(x,y)\}\, \delta\{c_1 - c_1(x,y)\} \cdots \delta\{c_K - c_K(x,y)\}, \quad (3.1.61)$$

have also to be evaluated.

In both cases, since the convergence rate is only $N^{-1/2}$, it is important to investigate possible ways of reducing the variance ω_I and hence the standard error δt_I of an estimate t_I. Hammersley and Handscomb (1964) and Schreider (1964) discuss several methods of variance reduction for the crude estimate t_1. These methods should only be applied with extreme caution to $D-$ dimensional integrals of the crude or hit-or-miss type. Thus, for example, for $D=6$ (as is the case for many of the integrals treated later in this thesis), one-dimensional rules employing 2, 3 or 4 function values, become rules employing 64, 729, and 4096 function values respectively.

In stratified sampling the range of integration of the integral θ_1 is divided into K intervals $h_I = (\alpha_{I-1}, \alpha_I)$, say, where $0 = \alpha_0 < \alpha_1 \cdots < \alpha_K = 1$, and, in each interval, the crude estimate is calculated independently. Hence

$$\theta_1 = \sum_{I=1}^{K} \int_{\alpha_{I-1}}^{\alpha_I} dx\, f(x) = \sum_{I=1}^{K} h_I \int_0^1 dx'\, f(\alpha_{I-1} + h_I x'), \quad (3.1.62)$$

has an unbiased stratified estimate t_3 given by

$$t_3 = \sum_{I=1}^{K} \frac{h_I}{N_I} \sum_{J=1}^{N_I} f(\alpha_{I-1} + h_I \xi_{IJ}), \quad (3.1.63)$$

where N_I is the predetermined number of function values to be selected

in each interval h_I . If each N_I is proportional to h_I, the stratification is uniform and the standard error δt_3 of the estimate t_3 is never worse than the error δt_1 . A non-uniform stratification may lead to better or to worse results. When each N_I is large an estimate w_3 of the variance is given by

$$w_3 = N \sum_{I=1}^{K} \frac{h_I^2}{N_I(N_I-1)} \sum_{J=1}^{N_I} \left(f_{IJ} - \bar{f}_I \right)^2 , \qquad (3.1.64)$$

where $N = \sum_{I=1}^{K} N_I$ is the total number of function evaluations,

$$f_{IJ} = f\left(\alpha_{I-1} + h_I \xi_{IJ} \right) , \qquad (3.1.65)$$

and

$$\bar{f}_I = \frac{1}{N_I} \sum_{J=1}^{N_I} f_{IJ} . \qquad (3.1.66)$$

The standard error δt_3 is therefore given by

$$\delta t_3 \simeq \left(\frac{w_3}{N} \right)^{1/2} . \qquad (3.1.67)$$

For an integral of the form θ_2 , both integration ranges may be stratified simultaneously. Suppose that the range of x is divided into K intervals h_I , and that the range of y is divided into L intervals $k_J = (\beta_{J-1}, \beta_J)$, where $0 = \beta_0 < \beta_1 < \ldots < \beta_L = 1$. In any stratum (I,J) of area $h_I k_J$ suppose that N_{IJ} function values are chosen. Then an unbiased hit-or-miss stratified estimate t_4 of the integral

$$\theta_2 = \sum_{J=1}^{L} \sum_{I=1}^{K} \int_{\beta_{J-1}}^{\beta_J} dy \int_{\alpha_{I-1}}^{\alpha_I} dx \; H\{f(x,y)\}$$

$$= \sum_{J=1}^{L} k_J \sum_{I=1}^{K} h_I \int_0^1 dy' \int_0^1 dx' \, H\{f(x,y)\} , \qquad (3.1.68)$$

where $x = \alpha_{I-1} + h_I x'$ and $y = \beta_{J-1} + k_J y'$, is given by

$$t_4 = \sum_{J=1}^{L} k_J \sum_{I=1}^{K} h_I \frac{M_{IJ}}{N_{IJ}} , \qquad (3.1.69)$$

where M_{IJ} is the number of points satisfying $f(x,y) \geq 0$ in the stratum (I,J) . When all the N_{IJ} are large and all the M_{IJ} are not too extreme, an estimate w_4 of the variance may be written

$$w_4 = \sum_{J=1}^{L} k_J \sum_{I=1}^{K} h_I \frac{M_{IJ}(N_{IJ}-M_{IJ})}{N_{IJ}(N_{IJ}-1)} , \qquad (3.1.70)$$

so that

$$\delta t_4 \doteq \left(\frac{w_4}{N}\right)^{1/2} . \qquad (3.1.71)$$

If several M_{IJ} are extreme with all N_{IJ} large, then the contributions to δt_4 from such strata may be calculated using equation (3.1.60) instead of equation (3.1.58). However, in practice, it is also possible to select a stratification scheme in which each N_{IJ} is unity. In this case equation (3.1.70) does not apply, but an upper bound to δt_4 may be obtained by substituting t_4 for t_2 in equation (3.1.58), or else in equation (3.1.60) for extreme t_4 . This scheme is usually more accurate than the hit-or-miss technique, since the density of points, at which the function $H\{f(x,y)\}$ is evaluated, is more stringently controlled, and, since the contributions to the area from all strata which do not intersect the boundary $f(x,y)=0$ are determined exactly by just one function evaluation.

The technique of stratification may be regarded as a particular case of importance sampling. In this approach for the integral θ_1 , a function $g(x)$ is sought so that $g(x) \geq 0$ for $0 \leq x \leq 1$ and, so the indefinite integral

$$y(x) = \int_0^x dx' \, g(x') , \qquad (3.1.72)$$

where $y(0)=0$ and $y(1)=1$, is known analytically. Then, since $y(x)$ can be inverted, in principle, to obtain $x(y)$ and as

$$\theta_1 = \int_0^1 dx\, f(x) = \int_0^1 dy\, f\{x(y)\}/g\{x(y)\}, \qquad (3.1.73)$$

the crude importance estimate t_5 of θ_1 together with the standard error δt_5 are given by substituting $f\{x(\xi_i)\}/g\{x(\xi_i)\}$ for $f(\xi_i)$ in equations (3.1.52) and (3.1.53). The combined uniform-stratified and importance estimates t_6 together with the standard error δt_6 are given by the corresponding substitution into equations (3.1.63) and (3.1.64). Importance methods will produce more accurate results than the crude estimate when the variation of $f(x)/g(x)$ is less than the variation of $f(x)$ alone. However, a poor choice of $g(x)$ can lead to less accurate estimates.

Importance sampling methods may also be applied to integrals of the form θ_2, but it must be remembered that each function value then has its own weight $1/g(x,y)$.

In the method of control variates let $\tilde{f}(x)$ be an approximation to $f(x)$, with known integral $\tilde{\theta}$. Then, the crude control estimate t_7 and the uniformly-stratified control estimate t_8 can be derived from the identity

$$\theta_1 = \tilde{\theta} + \int_0^1 dx\, \{f(x) - \tilde{f}(x)\}, \qquad (3.1.74)$$

where the second integral in this equation is estimated by crude or uniformly-stratified methods.

The control-variate technique is particularly simple in the case of

the integral θ_2 . Let $\tilde{f}(x,y)=0$ be an approximation of known area $\tilde{\theta}$ to the boundary $f(x,y)=0$. Then

$$\theta_2 = \tilde{\theta} + \int_0^1 dy \int_0^1 dx \left[H\{f(x,y)\} - H\{\tilde{f}(x,y)\} \right] . \quad (3.1.75)$$

In this equation the value of the integrand of the second integral is zero when $\left(f(x,y) \geqslant 0 \text{ and } \tilde{f}(x,y) \geqslant 0 \right)$, or when $\left(f(x,y) < 0 \text{ and } \tilde{f}(x,y) < 0 \right)$, is unity when $\left(f(x,y) \geqslant 0 \text{ and } \tilde{f}(x,y) < 0 \right)$, and has value -1 when $\left(f(x,y) < 0 \text{ and } \tilde{f}(x,y) \geqslant 0 \right)$. Suppose that the second integral in equation (3.1.75) is evaluated by the hit-or-miss technique. In the sample of N points suppose that the numbers of points lying inside the four mutually-exclusive regions defined above are a , d , b and c respectively. Then the hit-or-miss estimate of the original integral θ_2 , given by equation (3.1.54), is obtained by setting $M = a+b$. However, the hit-or-miss control estimate t_q is given by

$$t_q = \tilde{\theta} + \frac{(b-c)}{N} , \quad (3.1.76)$$

with

$$\delta t_q \doteq \left\{ \frac{(b+c)}{N(N-1)} - \frac{(b-c)^2}{N^2(N-1)} \right\}^{1/2} , \quad (3.1.77)$$

provided b and c are not too extreme. Similar results will be obtained if hit-or-miss sampling is replaced by uniformly-stratified sampling.

Of the remaining variance-reduction techniques the regression method generalises simply for higher-dimensional integrals. In this approach

several independent unbiased estimates of the unknown integral must be available. Then, since any weighted arithmetic mean of estimates is also an unbiased estimate, it is possible to determine one set of weights for which the variance is least. As an example, the least-variance estimate $t_{q\,min}$ obtained from the hit-or-miss and hit-or-miss control estimates of the integral θ_2 is given by

$$t_{q\,min}(a,b,c,d) = \frac{(ab+2bc+cd)(a+b)}{N(a+c)(b+d)} + \frac{(ad-bc)}{(a+c)(b+d)} \cdot \left\{ \tilde{\theta} + \frac{(b-c)}{N} \right\}, \qquad (3.1.78)$$

with

$$\delta t_{q\,min} \doteq \left\{ \frac{ab(c+d) + cd(a+b)}{N(N-1)(a+c)(b+d)} \right\}^{1/2}, \qquad (3.1.79)$$

provided a, b, c and d are not too extreme.

3.2 Collisions between Charged Particles and Neutral Hydrogenic Atoms

(a) Geometry

Let incident particle 1 have charge $z_1 = \pm e$ and mass m_1. Suppose the target atom 4 consists of two particles 2 and 3 of mass m_2 and m_3 and charges $z_2 = \mp e$ and $z_3 = \pm e$, respectively. If the magnitudes of the three charges are different, then the theory must be modified to allow for a long-range Coulomb attraction or repulsion in a rearrangement collision in which particles 1 and 2 form a bound system 6 and particle 3 is free. However, there is no restriction upon the masses of the particles.

(b) Initial Conditions

In the initial reference state the target body 4 is located at rest at the origin O of a laboratory Galilean coordinate system $O(\hat{\underline{x}}, \hat{\underline{y}}, \hat{\underline{z}})$. Let the reduced mass associated with the motion of particle 2 with respect to particle 3 be m and let the relative position and velocity vectors at time t be $\underline{r}$ and $\underline{v}$. Neglecting relativistic effects the total energy $E = -U$, where

$$\frac{1}{2} m v^2 - \frac{e^2}{r} = E = -\frac{1}{2} m v_0^2 \quad , \tag{3.2.1}$$

the angular-momentum vector $\underline{L}$, where

$$\underline{L} = m \underline{r} \times \underline{v} \quad , \tag{3.2.2}$$

and the Runge-Lenz (perihelion) vector $\underline{N}$, where

$$\underline{N} = \underline{v} \times \underline{L} - \frac{e^2}{r} \underline{r} \quad , \tag{3.2.3}$$

are all constants of the unperturbed motion (see, for example, Landau and Lifschitz 1960). The orbit of the bound relative motion is an ellipse. For a prescribed total energy $-U$ the semi-major axis a of the ellipse is given by

$$a = \frac{e^2}{2U} \quad . \tag{3.2.4}$$

The plane of the ellipse is perpendicular to the angular-momentum vector, whose magnitude is bounded by L_{max}, the angular-momentum magnitude in the circular orbit of the same total energy. Obviously,

$$L_{max} = m a v_o \quad . \tag{3.2.5}$$

The eccentricity ϵ of the orbit is given by

$$\epsilon^2 = 1 - \frac{L^2}{L_{max}^2} \quad . \tag{3.2.6}$$

The parameter β, defined as

$$\beta = \frac{L^2}{L_{max}^2} \quad , \tag{3.2.7}$$

is a convenient alternative to ϵ. The period T of the bound motion is independent of the angular momentum for a fixed energy. Hence

$$T = \frac{2\pi a}{v_o} \quad . \tag{3.2.8}$$

In a cartesian coordinate system $O(\hat{\underline{x}}', \hat{\underline{y}}', \hat{\underline{z}}')$ oriented so that $\hat{\underline{z}}'$ lies along $\underline{L}$ and $\hat{\underline{x}}'$ lies along $\underline{N}$, the relative position and velocity vectors $\underline{r}'$ and $\underline{v}'$ are conveniently parametrised by the eccentric anomaly u in the form

$$\underline{r}' = a \{ \cos(u) - \epsilon, (1-\epsilon^2)^{1/2} \sin(u), 0 \} \quad , \tag{3.2.9}$$

and

$$\underline{v}' = \frac{2\pi a^2}{T\,|\underline{r}'|}\left\{-\sin(u),\,(1-\epsilon^2)^{\frac{1}{2}}\cos(u),\,0\right\}, \qquad (3.2.10)$$

where the eccentric anomaly u and the time t relative to the time at the perihelion distance are related by Kepler's equation

$$\frac{2\pi t}{T} = u - \epsilon \sin u \quad . \qquad (3.2.11)$$

Formally, Kepler's equation has the following explicit solution for $u(t)$

$$u(t) = \frac{2\pi t}{T} + 2\sum_{s=1}^{\infty} \frac{J_s(s\epsilon)}{s} \sin\frac{2\pi s t}{T}, \qquad (3.2.12)$$

where $J_n(x)$ is the ordinary Bessel function with argument x and integral order n. However, for simple numerical work, equation (3.2.11) can be solved directly (see Abrines and Percival 1966a).

The orientation of the frame $O(\hat{\underline{x}}',\hat{\underline{y}}',\hat{\underline{z}}')$ with respect to the laboratory frame $O(\hat{\underline{x}},\hat{\underline{y}},\hat{\underline{z}})$ may be compounded from three successive rotations through the positive Euler angles ψ, θ and ϕ about the fixed $\hat{\underline{z}}$, $\hat{\underline{y}}$ and $\hat{\underline{z}}$ axes respectively, where $0 \le \psi \le 2\pi$, $0 \le \theta \le \pi$ and $0 \le \phi \le 2\pi$. The parameter μ where

$$\mu = \cos\theta \quad , \qquad (3.2.13)$$

is a convenient alternative to θ.

The state of relative motion may therefore be completely specified by the variables U, β, $\tau = t/T$, ϕ, ψ and μ. Abrines and Percival (1966a) show that if the variables β, τ, $\phi/2\pi$, $\psi/2\pi$ and $(1+\mu)/2$ are all selected independently from a uniform distribution $\rho(x)=1$ for $0 \le x \le 1$, the microcanonical

ensemble defined by equation (3.1.42) is generated with total energy $E=-U$. The specification of the initial reference state is completed by prescribing the time t_0 and the position $\underline{r}_{L1}$ and velocity $\underline{v}_{L1}$ of the incident particle.

For convenience, the time t_0 is chosen to be zero. The velocity of the incident particle is chosen, by convention, along the $\hat{\underline{z}}$ axis. It will be shown that this convention together with the Euler-angle conventions obscures a dynamical condition, which helps to discriminate between different possible final channels. The position of the incident particle may be fixed by the unmodified impact parameter $\underline{b}$ which may be chosen by convention along the $\hat{\underline{y}}$ axis, since the target distribution is spherically symmetric. Hence

$$\underline{r}_{L1} = (0, b, 0) , \tag{3.2.14}$$

$$\underline{v}_{L1} = (0, 0, v_{L1}) , \tag{3.2.15}$$

and the initial reference state is completely specified. Apart from border-line cases each initial reference state leads to a unique final reference state with a definite final channel. Abrines and Percival (1966a) have shown that total cross sections are obtained when the variable b^2 / b_{max}^2 is uniformly distributed in the range $[0, 1]$, where b_{max} is chosen sufficiently large to include all collisions of relevance. It is not difficult to show that the most efficient choice of b_{max} is the smallest possible value if Monte-Carlo methods are used to evaluate the cross sections. However this smallest value can

only be determined precisely from the results of a large number of orbits. In practice a guess for b_{max} is made. If it appears that the guess is too small, then it is always possible to choose additional orbits with b lying between the original guess and some larger value. Since the statistical errors in the total cross sections are proportional to b_{max}^2, it is important to determine whether an alternative coordinate to b can be used.

Suppose that the target atom consists of an electron and a much heavier nucleus. Then, if the velocity of the incident particle is much greater than the velocity in the circular orbit of the target atom, the energy transferred to the atom in a collision is given approximately by the energy transferred to the electron, treated as free from the nucleus during the collision, when the energy transfer is comparable to or greater than the ionization energy U. Thus, the energy transfer depends not upon the position of the nucleus relative to the position of the incident particle, but upon the position of the electron relative to the incident particle. The modified impact parameter b' is therefore measured from the projection of the position of the target electron in the $(\hat{\underline{x}},\hat{\underline{y}})$ plane at the initial reference state. Hence

$$\underline{r}_{L1} = (x_{Le}, y_{Le} + b', 0) \quad , \qquad (3.2.16)$$

where the position of the electron is $\underline{r}_{Le}$ at the initial reference state. It is not immediately obvious that b'^2 is uniformly distributed. However, suppose that the atomic state is held fixed, apart from the final Euler angle of rotation ϕ about the $\hat{\underline{z}}$ axis. Then, if instead, the rotation is performed upon the incident particle in the opposite sense,

the orbit is essentially unchanged. The distribution of the plane-polar coordinates (b, ϕ) of the incident particle corresponds to a uniform beam of particles crossing the $(\hat{x}, \hat{y})$ plane. This beam could be described equally-well by coordinates (b', ϕ') relative to the projection of the position of the electron in this plane. Since ϕ' is also uniformly distributed, then b'^2 must be uniformly distributed. Finally, if b'^2 is uniformly distributed for one atomic configuration, it is uniformly distributed for all atomic configurations.

For high incident velocities b'^2_{max} should be smaller than b^2_{max}, and hence the standard errors in the total cross sections for strong collisions, such as ionizations, should be reduced. For extremely weak collisions the cross sections are dominated by large impact parameters and the distinction between modified and unmodified impact parameters is negligible. For intermediate impact parameters it is not clear which technique yields more accurate results. The surprising accuracy of binary-encounter theory for strong collisions at lower incident velocities suggests that the strong collisions will be more concentrated in the modified impact parameter than in the unmodified impact parameter. The modified impact parameter is therefore preferable for strong collisions and all incident velocities of the order of v_0 and greater.

It is now clear why the restriction upon the mass ratio of the two target particles was made. If the two target particles have comparable mass, then both particles can receive significant energy transfers and hence orbits with large energy transfers may be grouped about either of the projections of the target particles in the $(\hat{x}, \hat{y})$ plane. Fortunately

this complication does not usually arise in practice.

It should be noted that the impact-parameter modification is taken relative to the projection of the position of the target electron in the plane passing through the centre of mass of the target atom and oriented perpendicular to the incident velocity. A vector modification is also possible, but, in order to prevent correlation between the projections of the positions of the incident particle and the target electron parallel to the incident velocity, it is necessary to introduce an additional time variable $\tau_{REL} = t_{REL}/T$, which is uniformly distributed in some unit range, say $[0,1]$, since the unperturbed motion of the target system has period T. Then, the vector impact-parameter modification is achieved if the incident particle is located at the point

$$\underline{r}_{L1} = (x_{Le}, y_{Le} + b', z_{Le} + v_{L1} t_{REL}) , \qquad (3.2.17)$$

in the initial reference state.

This technique suffers from the fact that an additional variable is needed to specify the initial reference state, but is essential for special applications in which arbitrarily close encounters between the incident particle and target electron are required.

The approximate initial scattering state is controlled by the dimensionless error parameter γ. The time $t_-(\gamma)$ at the initial scattering state is given by

$$t_-(\gamma) = -\frac{2a}{\gamma v_{L1}} . \qquad (3.2.18)$$

The initial scattering state is obtained by evolving the initial reference state in the initial non-interacting $(2+1)$-particle channel $|$ through

the time interval $(t_- - t_0)$. It is easy to show that the potential-energy terms between the incident particle and each of the target particles in the approximate initial scattering state is bounded by

$$V_{max} = \gamma^2 U + O(\gamma^3) . \qquad (3.2.19)$$

(c) The Numerical Solution of the Equations of Motion.

In the present work the approximate final scattering state is computed from the approximate initial scattering state by solving the equations of relative motion (3.1.23) and (3.1.24) approximately. The solution is advanced step-by-step using a standard fourth-order Runge-Kutta formula (see for example, Buckingham 1962, p.242, equation 8.41) with a time step which is recalculated at each step according to the formula derived by Abrines and Percival (1966a, equation 31) until an approximate final scattering state is attained. The overall accuracy is controlled by a dimensionless error parameter ε. The time-step formula is based upon the classical scaling laws for Coulomb interactions and is a generalisation of a simplified formula for the relative motion of two charged particles based on a Taylor expansion.

The most serious disadvantage of this method is that an absolute potential-energy error can become large if a relative distance becomes very small, even though the relative error may remain approximately constant. For weak collisions large potential-energy errors arise predominantly from highly-eccentric orbits of the target system. These errors can be moderated by multiplying the time step by an additional factor $\beta^{1/4}$ which is constant for a given orbit. A more detailed investigation by

Valentine (1968) showed that in any close approach of two particles, the absolute potential-energy error could be moderated by multiplying the time step by a factor $r_{RI}^{1/4}$, instead of $\beta^{1/4}$, where r_{RI} is the appropriate relative distance. However, Valentine claimed that the refinement improved only 1% or 2% of the individual orbits with increased computing time. In the present work the time step with the factor $\beta^{1/4}$ has therefore been used, though neither method is really as satisfactory as a perturbation expansion method, say.

(d) Exit Tests

The approximate final state is attained when prescribed exit tests are satisfied. These tests are listed in Abrines and Percival (1966a). For final direct and exchange channels the error parameter γ is used in a similar way to that in the construction of the approximate initial scattering state. For final ionization channels an additional dimensionless error parameter δ is employed. The approximate final state in an ionizing orbit is attained when, for each pair of particles, the absolute ratio of the potential energy to the binding energy is less than δ. Other simple exit tests are required to prevent orbits stopping prematurely.

(e) Scattering Parameters

In principle, the approximate final scattering state should be evolved backwards in time without interaction to determine the final reference state. All scattering parameters can then be calculated from the initial and final reference states. This procedure would be essential if, for

example, the final value of the modified impact parameter or the final value of the eccentric anomaly were required in a direct or exchange collision. However, in practice, the scattering variables of interest can be calculated from the initial and final scattering states.

(f) Determination of Suitable Error Parameters γ , ε , δ .

The values of the error parameters must be chosen with regard to the conflicting demands of time of computation and of accuracy.

The error parameter δ is important only for ionizations. Owing to the form of the adjustable time-step formula, the computing time is insensitive to large changes in δ . The value of δ may therefore be selected to yield errors of the same order of magnitude as those introduced by ε and γ .

The error parameter γ controls the initial potential-energy error bound defined in equation (3.2.19) and a similar final potential-energy error bound for final direct and exchange channels, where U is replaced by the corresponding final binding energy. In contrast, the round-off error in the numerical solution of the equations of motion is approximately inversely proportional to γ , since γ is roughly inversely proportional to the total time interval of evolution.

The truncation error in the numerical solution of the equations of motion is approximately proportional to ε^4, provided that the error is not too large. However, for small ε the round-off error is also approximately inversely proportional to ε . Thus, if the computing time were irrelevant, the most accurate choices of γ , ε and δ would be the smallest values above the limits of round-off error.

In practice the computing time is important. Usually, the total computing time is dominated by the time t_c required to solve the equations of motion. Neglecting complicated collisions

$$t_c \simeq \frac{kN}{\varepsilon \gamma v_{L1}} , \qquad (3.2.20)$$

where v_{L1} is the initial velocity of the incident particle, N is the total number of orbits and k is approximately a constant, whose value depends upon the computer available. If complicated collisions are important then this value of t_c is probably too small. For incident protons the value of k was found to vary by only about 20% for incident velocities in the range $0.4\, v_0 \leq v_{L1} \leq 2 v_0$.

In the present work the values of the error parameters γ, ε and δ are chosen by trial and error using a small sample of orbits. The usual criterion is that γ and ε are chosen as large as possible, subject to prescribed error bounds in the scattering variables of interest and in the constants of the motion. The value of δ is not normally critical. In this way a fixed computing time is used to calculate as many orbits as possible.

(g) Generation of Pseudorandom Numbers.

The uniform distribution of random numbers is generated from the pseudorandom sequence

$$\xi_i \equiv a\, \xi_{i-1} + c \quad (\text{modulo } m) , \qquad (3.2.21)$$

with $a = 127$, $m = 2^{29}$ and $c = 0$. Some of the properties of this sequence and of other similar formulae are

discussed by Hammersley and Handscomb (1964).

3.3 Exact-Classical Total Cross Sections for Protons Incident upon Atomic Hydrogen.

(a) Introduction

The earlier results of Abrines and Percival (1966b) were obtained using an EMA computer program which was run on the University of London Atlas computer. Their results are extended in this work to lower incident proton energies using the more general and flexible FORTRAN computer program developed by Percival and Valentine (see Valentine 1968). All computations have been performed on the Chilton Atlas computer.

All cross-section data are presented for target atoms in the ground state. Using the classical scaling laws the corresponding cross-sections for target atoms initially in a uniformly-populated (microcanonical) level n may be readily obtained. Although atomic units have been used throughout, it is convenient to express the incident proton energy in Kev. and also to use incident velocities for comparisons with infinite-mass models. The approximate relations that a proton moving with an atomic unit of velocity has an incident energy of about 918 a.u., which is approximately equivalent to 25 Kev., have been used.

(b) Calculations

In table (3.3.1) the incident energies in Kev., the maximum value of the square of the impact parameter in a_o^2, the error parameters ε, γ and δ, the total number of orbits successfully integrated, the total numbers in each of the mutually-exclusive final channels for direct excitation, ionization and charge transfer, and the approximate computing

E_1 in Kev.	b^2_{max} in a_o^2	ε	γ	δ	N_T	N_D	N_I	N_E	T in hours
7	18	0.16	0.04	0.005	500	384	0	116	3.0
10	20	0.17	0.04	0.005	699	580	1	118	3.6
20	17	0.18	0.04	0.005	1499	1139	34	326	5.3
68	11*	0.25	0.10	0.005	2500	1986	406	108	1.6

Table 3.3.1 Preliminary data for exact-classical p-H results. A * in the first column indicates modified impact parameter; otherwise unmodified. See text.

E_1 in Kev.	$\sigma_I(\pi a_o^2)$	$\sigma_E(\pi a_o^2)$	$\sigma_{Loss}(\pi a_o^2)$
7*	0 + 03	4.18 ∓ 34	4.18 ∓ 34
10*	0.03 ∓ 03	3.38 ∓ 28	3.40 ∓ 28
20*	0.39 ∓ 07	3.70 ∓ 18	4.08 ∓ 19
38.1	1.35 ∓ 13	2.19 ∓ 18	3.54 ∓ 22
54.4	1.69 ∓ 12	1.07 ∓ 12	2.76 ∓ 16
68	1.81 ∓ 13	0.55 ∓ 09	2.36 ∓ 15
68*	1.79 ∓ 08	0.48 ∓ 05	2.26 ∓ 09
81.6	1.63 ∓ 12	0.31 ∓ 08	1.94 ∓ 14
95.2	1.57 ∓ 11	0.17 ∓ 04	1.74 ∓ 12
108.8	1.39 ∓ 10	0.07 ∓ 03	1.46 ∓ 10
136	1.13 ∓ 09	0.01 ∓ 01	1.14 ∓ 09
163.2	0.96 ∓ 06	0 + 01	0.96 ∓ 06
217.6	0.73 ∓ 05	0 + 01	0,73 ∓ 05

Table 3.3.2 Total reduced exact-classical p-H cross sections; σ_I (ionization); σ_E (charge-transfer); σ_{Loss} (electron-loss). Errors represent approximate statistical 2/3 confidence limits. A * in the first column indicates present calculations; otherwise, those of Abrines and Percival (1966b).

time in hours are all listed.

The orbits with incident energy 68 Kev. were computed in order to check the improved FORTRAN program against the available results from the EMA program, since the FORTRAN program had not been used previously for production runs.

At incident energies below about 4 Kev. the computing time required to obtain reasonably accurate cross-sections is prohibitive with the present version of the program. Fortunately, below this incident energy, ionizing collisions are rare and the charge-transfer collisions have been treated approximately by Bates and Reid (1969b), using a classical adiabatic model together with the Bohr-Sommerfeld quantization rules for the hydrogen molecular ion. Thus, the present work fills the gap between the exact-classical results of Abrines and Percival (1966b) and the calculations of Bates and Reid.

(c) Results for Total Cross Sections.

The exact-classical total cross sections may be calculated using equations (3.1.46) and (3.1.56) with standard errors given by equations (3.1.58) or (3.1.60) in extreme cases.

The exact-classical total cross sections σ_I, σ_E and σ_{Loss} for ground-state targets are listed in table (3.3.2) in πa_0^2 together with the earlier results of Abrines and Percival (1966b). It should be recalled that σ_E includes capture into all final states. The exact-classical electron-loss cross section σ_{Loss} is just the sum of the ionization and capture (charge-transfer) cross sections σ_I and σ_E.

The statistical errors represent approximate $^2/_3$ confidence limits. Note that the statistical error in σ_{Loss} may be derived directly by using the sum (N_I+N_E) of orbits resulting in electron loss, rather than by combining the separate statistical errors in σ_I and σ_E, in which case a larger estimate may be obtained. The cross sections σ_I and σ_{Loss} are compared with various classical binary-encounter approximations in figure (2.10.1).

In figure (3.3.3) σ_I is compared with the averaged binary-encounter results of Vriens (1967) and the exact-classical ionization cross section of Percival and Valentine (1967) for incident positrons of the same velocity. Also displayed are the first-Born calculation of Bates and Griffing (1953) and the experimental values of Fite et al. (1960) and of Gilbody and Ireland (1964) in the specific case of ground-state target atoms.

In figure (3.3.4) σ_E is compared with the classical adiabatic resonant ground-state charge-transfer cross section of Bates and Reid (1969b) and with the corresponding averaged scaled cross sections for the initial level n, since their cross sections do not scale classically. Also shown are the exact-classical results of Percival and Valentine (1967) for incident positrons of the same velocity, the two-state quantal calculation of McElroy (1963) and the experimental results of Gilbody and Ryding (1966), both of which apply specifically for ground-state target atoms.

If $\sigma(v_i,v_o)$ is an exact-classical total cross section for an incident charged particle moving with initial velocity v_i, and v_o is the root-mean-square velocity of the electron in the ground state of

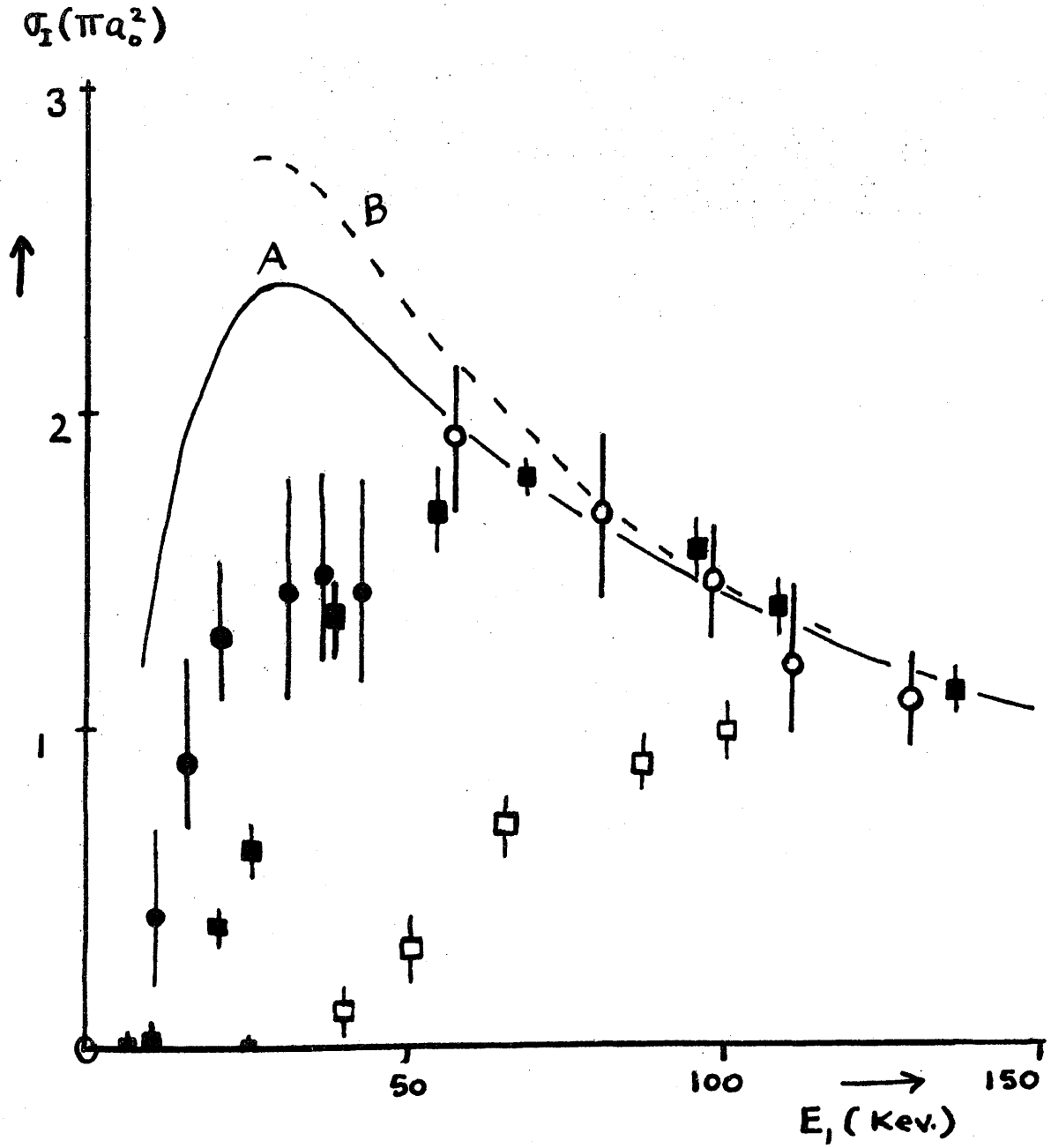

Figure 3.3.3 Ground-state p-H ionization cross sections. Curves; A (first-Born); B (binary-encounter). Experimental values; full circles (Fite et al.); open circles (Gilbody and Ireland). Exact-classical results; full squares (protons); open circles (positrons of same velocity). Error bars in exact-classical results represent approximate statistical 2/3 confidence limits

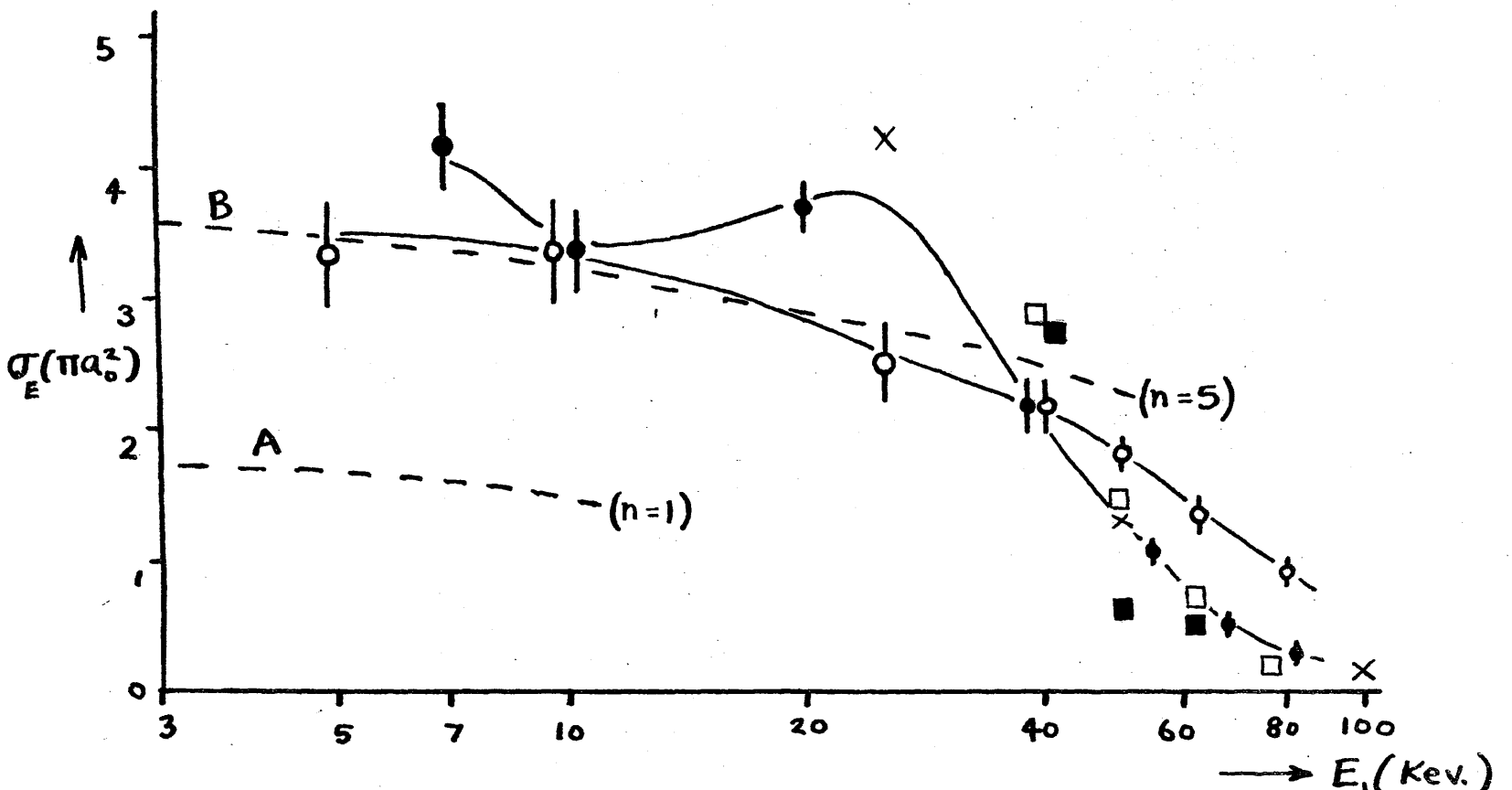

Figure 3.3.4 Total reduced classical p-H capture cross sections into all final states. Curves; A (adiabatic model of Bates and Reid for ground-state targets); B (similar reduced model for initial n = 5 target level). Exact-classical values; full circles (protons); open circles (positrons of the same velocity). Error bars in the exact-classical results represent approximate statistical 3/3 confidence limits. Experimental values; full squares, Gilbody and Ryding; open circles, Wittkower et al. (1966). Quantal two-state; crosses.

the target hydrogenic atom, then the corresponding cross section $\sigma'(v_1', v_0')$ for an incident particle of velocity v_1' and for a target atom in a uniformly-populated excited level n with root-mean-square velocity v_0' is given by the classical scaling law

$$\sigma'(v_1', v_0') = n^4 \sigma(v_1, v_0) , \qquad (3.3.1)$$

where

$$n v_0' = v_0 , \qquad (3.3.2)$$

and

$$n v_1' = v_1 . \qquad (3.3.3)$$

The exact-classical results for incident protons in the low velocity range $v_1 < v_0$ show a marked disagreement with experimental and quantal values for both ionization and total capture in the case of ground-state target atoms, in contrast to the excellent agreement at intermediate velocities $v_0 \leq v_1 \leq 4 v_0$, say. It is now well-established (see for example, Bates and Reid, 1969a,b) that for $v_1 < v_0$ barrier penetration plays a dominant role in charge-transfer processes and consequently also in ionizations. The exact-classical results are, therefore, not surprisingly, too small in this region. However, for corresponding atoms in an excited level n, the range of scaled velocities, over which barrier penetration is significant, should decrease as n increases and hence for sufficiently large n, the exact-classical cross sections should be accurate for the velocities considered. These results indicate clearly the danger of extrapolating experimental or quantal cross sections by classical scaling laws.

(d) The Validity of the Classical Model of Bates and Reid

The Bates and Reid model (1969b) is based upon the classical theory of the hydrogen molecular ion and employs only those classical orbits allowed by the Bohr-Sommerfeld quantization rules. Nevertheless, for large n, the averaged scaled cross sections should approximate the exact-classical microcanonical results, though for low n the models do not correspond. Apart from these differences Bates and Reid make two important assumptions in the low velocity limit which can be tested directly, although it may be argued that the present exact-classical results are not sufficiently low in incident velocity for the classical adiabatic theory to be valid. Firstly, they assume that for each allowed orbit, charge transfer takes place with probability $\frac{1}{2}$ if the nuclear separation R is less than $R(n,m,I)$ where n is the initial level of the hydrogen atom and m and I are subsidiary molecular quantum numbers. Secondly, they assume that non-resonant transfers are negligible. The scaled averaged low-velocity limit of the classical resonant charge-transfer cross section $\sigma_E(n)$ is given by

$$\sigma_E(n) = \tfrac{1}{2}\pi \sum_{I=0}^{n-1} \sum_{m=-I}^{I} \frac{R^2(n,m,I)}{n^4} \quad . \qquad (3.3.4)$$

As can be seen from figure (3.3.4) the cross section $\sigma_E(5)$ is in excellent agreement with the exact-classical cross section for capture into all states, though the apparent structure in the exact-classical cross section for higher incident velocities is not reproduced in their model. The extent of the agreement is demonstrated by the comparison between the exact-classical charge-transfer probability as a function of

the square of the unmodified impact parameter b and the contributions from equation (3.3.4) with

$$R(n,m,1) = n^2 b \ , \qquad (3.3.5)$$

as shown in figure (3.3.5).

However, in the exact-classical results, the spread in the distribution of final binding energies is not negligible at the incident velocities considered. At lower incident velocities the spread should decrease, but this is just the region where barrier penetration becomes more significant. The classical resonant capture cross sections of Bates and Reid for large n are therefore too large at higher incident velocities, because capture into different final levels is significant, but is not included, and are too small at lower incident velocities, because barrier penetration is neglected.

The reasons for the failure of classical methods in treating weak excitations at high incident velocities have been discussed by Percival and Richards (1970a). They claim that classical methods may only be applied if all quantum numbers and all changes in the quantum numbers are large compared with unity. The failure of the classical resonant capture cross sections of Bates and Reid even for large n may be due to similar reasons. Nevertheless, if these cross sections are interpreted as capture cross sections into all states, the values are accurate for sufficiently large n and for incident velocities above the region of importance of barrier penetration, but low enough for their approximate theory to be valid.

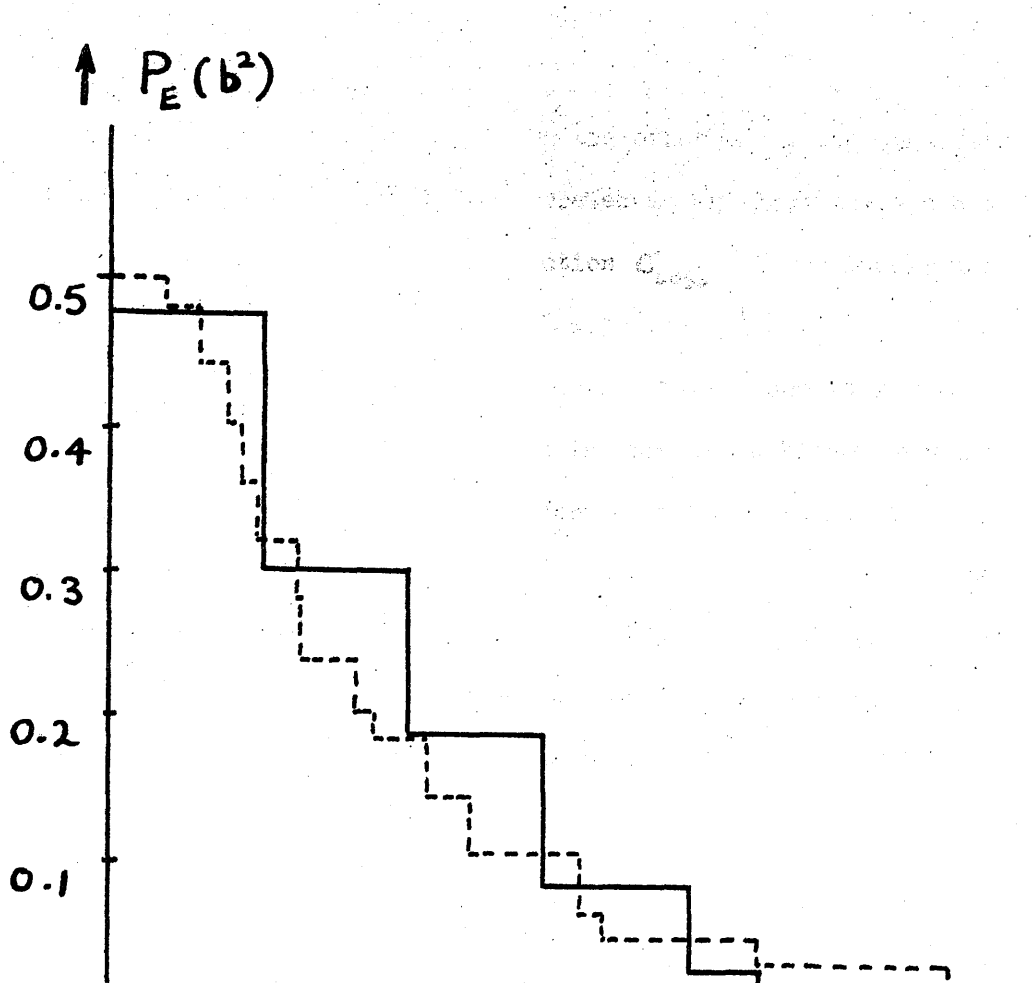

Figure 3.3.5 Reduced classical p-H capture probability versus the square b^2 of the unmodified impact parameter at the incident energy 7 Kev. Full curve (exact-classical); dashed curve (adiabatic model of Bates and Reid for initial n = 5 level).

(e) The Validity of the Binary-Encounter Approximation

It is evident from figure (2.10.1) that the binary-encounter approximation to σ_I seriously overestimates the exact-classical values for low incident proton velocities, even though such collisions involve close encounters. If, on the other hand, the binary-encounter ionization cross section is interpreted as an electron-loss cross section, then the exact-classical cross section σ_{Loss} is seriously underestimated by the binary-encounter model at low proton velocities. The latter result suggests that charge-transfer may take place at low incident velocities in collisions for which the predicted binary-encounter energy transfer is small. Since the binary-encounter results for total electron loss and total ionization are seriously in error for low incident proton velocities, the binary-encounter results for excitations by slow incident protons are likely to be even worse than the results for the stronger collisions. A similar discrepancy between binary-encounter and exact-classical total and differential ionization cross sections for incident electrons was found by Abrines, Percival and Valentine (1966), even for incident velocities larger than, but comparable to, the initial root-mean-square velocity v_0 of the target electron.

In the previous and present exact-classical work the value of b^2_{max} was chosen to include virtually all ionizing and charge-transferring collisions. Since contributions to the exact-classical continuous differential excitation cross section $\frac{d\sigma_D}{d\Delta E}$ occur with impact parameters outside this range, the estimate of $\frac{d\sigma_D}{d\Delta E}$ from impact parameters below b^2_{max} is a lower bound subject to statistical fluctuations. Nevertheless

for each individual collision the exact-classical and the binary-encounter values of the energy transfer ΔE may be computed. The exact-classical and binary-encounter contributions to $\frac{d\sigma_D}{d\Delta E}$ are sketched in figure (3.3.6) for the incident energies 68 Kev. and 20 Kev. The striking disagreement at 20 Kev. may be even worse, since small errors in the exact-classical orbit integration will tend to broaden the true results for small ΔE . The region of validity of the binary-encounter approximation as a classical model has been given by Percival and Richards (1967). They argue that the theory is valid when the collision time $t_{COL} = 2b'/v_1$ is short compared with the natural period $T = 2\pi a/v_o$ of the target atom, where a is the radius and v_o is the speed of the atomic electron in the circular orbit of the same binding energy. For low incident velocities $v_1 << v_o$, and so the region, in which the binary-encounter approximation is valid, yields a negligible contribution of order $\pi b_{COL}^2 = \pi a^2 \left(\frac{v_1^2}{v_o^2}\right)$ to the total electron-loss cross section σ_{Loss}, which is comparable to πa^2 .

For the first time the binary-encounter theory has been compared with exact-classical results for individual orbits, using the theory described in sections (2.1), (2.2) and (2.3) for the particular case of an incident finite-mass proton and a target electron. The comparison is made using the coordinates defined at the initial reference state, rather than those at the approximate initial scattering state, because, in the exact-classical model, the target electron is evolved backwards in time from the initial reference state to the initial scattering state on an elliptic orbit instead of a straight-line orbit, as required in the binary-encounter theory. Although, in principle, either state, or any intermediate

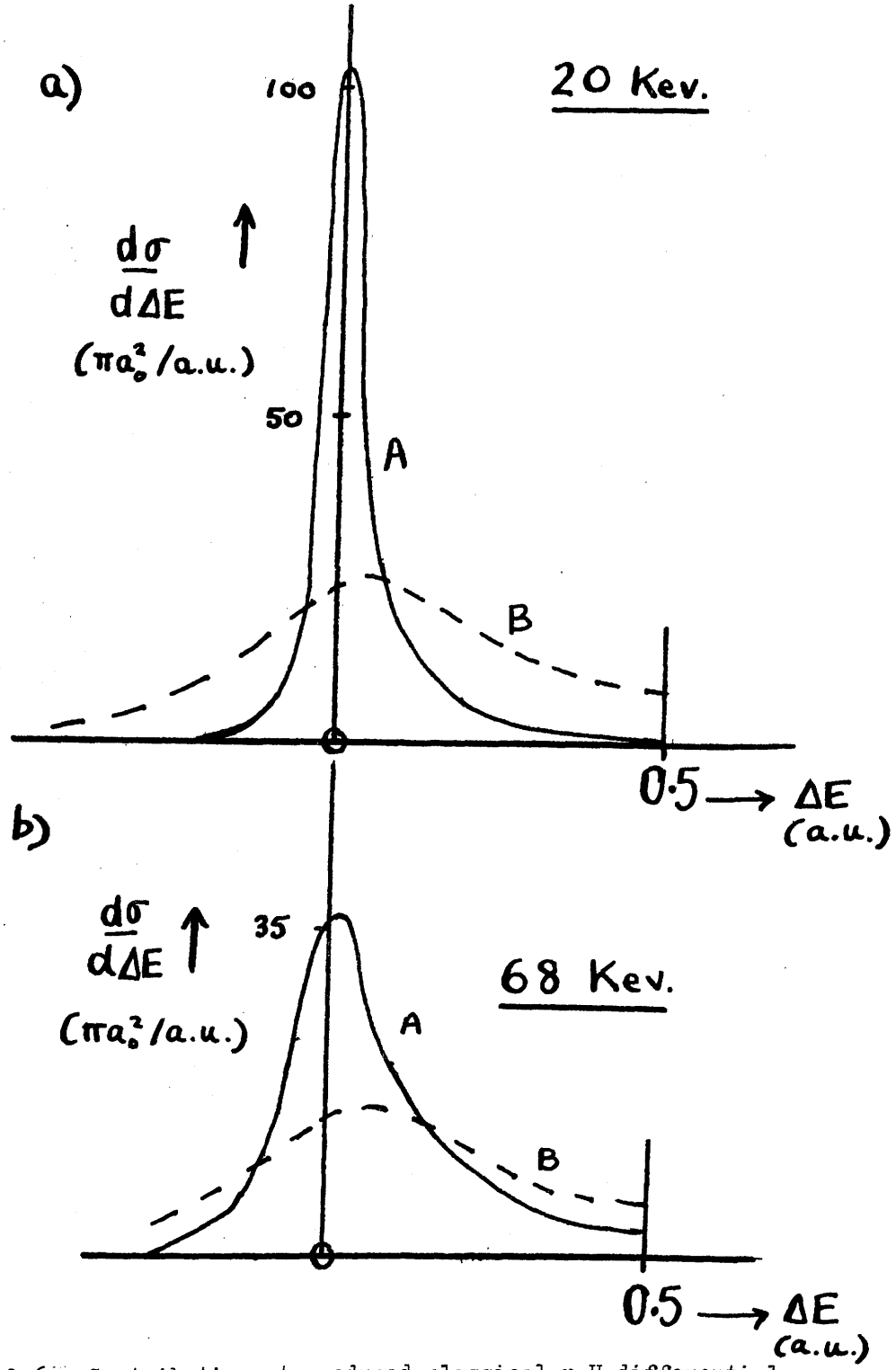

Figure 3.3.6 Contributions to reduced classical p-H differential excitation cross sections from impact parameters below b_{max} versus energy transfer. Case a) 20 Kev.; b) 68 Kev. Curves; A (exact-classical); B (binary-encounter).

state may be used, the correlation between the exact-classical and binary-encounter results should be greatest at the initial reference state, since the incident proton is at its position of closest approach relative to the centre of mass of the target atom, for each orbit at this state. Only at very high incident velocities will the correlation be insensitive to the initial state at which the comparison is made.

Each orbit must result in one of four mutually-exclusive final channels or cells according to whether the exact-classical final channel is electron-loss or direct excitation (or possibly de-excitation) and to whether the binary-encounter model predicts electron-loss or direct excitation (or possibly de-excitation). In this approach it is still possible for the energy transfer ΔE calculated by each theory to differ widely within the same cell.

At the incident energies 10 Kev. and 68 Kev. all exact-classical orbits have been used in the comparison. At the incident energies 7 Kev. and 20 Kev. only the first 500 and 600 orbits respectively have been compared. A particularly attractive feature of this approach is that the binary-encounter results, together with a variety of other predictors, may be evaluated in a separate computer program with little additional computing time, since the initial conditions can be regenerated quickly. Then, all that is required from the exact-classical orbits is the value of the final channel. In this way all earlier exact-classical orbits may be compared with binary-encounter predictions, provided that the exact initial conditions can be reproduced and that the exact-classical channels are known.

The total numbers of orbits, which fall into each cell, are presented in the first column of two-by-two contingency tables in table (3.3.7). The results, which would be expected if the binary-encounter theory were not correlated with the exact-classical values, are presented in the second column. In this case the number in each cell is given by the product of the appropriate row sum and column sum, divided by the total number of orbits. The results in the second column have been rounded to the nearest integer. The numbers, which would be expected if every orbit, for which the binary-encounter model predicts electron-loss, results in electron-loss, are listed in the third column. In this case the region of initial conditions, for which the binary-encounter model predicts electron-loss, is contained within the corresponding exact-classical region. Since, for each contingency table, there is only one degree of freedom, a measure of the relevance of the binary-encounter model can be derived by noting that any cell total N_{IJ1} selected from the first column may be written in the form

$$N_{IJ1} = (1-\chi)\, N_{IJ2} + \chi\, N_{IJ3} \quad , \qquad (3.3.6)$$

where N_{IJ2} and N_{IJ3} are the corresponding cell totals in the second and third columns respectively, and where χ depends only upon the incident velocity. The factor $(1-\chi)$ may be regarded as a measure of the random component in the comparison and the fraction χ may be interpreted as a measure of the significance of the approximate theory. Approximate standard errors in χ may be gauged by adding to, and subtracting from, the smallest cell total its own square root. Negative values of χ are permissible though unlikely since this would imply a negative correlation

a) 7 Kev.

	BL	BD	T
EL	8	108	116
ED	16	368	384
T	24	476	500

	BL	BD	T
EL	6	110	116
ED	18	366	384
T	24	476	500

	BL	BD	T
EL	24	92	116
ED	0	384	384
T	24	476	500

b) 10 Kev.

	BL	BD	T
EL	19	100	119
ED	42	538	580
T	61	638	699

	BL	BD	T
EL	10	109	119
ED	51	529	580
T	61	638	699

	BL	BD	T
EL	61	58	119
ED	0	580	580
T	61	638	699

c) 20 Kev.

	BL	BD	T
EL	55	78	133
ED	39	428	467
T	94	506	600

	BL	BD	T
EL	21	112	133
ED	73	394	467
T	94	506	600

	BL	BD	T
EL	94	39	133
ED	0	467	467
T	94	506	600

d) 68 Kev.

	BL	BD	T
EL	305	209	514
ED	164	1822	1986
T	469	2031	2500

	BL	BD	T
EL	96	418	514
ED	373	1613	1986
T	469	2031	2500

	BL	BD	T
EL	469	45	514
ED	0	1986	1986
T	469	2031	2500

Table 3.3.7 p-H contingency tables at various incident energies for comparisions between exact-classical values (E) and binary-encounter predictions of the final channels of electron-loss (L) and of direct excitation (D) for sets of individual orbits. Row and column totals are denoted by T. The actual results obtained are presented in the first column of contingency tables. See text for the remaining tables.

between the two models.

The binary-encounter comparison may be used to determine a control estimate of the exact-classical cross section σ_{Loss}, using equation (3.1.76) with standard error given approximately by equation (3.1.77), though there is no guarantee that the results will be more accurate than the direct hit-or-miss estimates in table (3.3.2). In order to obtain a control estimate, the Fock-averaged binary-encounter electron-loss cross section for a finite-mass incident proton must also be known. However, since the difference between the finite-mass and infinite-mass binary-encounter models is small at these incident velocities, the simpler infinite-mass results may be employed, particularly since the standard error of the control estimate is independent of the approximate analytic integral.

The theoretical values for the infinite-mass binary-encounter electron-loss cross section $\sigma_{Loss,BE}$ are $1.93\pi a_0^2$ at 68 Kev. and $1.75\ \pi a_0^2$ at 10 Kev. The hit-or-miss estimates of $\sigma_{Loss,BE}$ are $2.06 \pm .09\pi a_0^2$ and $1.75 \pm .21\pi a_0^2$ respectively, and the control estimates of the exact-classical σ_{Loss} are $2.13 \pm .09\ \pi a_0^2$ and $3.40 \pm .34\ \pi a_0^2$ respectively. If any bias in the random sample of initial conditions at 68 Kev. affects $\sigma_{Loss,BE}$ and σ_{Loss} similarly, then this work suggests that the hit-or-miss value listed in table (3.3.2) is larger than it should be. However, the earlier independent estimate by Abrines and Percival (1966b) is then even larger. Although the control-estimate approach is more satisfactory aesthetically, the statistical errors are, at both incident energies, at least as large, for these cases, as the original hit-or-miss errors. Thus the binary-encounter model for individual orbits is not sufficiently close to the exact-classical

model, to reduce the statistical errors at these incident velocities. Although this approximation may be more useful at higher velocities, the exact-classical and binary-encounter electron-loss cross sections are known to agree closely (at least statistically) in this region. Nevertheless, the individual-orbit binary-encounter model is useful in comparisons with exact-classical results, especially when subsamples of initial conditions are selected for investigation by the exact-classical technique. In such cases the analytic binary-encounter results may not have been determined, for example, a sub-sample of orbits with b^2 distributed uniformly in the range $(0,2)a_0^2$ only, say.

3.4 Exact-Classical Charge-Transfer Probabilities in Close Collisions of Protons with Hydrogen Atoms.

(a) Introduction

The first measurement of the charge-transfer probability in close collisions of protons and ground-state hydrogen atoms was made by Lockwood and Everhart (1962). Their results for incident proton energies in the range 0.7 Kev. to 40 Kev. at a fixed scattering angle of 3° revealed that the charge-transfer probability p_E was an oscillating function of incident energy. More recently Helbig and Everhart (1965) repeated and extended these measurements to include incident energies from 0.13 Kev to 150 Kev. and scattering angles between 0.2° and 6°. It was found that p_E was also a resonant function of scattering angle. However, over the range 4 Kev. to 150 Kev. p_E was independent of the scattering angle, provided the angle was at least 2°.

Early quantum-mechanical calculations failed to predict the location of the maxima and overestimated the amplitude of the oscillations in p_E (see, for example, Wilets and Gallaher, 1966, and the references therein). However the Sturmian close-coupling calculations of Gallaher and Wilets (1968) and the variable screened nuclear-charge model of Cheshire (1968) are in better agreement with experiment.

There are two simple explanations for the resonant behaviour of p_E. The first explanation is easy to formulate within the framework of quantum mechanics, since the symmetry of the field experienced by the electron leads naturally to both gerade and ungerade molecular wavefunctions. Then, the interference between these states can give rise to resonant

phenomena in p_E . Since this process has no analogue in a purely-classical description, such resonances are non-classical and cannot be reproduced by a purely-classical model.

A second mechanism was proposed by Cheshire (1968) and may be worded in the following way. At high incident-proton energies the atomic electron does not have enough time to "jump" to the passing proton during the collision and therefore p_E should be small. As the incident energy is decreased, p_E should increase until an optimum incident energy is reached (at about 25 Kev.) at which the atomic electron has sufficient time to "jump" to the passing proton, but not enough time to return to the target proton. In the neighbourhood of this incident energy, p_E should have its first maximum in terms of decreasing incident energy. At lower incident energies multiple transfers are possible and a series of maxima and minima in p_E may be expected.

Unlike the first explanation Cheshire's mechanism may be interpreted classically. In this section the exact-classical values of p_E are determined to discover whether the Lockwood and Everhart effect has a classical explanation. The exact-classical results are also useful as a test for possible approximate classical collision models.

(b) Calculations

The preliminary data for the calculations is displayed in table (3.4.1). The range of incident energies is chosen to correspond to the experimental range over which p_E was found to be insensitive to scattering angles about 3°. Scattering angles close to 3° are selected because of the large amount of experimental and quantal theoretical

E_1 in Kev.	b^2 in a_o^2	ϵ	γ	δ	N_T	N_D	N_I	N_E	T in hours
4	1.667	0.15	0.04	0.005	597	318	11	268	5.4
5	1.067	0.16	0.04	0.005	498	261	11	226	3.9
7	0.544	0.16	0.04	0.005	499	273	23	203	3.1
8	0.416	0.16	0.04	0.005	700	404	22	274	4.1
10	0.267	0.17	0.04	0.005	700	381	33	286	3.6
14	0.137	0.16	0.04	0.005	400	166	31	203	1.9
20	0.067	0.18	0.04	0.005	1000	245	103	652	3.4
30	0.029	0.17	0.04	0.005	600	129	105	366	1.8
50	0.010	0.17	0.04	0.005	700	209	207	284	1.7
100	0.003	0.17	0.04	0.005	600	299	247	54	1.4*
a)100	0.003*	0.20	0.10	0.005	300	230	69	1	1.9
b)100	0.003*	0.20	0.10	0.005	266	95	127	44	1.6

Table 3.4.1 Preliminary data for close p-H collisions. A * in the second column denotes impact parameters modified relative to the target proton; otherwise, unmodified. A * in the final column indicates the value to be multiplied by a factor of ten. Data at 100 Kev.; a) initial conditions with τ in the range (0.25,0.6) only; b) τ in the range (-0.4,0.25) only. The marked differences in these two cases indicate that τ is a significant initial variable at high energies. See section (4.2).

results available for comparison.

It is not practical to determine the appropriate initial conditions which yield a scattering angle of exactly 3° for each individual orbit. Instead, as in the calculation of Cheshire (1968) and Gallaher and Wilets (1968), the impact parameter relative to the centre of mass of the target system is chosen to be a function of the incident energy alone. The Rutherford formula for the scattering of the protons, alone, yields

$$b E_1 = 0.519 \ , \qquad (3.4.1)$$

where b is expressed in a_0 and E_1 in Kev. Since this formula does not allow for the screening of the target proton by the atomic electron, a more accurate value of b was found by trial and error at 7 Kev. This value may be used to obtain impact parameters at different incident energies employing the approximate relation

$$b E_1 = 0.516 \ . \qquad (3.4.2)$$

The corresponding values of b^2 are listed in table (3.4.1). In all cases, except at the highest energy 100 Kev., the spread in the angles of scattering close to 3° is less than, but comparable to, the angular resolution quoted by Lockwood and Everhart (1962). For incident energies of 100 Kev. and above the excessive spread in scattering angle is caused by b being not much larger than the unperturbed radius of the orbit of the target proton. The spread is reduced by choosing b relative to the target proton rather than to the centre of mass.

The incident energies in the range 4 Kev. to 50 Kev. inclusive were computed on the Chilton Atlas. The calculations at 100 Kev. were

performed on the University of Stirling ICL 4130.

(c) Results for the Exact-Classical Probabilities.

The values of the exact-classical probabilities of total direct excitation p_D, of total ionization p_I and of total charge transfer p_E are shown in figure (3.4.2). The error bars represent approximate $^2/_3$ confidence limits. Smooth curves have been drawn through the points by hand to avoid possible confusion. The upper horizontal scale is non-linear and shows the incident energy E_1 in Kev. The lower horizontal scale is linear in a convenient dimensionless parameter t, which is the ratio of the incident energy E_1 in Kev. to the incident energy (E_1+25) in Kev. The value $t = ½$ corresponds to the incident energy 25 Kev. at which the incident proton velocity v_1 and the root-mean-square velocity v_0 of the atomic electron are almost equal. Note that the incident energy range considered is therefore approximately equivalent to the incident velocity range

$$0.4\, v_0 \leq v_1 \leq 2\, v_0 \quad .$$

It is immediately apparent that the charge-transfer probability p_E is an undulating function of E_1, and has a maximum value of about 0.68 close to 25 Kev. There is also strong evidence for a minimum value of about 0.39 close to 8 Kev. There appears to be no further significant structure below 7 Kev. Since there is no significant structure below 7 Kev., the maxima and minima for the high-order transfers predicted by Cheshire (1968) are rapidly damped in the classical approach. In this region any strong oscillations in p_E must be purely-quantal in origin. In contrast, above 7 Kev. significant oscillations are present in the

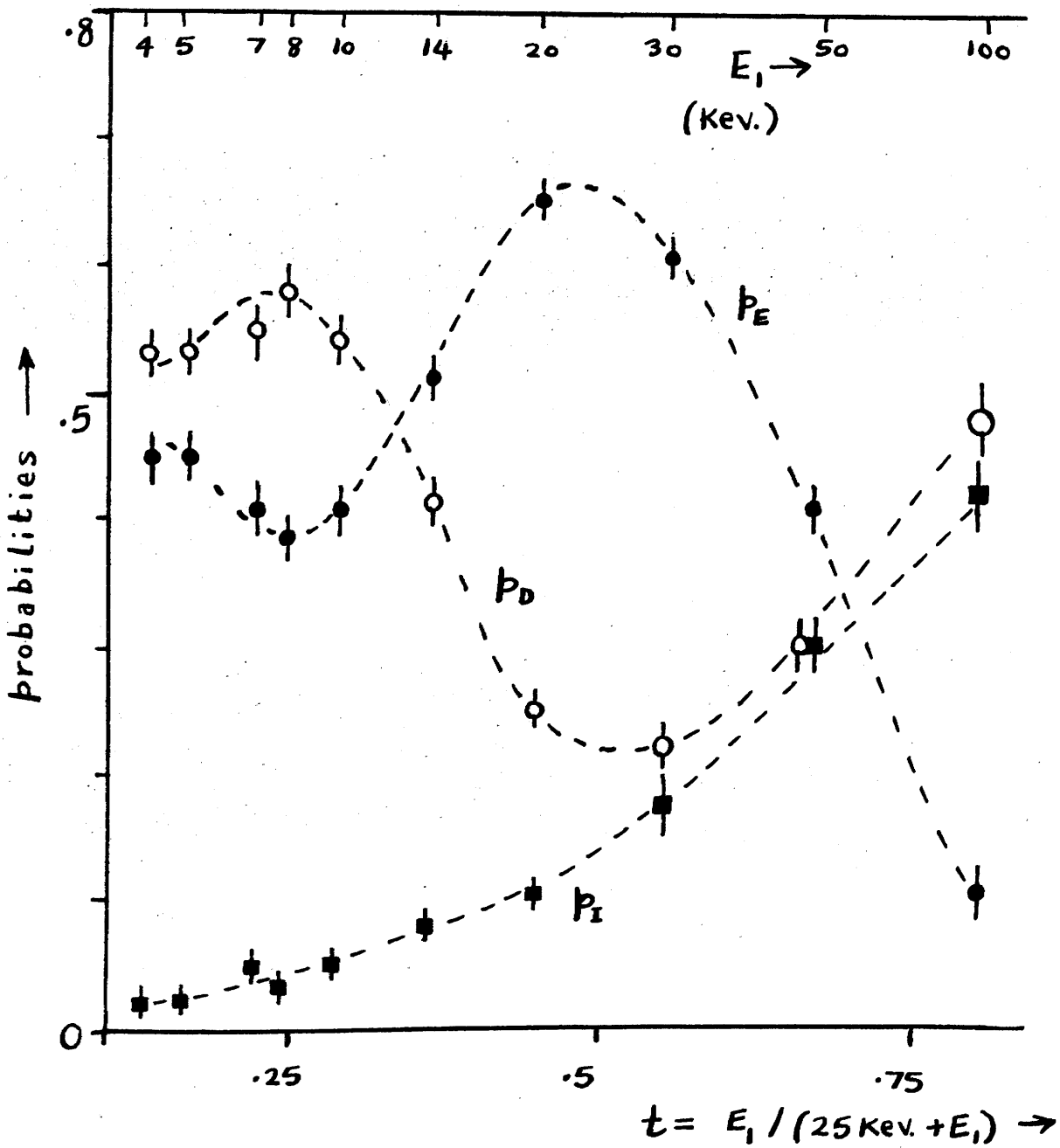

Figure 3.4.2 Exact-classical close p-H total probabilities versus incident energy. Full squares (ionization); full circles (total capture); open circles (direct excitation). Error bars represent approximate statistical 2/3 confidence limits.

classical results and hence the purely-quantal effects may not be dominant.

In figure (3.4.3) the exact-classical results for P_E are compared with the quantal calculations of Cheshire (1968) and of Gallaher and Wilets (1968) and with the experimental values of Lockwood and Everhart (1962). Unlike early quantal theories, the exact-classical results are "in phase" with the experimental values for incident energies above 7 Kev. The classical amplitudes are too small by approximately the same factor as the quantal results of Cheshire and of Wilets and Gallaher are too large.

As in other exact-classical calculations, an important advantage of the classical method is the ability to discriminate between phenomena which are purely-quantal and those which can be described equally-well classically. This leads, not only to a better understanding of the mechanisms involved, but also enables more accurate extrapolations for corresponding processes involving initially excited levels. A second advantage of the classical approach is the possibility of testing approximate hypotheses used either in classical or in quantal treatments. In the present case the failure of the hydrogenic expansion of Wilets and Gallaher (1966) and of the calculation of Cheshire (1968) at incident energies above 7 Kev. is not surprising since they neglect ionization channels. As can be seen from figure (3.4.2) the exact-classical ionization probability is not negligible in this energy range and it is therefore not unreasonable to expect the true ionization probability to be significant here. If this is so, the results of Wilets and Gallaher

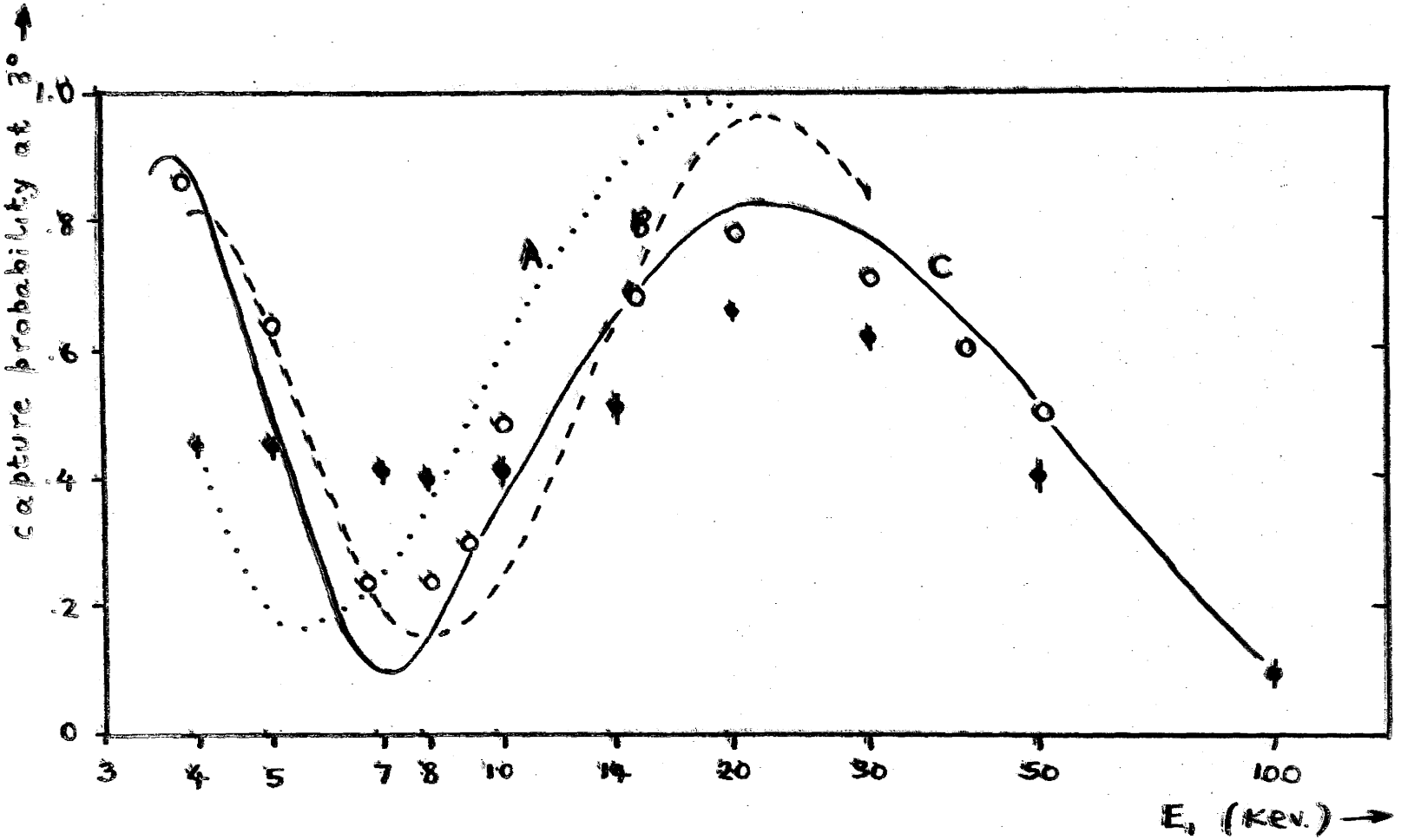

Figure 3.4.3 Ground-state p-H 3^{o} scattering total capture probabilities. Quantal calculations: A (Wilets and Gallaher); B (Cheshire); C (Gallaher and Wilets). Open circles (experimental values of Lockwood and Everhart); full circles (exact-classical results). Error bars represent approximate statistical 2/3 confidence limits.

and of Cheshire are too large at higher incident energies. In contrast the results of Gallaher and Wilets (1968) contain the possibility of ionization implicitly in the Sturmian expansion. Their results are in best agreement with experiment.

(d) Differential Distributions

The continuous differential probabilities $p_D(\beta)$ and $p_E(\beta)$ show little structure as a function of the initial angular-momentum parameter $\beta = L^2/L^2_{max}$. In contrast the differential probability $p_I(\beta)$ indicates a complete reversal of bias over the incident range considered, as can be seen in figure (3.4.4).

The distributions $\rho_D(U_f)$ and $\rho_E(U_f)$ of final binding energy U_f for direct and charge-transfer collisions are, of course, also continuous. The distributions may be characterised by their means and standard deviations, though since $\rho_D(U_f)$ and $\rho_E(U_f)$ are not equal to the normal distribution, higher moments may also be important. The means and standard deviations are plotted in figure (3.4.5) as a function of the incident energy. The error bars represent approximate $^2/_3$ confidence limits in the values determined from the finite samples of orbits. Again, smooth curves have been drawn through the points by hand to avoid possible confusion. At low incident energies, as expected, the distributions $\rho_D(U_f)$ and $\rho_E(U_f)$ are very similar. Over the energy range considered, the apparent structure in the distributions is extremely complicated. It would therefore appear that the possibility of finding an approximate classical theory in this energy range is extremely unlikely.

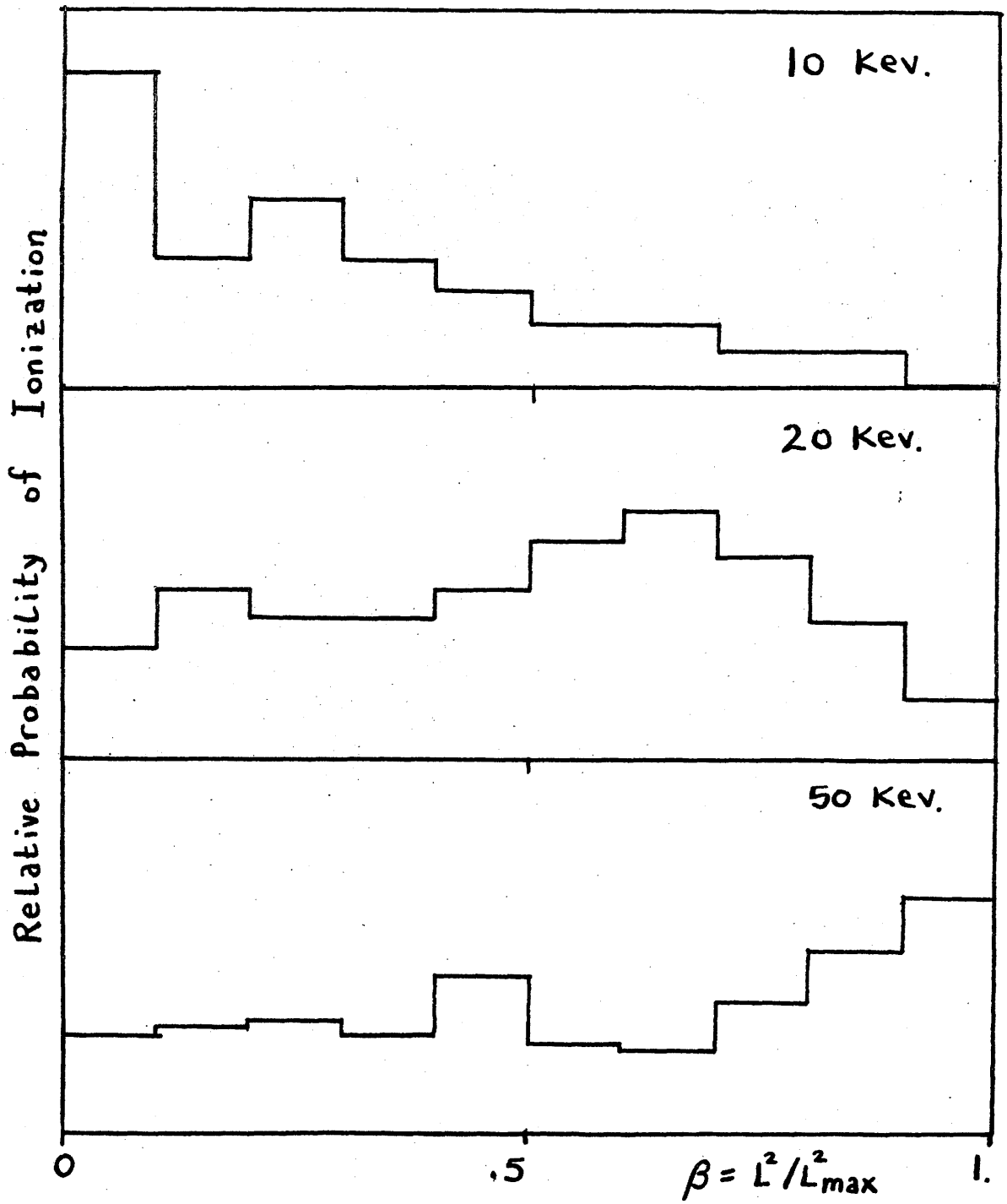

Figure 3.4.4 Exact-classical relative differential ionization probabilities in close p-H collisions versus the initial angular-momentum parameter β for incident energies 10 Kev., 20 Kev., and 50 Kev.

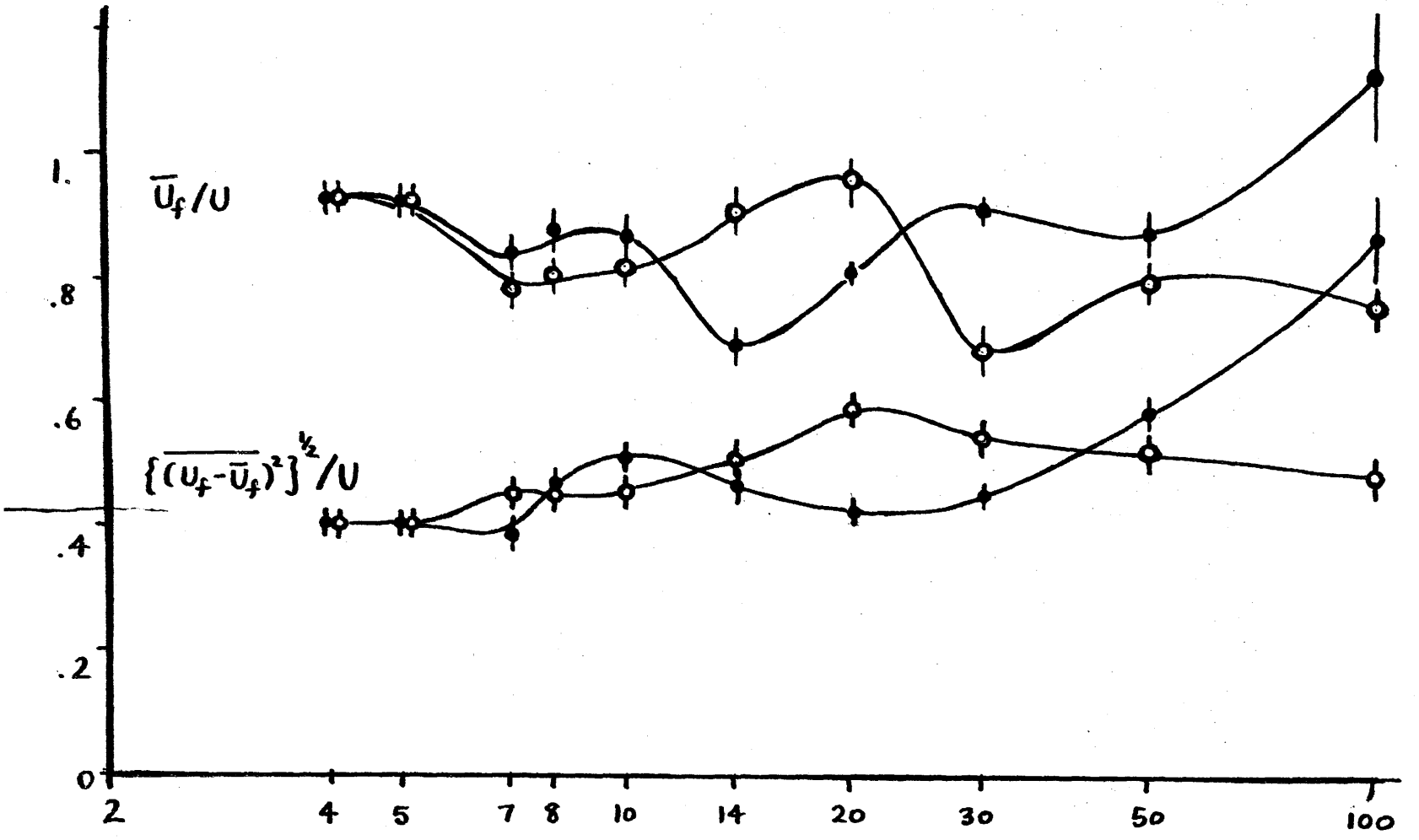

Figure 3.4.5 Means $\bar{U}_f/U$ and standard deviations $\{\overline{(U_f-\bar{U}_f)^2}\}^{1/2}/U$ of exact-classical final binding energies U_f versus incident energy. Full circles (total capture); open circles (total direct excitation).

However, both below and above this energy range approximate theories appear feasible.

The continuous differential distribution $\rho_E(\beta_F)$, where β_F is the final angular-momentum ratio L^2/L^2_{max}, is insensitive to β_F for low and intermediate energies, but for incident energies of 50 Kev. and above, electrons are captured preferentially into orbits with low angular momenta, as was found by Abrines and Percival (1966b) in the case of total charge transfer. Again, as in their work, the results for low β_F arising from orbits with β large initially may not be accurately determined.

3.5 Simultaneous Angle and Energy Distributions of Electrons Ejected from Ground-State Helium Atoms by Protons of Intermediate Energy.

The 3-particle exact-classical FORTRAN computer program of Percival and Valentine (see Valentine 1968) has been used to investigate classical collisions of protons incident upon ground-state helium atoms.

A direct classical treatment of the 4-particle problem was not attempted for two important reasons. Firstly, it would have been difficult, if not impossible, to construct a stable classical model of an isolated ground-state helium atom with two orbiting electrons, since it is always possible for such a classical system to autoionize. In order to avoid autoionization the two-electron model was approximated by two independent one-electron models. The second main reason for reducing the 4-particle problem to a 3-particle problem was that extensive modifications to the computer program would have been required to treat four particles.

Two alternative classical one-electron models of ground-state helium atoms were considered. The former was an extremely simple but crude scaled-hydrogenic model, in which the atom was represented as an electron orbiting around a structureless particle whose mass and charge were taken to be that of a singly-charged helium ion. This model, therefore, implied that the single electron was completely screened by the other electron from the doubly-charged nucleus. Hence this model was most realistic for high singly-excited states of helium rather than for the ground state. Nevertheless, this model had the advantages that equivalent approximations had been made in the first-Born calculations of Rudd, Sautter and Bailey(1966),

and that the classical computer program could be used without modification.

A more realistic variable-nuclear-charge model was also investigated using a simple expression

$$Z(r) = \{1 + \exp(-kr)\}e, \qquad (3.5.1)$$

for the effective nuclear charge $Z(r)$ as a function of the radius r of the electron orbit, where k was a suitable constant. This model had the advantage that a variation in the screening of the nuclear charge was incorporated, but the main disadvantages were that, since the period of the bound motion of the electron was no longer independent of its angular momentum for a fixed binding energy, the wind-back procedure was more complicated than the Kepler motion, that the best choice of angular-momentum distribution to represent the ground state was not obvious, that several parts of the classical computer program required modification, and that the solution of Newton's equations of motion using equation (3.5.1) was probably more time-consuming owing to the need for a smaller time-step.

For these reasons, the simpler model was selected for a preliminary investigation, but the necessary modifications to the computer program were also carried out for the more realistic model, in the event that the classical results using the simple model were not in satisfactory agreement with the experimental results of Rudd and Jorgenson (1963) and of Rudd, Sautter and Bailey (1966), especially for small angles of ejection, where the experimental results are typically larger than the binary-encounter results of Bonsen and Vriens (1970) and the Born calculations of Rudd et al. by at least a factor of ten.

The details of this calculation, the results and the comparison with experiment and with Born and binary-encounter theories have been published by Bonsen and Banks (1971) (see, for example, the end of this thesis). The results obtained from the simple classical model are in such close agreement with experiment at low ejection angles that a further investigation using the more sophisticated model is not justified, because the remaining discrepancy could be due predominantly to the classical approximation itself.

Since the binary-encounter results are too low at low angles, genuine three-body effects must be responsible for the enhancement at low ejection angles. The remarkable agreement using the simple classical model suggests that the effect depends crucially on the final long-range interactions between the three bodies, rather than upon specific initial atomic properties.

In contrast, at large angles of ejection, the Born calculations are considerably larger than the results of the accurate-classical and binary-encounter models, and are in much better agreement with experiment. In this region, since the accurate-classical and binary-encounter results are similar, three-body effects are not important. The failure of the classical results has been attributed by Percival (1971) to the dominance of a purely-quantal two-body mechanism, termed super-barrier reflection, between the ejected electron and the helium ion.

This work again demonstrates that simple quantal theories (in this case the first-Born approximation) and accurate-classical models are complementary, even for low quantum numbers, and that the complementarity

may not be evident unless a sufficiently-accurate classical model is used.

CHAPTER 4

ADDITIONAL AND CONCLUDING REMARKS

4.1 Classical Models for Hydrogenic Atoms and Ions

There are two similar but distinct classical models of hydrogenic atoms and ions. In the Bohr-Sommerfeld model (see, for example, Born 1960) a direct correspondence is made between the quantum numbers (n,l,m) of a quantal excited state of a hydrogenic atom or ion in spherical-polar coordinates, and discrete values only of the classical action variables (n_c,l_c,m_c) in spherical-polar coordinates. The Bohr-Sommerfeld model, therefore, consists of a classical ensemble of similar orbits each with prescribed classical action variables, but with arbitrary values of the canonically-conjugate angle variables, by virtue of the uncertainty principle. The natural distribution, from which to select the angle variables independently, is the uniform rectangular distribution defined over a range $[0,2\pi]$, say. This ensemble may be generalised to treat the two cases in which firstly atoms in a given level (n,l) are uniformly populated in the $(2l+1)$ m-states and secondly, in which atoms in a given level n are uniformly populated in the n^2 (l,m)-states. However, the classical ensembles which represent these levels are not usually spherically symmetric, unlike the quantal treatment; for example, the ensemble representing the level $(n_c=2,l_c=1)$, averaged uniformly over the m_c-states, $m_c=-1,0,1$, is not spherically symmetric, since the orbits with $m_c=\pm1$ lie entirely

in the $(\underline{\hat{x}},\underline{\hat{y}})$ plane, whereas orbits with $m_c=0$ are spherically distributed. Only in the limit of large n_c and l_c will these distributions approach a spherical form for non-zero values of l_c .

A well-known alternative to the Bohr-Sommerfeld model for a uniformly-populated level n is the classical microcanonical model. However, no alternative to the Bohr-Sommerfeld model for a uniformly-populated level (n,l) has previously been given. A possible model is formulated in this section. In the classical microcanonical model a correspondence is made between n and n_c , as in the Bohr-Sommerfeld case, but not between (l,m) and discrete values of (l_c, m_c) . Instead, the level n is represented by a different average of ensembles of the Bohr-Sommerfeld type with prescribed (n_c, l_c, m_c) . This average is taken over all values of m_c in the complete continuous range $[-l_c, l_c]$ and over all l_c in the complete continuous range $[0, n_c]$, in such a way that the dimensionless variables $\beta = l_c^2/n_c^2$ and $\mu = m_c/l_c$ are independently and uniformly distributed in the ranges $[0,1]$ and $[-1,1]$ respectively. The classical microcanonical model is therefore the approximation to the Bohr-Sommerfeld model for a level n , obtained by replacing the summations by integrations. However, the classical microcanonical model has two advantages over the Bohr-Sommerfeld model. Firstly the classical ensemble is spherically distributed for all n , as in the quantal treatment. Secondly, the momentum distribution derived from the microcanonical ensemble is correct for all levels n . For these reasons, the classical microcanonical model for a uniformly-populated

level n is more attractive than the Bohr-Sommerfeld model. A similar model of a uniformly-populated level (n,l) is sought with the same additional properties.

The key to this construction is the correspondence between the quantum numbers n and l and a classical distribution function $\rho_{nl}(\beta)$. This can be seen from the fact that for any level (n,l) the spherical quantum momentum distribution is defined over the entire range of magnitudes of momentum, whereas in the classical case barriers exist unless straight-line orbits are permitted. By comparison with the known microcanonical model in which $\rho_n(\beta)=1$, the distribution $\rho_{nl}(\beta)$ must satisfy the Fock identity, namely

$$\sum_{l=0}^{n-1} \frac{(2l+1)}{n^2} \rho_{nl}(\beta) = \rho_n(\beta) = 1 \quad , \tag{4.1.1}$$

for all n. In particular, for $n=1$, $l=0$

$$\rho_{nl}(\beta) = 1 = \rho_n(\beta) \quad . \tag{4.1.2}$$

The simplest possible postulate for $\rho_{nl}(\beta)$ is a polynomial of degree $(n-1)$ with coefficients which depend upon n and l. For a given value of β the classical ensemble of orbits, obtained by averaging over the three angle variables and the variable μ, leads to the classical momentum distribution $\rho^c_{p_0\beta}(p)$ given by

$$\rho^c_{p_0\beta}(p) = \frac{4}{\pi} \cdot \frac{p_0^3}{(p^2+p_0^2)^2} \cdot \frac{H(\beta_{max}-\beta)}{(1-\beta/\beta_{max})^{1/2}} \quad , \tag{4.1.3}$$

where $p_0^2 = 2mU$ and $\beta_{max} = 4p^2p_0^2/(p^2+p_0^2)^2$. This distribution may be obtained from the position distribution defined by Hapleton (1966) for

a fixed classical angular-momentum magnitude, by using the energy equation

$$\frac{1}{2m}p^2 - \frac{Ze^2}{r} = -U = -\frac{1}{2m}p_o^2 \quad . \tag{4.1.4}$$

The precise analytic form of β_{max} is essential to the correspondence with the quantal momentum distributions. The physical reason for the upper bound β_{max}, which is never greater than unity, is that if p is different to p_o, then a circular orbit must be forbidden and hence β cannot be unity.

The distribution $\rho^c_{p_o\beta}(p)$ is normalised according to

$$\int_{p_{min}}^{p_{max}} dp\, \rho^c_{p_o\beta}(p) = 1 \quad , \tag{4.1.5}$$

where

$$p_{max} = p_o \left(\frac{1+\epsilon}{1-\epsilon}\right)^{1/2} \quad , \tag{4.1.6}$$

$$p_{min} = p_o \left(\frac{1-\epsilon}{1+\epsilon}\right)^{1/2} \quad , \tag{4.1.7}$$

and

$$\epsilon = (1-\beta)^{1/2} \quad , \tag{4.1.8}$$

is the eccentricity of the ensemble of orbits.

It is not difficult to show that the classical microcanonical momentum distribution $\rho^c_{p_o}(p)$ is generated by

$$\rho^c_{p_o}(p) = \int_0^1 d\beta\, \rho_{IS}(\beta)\, \rho^c_{p_o\beta}(p) \quad , \tag{4.1.9}$$

where $\rho_{IS}(\beta) = 1$. Then

$$\rho^c_{p_o}(p) = \frac{32}{\pi} \frac{p_o^5 p^2}{(p^2+p_o^2)^4} \quad . \tag{4.1.10}$$

Let

$$\rho^{c}_{n\ell}(p) = \int_0^1 d\beta\, \rho_{n\ell}(\beta)\, \rho^{c}_{p_0\beta}(p) \quad , \tag{4.1.11}$$

be the classical momentum distribution derived from $\rho_{n\ell}(\beta)$.

In particular, if $\rho_{2p}(\beta) = 2\beta$ then

$$\rho^{c}_{2p}(p) = \frac{8}{\pi} \frac{p_0^3}{(p^2+p_0^2)^2} \int_0^{\beta_{max}} d\beta\, \beta\, (1-\beta/\beta_{max})^{-1/2} ,$$

giving

$$\rho^{c}_{2p}(p) = \frac{32}{\pi} \cdot \frac{p_0^5 p^2}{(p^2+p_0^2)^4} \cdot \frac{16}{3} \frac{p_0^2 p^2}{(p^2+p_0^2)^2} \quad , \tag{4.1.12}$$

which is the exact quantal momentum distribution for the $2p$ level.

Similarly, if $\rho_{2s}(\beta) = 4-6\beta$ then

$$\rho^{c}_{2s}(p) = \frac{32}{\pi} \frac{p_0^5 p^2}{(p^2+p_0^2)^4} \cdot \frac{4(p^2-p_0^2)^2}{(p^2+p_0^2)^2} \quad , \tag{4.1.13}$$

which is also the exact quantal momentum distribution for the $2s$ level.

As a check, note that

$$\frac{1}{4}\rho_{2s}(\beta) + \frac{3}{4}\rho_{2p}(\beta) = 1 \quad , \tag{4.1.14}$$

and

$$\frac{1}{4}\rho^{c}_{2s}(p) + \frac{3}{4}\rho^{c}_{2p}(p) = \rho^{c}_{p_0}(p) = \frac{32}{\pi} \frac{p_0^5 p^2}{(p^2+p_0^2)^4} . \tag{4.1.15}$$

Further, the following simple relations hold

$$\left.\begin{aligned} \int_0^1 d\beta\, \rho_{1s}(\beta) = \int_0^1 d\beta\, \rho_{2s}(\beta) = \int_0^1 d\beta\, \rho_{2p}(\beta) = 1 \\ \int_0^1 d\beta\, \rho_{2s}(\beta)\, \rho_{2p}(\beta) = 0 \\ \int_0^1 d\beta\, \beta\, \rho_{1s}(\beta)\, \rho_{2s}(\beta) = 0 \end{aligned}\right\} \tag{4.1.16}$$

and

There remains only one awkward problem. For $\beta > 2/3$, $\rho_{2s}(\beta)$

is negative. The explanation is, however, extremely simple. Since the quantal momentum-space wave functions for the $1s$ and $2s$ states must be orthogonal in their "radial" part, the latter must have a simple zero at a finite but non-zero value of p, and so the momentum distribution for this level must have a node at this point. Clearly, the node occurs at $p=p_0$, where the distribution takes the form $k(p-p_0)^2$. In order to reproduce this behaviour some classical contributions near $p=p_0$ must be subtracted, not added. It may be argued that such negative distributions are unacceptable, yet they do not arise inherently from classical distribution theory, but are consequences of the correspondence between classical and quantal systems. In spite of this difficulty it is extremely surprising that such a simple extension gives exact results.

For an arbitrary level (n,l) the quantal momentum distribution $\rho^Q_{nl}(p)$ may be written

$$\rho^Q_{nl}(p) = \frac{32}{\pi}\frac{p_0^5 p^2}{(p^2+p_0^2)^4}\cdot\frac{(2^l l!)^2(n-l-1)!}{(n+l)!}\cdot n\beta_{max}^l\left\{C_{n-l-1}^{l+1}(\epsilon_{max})\right\}^2, \qquad (4.1.17)$$

where

$$\epsilon_{max} = (p^2-p_0^2)/(p^2+p_0^2), \qquad (4.1.18)$$

and

$$\beta_{max} = 1-\epsilon_{max}^2, \qquad (4.1.19)$$

(see for example Bethe and Salpeter 1957, Vol. 35, pp. 125-6). The function $C_n^\nu(x)$ is the Gegenbauer polynomial of degree n with parameter ν and argument x (see, for example, Abramowitz

and Stegun 1965, pp. 773-803). Now, since $C_n^{\nu}(x)$ is even or odd according to whether n is even or odd, the function $\{C_n^{\nu}(x)\}^2$ is a polynomial in x^2 and hence also a polynomial in $(1-x^2)$. Thus, by equation (4.1.19) the expression $\{C_{n-l-1}^{l+1}(\epsilon_{max})\}^2$ is always a polynomial in β_{max} of degree $j = n-l-1$, the number of zeros in the "radial" momentum-space wave function. Hence, it is always possible to write

$$\left\{ C_{n-l-1}^{l+1}(\epsilon_{max}) \right\}^2 = \sum_{k=0}^{j} D_{jk}^{l+1} \beta_{max}^{k} , \qquad (4.1.20)$$

so that

$$\rho_{nl}^{Q}(p) = \frac{32}{\pi} \frac{p_o^5 p^2}{(p^2+p_o^2)^4} \cdot \frac{(2^l \cdot l!)^2 j! n}{(n+l)!} \cdot \sum_{k=0}^{j} D_{jk}^{l+1} \beta_{max}^{k+l} . \qquad (4.1.21)$$

In order to reproduce this quantal distribution in the classical model, suppose $\rho_{nl}(\beta) = \sum_{k=0}^{n-1} A_{nlk} \beta^k$. Use this in equation (4.1.11) Then

$$\rho_{nl}^{c}(p) = \frac{4}{\pi} \cdot \frac{p_o^3}{(p^2+p_o^2)^2} \cdot \int_0^{\beta_{max}} d\beta \, (1-\beta/\beta_{max})^{-1/2} \sum_{k=0}^{n-1} A_{nlk} \beta^k ,$$

so that

$$\rho_{nl}^{c}(p) = \frac{32}{\pi} \cdot \frac{p_o^5 p^2}{(p^2+p_o^2)^4} \cdot \sum_{k=0}^{n-1} W_{2k+1} A_{nlk} \beta_{max}^{k} , \qquad (4.1.22)$$

where $W_{2k+1} = (2^k k!)^2/(2k+1)!$. Hence $\rho_{nl}^{c}(p)$ is identical to $\rho_{nl}^{Q}(p)$ if the A_{nlk} are chosen to satisfy

$$\left.\begin{aligned} A_{nl(l-r-1)} &= 0 \quad , \text{ for } r = 0, l-1 ; \\ A_{nl(l+r)} &= \frac{(2^l \cdot l!)^2 j! n}{(n+l)! \, W_{2l+2r+1}} \cdot D_{jr}^{l+1} , \\ &\text{for } r = 0, n-l-1 . \end{aligned}\right\} \qquad (4.1.23)$$

The coefficients D^{l+1}_{jr} are assumed to be known from the quantal model and so the classical polynomial distribution $\rho_{nl}(\beta)$ is uniquely determined. Since the coefficient D^{l+1}_{jr} depends upon properties of the Gegenbauer polynomials, an explicit expression is not necessarily easy to obtain. However a direct guess $A^{*}_{nl\,l+r}$ for $A_{nl\,l+r}$ with

$$A^{*}_{nl\,l+r} = \frac{(-1)^{r}\,(n+l+r)!\,n}{(n-l-r-1)!\,(2l+r+1)!\,r!}\,, \qquad (4.1.24)$$

satisfies the necessary constraint given by equation (4.1.1) and has been checked in many cases. This guess leads to the expression

$$\rho^{*}_{nl}(\beta) = \frac{n\,(n+l)!}{(n-l-1)!\,(2l+1)!}\,\beta^{l}\,F_{n-l-1}(2l+2,\,2l+2,\,\beta)\,, \qquad (4.1.25)$$

where $F_n(p,q,x)$ is the Jacobi polynomial defined by Abramowitz and Stegun (1965, pp. 773-803). The orthogonality relations for these polynomials imply automatically that

$$\left.\begin{aligned} &\int_0^1 d\beta\;\rho^{*}_{nl}(\beta) = 1 \quad \text{for all } n,l \\ \text{and}\quad &\int_0^1 d\beta\;\rho^{*}_{nl}(\beta)\,.\,\beta\,.\,\rho^{*}_{n'l}(\beta) = 0 \quad \text{for } n' \neq n\,. \end{aligned}\right\} \qquad (4.1.26)$$

It further appears that

$$\int_0^1 d\beta\;\rho^{*}_{nl}(\beta)\,\rho^{*}_{nl'}(\beta) = 0 \quad \text{for } l' \neq l\,. \qquad (4.1.27)$$

In particular

$$\rho_{n\,n-1}(\beta) = n\,\beta^{n-1}\,, \qquad (4.1.28)$$

and

$$\rho_{n\,n-2}(\beta) = 2n(n-1)\beta^{n-2} - n(2n-1)\beta^{n-1} , \qquad (4.1.29)$$

are completely consistent with equations (4.1.25) - (4.1.27).

4.2 Miscellaneous Initial Variables

In principle, the initial conditions of an exact-classical orbit can be generated from any alternative set of initial variables equivalent to the original set. If, however, exact-classical orbits with known initial conditions are available from previous work, then there are two main reasons why, in practice, it is important to investigate whether there are alternative significant initial variables. In this work a significant initial variable may be defined as one for which orbits of a similar type, say ionization, are significantly concentrated in limited regions of the allowed range of the variable, even when the orbits have been averaged over all other initial variables. In contrast, an insignificant initial variable may be defined as one for which the concentration of orbits of a similar type is insensitive to the value of the initial variable over its entire range, once the orbits have been averaged over all other initial variables.

The first important reason for such an investigation is that the significance (or even the lack of significance) of a particular initial variable can suggest (or even reject) the possibility of a simplified treatment of the collisions. Such a procedure may therefore provide insight into the classical mechanisms involved in specific many-particle collisions. Further, the success (or failure) of a classical dynamical approximation may be used to suggest (or criticise) an equivalent quantal dynamical approximation.

The second reason applies particularly to the Monte-Carlo methods of integration. The more refined techniques, such as stratification, importance sampling and control-variate methods (see, for example, section (3.1)), only have increased efficiency over the crude and hit-or-miss methods, if as many as possible of the initial variables are significant, otherwise the gain in efficiency is usually small.

A detailed investigation of ionization and charge-transfer collisions was made at the incident proton energy 68 Kev. (see section (3.3)). The dependence of these strong collisions was sought as a separate function of each of the original and of several simple alternative initial variables, though dependences for two or more variables at a time were postponed until significant variables could be found.

The results of the investigation were, in general, disappointing, but perhaps it was too much to expect that all the original initial variables could be replaced by alternative simple significant initial variables.

The first of the significant variables was found to be the square b'^2 of the modified impact parameter, which was already known from earlier work. Strong collisions were indeed more closely grouped than in the corresponding unmodified square b^2 at this incident energy. The significance of b'^2 is suggested from the binary-encounter theory. Indeed, in the Thomson model, the energy transfer is a simple function of b'^2 and is independent of the other five initial variables. However, in the Thomas model, in which allowance is made for the motion of the

target electron, the energy transfer is a complicated function of b'^2 and of the other initial variables. In fact, only four of these five variables are required, since the Thomas energy transfer is invariant under rotations of the position of the target electron about the axis through the centre of mass of the atom in the direction of the incident velocity. Unfortunately this angle is not one of the original set of initial variables. Since b' is measured along a fixed axis, and not radially, different values of this angle produce different unmodified impact parameters b so that the exact-classical orbits are not invariant under this rotation, though the angular dependence of strong collisions was not found to be sufficiently significant to be useful in later work. The Thomas binary-encounter model was found to be particularly disappointing, as the gain over the Thomson model was only marginal at this energy. Nevertheless, the binary-encounter theory does provide the variable b'^2 .

A second significant variable was suggested originally by Percival and Richards (1971a,b), where they found that their analytic work for weak excitations simplified if the incident-velocity direction is chosen along $\hat{\underline{y}}$ axis instead of the $\hat{\underline{z}}$ axis. They found that the Euler rotation-matrix elements were more symmetric and that the expression $(1-\mu^2)^{1/2} = \sin\theta$ could be entirely eliminated with this choice of incident-velocity direction. Since, in the exact-classical work the incident direction had been chosen by convention along the $\hat{\underline{z}}$ axis, it was decided to investigate the dependence of strong collisions on each of

the rotation-matrix elements. This had not been considered previously. It was found, surprisingly that the dependence on the element R_{13} $(= -\cos\phi \sin\theta$ in terms of the original variables) was significant for both ionization and charge transfer. Further, the dependence was found to be very close to that predicted by the classical first-order dipole perturbation theory of Percival and Richards (1967) for the special case of circular orbits and large values of the adiabaticity parameter $\omega b'/v_1$. The element R_{13} is simply the scalar product $\hat{\underline{L}}.\hat{\underline{x}}$ in the original coordinate system where $\underline{L}$ is the initial orbital angular momentum of the target electron. If the impact parameter is unmodified, or even if it is modified, but much larger than the mean atomic radius a , then $\hat{\underline{x}}$ is directed along the initial angular momentum $\underline{L}_1$ of the incident particle, though this is not true for small modified impact parameters. For this reason the dependence of strong collisions was also investigated as a function of $\hat{\underline{L}}_1.\hat{\underline{L}}$ but it was found to be so close to the dependence with respect to $\hat{\underline{L}}.\hat{\underline{x}}$ that the simpler uniformly-distributed variable $\hat{\underline{L}}.\hat{\underline{x}}$ could be used in preference. If the velocity is directed along the $\hat{\underline{y}}$ axis, then $\hat{\underline{L}}.\hat{\underline{x}}$ is simply the new initial Euler-angle variable μ' . Hence the classical adiabatic perturbation theory provides the significant variable μ' . Physically, this means that, for large impact parameters, strong collisions are concentrated in the region where the orbits are almost planar, as might have been expected from first principles.

At lower incident energies b'^2 is less significant than b^2 , but

the significance of μ' persists, as can be seen from figure (4.2.1), where the dependence of charge transfer (ionization being negligible in this case) is displayed simultaneously as a function of the variables b^2/b^2_{max} and $\frac{(1-\mu')}{2}$, using the first 400 orbits of the exact-classical results for 7 Kev. incident protons. The dependence is extremely striking at such a low incident energy. It should be noted that each cell would be expected to contain approximately the same number of charge-transfer orbits, if these variables were insignificant. In this case the shape of the distribution suggests that an alternative product variable $q = b^2(1-\mu')/(2b^2_{max})$ would be even more significant. However, first, care is needed, since the product q of the two independent and uniformly-distributed variables x and y say, is not uniformly distributed, even though all are defined in the range $[0,1]$. Instead, the variable $u = q - q\log q$ is uniformly distributed on this range. In the above case, all charge-transfer orbits possess values of u in the restricted range $[0, 0.6]$ approximately, which implies that the remaining 40% of the total orbits could have been omitted, if the significance of this variable and its precise cut-off value were known beforehand. The only difficulty which could arise from using this variable is that its value depends upon b^2_{max}. It is therefore probably better to use this variable only if b^2_{max} is known to include all orbits of interest and is not to be varied.

Of the remaining distributions the dependences upon the variables $\beta = L^2/L^2_{max}$ and the electron phase parameter $\tau/2\pi$ are probably most significant at intermediate and high incident energies, but only for

a)

0.0 b^2/b^2_{max} →					1.0
4	0	0	0	0	4
8	1	0	0	0	9
10	3	1	0	0	14
12	5	13	4	0	34
8	10	7	5	3	33
42	19	21	9	3	94

1.0

$(1-\mu')/2$ ↑

0.0

b)

18	13	15	15	14	75
19	18	14	17	16	84
17	12	15	21	10	75
17	15	23	21	18	94
18	17	15	13	9	72
89	75	82	87	67	400

1.0

$(1-\mu')/2$ ↑

0.0

0.0 b^2/b^2_{max} → 1.0

Table 4.2.1 Double-plot of p-H charge-transfer probability versus the initial variables b^2/b^2_{max} and $(1-\mu')/2$ for 7 Kev. protons. Case a) orbits resulting in charge-transfer only; b) all orbits.

charge-transfer, not for ionization. These two variables are just those needed to define the initial radius r of the electron and hence also its speed, using the energy equation. It would appear that the variable $g(r)$, where

$$g(r) = \frac{2}{\pi}\tan^{-1}\left(\frac{r}{2a-r}\right)^{1/2} - \frac{1}{\pi a^3}(a+r)\left(a-\frac{2r}{3}\right)\left[r(2a-r)\right]^{1/2}, \qquad (4.2.1)$$

which is uniformly distributed in the range $[0,1]$, is a convenient alternative to the pair (β,τ). It is interesting that this variable arises naturally in the approximate classical treatment of charge transfer at high incident energies (see, for example, Thomas 1927c, Bates and Kingston 1970).

REFERENCES

ABRAMOWITZ, M., and STEGUN, I.A., (Eds), 1965, Handbook of Mathematical Functions (New York : Dover Publications).

ABRINES, R., and PERCIVAL, I.C., 1966a, Proc. Phys. Soc., 88, 861.

- - - -1966 b, Proc. Phys. Soc., 88, 873.

ABRINES, R., PERCIVAL, I.C., and VALENTINE, N.A., 1966, Proc. Phys. Soc., 89, 515.

BANKS, D., PERCIVAL, I.C., and VALENTINE, N.A., 1969, Abstr. 6th Int. Conf. Electronic and Atomic Collisions (Cambridge: MIT Press), p.215.

BANKS, D., PERCIVAL, I.C., and WILSON, J.McB., 1971, Computer Phys. Commun., 2, 114.

- - - - 1972a, Computer Phys. Commun., in press.

- - - - 1972b, Computer Phys. Commun., in press.

- - - - 1972c, Computer Phys. Commun., in press.

BANKS, D., and VALENTINE, N.A., 1969, Abstr. 6th Int. Conf. Electronic and Atomic Collisions (Cambridge : MIT Press), p.123.

BANKS, D., VRIENS, L., and BONSEN, T.F.M., 1969, J. Phys. B (Atom. Molec. Phys.), 2, 976.

BATES, D.R., and GRIFFING, G.W., 1953, Proc. Phys. Soc., A66, 961.

BATES, D.R., and KINGSTON, A.E., 1970, Advances in Atomic and Molecular Physics, Vol. 6, Eds D.R. Bates and I. Estermann (New York: Academic Press), p. 269.

BATES, D.R., and REID, R.H.G., 1969a, J. Phys. B (Atom. Molec. Phys.), 2, 851.

- - - - 1969b, J. Phys. B (Atom. Molec. Phys.), 2, 857.

BETHE, H.A., and SALPETER, E.E., 1957, Encyclopedia of Physics, Vol. 35, Ed S. Flügge (Berlin : Springer-Verlag).

BOISEN, T.F.M., and BANKS, D., 1971, J. Phys. B (Atom. Molec. Phys.), 4, 706.

BOISEN, T.F.M., and VRIENS, L., 1970, Physica, 47, 307.

BORN, M., 1960, Mechanics of the Atom (London : Bell).

BRATTSEV, V.F., and OCHKUR, V.I., 1967, Soviet Phys. JETP, Vol. 25, 4, 631.

BURGESS, A., 1963, Proc. 3rd Int. Conf. Electronic and Atomic Collisions, Ed M.R.C. McDowell (Amsterdam : North-Holland), p.237.

- - - - 1964, Proc. Symp. Atomic Collision Processes in Plasmas, Culham (A.E.R.E. Rep. 4818), p.63.

BURGESS, A., and PERCIVAL, I.C., 1968, Advances in Atomic and Molecular Physics, Vol. 4, Eds D.R. Bates and I. Estermann (New York: Academic Press), p. 109.

CATLOW, G.W., and McDOWELL, M.R.C., 1967, Proc. Phys. Soc., 92, 875.

CHESHIRE, I.M., 1968, Proc. Phys. Soc., 113, 428.

CORBEN, H.C., and STEHLE, P., 1966, Classical Mechanics, 2nd Edn (London : John Wiley).

FITE, W.L., STEBBINGS, R.F., HUMMER, D.G., and BRACKMANN, R.T., 1960, Phys. Rev., 119, 663.

FLANNERY, M.R., 1970a, Astrophys. Letters, 7, 85.

- - - - 1970b, J. Phys. B (Atom. Molec. Phys.), 3, 1610.

FOCK, V., 1935, Z. Phys., 98, 145.

GALLAGHER, D.F., and WILETS, L., 1968, Phys. Rev., 169, 139.

GERJUOY, E., 1966, Phys. Rev., 148, 54.

GILBODY, H.B., and IRELAND, J.V., 1964, Proc. Roy. Soc., A277, 137.

GILBODY, H.B., and RYDING, G., 1966, Proc. Roy. Soc., A291, 438.

GRYZINSKI, M., 1959, Phys. Rev., 115, 374.

- - - - 1965a, Phys. Rev., 138, A305.

- - - - 1965b, Phys. Rev., 138, A322.

- - - - 1965c, Phys. Rev., 138, A336.

HAMMERSLEY, J.M., and HANDSCOMB, D.C. , 1964, Monte Carlo Methods (London : Methuen).

HAYS, W.L., 1963, Statistics (London : Holt, Rinehart and Winston), p. 291.

HELBIG, H.F., and EVERHART, E., 1965, Phys. Rev., 140, A715.

KINGSTON, A.E., 1966, Proc. Phys. Soc., 87, 193.

- - - - 1968, J. Phys. B (Proc. Phys. Soc.), 1, 559.

LANDAU, L.D., and LIFSCHITZ, E.M., 1960, Mechanics (London : Pergamon Press).

LOCKWOOD, G.L., and EVERHART, E., 1962, Phys. Rev., 125, 567.

McDOWELL, M.R.C., 1966, Proc. Phys. Soc., 89, 23.

McDOWELL, M.R.C., and COLEMAN, J.P., 1970, Introduction to the Theory of Ion-Atom Collisions (Amsterdam : North-Holland), Chap. 1 and3.

McELROY, M.B., 1963, Proc. Roy. Soc., A272 , 542.

MAPLETON, R.A., 1966, Proc. Phys. Soc., 87, 219.

MOTT, N.F., and MASSEY, H.S.W., 1965, Theory of Atomic Collisions, 3rd Edn (Oxford : Clarendon Press).

NORCLIFFE, A., 1970, Ph D thesis, University of Stirling.

OCHKUR, V.I., and PETRUN'KIN, A.N., 1963, Optics Spectrosc., 14, 245.

PERCIVAL, I.C., 1966, Nuclear Fusion, 6, 182.

- - - - 1969, Physics of the One-and Two- Electron Atoms, Eds F. Bopp and H. Kleinpoppen (Amsterdam : North-Holland), p. 252.

- - - - 1971, Proc. 2nd Int. Conf. Atomic Phys., Ed P.G.H. Sandars (London : Plenum Press), p. 345.

PERCIVAL, I.C., and RICHARDS, D., 1967, Proc. Phys. Soc., 92, 311.

- - - - 1970a, J. Phys. B (Atom. Molec. Phys.), 3, 315.

- - - - 1970b, J. Phys. B (Atom. Molec. Phys.), 3, 1035.

- - - - 1971a, J. Phys. B (Atom. Molec. Phys.), 4, 918.

- - - - 1971b, J. Phys. B (Atom. Molec. Phys.), 4, 932.

PERCIVAL, I.C., and VALENTINE, N.A., 1966, Proc. Phys. Soc., 88, 885.

- - - - 1967, Abstr. 5th Int. Conf. Electronic and Atomic Collisions (Leningrad : Nauka), p, 121.

PETERKOP, R., 1971, J. Phys. B (Atom. Molec. Phys.), 4, 21.

PETERKOP, R., and LIEPINSH, A., 1969, Abstr. 6th Int. Conf. Electronic and Atomic Collisions (Cambridge : MIT Press), p. 212.

PETERKOP, R., and TSUKERMAN, P., 1969, Abstr. 6th Int. Conf. Electronic and Atomic Collisions (Cambridge : MIT Press), p. 209.

RUDD, M.E., and JORGENSON, Jr. T., 1963, Phys. Rev., 131, 666.

RUDD, M.E., SAUTTER, C.A., and BAILEY, C.L., 1966, Phys. Rev., 151, 20.

SCHREIDER, Y.A., (Ed), 1964, Method of Statistical Testing (Amsterdam : Elsevier), chap. 1-3.

STABLER, R.C., 1964, Phys. Rev., 133, A1268.

THOMAS, L.H., 1927a, Proc. Camb. Phil. Soc., 23, 713.

- - - - 1927b, Proc. Camb. Phil. Soc., 23, 829.

- - - - 1927c, Proc. Roy. Soc., A114, 561.

THOMSON, J.J., 1912, Phil. Mag., 23, 449.

TRIPATHI, A.N., MATHUR, K.C., and JOSHI, S.K., 1969, J. Phys. B (Atom. Molec. Phys.), 2, 878.

VALENTINE, N.A., 1968, Ph D thesis, University of London.

VRIENS, L., 1966a, Phys. Rev., 141, 88.

- - - - 1966b, Proc. Phys. Soc., 89, 13.

- - - - 1967, Proc. Phys. Soc., 90, 935.

- - - - 1969, Case Studies in Atomic Collisions, Eds E.W. McDaniel and M.R.C. McDowell (Amsterdam : North-Holland), chap. 6.

VRIENS, L., and BONSEN, T.F.M., 1968, J. Phys. B (Proc. Phys. Soc.), 1, 1123.

WANNIER, G.H., 1953, Phys. Rev., 90, 817.

WHITTAKER, E.T., 1965, A Treatise on the Analytic Dynamics of Particles and Rigid Bodies (Cambridge : Cambridge University Press).

WILETS, L., and GALLAHER, D.F., 1966, Phys. Rev., 147, 13.

WILLIAMS, E.J., 1927, Nature, 119, 489.

- - - - 1945, Rev. Mod. Phys., 17, 217.

ZUBIN, J., 1935, Journal of Applied Psychology, 19, 2, 213.

Addenda

BUCKINGHAM, R.A., 1962, Numerical Methods (London : Pitman).

RUDGE, M.R.H., and SEATON, M.J., 1965, Proc. Roy. Soc., A283, 262.

WITTKOWER, A.B., RYDING, G., and GILBODY, H.B., 1966, Proc. Phys. Soc., 89, 541.

J. PHYS. B (ATOM. MOLEC. PHYS.), 1969, SER. 2, VOL. 2. PRINTED IN GREAT BRITAIN

Initial-state m quantization in binary-encounter theory

D. BANKS†, L. VRIENS‡ and T. F. M. BONSEN§

† Department of Physics, University of Stirling
‡ F.O.M.–Instituut voor Atoom-en Molecuulfysica, Amsterdam, The Netherlands
§ Fysisch Laboratorium der Rijksuniversiteit, Utrecht, The Netherlands

MS. received 6th March 1969

Abstract. A detailed comparison has been made between the binary-encounter and Bethe theories for ionization of the (2p, 0) hydrogen atom by a fast incident charged particle. For this purpose we have mathematically reformulated the binary-encounter theory to treat the non-isotropic velocity distribution in the initial state of the atom considered. The pronounced dip found before in the Bethe theory is reproduced in the binary-encounter theory and is shown to be caused solely by the angular part of the initial-state wave function. Good agreement between the theories is found for energy transfers $\epsilon > 1$ ryd. Applications to other initial states and other atoms are discussed.

1. Introduction

A new wave of interest in binary-encounter collision theory was created by the publication of Gryzinski's (1959) paper, where remarkably good agreement between classical total cross sections and experiment was found for a vast range of charged-particle–atom collisions. However, these formulae contained certain errors which were corrected by Stabler (1964) and as a result the agreement with experiment suffered. The agreement was improved for electron–atom collisions by Burgess (1963) and Vriens (1966) by formulating a symmetric collision model and partly allowing for electron exchange by using a quantal instead of a classical treatment. Kingston (1968) gave a quantitative comparison between the binary-encounter collision theory and Bethe (first Born) theory for ionization of ground-state and excited hydrogen atoms by fast charged particles, and so studied the range of validity of the binary-encounter collision theory for total cross sections. His results agree with the qualitative results afforded by the correspondence principle (see e.g. Abrines and Percival 1966, Burgess and Percival 1968, Vriens 1969). This approach was extended to a comparison of the differential cross sections by Vriens and Bonsen (1968, to be referred to as I) for ionization of atomic hydrogen from the initial 'configurations' 1s, 2s, 2p and 2. Here 1s and 2s are single states, 2p is the arithmetic mean of (2p, 0), (2p, +1) and (2p, −1), and 2 is the arithmetic mean of 2s, (2p, 0), (2p, +1) and (2p, −1). All of these 'configurations' have isotropic velocity distributions. 2s and 2p have the same ionization energy, but differ in the form of the velocity distributions. It was shown in I that, by using the quantal velocity distribution in the binary-encounter collision theory, good agreement was found with the corresponding Bethe results. This established how 'initial-state l quantization', as we have called it, should be accounted for in the binary-encounter collision theory. In this paper we extend the comparison to include 'initial-state m quantization'. This introduces a new feature, viz. non-isotropic initial velocity distributions, and we have modified the binary-encounter collision theory accordingly. This work was also motivated by the pronounced 'dip' which develops in the Bethe generalized oscillator strength $f_E(K)$ for ionization from the initial (2p, 0) state of hydrogen. We have hereby completed the quantization in the initial state. In contrast no consistent method has yet been found to account for final-state quantization (necessary, for example, in excitation and charge transfer). Throughout this paper we neglect exchange effects, and hence for the case of incident electrons the formulae only apply for sufficiently high incident energies. We also neglect all relativistic effects.

2. Binary-encounter theory

In a binary encounter the differential cross section $\partial^3\sigma/\partial E\,\partial P\,\partial(\cos\chi)$, abbreviated hereafter by ${}_s\sigma_{E,P,\chi}$, for an energy transfer E and a simultaneous momentum transfer $\boldsymbol{P}$

from an incident particle of charge z_1e and velocity $\boldsymbol{v}_1$ to a target electron with velocity $\boldsymbol{v}$ is given by Vriens (1966) for incident electrons only, Banks (unpublished) for arbitrary masses; Banks's method is described by Vriens (1969)

$$\sigma_{E,P,\chi} = \frac{8z_1{}^2e^4}{v_1{}^2vP^4}\frac{H(X)}{X^{1/2}} \tag{1}$$

where

$$X = 1+2(\hat{\boldsymbol{v}}_1 \cdot \hat{\boldsymbol{P}})(\hat{\boldsymbol{v}} \cdot \hat{\boldsymbol{P}})(\hat{\boldsymbol{v}}_1 \cdot \hat{\boldsymbol{v}})-(\hat{\boldsymbol{v}}_1 \cdot \hat{\boldsymbol{P}})^2-(\hat{\boldsymbol{v}} \cdot \hat{\boldsymbol{P}})^2-(\hat{\boldsymbol{v}}_1 \cdot \hat{\boldsymbol{v}})^2 \tag{2}$$

$H(X) = 1$ for $X \geqslant 0$ and $H(X) = 0$ otherwise, and $\hat{\boldsymbol{v}}_1 \cdot \hat{\boldsymbol{v}} = \cos\chi$.

In applications to charged-particle–atom collisions equation (1) must be averaged over the velocity distribution $f(\boldsymbol{v})$ of the atomic electron(s) relevan tto the target atoms considered, i.e.

$$\sigma_{E,\,P} = \int_0^\infty v^2\,\mathrm{d}v f_v(v)\int_{-1}^{1}\mathrm{d}(\cos\chi)f_\chi(\chi)\int_0^{2\pi}\mathrm{d}\eta\, f_\eta(\eta)\sigma_{E,P,\chi} \tag{3}$$

where η is the azimuthal angle of $\boldsymbol{v}$ around $\boldsymbol{v}_1$ and

$$\int_0^\infty v^2\,\mathrm{d}v f_v(v)\int_{-1}^{1}\mathrm{d}(\cos\chi)f_\chi(\chi)\int_0^{2\pi}\mathrm{d}\eta\, f_\eta(\eta) = 1. \tag{4}$$

For isotropic velocity distributions $f_\eta(\eta) = 1/2\pi$ and $f_\chi(\chi) = \frac{1}{2}$, so that the angular integrations in equation (3) yield (see Thomas 1927, Vriens 1966, 1967)

$$\sigma_{E,P,v} = \frac{4\pi z_1{}^2e^4}{v_1{}^2vP^4} \tag{5}$$

and

$$\sigma_{E,P} = \int_0^\infty v^2\,\mathrm{d}v\, f_v(v)\sigma_{E\,P,v}. \tag{6}$$

For non-isotropic velocity distributions equation (3) will first be expressed in a more convenient form.

Let $\mathrm{O}(\hat{\boldsymbol{X}}, \hat{\boldsymbol{Y}}, \hat{\boldsymbol{Z}})$ be a Cartesian frame of reference oriented so that $\hat{\boldsymbol{Z}}$ is in the direction of $\boldsymbol{v}_1$ and so that $\boldsymbol{P}$ lies in the $(\hat{\boldsymbol{Z}}, \hat{\boldsymbol{X}})$ plane. Then $\hat{\boldsymbol{v}}$ is conveniently described by the usual spherical polar angles χ and η, where $\cos\chi = \hat{\boldsymbol{v}}_1 \cdot \hat{\boldsymbol{v}}$.

Let $\mathrm{O}(\hat{\boldsymbol{x}}, \hat{\boldsymbol{y}}, \hat{\boldsymbol{z}})$ be another Cartesian frame of reference oriented so that $\hat{\boldsymbol{x}}$ coincides with $\hat{\boldsymbol{Y}}$ and so that $\hat{\boldsymbol{z}}$ lies along $\boldsymbol{P}$ (see figure 1). In this frame $\hat{\boldsymbol{v}}$ is described by the spherical polar angles θ and ϕ, where $\cos\theta = \hat{\boldsymbol{v}} \cdot \hat{\boldsymbol{P}}$.

It can easily be shown (Vriens 1966, 1969) that $\hat{\boldsymbol{v}}_1 \cdot \hat{\boldsymbol{P}}$ and $\hat{\boldsymbol{v}} \cdot \hat{\boldsymbol{P}}$ are uniquely determined by v_1, P, E and v, all of which are here considered fixed in the integration over angles (the integration over v being the final one). Let $\cos\alpha = \hat{\boldsymbol{v}}_1 \cdot \hat{\boldsymbol{P}}$. Geometrically the condition $\hat{\boldsymbol{v}} \cdot \hat{\boldsymbol{P}}$ is a constant means that $\hat{\boldsymbol{v}}$ is restricted to a circle Γ whose centre lies on $\boldsymbol{P}$ and whose plane is normal to $\hat{\boldsymbol{P}}$. The angles χ, θ, ϕ and α are related by

$$\cos\chi = \sin\alpha\sin\theta\sin\phi + \cos\alpha\cos\theta. \tag{7}$$

Now

$$X^{1/2} = \sin\theta\sin\alpha\cos\phi \tag{8a}$$

and

$$\frac{\mathrm{d}(\cos\chi)}{\mathrm{d}\phi} = \sin\theta\sin\alpha\cos\phi \tag{8b}$$

so that

$$\frac{\mathrm{d}(\cos\chi)}{X^{1/2}} = \mathrm{d}\phi. \tag{9}$$

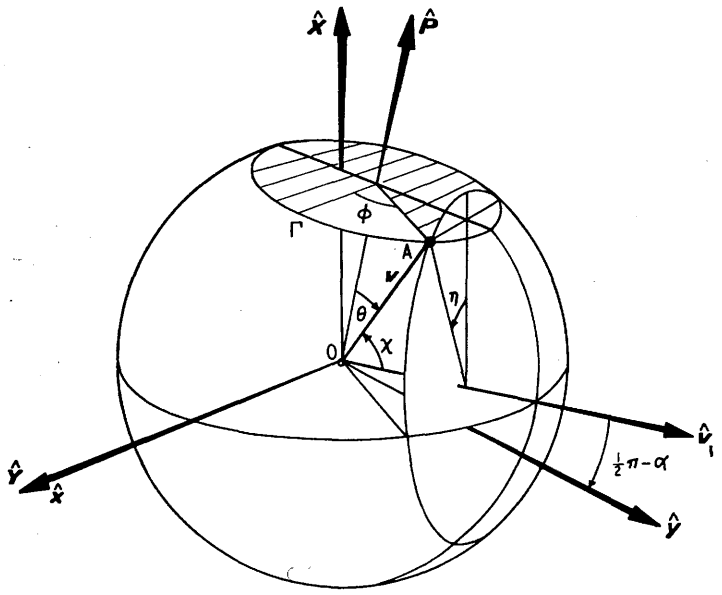

Figure 1. Velocity space diagram for the binary encounter. When $\boldsymbol{P}$, E, $\boldsymbol{v}_1$ and the magnitude of $\boldsymbol{v}$ are all fixed, the vector $\boldsymbol{v}(\overrightarrow{OA})$ must lie on the circle Γ, whose plane is perpendicular to $\boldsymbol{P}$ and whose centre lies on $\boldsymbol{P}$.

Hence, for the case of isotropic velocity distributions, we can replace the non-uniform integration over $\cos\chi$ by a uniform and much simpler integration over ϕ, where ϕ is the most convenient representation for $\hat{\boldsymbol{v}}$. Thus we can write

$$\sigma_{E,P,\phi} = \frac{4\pi z_1^2 e^4}{v_1^2 v P^4} \tag{10}$$

where

$$\frac{1}{2\pi}\int_0^{2\pi} \mathrm{d}\phi\, \sigma_{E,P,\phi} = \frac{1}{2}\int_{-1}^{1} \mathrm{d}(\cos\chi)\, \sigma_{E,P,\chi}.$$

For non-isotropic distributions of $\hat{\boldsymbol{v}}$, because θ is fixed,

$$\sigma_{E,P,\theta,\phi} = \frac{8\pi z_1^2 e^4}{v_1^2 v P^4}\delta(\cos\theta - \mu) \tag{11}$$

where $\delta(x)$ is the well-known Dirac δ-function and

$$\mu = \frac{2m_e E - P^2}{2m_e v P} \tag{12}$$

where m_e is the electron mass.

Equation (10) is a simpler and more elegant version of equation (1). Equation (11) is fully normalized in that

$$\int_{-1}^{1} \tfrac{1}{2}\,\mathrm{d}(\cos\theta)\int_0^{2\pi}\frac{1}{2\pi}\,\mathrm{d}\phi\,\sigma_{E,P,\theta,\phi} = \frac{4\pi z_1^2 e^4}{v_1^2 v P^4}.$$

With equation (11) we have reproduced a formula derived by Nijboer (1968, private communication) in an entirely different way. He used the first Born matrix element for charged-particle–atom collisions as a starting point and not relations for scattering of free-moving particles. Nijboer's method is described in the review by Vriens (1969).

Let the velocity (momentum) space wave function $\psi_{nlm}(\boldsymbol{v})$ of the hydrogen atom in the initial bound state be written

$$\psi_{nlm}(\boldsymbol{v}) = \rho_{nl}(v)Y_{lm}(\theta, \phi) \tag{13}$$

where $\rho_{nl}(v)$ is the radial velocity space wave function,

$$\int_0^\infty v^2 \, \mathrm{d}v|\rho_{nl}(v)|^2 = 1$$

and $Y_{lm}(\theta, \phi)$ is the normalized spherical harmonic (see Bethe and Salpeter 1957, p. 91, pp. 122–5). Then

$$\sigma_{E,P} = \left\langle nlm\left| \frac{8\pi {z_1}^2 e^4}{{v_1}^2 v P^4} \delta(\cos\theta - \mu) \right| nlm \right\rangle$$
$$= \frac{8\pi {z_1}^2 e^4}{{v_1}^2 P^4} \left\langle nlm\left| \frac{1}{v} \delta(\cos\theta - \mu) \right| nlm \right\rangle. \tag{14}$$

3. The generalized oscillator strength in binary-encounter theory

The 'binary-encounter generalized oscillator strength' $f_E(K)$ (denoted before in I as $\mathrm{d}f(Q)/\mathrm{d}\epsilon$) is related to the high incident velocity limit of the binary-encounter cross section $\sigma_{E,P}$ by

$$f_E(K) = \frac{PE{v_1}^2}{8\pi {a_0}^2 {z_1}^2 {v_0}^2} \sigma_{E,P} \tag{15}$$

where $\boldsymbol{K} = \boldsymbol{P}/\hbar$ (hence Ka_0 is dimensionless) and $v_0 = e^2/\hbar$. Hence

$$f_E(K) = \frac{E/R}{(Ka_0)^3} \left\langle nlm\left| \frac{v_0}{2v} \delta(\cos\theta - \mu) \right| nlm \right\rangle$$
$$= \frac{E/R}{(Ka_0)^2} \left\langle nlm\left| \delta\left(\frac{E - \hbar \boldsymbol{K} \cdot \boldsymbol{v} - \frac{1}{2}\hbar^2 K^2/m_e}{R} \right) \right| nlm \right\rangle \tag{16}$$

where R is the Rydberg energy ($m_e e^4/2\hbar^2$). Here we used the relation $|a|\delta(ax) = \delta(x)$. Equation (16) is actually the formula derived by Nijboer and mentioned before. Using the notation $Q = (Ka_0)^2$ and $\epsilon = E/R$,

$$\mu = \frac{\epsilon - Q}{2Q^{1/2}} \frac{v_0}{v}$$

and, since $\mu^2 \leqslant 1$, $v^2 \geqslant {v_{\min}}^2$ where

$$v_{\min} = \frac{|\epsilon - Q|}{2Q^{1/2}} v_0.$$

In particular for the (2p, 0) initial hydrogenic state

$$Y_{10} = \left(\frac{3}{4\pi}\right)^{1/2} \cos\theta$$

and

$$\rho_{21}(v) = \frac{128}{(3\pi)^{1/2}} \frac{{v_0}^{7/2} v}{(4v^2 + {v_0}^2)^{3}}$$

Performing the angular integration only, we obtain

$$f_{E,v}(K) = \frac{2^{10}}{\pi} \frac{\epsilon(\epsilon - Q)^2}{Q^{5/2}} \frac{{v_0}^{10} v}{(4v^2 + {v_0}^2)^6} H(v - v_{\min}) \tag{17}$$

and

$$f_E(K) = \int_0^\infty \mathrm{d}v \, f_{E,v}(K).$$

It can immediately be seen that $f_{E,v}(K)$ is zero for $\epsilon = Q$ and non-zero around this region. Performing the integration over v, we obtain

$$f_{E,(2p,0)}(K) = \frac{128}{5\pi} \frac{\epsilon Q^{5/2}(\epsilon - Q)^2}{\{(\epsilon - Q)^2 + Q\}^5}. \tag{18}$$

Similarly, for the (2p, ± 1) initial state

$$Y_{1\pm1}(\theta, \phi) = \left(\frac{3}{8\pi}\right)^{1/2} \sin\theta \exp(\pm i\phi)$$

and the complete integration yields

$$f_{E,(2p,\pm1)}(K) = \frac{16}{5\pi} \frac{\epsilon Q^{5/2}}{\{(\epsilon - Q)^2 + Q\}^4}. \tag{19}$$

Now

$$f_{E,2p}(K) = \tfrac{1}{3}\{f_{E,(2p,0)}(K) + 2f_{E,(2p,\pm1)}(K)\}$$

i.e.

$$f_{E,2p}(K) = \frac{32}{15\pi} \frac{\epsilon Q^{5/2}\{5(\epsilon - Q)^2 + Q\}}{\{(\epsilon - Q)^2 + Q\}^5}. \tag{20}$$

which is in agreement with equation (7*c*) of I.

4. The generalized oscillator strength in Bethe theory

The generalized oscillator strength $f_E(K)$ is defined by

$$f_E(K) = \frac{\epsilon}{Q} \left| (\psi_f | \exp(iK \cdot r) | \psi_{nlm}) \right|^2 \tag{21}$$

where, as before, ψ_{nlm} is the initial-state wave function of the target atom, ψ_f is the final wave function and r is the position vector of the atomic electron. For ionization of the hydrogen atom from the initial state (n, l, m) (see I and the references therein)

$$f_E(K) = \xi_{nlm} \left\{1 - \exp\left(\frac{-2\pi}{k_n}\right)\right\}^{-1} \exp\left\{\frac{-2}{k_n} \arctan\left(\frac{2k_n/n}{Q - k_n^2 + 1/n^2}\right)\right\} \tag{22}$$

where $k_n^2 = \epsilon - 1/n^2$. In particular, for ionization from the (2p, 0) hydrogen atom

$$\xi_{210} = \frac{4\epsilon}{15\{(\epsilon - Q)^2 + Q\}^5} \{7(\epsilon - Q)^4 + (64Q + 4)(\epsilon - Q)^3 + (192Q^2 + 54Q)(\epsilon - Q)^2 + 80Q^2(\epsilon - Q) + 15Q^2\}. \tag{23}$$

5. Comparison of the theories

We used equations (18), (22) and (23) to calculate the K dependence of $f_{E,(2p,0)}(K)$ for different values of E. The results are displayed in figures 2, 3 and 4. The most striking feature of the Bethe theory formula is the gradually developing dip at $Q = \epsilon$ which deepens with increasing ϵ. For this state the binary-encounter theory approach gives an exact zero at $Q = \epsilon$ for all ϵ. The differences in the two theories arise from the fact that the effect of the nucleus on the atomic electron is only partly allowed for (initial state) in the binary-encounter approach, whereas the Bethe theory contains the full effect of the nucleus (initial and final state) on the atomic electron. In both theories the effect of the nucleus on the incident particle is ignored. This is valid provided the incident velocity is sufficiently large. It can be seen that there is remarkable agreement for $\epsilon = 15$ (see figure 4) and that reasonable agreement is already found for $\epsilon \geqslant 1$, which exceeds the threshold energy for ionization by a factor of 4. As in I, we find that the binary-encounter theory gives an incorrect description of the collision process for small K.

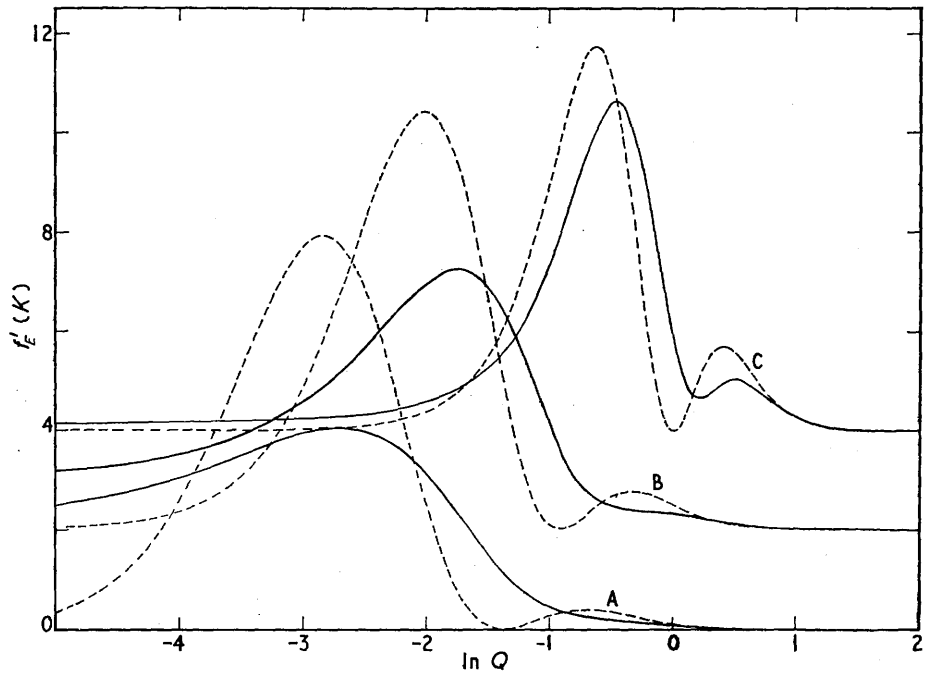

Figure 2. Bethe (full curves) and binary-encounter (broken curves) generalized oscillator strengths for ionization of the hydrogen atom from the $n = 2$, $l = 1$, $m = 0$ state for different energy transfers. Curve A, $\epsilon = 0{\cdot}25$ and $f_E(K) = f_E'(K)$; curve B, $\epsilon = 0{\cdot}4$ and $f_E(K) = 0{\cdot}5(f_E'(K)-2)$; curve C, $\epsilon = 1$ and $f_E(K) = 0{\cdot}2(f_E'(K)-4)$.

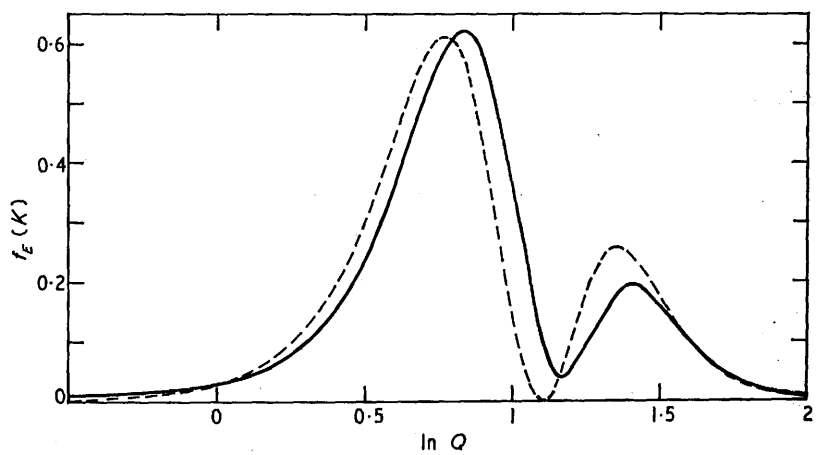

Figure 3. Bethe (full curve) and binary-encounter (broken curve) generalized oscillator strengths for ionization of the hydrogen atom from the $n = 2$, $l = 1$, $m = 0$ state for $\epsilon = 3$.

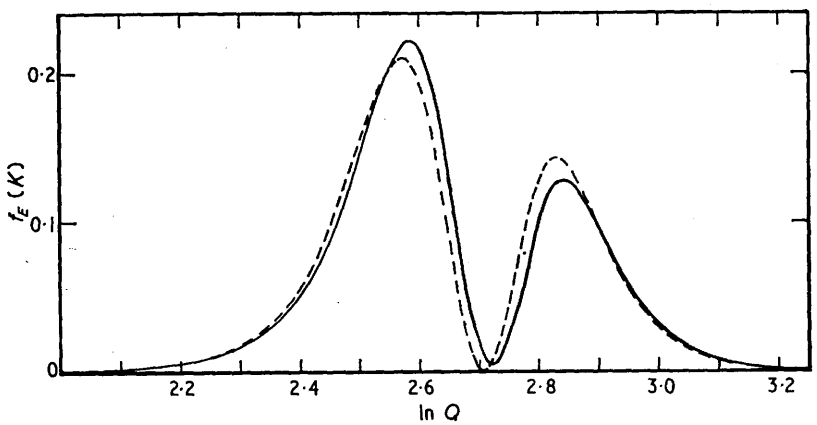

Figure 4. As in figure 3 for $\epsilon = 15$.

6. *m*-quantization axis

In both theories the axis of m quantization was taken along the direction of the momentum transfer vector $\boldsymbol{P}$, which is fixed once $\boldsymbol{v}_1$ and $\boldsymbol{v}_1'$, the final velocity of the incident particle (energy loss and direction of scattering), are chosen (e.g. in an experiment). Hence the cases considered are realistic in that it is experimentally possible to make a beam of atoms with m either 0 or 1 along the $\hat{\boldsymbol{P}}$ direction. In principle one can thus observe the pronounced dip found here.

It is interesting to note that, if in the binary-encounter theory we choose the initial state m-quantization axis along the direction of $\boldsymbol{v}_1$, then for the (2p, 0) state of atomic hydrogen we obtain equation (19) which equals the result arising from the (2p, ± 1) state with the m-quantization axis along $\boldsymbol{P}$. This is surprising because, even though

$$\hat{\boldsymbol{v}}_1 \cdot \hat{\boldsymbol{P}} = \frac{2m_1E + P^2}{2m_1v_1P}$$

is small for large v_1 and therefore $\boldsymbol{P}$ is almost perpendicular to $\boldsymbol{v}_1$, the resulting angular distributions are different. The former distribution has axial symmetry about the $\hat{\boldsymbol{v}}_1$ direction, whereas the latter has toroidal symmetry about the $\hat{\boldsymbol{P}}$ direction.

7. Additional remarks

Because of the simple structure of equation (16), the method can easily be extended to higher excited states of hydrogen and to other target atoms. The zeros (or minima) in the binary-encounter generalized oscillator strength for large E and P give the location of possible dips in the Bethe and experimentally measured generalized oscillator strengths. The nature of these dips arises essentially from the angular integration and thus from the *angular* part of the initial-state wave function, as can be seen from equations (16) and (17). The dips (troughs) recently discussed by Kim *et al.* (1968) arise in a different way. They considered excitation to bound states and ionization with small E. In their cases the dips arise from the *radial* parts of the initial- and final-state wave functions.

Acknowledgments

We should like to thank Professor B. R. A. Nijboer for informing one of us about his method, which largely influenced our mathematical formulation, and also Professor I. C. Percival for useful discussions. D.B. would also like to thank the F.O.M.–Instituut voor Atoom-en Molecuulfysica for their hospitality while part of this work was being done and is indebted to the Science Research Council for providing a research grant. The work of L.V. and T.F.M.B. is part of the research programme of the 'Stichting voor Fundamenteel

Onderzoek der Materie' (F.O.M.) and was financially supported by the 'Nederlandse Organisatie voor Zuiver Wetenschoppelijk Onderzoek' (Z.W.O.).

References

ABRINES, R., and PERCIVAL, I. C., 1966, *Proc. Phys. Soc.*, **88,** 861–72.

BETHE, H. A., and SALPETER, E. E., 1957, *Encyclopedia of Physics*, Vol. 35, Ed. S. Flügge (Berlin: Springer-Verlag), pp. 88–126.

BURGESS, A., 1963, *Proc. 3rd Int. Conf. on Electronic and Atomic Collisions, London*, 1963, Ed. M. R. C. McDowell (Amsterdam: North-Holland), pp. 237–42.

BURGESS, A., and PERCIVAL, I. C., 1968, *Advances in Atomic and Molecular Physics*, Vol. 4, Eds D. R. Bates and I. Estermann (New York: Academic Press), pp. 109–41.

GRYZINSKI, M., 1959, *Phys. Rev.*, **115,** 374–83.

KIM, Y.-K., INOKUTI, M., CHAMBERLAIN, G. E., and MIELCZAREK, S. R., 1968, *Phys. Rev. Lett.*, **21,** 1146–8.

KINGSTON, A. E., 1968, *J. Phys.* B (*Proc. Phys. Soc.*), [2], **1,** 559–66.

STABLER, R. C., 1964, *Phys. Rev.*, **133,** A1268–73.

THOMAS, L. H., 1927, *Proc. Camb. Phil. Soc.*, **23,** 713–6.

VRIENS, L., 1966, *Proc. Phys. Soc.*, **89,** 13–21.

—— 1967, *Proc. Phys. Soc.*, **90,** 935–44.

—— 1969, *Case Studies in Atomic Collisions*, Eds E. W. McDaniel and M. R. C. McDowell (Amsterdam: North-Holland), chap. 6.

VRIENS, L., and BONSEN, T. F. M., 1968, *J. Phys.* B (*Proc. Phys. Soc.*), [2], **1,** 1123–30.

J. Phys. B: Atom. Molec. Phys., 1971, Vol. 4. Printed in Great Britain

Angular distribution of electrons ejected by charged particles
III. Classical treatment of forward ejection

T. F. M. BONSEN† and D. BANKS‡

† Fysisch Laboratorium der Rijksuniversiteit, Utrecht, The Netherlands
‡ Department of Physics, University of Stirling, Stirling, Scotland

MS. received 15*th January* 1971

Abstract. Differential cross sections for the ejection of electrons from helium by 100 and 300 keV protons are calculated using a classical three body collision theory. Comparisons are made with the experimental and quantum mechanical results. For not too large angles of ejection the classical orbit integration cross sections agree very well with the experimental values, in contrast to the quantum mechanical Born calculations.

1. Introduction

The energy and angular distribution of electrons ejected by 100 to 300 keV protons from helium has been measured by Kuyatt and Jorgenson (1963), Rudd and Jorgenson (1963, to be referred to as RJ) and by Rudd, Sauter and Bailey (1966, to be referred to as RSB). RSB also performed Born calculations (hydrogenic, scaled on the ionization energy) for this process. An extension of the Born calculations was made by Salin (1969) for atomic hydrogen. He took into account the interaction of the ejected electron with the scattered proton by introducing a velocity dependent effective charge. Macek (1970) took account of the final state wave distortion due to the proton by calculating the first term of the Neumann expansion of the solutions of the Faddeev equation. Another theoretical approach, the binary encounter theory, has been employed by Bonsen and Vriens (1970). From their comparison of the (simple) binary encounter theory with the experiment and Born calculations of RSB, they concluded that (i) the binary encounter theory and all classical theories fail in describing the backward ejection, since this is caused by a purely quantum mechanical interaction of the ejected electron with the rest of the atom and (ii) for velocities of the ejected electron which are of the same order of magnitude as the velocity of the incident proton a three (or more) body theory has to be used to describe the experimental results in the forward direction.

These conclusions encouraged us to calculate the cross sections for small angle ejection of electrons by protons from helium using the classical three body theory developed and applied to collisions of protons with hydrogen atoms by Abrines and Percival (1966 a,b, to be referred to as AP). Abrines *et al.* (1966) also applied the original Ema program developed by AP to collisions of electrons with hydrogen atoms. The total p–H ionization cross sections, obtained by AP had normal statistical errors of about 10% and agreed with experiment to within 15% over the entire range of incident proton energies (40–225 keV). In their treatment, the only approximation was the classical one, whereas in all other classical theories (Gryzinski 1959, Burgess 1964, Stabler 1964 and Ochkur and Petrun'kin 1963) a second approximation (the impulse or binary encounter approximation) was also made. Our program was based on the more general and flexible Fortran three body Monte Carlo program of

Percival and Valentine (see Valentine 1968, Banks, *et al.* 1969 and Banks and Valentine 1969).

In this paper we make extensive comparisons with the experiment and Born calculations of RSB and RJ, and with the binary encounter theory. Double differential cross sections are calculated so that we are able to test the validity of the classical approximation in detail.

2. Classical model for the helium atom

Because of the fact that the atom contains two electrons, an additional approximation has to be made. The two electrons will be described as independent scattering centres, so the four particle collision can be replaced by two independent three particle (p–H) collisions. The classical microcanonical velocity distribution in the field of the nucleus can be written as

$$\rho(v) = \frac{8v_0^5}{\pi^2(v^2+v_0^2)^4} \tag{1}$$

in which $mv_0^2 = -2E_0$, E_0 being the binding energy. This distribution has also been shown by Bonsen and Vriens (1970) to represent the quantum mechanical velocity distribution of the electrons in the helium atom very well if E_0 was chosen to be equal to the mean kinetic energy of the electron (39·49 eV). However, since the ionization threshold is equal to E_0 in the classical model, we had to choose E_0 equal to the ionization energy (24·58 eV). This represents the same scaling as has been performed in the Born approximation.

3. Numerical method

We used the program described by Valentine (1968) to construct the classical proton–helium atom system and obtained the differential cross sections for ejection of electrons for two incident energies (100 keV and 300 keV). The values of the error parameters ϵ, γ and δ defined by AP were chosen to be 0·3, 0·2 and 0·005 respectively. With these error parameters the statistical errors were larger than the numerical and truncation errors arising from the Runge Kutta integration of the equations of motion and from the neglect of the asymptotic interaction. Although a very small value of δ was used the extra computing time was relatively short. The range of modified impact parameters was chosen to be $\sqrt{3}\cdot 37\, a_0$ for 100 keV proton impact and $\sqrt{3}\, a_0$ for 300 keV proton impact. From a sample of orbits uniform in the whole range of modified impact parameters (3000 orbits in the case of 100 keV impact and 1000 orbits for 300 keV impact) the following remarks could be made:

(i) In order to obtain normal statistical errors less than 20% for the small angle ionization cross sections in the interesting ejection energy range (40–200 eV for 100 keV impact and 100–600 eV for 300 keV impact), the total number of orbits necessary with a uniform impact parameter distribution would be 25 000 for 100 keV and as many as 75 000 for 300 keV proton impact.

(ii) For all ejection angles, large ejection energies arose from collisions in which small modified impact parameters were involved.

To reduce the computing time, which was about thirty seconds for each orbit on the Stirling University ICL 4100 as well as on the Utrecht University EL–X8 we made use of (ii) and used a weighted distribution of modified impact parameters for the calculations of the cross sections (Abrines and Percival 1966 b). By taking the

distribution of figures 1*a* and 1*b* for 100 and 300 keV proton impact respectively, we obtained normal statistical errors less than 20% for the cross sections in the interesting range of energy and angle with 8000 orbits in the case of 100 keV proton impact and 9300 in the case of 300 keV proton impact.

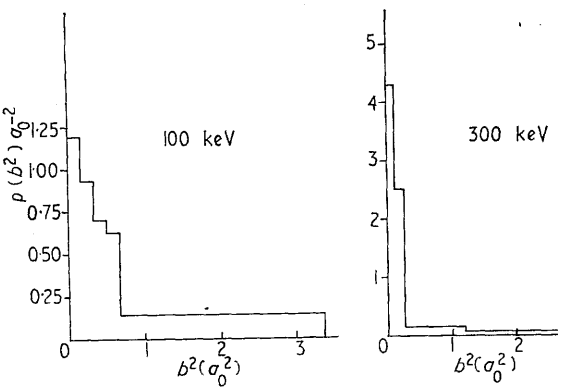

Figure 1. Impact parameter distribution used for the calculations of collisions of 100 and 300 keV protons on helium.

4. Statistics

The impact parameter distributions used to calculate the double differential cross sections can be written as:

$$\rho(b^2) = \theta(b^2) \sum_{j=1}^{n} c_j \theta(b_j{}^2 - b^2) \tag{2}$$

in which $\theta(x)$ is the unit step function; so between two values b_{i-1} and b_i of the modified impact parameter the distribution is uniform. For the range of impact parameters between b_{i-1} and b_i we can calculate the contribution $\sigma_i(E, \theta)$ to the double differential cross section $\sigma(E, \theta)$. Suppose that n_i collisions take place with impact parameter between b_{i-1} and b_i, then $n_i = N\Sigma_{j=i}^{n} c_j$, in which N is the total number of orbits. Further let the number of collisions resulting in ionization of the atom with the ejected electron moving in a direction between $\theta - \frac{1}{2}\Delta\theta$ and $\theta + \frac{1}{2}\Delta\theta$ with respect to the incident proton and with an energy between $E - \frac{1}{2}\Delta E$ and $E + \frac{1}{2}\Delta E$ be denoted by $n_i(E, \theta)$. Then the contribution $\sigma_i(E, \theta)$ to the double differential cross section $\sigma(E, \theta)$ can be written as:

$$\sigma_i(E, \theta) = \frac{n_i(E, \theta)}{2n_i \Delta\theta \Delta E \sin\theta}(b_i{}^2 - b_{i-1}{}^2) \qquad \text{where } b_0 = 0. \tag{3}$$

Assuming that no ionization takes place for impact parameters larger than b_n, the double differential cross section $\sigma(E, \theta)$ for ejection of an electron is simply

$$\sigma(E, \theta) = \sum_{i=1}^{n} \sigma_i(E, \theta). \tag{4}$$

Since in practice $n_i \gg n_i(E, \theta)$ the standard error is given by

$$\Delta\sigma(E, \theta) = \frac{1}{2\Delta\theta \Delta E \sin\theta} \left\{ \sum_{i=1}^{n} \frac{n_i(E, \theta)}{n_i{}^2} (b_i{}^2 - b_{i-1}{}^2)^2 \right\}^{1/2}. \tag{5}$$

In our calculations we choose $\Delta\theta = 10°$ for both incident energies. We took $\Delta E = 25$ eV for 100 keV proton impact and $\Delta E = 50$ eV for 300 keV proton impact. The standard errors were found to be of the order of 20%, except for very large ejection energies and large ejection angles where the errors may be as large as 100%.

Note that to obtain good statistics from an economical number of orbits we require fairly large tolerances in energy and angle. This may result in a smoothing of the double differential cross section. Experimentalists are faced with similar difficulties but in this case our tolerances are larger than those of RSB. However for a given atomic model we have 100% counting efficiency so that we do not have additional normalization problems.

5. Double differential cross sections

For ejection angles smaller than 90° we calculated the cross sections $\sigma(E, \theta)$ and compared our values with the corresponding experimental cross sections of RSB, the binary encounter results of Bonsen and Vriens (1970) and the Born cross sections of RSB, which agree with the binary encounter cross sections to within 10%. For 100 keV proton impact on helium the results are given in figure 2.

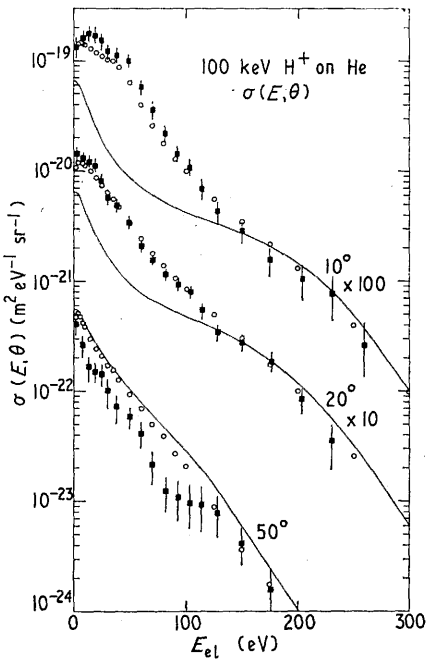

Figure 2. Energy distributions of electrons ejected from helium at various angles with respect to 100 keV proton beam. The sets of data for 10° and 20° ejection are multiplied by a factor of 100 and 10 respectively. ■ our calculations; O experiment of RSB; full curve, Born approximation.

The three sets of data have been displaced along the ordinate axis. In the upper set the ejection angle is 10°. The agreement between the experiment and the classical results is extremely good. The remaining discrepancies may be due to the approximate velocity distribution. In the energy region where both Born and binary encounter

theory give results which are about a factor of six smaller than the experiment, the Monte Carlo results are somewhat larger even than the experimental ones. This is rather surprising since the omission of quantal tunnel effects should produce the opposite. This discrepancy is unlikely to be due to the approximate velocity distribution since Bonsen and Vriens (1970) demonstrated that (in the binary encounter approximation) the use of a more accurate velocity distribution raised the cross sections in this energy region. The calculated energy distribution for 20° ejection (the middle set of data) agrees completely with the experimental cross section over the whole range of energy to within the statistical errors. For higher ejection angles (see for instance the lower set for 50° ejection) it can be seen that the classical approximation no longer holds.

The Monte Carlo results for 300 keV proton impact on helium are presented in figure 3 together with experimental and Born results of RSB. The results for 10°

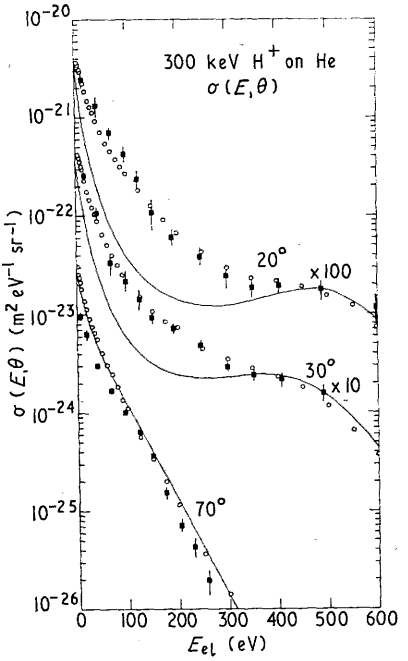

Figure 3. Energy distribution of electrons ejected by 300 keV protons from helium at various angles. The set of data for 20° and 30° ejection are multiplied by a factor of 100 and 10 respectively. ■ our calculations; ○ experiment of RSB; full curve, Born approximation.

ejection are not presented since the statistical errors are too large to make decisive conclusions. For 20° ejection the cross sections are given in the upper part of the figure. Though the statistical errors are not small the agreement between the classical theory and the experiment is extremely good. This is also the case for 30° ejection. For higher ejection angles the classical theory underestimates the cross sections but even for 70° ejection (see the lower set of data of figure 3) the calculated energy distribution is in quite good agreement with experiment.

Comparison with the Born (as well as the binary encounter) approximation shows that the interaction between the projectile and the atom in the region where the

velocity of the incident proton is about the same as the velocity of the ejected electron (50 eV for 100 keV protons and 150 eV for 300 keV protons) is essentially a four particle interaction, which can be described very well classically by two independent three particle collisions.

6. Single differential cross sections

In figures 4 and 5 the cross sections $\sigma(\theta)$ are presented and compared with the corresponding experimental results of RSB and RJ and with Born and binary

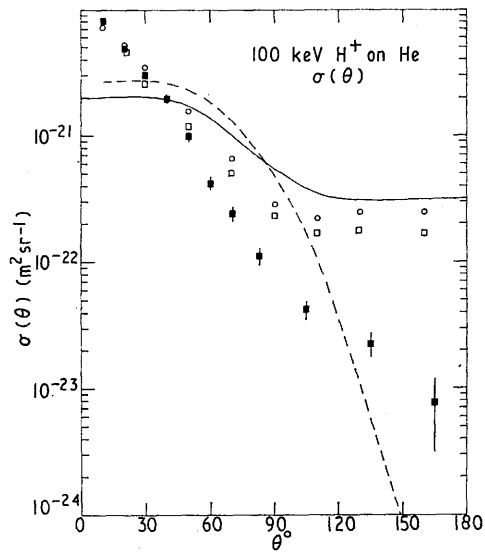

Figure 4. Angular distribution of electrons ejected by 100 keV protons from helium. ■ our results; □ experiments of RJ; ○ experiments of RSB; full curve, Born approximation; broken curve, binary encounter theory.

encounter calculations. From these figures it is clear that the classical approach is not valid for backward ejection as has been explained previously by Bonsen and Vriens (1970). In the forward direction the angular distribution calculated using the Monte Carlo method is in very close agreement with experiment. For lower angles the statistical errors become large owing to the small size of the ionization channel. For higher impact energies the range of validity of the classical theory approaches 90°. The results of RJ seem to be somewhat more realistic than the measurements of RSB.

In figure 6 the energy distributions of the ejected electrons are presented for both incident energies. The agreement between all experiments and theories is close for all ejection energies. It is clear that large angle ejection does not contribute significantly to $\sigma(E)$ for ejection energies larger than about 30 eV. For very small ejection energies (< 20 eV) the results of RJ are in closer agreement with our calculations than the measurements of RSB. In the energy range where the velocities of ejected electron and incident proton are about equal, the classical cross sections are slightly better than Born and binary encounter values which follows directly from the double differential cross section calculations.

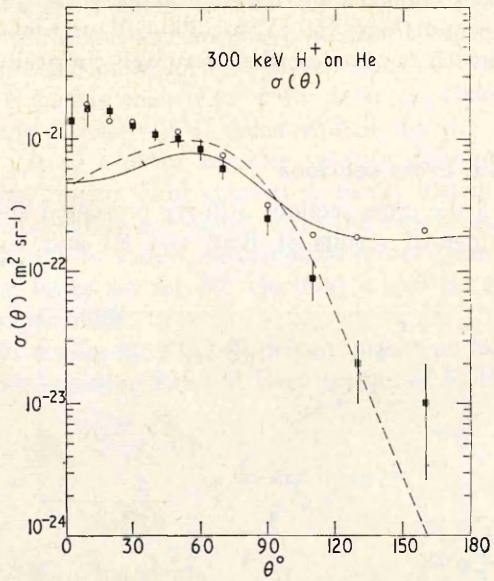

Figure 5. Angular distribution of electrons ejected by 300 keV protons from helium. ■ our results; ○ experiments of RSB; full curve, Born approximation; broken curve, binary encounter approximation.

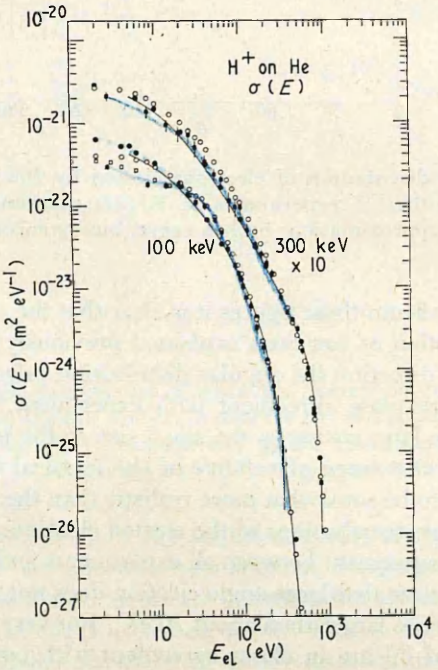

Figure 6. Energy distributions of electrons ejected by 100 and 300 keV protons from helium. The 300 keV sets of data have been multiplied by 10. ■ our results; □ experiments of RJ; ○ experiments of RSB; ● binary encounter theory; full curve, Born approximation.

7. Total ionization cross sections

In table 1 the classical total ionization cross sections are presented for both incident energies and compared with previous results.

Table 1. Total ionization cross sections for ionization of helium by protons

E_p (keV)	RSB	RJ	Born	Binary encounter	Our results
100	11·9	10·0	11·0	11·9	9·25 ±0·25
300	7·13	—	5·47	5·74	5·44 ±0·25

All cross sections are in units of 10^{-21}m^2.

It can be seen that the classical result, which is in very close agreement with previous calculations of AP for p–H collisions, in both cases is about 20% smaller than the RSB results. The cross sections of RJ for 100 keV protons agree to within 7% with our calculations. The main difference between classical theory and both experiments is due to small energy (< 20 eV) large angle ($> 70°$) ejection as can be seen from figures 4 to 6. For 100 keV proton impact a fortuitous agreement exists between the quantum mechanical (Born as well as binary encounter) theories and the experiment of RSB. From figure 4 it can be seen that a compensation of the errors occurs in forward and intermediate angles. For 300 keV proton impact this compensation does not occur to the same extent and the total cross section in both theories is smaller than the experimental value.

8. Conclusion

The classical three body approximation describes the angular and energy distribution of electrons ejected by protons from helium very well for small and intermediate ejection angles and for all ejection energies. In this region the classical approach is even superior to the Born approximation. For large ejection angles a quantum mechanical approach has to be used. To calculate total cross sections for intermediate energies of the proton the classical three body approximation is as good as any quantum mechanical approach. However to obtain good statistics within reasonable time a fast computer has to be used for the Monte Carlo program.

The proton and electron ionization cross sections obtained by Abrines and Percival (1966 b) and by Abrines *et al.* (1966) were determined as functions of incident energy only. It is possible, that the agreement between Monte Carlo and experiment on ground-state atoms is fortuitous. Particularly since the experiments of Lassettre and his collaborators there is increasing insistance that comparisons of the differential cross sections should be required before theory and experiment are said to agree. On this basis the present results for double differential cross sections show that classical orbit integration methods are valid in important regions of incident energy, energy transfer and ejection angle even for low quantum numbers.

Acknowledgments

We are indebted to Professor M. E. Rudd for generously providing us with very extensive tabular data on his experimental and Born cross sections. We should like to thank Professor I. C. Percival for starting this investigation.

TFMB would also like to thank the Physics Department of the University of Stirling for their hospitality while part of this work was being done. The work of TFMB is part of the research programme of the Foundation for Fundamental Research on Matter (FOM) and was financially supported by the Netherlands Organization for the advancement of Pure Research (ZWO). DB is indebted to the Science Research Council for providing a research grant.

References

ABRINES, R., and PERCIVAL, I. C., 1966 a, *Proc. Phys. Soc.*, **88,** 861–72.
—— 1966 b, *Proc. Phys. Soc.*, **88,** 873–83.
ABRINES, R., PERCIVAL, I. C., and VALENTINE, N. A., 1966, *Proc. Phys. Soc.*, **89,** 515–23.
BANKS, D., PERCIVAL, I. C., and VALENTINE, N. A., 1969, *Abstr. 6th Int. Conf. on the Physics of Electronic and Atomic Collisions* (Cambridge Mass.: M.I.T. Press) pp. 215–6.
BANKS, D., and VALENTINE, N. A., 1969, *Abstr. 6th Int. Conf. on the Physics of Electronic and Atomic Collisions* (Cambridge Mass.: M.I.T. Press) p. 123.
BONSEN, T. F. M., and VRIENS, L., 1970, *Physica*, **47,** 307–19.
BURGESS, A., 1964, *Proc. 3rd Int. Conf. on the Physics of Electronic and Atomic Collisions, London*, 237–42.
GRYZINSKI, M., 1959, *Phys. Rev.*, **115,** 374–83.
KUYATT, C. E., and JORGENSON, JR, T., 1963, *Phys. Rev.*, **130,** 1444–55.
MACEK, J., 1970, *Phys. Rev.*, A, **1,** 235–41.
OCHKUR, V. I., and PETRUN'KIN, A. M., 1963, *Optics Spectrosc.*, **14,** 245–8.
RUDD, M. E., and JORGENSON, Jr. T., 1963, *Phys. Rev.*, **131,** 666–75.
RUDD, M. E., SAUTER, C. A., and BAILEY, C. L., 1966, *Phys. Rev.*, **151,** 20–7.
SALIN, A., 1969, *J. Phys.* B: *Atom. molec. Phys.*, **2,** 631–9.
STABLER, R. C., 1964, *Phys. Rev.*, **133,** A 1268–73.
VALENTINE, N. A., 1968, *PhD thesis*, University of London.

COMPUTER PHYSICS COMMUNICATIONS 2 (1971) 114-123. NORTH-HOLLAND PUBLISHING COMPANY

CLASSICAL RELATIVE MOTION OF 2 PARTICLES

D. BANKS, I. C. PERCIVAL and J. McB. WILSON
Department of Physics, University of Stirling, Scotland

Received 1 October 1970

PROGRAM SUMMARY

Title of program (32 characters maximum): EVAR

Catalogue number: ACQT

Computer for which the program is designed and others upon which it is operable

Computer: ELLIOT 4130. *Installation*: University of Stirling, Scotland

Operating system or monitor under which the program is executed: ENL 23

Programming languages used: FORTRAN

High speed store required: 20000 words. *No. of bits in a word*: 24.

Is the program overlaid? No

No. of magnetic tapes required: None

What other peripherals are used? Card Reader; Line Printer

No. of cards in combined program and test deck: 3452

Card punching code: IBM 029 EBCDIC

Keywords descriptive of problem and method of solution: Atomic, Molecular, Astrophysics, Classical, Coulomb, Diatomic, Euler, Forces, Frame, Gravitational, Hydrogen, Interatomic, Kepler, Newtonian, Orbit, Particle, Runge-Kutta, Scattering, State, Vibrational.

Nature of the physical problem

Flexible representation of the classical relative motion of two particles interacting through a general central force.

Method of solution

A general terminology of states and frames is introduced which allows changes from one state or frame to another to be defined. The frame changes are analytic. The state changes are made by solution of Newton's equations of motion using a fourth-order Runge-Kutta formula [1].

Restrictions on the complexity of the problem

Limited to central forces.

Typical running time

This depends on the form of the potential, the boundary conditions and the integration time specified.

Reference

[1] R. A. Buckingham, Numerical methods (Pitman, London, 1962).

LONG WRITE-UP

1. INTRODUCTION

Programs for the numerical solution of the newtonian equations for the relative motion of 2 particles interacting through a central force have wide application. Frequently solutions are required as part of the solution of a problem involving 3 or more particles.

This package is designed to provide a *flexible, comprehensible and machine-independent* set of routines for the 2-particle relative-motion problem, rather than routines which compute quickly, although speed has not been neglected. Some of the conventions adopted may appear unnecessary, but their significance becomes apparent in using the package as part of a larger problem.

Because the problem of the relative motion of 2 particles is equivalent to that of the motion of a single particle (with their reduced mass) in a given external field [1, p. 29], the masses, co-ordinates and velocities of the individual particles are not relevant to this package. Furthermore this package may be used directly to obtain solutions of the equivalent problem of a single particle in a given fixed external field.

Although most computing time is spent in integrating equations of motion, in practice, much programming is concerned with setting up initial conditions and analysing data. We have found that this programming is greatly assisted by the introduction of a terminology of classical frames and states. The routines of the package are concerned with changes in frame in addition to the integration of equations of motion, which is required for changes in state. The latter is carried out using a fourth-order Runge-Kutta method [2] with a step length which is recalculated at each step.

Provision is made for obtaining and working in a frame of reference (x', y', z') for which the relative motion is in the x', y' plane, but no attempt is made to separate the radial and angular motions, since the use of similar integration methods for 2-particle and 3-particle systems should reduce certain numerical errors accumulated along orbits. The form of the force field is chosen so that the user may include his own force terms. There is also special provision for the inverse-square force term. The package may be used for both bound systems and scattering problems.

The programming standards adopted in this package are comparable to those proposed by Roberts in ref. [3].

2. BODY AND STATES

There is only 1 body in a 2-particle relative-motion system. This is called the *reduced mass*. It is labelled by any of

IBODR, JBODR, ..., NBODR, (IBODR = 1),
BODR (abbreviation).

This body has a mass EMR2(IBODR).

The

2 (abbreviation)

as for EMR2(IBODR) is used to denote a variable or routine associated specifically with a 2-particle system. This is convenient when the package is used as part of a larger package or program.

Time (epoch) for the 2-particle relative-motion system is denoted by TIMR2 and is measured (in some system of units which must be used consistently throughout) with respect to a standard origin of time which is supposed fixed.

At a given time TIMR2 the body has a position $\boldsymbol{R}$ and velocity $\boldsymbol{V}$ relative to the standard (laboratory or LAB) co-ordinate system whose origin coincides with the centre of force. $\boldsymbol{R}$ and $\boldsymbol{V}$ are represented collectively by 6 numerical co-ordinates (in some system of units which must be used consistently throughout).

The 6 co-ordinates constitute the *RV-vector* of the body and are labelled by any of

IRV, JRV, ..., NRV, (IRV = 1 to 6), in which
IRV = 1, 2, 3 label the position co-ordinates and
IRV = 4, 5, 6 label the corresponding velocity co-ordinates.

The

RV (abbreviation)

refers to co-ordinates of position and velocity. We have found that velocity is preferable to momentum for numerical computation of orbits.

The motion of the system at all times, or evolution of the system, can be obtained if a time TIMR2 and the RV-vector of the body (with respect to the standard cartesian axes at that time) are defined. This set of 7 real numbers defines a state of the 2-particle relative-motion system in the standard frame, or a point in the 7-dimensional RVT-space. Any equivalent set of 7 or more real numbers which defines this point also defines the state. States are labelled by any of

ISTR, JSTR, ..., NSTR, (ISTR = 1 to KRSTM2),
ST (abbreviation).

A typical state might be that at the beginning of an integration of the equations of motion, called the *initial state*, labelled ISTR = JSTR, or the state after integration, called the *final state*,

labelled ISTR = MSTR. When different forms of interaction or different stages in the integration are introduced, more states are needed. The choice of numerical values of ISTR labels is left to the user. We have made provision for 7 states but this maximum number 7 may be altered by changing dimension statements and redefining KRSTM2.

The time at which the system reaches state ISTR is denoted by

TIMR2 (1, ISTR) .

As the calculation proceeds, the RV-vectors are stored in a 3-dimensional array:

RVREL2 (IRV, IBODR, ISTR)

with locations for each of the 6 co-ordinates IRV of the RV-vector of the body IBODR in each state ISTR.

3. FRAMES

At a given stage in a computation not all of the elements of the RVREL2 array will be obtained. For a given state ISTR only the time TIMR2 and the 6 values of RVREL2 defining the position and velocity of the body are required to define the state. But any equivalent set of 7 or more real numbers also defines the state. Only some of these equivalent sets are significant or useful and we call these *frames*, which may be considered as particular co-ordinate systems in the 7-dimensional RVT-state space. If more than 7 numbers are given by a frame, then they are related and the frame is reducible. Such frames are nevertheless significant.

The frames are labelled by any of
IFRAM, JFRAM, ..., NFRAM,
(IFRAM = 1, 2, 3, 4, 5),
IFRAM (abbreviation).

The frame IFRAM = 1 has been defined above and is the *standard frame*. Thus, in a given state ISTR, for IFRAM = 1:

$$\text{give TIMR2}(1,\text{ISTR}),\quad \text{RVREL2}(\text{IRV},1,\text{ISTR}),\ \text{IRV} = 1 \text{ to } 6. \tag{1}$$

(That is to say, if TIMR2(1,ISTR), RVREL2(IRV,1,ISTR) are given then IFRAM = 1 is available.)

The frame IFRAM = 2 is the *rotation-matrix frame*. In this frame a new set of axes with unit vectors $\hat{x}'$, $\hat{y}'$, $\hat{z}'$ is defined with standard cartesian co-ordinates

XDASH2(IR,1,ISTR), IR = 1 to 3 ,
YDASH2(IR,1,ISTR), IR = 1 to 3 ,
ZDASH2(IR,1,ISTR), IR = 1 to 3 ,

respectively. The nine values constitute a 3×3 rotation matrix M which relates co-ordinates in the two co-ordinate systems. The components with IR = 4 are described in routine AXES2.

In the dashed co-ordinate system the x', y' plane is taken to be the plane of relative motion so that the angular momentum vector is in the direction of the z' axis. For the Coulomb force the x' axis is taken to be in the direction of the perihelion vector (shortest radius vector). When no Coulomb force is present the x' axis is taken perpendicular to the initial velocity vector so that the y' axis is parallel to this velocity vector. Combinations of Coulomb and non-Coulomb forces and the special cases that arise when some of the quantities are very large or small, are described in the comments of routine AXES2.

In the dashed co-ordinate system only the co-ordinates 1, 2, 4 and 5 are required to define the RV-vector as the z'-components are zero.

The RV-vector is called

RVRXV2(IRV,1,ISTR) ,

where RXV denotes the vector $\boldsymbol{R} \times \boldsymbol{V}$ which is used to define the new frame. The values for IRV = 3 and IRV = 6 are always zero.

Both this RV-vector and the rotation matrix are needed to define the given state ISTR of relative motion, so that for IFRAM = 2:

$$\begin{aligned}&\text{give TIMR2}(1,\text{ISTR}),\text{XDASH2}(\text{IR},1,\text{ISTR}),\\ &\quad \text{YDASH2}(\text{IR},1,\text{ISTR}),\text{ZDASH2}(\text{IR},1,\text{ISTR}),\\ &\quad \text{IR} = 1 \text{ to } 3 ,\\ &\quad \text{RVRXV2}(\text{IRV},1,\text{ISTR}),\text{IRV} = 1,\ 2,\ 4,\ 5.\end{aligned} \tag{2}$$

Clearly this frame is very reducible.

The reducibility is lessened by defining the rotation in terms of the Euler angles instead of the matrix. With the definition given by Whittaker [4, p. 9] of the Euler angles $(\phi_2, \theta_2, \psi_2) \hat{=}$ (PHI2, THETA2, PSI2) or with $\mu_2 \hat{=} \text{EMU2} \hat{=} \cos\theta_2$ as a useful alternative parameter, the *Euler-angle frames* are defined as follows. For IFRAM = 3:

$$\begin{aligned}&\text{give TIMR2}(1,\text{ISTR}),\text{PHI2}(1,\text{ISTR}),\\ &\quad \text{THETA2}(1,\text{ISTR}),\text{PSI2}(1,\text{ISTR}),\\ &\quad \text{RVRXV2}(\text{IRV},1,\text{ISTR}),\ \text{IRV} = 1,\ 2,\ 4,\ 5 .\end{aligned} \tag{3}$$

For IFRAM = 4 :

$$\begin{aligned}&\text{give as IFRAM} = 3,\\ &\quad \text{but EMU2}(1,\text{ISTR}) \text{ in place of}\\ &\quad \text{THETA2}(1,\text{ISTR}) .\end{aligned} \tag{4}$$

The fifth frame requires an alternative definition of the rotation in terms of the complex

Cayley-Klein parameters [4, p. 12] $(\alpha_2, \beta_2, \gamma_2, \delta_2)$ $\hat{=}$ (ALPHA2, BETA2, GAMMA2, DELTA2) so that for IFRAM = 5:

give TIMR2(1, ISTR), ALPHA2(1, ISTR),
BETA2(1, ISTR), GAMMA2(1, ISTR),
DELTA2(1, ISTR), RVRXV2(IRV, 1, ISTR), (5)
IRV = 1, 2, 4, 5.

The equations of relative motion are usually integrated in the rotation-matrix frame, but since only TIMR2 and RVRXV2 are required, any but the standard frame would do.

Initial conditions are sometimes set up in the Euler angle frame [5]. The Cayley-Klein frame is included for completeness.

4. SIGNALS AND SIGNAL RULES

These play a key role in the operation of the package. At the beginning of a run for a given orbit none of the frames will be available for any state of that orbit. The initial state (say ISTR = 1) for the relative motion may then be set up by the user in any one of the 5 frames, but it may be required at a later stage in any other frame. A routine UFRAM2 is provided for obtaining one frame from another, but this will not work unless a record is kept of which particular frame or frames is available. This service is provided by a *signal array*:

KSFRM2(IFRAM, 1, ISTR) ,

whose value for each IFRAM, ISTR is either 0, which is called *red*, or 1, which is called *green*. The package will function properly only if the *signal rules* are strictly kept by the user.

At the beginning of the run for a given orbit the whole signal array must be set to red (zero) by the user. For a given state ISTR, if the user provides the frame IFRAM without using the package, say to set up the initial conditions, he must set the appropriate signal to green (1). If the package routines are used to obtain frames, they set the signals automatically.

As each frame is obtained the corresponding signal is set to green. If a routine of the package requires a particular frame it first observes the corresponding signal. If it sees green it proceeds. If it sees red it means that the required frame is not available, and either it obtains the frame from an available frame, or, if none is available, a FAULT routine is called. If the user wishes to write routines using particular frames he is advised to use the signal KSFRM2 in the same way.

The signal arrays KSCAL2 and KSAXE2 will be described in the context of the routines that use them.

The signal rules described above must be obeyed by the user, or the routines of the package may produce nonsense, using RV-vectors with incorrect components as data. When the rules are obeyed they allow rapid and relatively simple programming.

5. EQUATIONS OF MOTION, ERROR PARAMETERS

The frames are derived from one another using analytic relations. A state ISTR can in general only be obtained from another by numerical integration of the equations of motion, called numerical evolution.

The equations of relative motion are

$$\dot{\boldsymbol{R}} = \boldsymbol{V}, \qquad \dot{\boldsymbol{V}} = \frac{1}{M} F\hat{\boldsymbol{R}} , \tag{6}$$

where M is the mass of the body, $F\hat{\boldsymbol{R}}$ is the external central force acting upon it, and the dot denotes differentiation with respect to time. We call F the scalar central force. F differs from the magnitude of the force by the inclusion of a sign (negative if attractive).

The 6 equations of relative motion are first order differential equations for RVREL2 with respect to TIMR2. The 4 equivalent equations for the corresponding co-ordinates RVRXV2 are solved (by routine USTR2) in frame 2 by a step-by-step procedure.

Numerical integration, like many other computations, requires a judgement to be made on the conflicting demands of speed of computation and accuracy of the results. Unfortunately this judgement often cannot be made without many test runs, so in this and later packages and programs speed and accuracy of computation are under the control of *error parameters*

ERRP (abbreviation) ,

which are part of the input data.

Normally if an error parameter is small the accuracy is relatively good, but the speed of computation is relatively low, and vice versa.

For a given accuracy we like the speed to be as high as possible. For the equations of relative motion the speed depends critically on the optimum length of the time-step STEP2 in the step-by-step integration, which is a function of the current force, and thus of the stage of integration.

We find it appropriate to recalculate STEP2 at

every step, normally according to the formula

$$\mathrm{STEP2} = \frac{\pm \mathrm{ERRP2(1)}}{\mathrm{SQRT}(|\boldsymbol{V}\cdot\boldsymbol{F}/M|)} \qquad (7)$$

where ERRP2(1) is an error parameter, and have for this reason used fourth-order Runge-Kutta integration and not a nominally faster numerical integration procedure for which a change of step length is difficult.

In exceptional circumstances, e.g. near a singularity or zero of the force, STEP2 as defined above may approach zero or infinity, and the routine STEPL2 which calculates STEP2 then keeps its magnitude within specified bounds.

6. SUBROUTINES AND FUNCTIONS

In writing routines it is advisable to allow for exceptional occurrences, such as position and velocity vectors being in the same direction. We have found that such exceptional cases require considerable programming, which detracts from the clarity of the routines of the package. We have therefore separated many routines into *normal modes* and *special* or *exceptional modes*. At first reading the special modes should be ignored. However, it should be pointed out that analytically "simple" orbits, such as circular and straight line orbits frequently require special modes of operation of the routines.

The general flow through the routines is given in fig. 1.

USTR2(WTIM, JSTR, MSTR) and its daughters
USTR2 is the most important routine of the 2-particle relative-motion package and, with the aid of its descendants, carries out the numerical evolution.

Explicitly, USTR2 obtains the final state MSTR of the relative motion in the standard frame from the initial state JSTR, in any frame, and the time interval WTIM.

USTR2 uses UFRAM2 to obtain the co-ordinates of relative motion in the dashed co-ordinate system, and then normally carries out step-by-step evolution with full interaction in that frame. For each step, USTR2 calculates the current time step STEP2 (increment or decrement) using STEPL2 and evolves the state approximately for that step in time using RUNGE2. When the time interval WTIM has lapsed (overshoot is automatically prevented) USTR2 sets KSFRM2(2,1,MSTR) = 1 and uses UFRAM2 to obtain the co-ordinates of relative motion in the standard frame IFRAM = 1. If during evolution

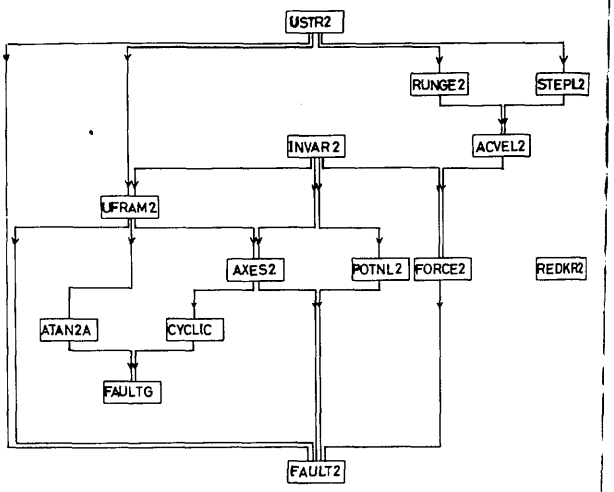

Fig. 1. Package structure. Each (mother) routine shown at the tail of each arrow calls (daughter) routines at the head of the arrow, which in their turn call further (descendant) routines.

the number of steps exceeds a given tolerable maximum number KINTM2, USTR2 calls FAULT2(2,JSTR).

Exceptional modes are described in the comments of USTR2.

RUNGE2
RUNGE2 carries out a single step in the numerical evolution using ACVEL2 to obtain the vector accelerations and velocities (derivatives of velocities and positions) as functions of position and velocity. The 4th-order Runge-Kutta method [2] is used.

STEPL2
STEPL2 calculates the current step in time for the step-by-step numerical evolution using eq. (7).

ACVEL2
ACVEL2 obtains the current relative vector acceleration and velocity in the dashed co-ordinate system, using FORCE2 to calculate the required current scalar force as a function of the current radial distance.

FORCE2
FORCE2 obtains the current scalar central force FRC2(1) which acts on the body (negative if attractive).

It is used to obtain the vector forces for

numerical integration and for calculation of the current step length.

FORCE2 is used and operates in 3 different modes, which we describe separately.

FORCE2 (inverse-square mode)
Only the inverse-square (or Coulomb) force is present. For use, set SCALE2(1,1) equal to the force constant (product of the charges), and KSCAL2(1,1) and KSCLM2(1) equal to 1. Before each call ensure R2(1) is equal to the distance from the force centre and then call the routine FORCE2 to obtain the scalar inverse-square force.

FORCE2 (general mode)
Central force (chemical) terms are present which are not inversely proportional to RSQ2(1). The total scalar force is a sum of KSCLM2(1) (10 or less) terms. For use in this mode the *routine must be modified by the programmer* as described in the comments of FORCE2. In addition to the modification KSCLM2(1) must be set to the number of terms in the force, KSCAL2(1,LPTL) set to 0 if the term LPTL is zero; and 1 otherwise, where the term LPTL = 1 is always of inverse-square form. The scale factors SCALE2(1,LPTL) must be assigned by the user. Also KSHPM2(1) must be set to the number (10 or less) of shape parameters and SHAPE2(1,LSHP) must be set to their correct values.

FORCE2 obtains the scalar force by calculating the KSCLM2(1) force terms (using the KSHPM2(1) shape parameters) and adding them together.

FORCE2 (chemical mode)
As in the general mode but the inverse-square term is never present.

UFRAM2 and AXES2
These form a different branch of the USTR2 family from those considered in the previous section. They are often used on their own, independently of USTR2.

UFRAM2(MFRAM2,JSTR)
UFRAM2 is used to obtain a required frame MFRAM2 for a given state JSTR of the relative motion of a 2-particle system if any of the 5 frames is available.

For instance the initial conditions of relative motion may be known in the standard frame IFRAM = 1, that is the vectors of relative position and velocity in the co-ordinate system of that frame. They are required (by USTR2) in one of the other frames in which the motion is in the x', y' plane in order to perform the numerical integration of the equations of motion.

The signal rules must be obeyed for UFRAM2 to work.

UFRAM2 looks at the signal KSFRM2(MFRAM2,1,JSTR) and if it is green, UFRAM2 assumes frame MFRAM2 is available and returns. If that signal is red, UFRAM2 looks at the other signals KSFRM2 for the state JSTR of relative motion to see if any one is green, and if so assumes the corresponding frame IFRAM2 is available. From frame IFRAM2 it then calculates the variables of MFRAM2, and of any intermediate frames that it may be convenient to use. It switches KSFRM2 to green for MFRAM2 *and* for any such intermediate frame of state JSTR and returns. If KSFRM2(IFRAM,1,JSTR) is red for all five frames, UFRAM2 calls FAULT2(4,JSTR) and returns.

AXES2(JSTR)
AXES2 obtains the standard co-ordinates (direction cosines) of the dashed axes x', y', z' for the state JSTR from the relative position and velocity RV-vector RVREL2. It also finds the following simple dynamical frame invariants in the state JSTR:

1) the relative distance RST2(1,JSTR),
2) the relative speed VST2(1,JSTR),
3) the magnitude of the angular momentum vector ZDASH2(4,1,JSTR) (if possible),
4) the magnitude of the Runge-Lenz vector XDASH2(4,1,JSTR) (if possible).

It has 3 normal modes of operation which we describe here and many exceptional modes which are needed for singular conditions and which are described only in the detailed comments of AXES2. In all normal modes the motion is confined to the x', y' plane.

AXES2 (inverse-square mode)
This is the normal mode when only an inverse-square force is present. The x' axis is in the direction of the perihelion of the orbit of relative motion, that is, in the direction of the Runge-Lenz vector [1, eq. (15.17)] of relative motion

$$M\boldsymbol{V}\times(\boldsymbol{R}\times\boldsymbol{V})+K\boldsymbol{R}/|\boldsymbol{R}|\ , \qquad (8)$$

where $K \hat{=}$ SCALE2(1,1) is the inverse-square force constant.

The Runge-Lenz vector is a constant of the motion and is approximately so during numerical evolution.

AXES2 (chemical mode)
This is the non-singular mode when chemical terms (see FORCE2, chemical mode) but no inverse-square term is present. The x' axis is in the direction of the first term in formula (8). During numerical evolution the x' axis remains constant at its initial-state value.

AXES2 (general mode)
Both chemical and inverse-square terms are present. The x' axis is in the direction of the vector (8) but this is not usually the direction of the perihelion of the relative motion. The same applies to numerical evolution as for the chemical mode. However, if the chemical terms are relatively small, the x' axis is approximately in the direction of the perihelion and AXES2 may be used to investigate the precession of the perihelion.

7. AUXILIARY ROUTINES AND FUNCTIONS

POTNL2
POTNL2 obtains the potential energy of the body (reduced mass). It has the same general structure as FORCE2.

INVAR2(JSTR)
INVAR2 obtains some of the simple dynamical frame invariants of the relative state JSTR.

REDKR2
REDKR2 sets to red (0) all the signals which can be altered by this package.

FAULT2(JFAULT, MFAULT)
FAULT2 writes fault messages for faults detected in the 2-particle relative-motion package into the output stream labelled by KOUT.

ATAN2A(WY, WX)
The function ATAN2A obtains the plane polar angle ATAN2A (in radians) in the range $(0, 2\pi)$ of a point in a plane with cartesian co-ordinates (WX, WY). This function is necessary for machine-independent operation, as the range of definition of ATAN2(X, Y) can be different for different installations. ATAN2A(WY, WX) requires the standard tangent function ATAN(X) for X in the range $(0, \pi/2)$ only.

CYCLIC(JI, MJ, MK)
CYCLIC makes (JI, MJ, MK) a cyclic permutation of (1, 2, 3) if possible, given JI only.

FAULTG(JFAULT)
FAULTG writes fault messages for faults detected in ATAN2A or CYCLIC into the output stream labelled by KOUT.

Common blocks

Block name	Contents
C2ANGL	ALPHA2(1,7), BETA2(1,7), DELTA2(1,7), EMU2(1,7), GAMMA2(1,7), PHI2(1,7), PSI2(1,7), THETA2(1,7)
C2AXES	KSAXE2(1,7), RVRXV2(6,1,7), XDASH2(4,1,7), YDASH2(4,1,7), ZDASH2(4,1,7)
C2BODR	KSFRM2(5,1,7), RVREL2(6,1,7), TIMR2(1,7)
C2FCPT	FRCN2(1,10), PTLN2(1,10)
C2INPR	EMR2(1), ERRP2(5), KINTM2, KRSTM2, KSCAL2(1,10), KSCLM2(1), KSHPM2(1), SCALE2(1,10), SHAPE2(1 10)
C2INVR	EKST2(1,7), ETST2(1,7), FRCST2(1,7), PTLST2(1,7), RST2(1,7), VST2(1,7)
C2USTR	FF2(4), FRC2(1), KINT2, PTL2(1), R2(1), RSQ2(1), RV2(4), STEP2, TIME2, V2(1), VSQ2(1)
CINOUT	AZERO, KIN, KOUT

For definitions of common block variables see dictionary.

8. ESSENTIAL INFORMATION REQUIRED BY THE PACKAGE

The package will function correctly if the following instructions are obeyed.

1) Include all common blocks of the package in the calling routine.

2) Define all the input constants. These constitute the common blocks CINOUT and C2INPR.

3) Call REDKR2.

4) Define *any* of the 5 frames for some state JSTR and set the corresponding signal (s) to GREEN (1).

5) Define WTIM if a new state MSTR is to be obtained by numerical evolution.

9. TEST RUN

The package is tested with the aid of the driver program REL MOTION TEST which consists of the main routine MAIN TEST and 4 auxiliary routines ZEROR2(JSTM2), INOUT2(JSTR, JIN, WNAME),

OUTST2(JSTR, WNAME) and OUT2(WNAME). Using the package, the driver program carries out the numerical evolution of the motion of an electron relative to a proton with a non-relativistic inverse-square attractive force between them, using atomic units. It then includes a harmonic perturbation term.

The first step of the main routine is to set all the common variables in the package for the states 1, 2, 3, 4, and 5 to zero. This is achieved by routine ZEROR2. The input constants and the initial state of the atom in the standard frame 1 are assigned in INOUT2, which also reads and writes the names QNAME of all the common variables. INOUT2 then writes out the complete common list, showing the input constants and the initial state of the atom in a standardised form. The output variables for state 1 are then calculated and written out. The main program next evolves state 1 for a complete period QWTIM of the bound motion, placing the results into state 2. The values of the common variables of state 2 are determined and written out. As the system has been evolved for a complete period, exact integration should return all the variables save WTIM to their original values. A good approximation to this situation can be obtained by choosing a sufficiently small ERRP2(1). At time QWTIM a perturbing term of the form $+\frac{1}{2}\omega^2 r^2$ (where $-\omega^2$ = SCALE2(1,2)) is added to the existing potential and the corresponding term $-\omega^2 r$ is added to the scalar force. As a result, some of the values of the common variables are altered and so the state is renamed state 3 and the complete common list written out again. The system is evolved from state 3 for a further time interval QWTIM forwards in time to state 4 and then backwards in time (time interval -QWTIM) to state 5. The values of all common variables are written out for the states 4 and 5 as each state is obtained. The results are not identical because the perturbed system has a different period to that of the unperturbed system. A fully comprehensive test of the package has been made but is too long for presentation. This program tests only those branches of routines which are required in a typical application of the package.

Data for the test run

The data consists of the names of all of the common variables.

Output from the test run

This consists of the listing of the input data followed by six pages showing the progression through the five states as described above. The input data and the first three of these pages are reproduced below.

ACKNOWLEDGEMENTS

The authors are indebted to the Science Research Council for providing a research grant. They would also like to thank Dr. K. V. Roberts, Dr. A. S. Dickinson, Mr. D. Richards and Dr. A. Norcliffe for useful discussions.

REFERENCES

[1] L. D. Landau and E. M. Lifshitz, Course of theoretical physics, Vol. 1, Mechanics (Pergamon Press, London, 1960).
[2] R. A. Buckingham, Numerical methods (Pitman, London, 1962).
[3] K. V. Roberts, Computer Phys. Commun. 1 (1969) 1.
[4] E. T. Whittaker, A treatise on the analytic dynamics of particles and rigid bodies (Cambridge Univ. Press, London, 1965).
[5] R. Abrines and I. C. Percival, Proc. Phys. Soc. (London) 88 (1966) 861.

TEST RUN OUTPUT

```
        DATA CARDS
        ---- -----
AZERO KIN   KOUT  ERRP2 KINTM2KSCAL2KSCLM2KSHPM2SCALE2SHAPE2ERCN2 PTLN2
FF2   FRC2  KINT2 PTL2  R2    RSQ2  RV2   STEP2 TIME2 V2    VSQ2  EMU2
KRSTM2KSFRM2RVREL2TIMR2 KSAXE2RVRXV2YDASH2YDASH2ZDASH2ALPHA2BETA2 DELTA2
EMU2  GAMMA2PHI2  PSI2  THETA2EKST2 ETST2 FRCST2PTLST2RST2  VST2
```

```
        INPUT VALUES OF ALL COMMON VARIABLES IN THE RELATIVE STATE 1 ARE AS FOLLOWS.
        ===== ====== == === ====== ========= == === ======== ===== = === == ========

 INPUT CONSTANTS
 ----- ----------
  AZERO      0.100000E-09
  KIN                   7
  KOUT                  2
  ERRP2      0.400000E-01    0.000000E+00    0.000000E+00    0.100000E-01    0.100000E+02
  KINTM2                1000
  KSCAL2                1                0
  KSCLM2                2
  KSHPM2                1
  SCALE2    -0.100000E+01   -0.100000E-01
  SHAPE2     0.000000E+00
 FRAME VARIABLES
 ----- ---------
  EMR2       0.999460E+00
  KRSTM2                5
  KSFRM2                1               0               0               0               0
  RVREL2     0.000000E+00    0.200000E+00    0.000000E+00    0.000000E+00    0.000000E+00    0.300000E+01
  TIMR2      0.000000E+00
  KSAXE2                0
  RVRXV2     0.000000E+00    0.000000E+00    0.000000E+00    0.000000E+00    0.000000E+00    0.000000E+00
  XDASH2     0.000000E+00    0.000000E+00    0.000000E+00    0.000000E+00
  YDASH2     0.000000E+00    0.000000E+00    0.000000E+00    0.000000E+00
  ZDASH2     0.000000E+00    0.000000E+00    0.000000E+00    0.000000E+00
  ALPHA2     0.000000E+00    0.000000E+00
  BETA2      0.000000E+00    0.000000E+00
  DELTA2     0.000000E+00    0.000000E+00
  EMU2       0.000000E+00
  GAMMA2     0.000000E+00    0.000000E+00
  PHI2       0.000000E+00
  PSI2       0.000000E+00
  THETA2     0.000000E+00
  EKST2      0.000000E+00
  ETST2      0.000000E+00
  FRCST2     0.000000E+00
  PTLST2     0.000000E+00
  RST2       0.000000E+00
  VST2       0.000000E+00
 INTERACTION TERMS
 ----------- -----
  ERCN2      0.000000E+00    0.000000E+00
  PTLN2      0.000000E+00    0.000000E+00
 CURRENT VARIABLES OF STEP-BY-STEP EVOLUTION
 ------- --------- -- ------------ ---------
  FF2        0.000000E+00    0.000000E+00    0.000000E+00    0.000000E+00
  FRC2       0.000000E+00
  KINT2                 0
  PTL2       0.000000E+00
  R2         0.000000E+00
  RSQ2       0.000000E+00
  RV2        0.000000E+00    0.000000E+00    0.000000E+00    0.000000E+00
  STEP2      0.000000E+00
  TIME2      0.000000E+00
  V2         0.000000E+00
  VSQ2       0.000000E+00
```

```
        OUTPUT VALUES OF ALL COMMON VARIABLES IN THE RELATIVE STATE 1 ARE AS FOLLOWS.
        ====== ====== == === ====== ========= == === ======== ===== = === == ========

 INPUT CONSTANTS
 ----- ----------
  AZERO      0.100000E-09
  KIN                   7
  KOUT                  2
  ERRP2      0.400000E-01    0.000000E+00    0.000000E+00    0.100000E-01    0.100000E+02
  KINTM2                1000
  KSCAL2                1                0
  KSCLM2                2
  KSHPM2                1
  SCALE2    -0.100000E+01   -0.100000E-01
  SHAPE2     0.000000E+00
 FRAME VARIABLES
 ----- ---------
```

```
 EMR2      0.999460E+00
 KRSTM2               5
 KSFRM2               1              1              1              1              1
 RVREL2    0.000000E+00   0.200000E+00   0.000000E+00   0.000000E+00   0.000000E+00   0.300081E+01
 TIMR2     0.000000E+00
 KSAXE2               4
 RVRXV2    0.200000E+00   0.000000E+00   0.000000E+00   0.000000E+00   0.300081E+01   0.000000E+00
 XDASH2    0.000000E+00   0.100000E+01   0.000000E+00   0.800000E+00
 YDASH2    0.000000E+00   0.000000E+00   0.100000E+01   0.100000E+01
 ZDASH2    0.100000E+01   0.000000E+00   0.000000E+00   0.599838E+00
 ALPHA2    0.500000E+00   0.500000E+00
 BETA2     0.500000E+00   0.500000E+00
 DELTA2    0.500000E+00  -0.500000E+00
 EMU2      0.000000E+00
 GAMMA2   -0.500000E+00   0.500000E+00
 PHI2      0.000000E+00
 PSI2      0.157080E+01
 THETA2    0.157080E+01
 EKST2     0.450000E+01
 ETST2    -0.500001E+00
 FRCST2   -0.250000E+02
 PTLST2   -0.500000E+01
 RST2      0.200000E+00
 VST2      0.300081E+01
INTERACTION TERMS
----------- -----
 FRCN2    -0.250000E+02   0.000000E+00
 PTLN2    -0.500000E+01   0.000000E+00
CURRENT VARIABLES OF STEP-BY-STEP EVOLUTION
------- --------- -- ------------ ---------
 FF2       0.000000E+00   0.000000E+00   0.000000E+00   0.000000E+00
 FRC2     -0.250000E+02
 KINT2                0
 PTL2     -0.500000E+01
 R2        0.200000E+00
 RSQ2      0.400000E-01
 RV2       0.000000E+00   0.000000E+00   0.000000E+00   0.000000E+00
 STEP2     0.000000E+00
 TIME2     0.000000E+00
 V2        0.000000E+00
 VSQ2      0.000000E+00
```

```
      OUTPUT VALUES OF ALL COMMON VARIABLES IN THE RELATIVE STATE 2 ARE AS FOLLOWS.
      ====== ====== == === ====== ========== == === ======== ===== = === == ========

INPUT CONSTANTS
----- ---------
 AZERO     0.100000E-09
 KIN                  7
 KOUT                 2
 ERRP2     0.400000E-01   0.000000E+00   0.000000E+00   0.100000E-01   0.100000E+02
 KINTM2               1000
 KSCAL2               1                0
 KSCLM2               2
 KSHPM2               1
 SCALE2   -0.100000E+01  -0.100000E-01
 SHAPE2    0.000000E+00
FRAME VARIABLES
----- ---------
 EMR2      0.999460E+00
 KRSTM2               5
 KSFRM2               1              1              1              1              1
 RVREL2    0.000000E+00   0.200000E+00   0.118001E-03   0.000000E+00  -0.984581E-03   0.300081E+01
 TIMR2     0.628149E+01
 KSAXE2               4
 RVRXV2    0.200000E+00   0.117856E-03   0.000000E+00  -0.982395E-03   0.300081E+01   0.000000E+00
 XDASH2    0.000000E+00   0.100000E+01   0.728302E-06   0.800000E+00
 YDASH2    0.000000E+00  -0.728302E-06   0.100000E+01   0.100000E+01
 ZDASH2    0.100000E+01   0.000000E+00   0.000000E+00   0.599838E+00
 ALPHA2    0.500000E+00   0.500000E+00
 BETA2     0.500000E+00   0.500000E+00
 DELTA2    0.500000E+00  -0.500000E+00
 EMU2      0.000000E+00
 GAMMA2   -0.500000E+00   0.500000E+00
 PHI2      0.000000E+00
 PSI2      0.157080E+01
 THETA2    0.157080E+01
 EKST2     0.450000E+01
 ETST2    -0.500001E+00
 FRCST2   -0.250000E+02
 PTLST2   -0.500000E+01
 RST2      0.200000E+00
 VST2      0.300081E+01
INTERACTION TERMS
----------- -----
 FRCN2    -0.250000E+02   0.000000E+00
 PTLN2    -0.500000E+01   0.000000E+00
CURRENT VARIABLES OF STEP-BY-STEP EVOLUTION
------- --------- -- ------------ ---------
 FF2      -0.984992E-03   0.300081E+01  -0.250135E+02  -0.147568E-01
 FRC2     -0.250000E+02
 KINT2                168
 PTL2     -0.500000E+01
 R2        0.200000E+00
 RSQ2      0.400000E-01
 RV2       0.200000E+00   0.118001E-03  -0.984581E-03   0.300081E+01
 STEP2     0.695306E-03
 TIME2     0.628149E+01
 V2        0.300077E+01
 VSQ2      0.900465E+01
```